Shells on a Sphere: Tectonic Plate Motion and Plate Boundary Deformation

by

Edwin Victor Apel III

A dissertation submitted in partial satisfaction
of the requirements for the degree of

Doctor of Philosophy

in

Earth and Planetary Science

in the

GRADUATE DIVISION

of the

UNIVERSITY OF CALIFORNIA, BERKELEY

Committee in charge:

Professor Roland Bürgmann, Chair
Professor Richard Allen
Professor Nicolas Sitar

Fall 2011

Shells on a Sphere: Tectonic Plate Motion and Plate Boundary Deformation

by

Edwin Victor Apel III

Abstract

Shells on a Sphere: Tectonic Plate Motion and Plate Boundary Deformation

by

Edwin Victor Apel III

Doctor of Philosophy in Earth and Planetary Science

University of California, Berkeley

Professor Roland Bürgmann, Chair

Plate motion models have matured from being based only on geology and seismicity to incorporating space-based geodetic methods like GPS. I use a block modeling approach to incorporate both rigid block rotation and near-boundary elastic strain accumulation effects in a formal inversion of GPS velocities.

Independent Okhotsk and Amurian microplate motions are tested using GPS velocities that constrain the plate kinematics of northeast Asia. Modeling favors scenarios with independent OKH and AMU motion, based on the application of F-test statistics. The plate-motion parameters of the independent plates are consistent with the kinematics inferred from earthquake focal mechanism solutions along their boundaries.

GPS-measured velocities (15 from continuously recording stations within the stable India plate interior) geodetically constrain India plate motion, intraplate strain, and plate boundary deformation around the India plate. Dense station coverage from previously published studies allows rigorous testing of boundary parameterizations. I develop robust India plate motion parameters and see good agreement between predicted plate directions from the preferred model and the seismological data.

Available GPS data in and around the Aegean region is combined and used to evaluate plate motion models, elastic plate boundary deformation and its relationship to seismogenic coupling along the Hellenic subduction zone. The A.D. 365 M ˜8.4, the A.D. 1303 M ˜8 Crete suggest that portions of the plate interface must be locked. The primary focus of this study is to examine potential upper plate deformation resulting from a locked subduction interface, active hanging-wall extension, or both. I consider multiple model scenarios in an attempt to interpret the both the horizontal and vertical geodetic signals in the region and its implications for earthquake hazard assessment.

To my wife Jessica, I could not have done this without you.

Contents

List of Figures

List of Tables

Acknowledgements

"All models are wrong but some prove to be useful."

– Professor George Box, 1979

Perhaps one of the most difficult things to accept as a scientist is that we are all wrong. However, there is a small modicum of relief in knowing that, while scientific models may be wrong they can still provide insight and utility. This dissertation is no different. It is filled with models that are wrong. Some models simplify the natural world into manageable means. Others are mere approximations. These models are wrong in that we know the earth to be vast complex system that is not fully captured by models with assumptions and approximations. Even so, these models allow us to gain further insight into the processes of the natural world and provide a basis for scientific understanding.

While it may take a village to raise a child, it takes an army to finish a dissertation. I would not have finished without the support and sacrifices of my friends, colleagues and family. To my friends, thank you for babysitting my children, making me dinners, and continuing to push me to finish. I am a better man for it.

I owe a great deal of thanks to the graduate students who came before me. Matt d'Alessio, Ingrid Johanson, and Mark Wenzel provided invaluable advice and instruction as well as many tips and tricks that made my research progress more efficient.

Roland Bürgmann, my advisor, has been one of the few people in my life who has been able to pat my on the back and kick me in the butt at the same time. Thank you for never giving up on me and helping me see this dissertation through to the end.

Last, but not least, I want thank my wife, Jessica. Thank you for agreeing to move away from your family and come with me to California when I was accepted into the Ph.D. program at UC Berkeley. You have made more sacrifices for this dissertation than anyone else. I could not have done this without you. I love you.

Chapter 1

Introduction

As scientific theories go Plate Tectonics is relatively young. Although Alfred Wegner proposed the idea of continental drift as early as 1912, a lack of a driving mechanism for moving the continents prevented the idea from taking hold in the scientific community. It wasn't until seafloor spreading was documented via magnetic reversals on the ocean floor [*Vine and Matthews*, 1963; *Vine and Wilson*, 1965] that the theory gained traction and continues to evolve to this day.

The elegance of Plate Tectonic theory is that any plate's motion can be described with Eulers fixed point theorem which states that: The most general displacement of a rigid body over the surface of a sphere can be regarded as a rotation about a suitable axis which passes through the center of that sphere. Therefore, assuming the earth is spherical, any rigid tectonic plate follows the curvature of the earth and can be considered a shell upon that sphere. Moreover, any tectonic plate motion can then be described with a single vector that passes through the center of the earth. The point on the surface of the earth where this vector intersects is often referred to as an Euler pole, described by a latitude, longitude and rotate rate.

Early geologic plate motion models [*McKenzie and Parker*, 1967; *Le Pichon*, 1968] took advantage of Eulers theorem and developed current plate motions based primarily on sea-floor spreading rates, transform fault azimuths, and earthquake slip vectors. As more sea-floor surveys were completed, subsequent global plate motion models included this data [*Chase*, 1978; *Minster and Jordan*, 1978] and tests for self-consistency [*DeMets et al.*, 1990] making global geologic plate motion models quite robust. Euler poles from these models could then be used to predict specific velocities on a tectonic plate anywhere in the world.

Geologic plate models, however, are largely based on magnetic anomaly data averaged over ˜3 Ma or as little as 0.78 Ma [*DeMets et al.*, 2010] for the most recent models. Plate motions are also difficult to estimate in areas of low seismicity or near continental plate boundaries that lack no sea-floor spreading. To measure and estimate instant plate tectonic motion data that span a significantly smaller temporal window is required. Space-based

geodesy can measure very accurate (millimeter) positions on the surface of the earth over time spans of months to years, the most prolific of which is GPS. Velocities estimated from global positioning system data can be inverted (in a least squared sense) to derive Euler poles.

Euler poles from geodetic plate motion models are generally consistent with geologic plate models to within 95% confidence [*Sella et al.*, 2002]. Both geologic plate models [*DeMets et al.*, 2010, e.g.] and geodetic plate models [*Sella et al.*, 2002, e.g.] assumes that tectonic plates are rigid, in fact, citetsella02 excluded many GPS velocities near plate boundaries the capture non-rigid plate processes. In order to make use of this data models that includes the effects of block rotations and interseismic strain accumulation are required [*Meade and Hager*, 2005; *Apel et al.*, 2006]. The block model formulation implicitly enforces a path integral constraint that ensures that the relative plate motion is accommodated everywhere along the length of the plate boundary zone.

In this thesis I present GPS data from three tectonic regimes using a block modeling approach to incorporate both rigid block rotation and near-boundary elastic strain accumulation effects in a formal inversion of GPS velocities.

In Chapter 2, I test for independent Okhotsk and Amurian microplate motions using GPS velocities that constrain the plate kinematics of northeast Asia. Elucidating the current plate kinematics of the region is complicated by subduction-dominated deformation in the east and little differential plate motion in the west resulting in diffuse and sparse seismicity obfuscating the plate boundaries. Modeling favors scenarios with independent OKH and AMU motion, based on the application of F-test statistics. The plate-motion parameters of the independent plates are consistent with the kinematics inferred from earthquake focal mechanism solutions along their boundaries.

In Chapter 3, I use GPS-measured velocities (15 from continuously recording stations within the stable India plate interior) to geodetically constrain India plate motion, intraplate strain, and plate boundary deformation around the India plate. Dense station coverage from previously published studies allows rigorous testing of boundary parameterizations. I develop robust India plate motion parameters and see good agreement between predicted plate directions from the preferred model and the seismological data.

In Chapter 4, available GPS data in and around the Aegean region is combined and used to evaluate plate motion models, elastic plate boundary deformation and its relationship to seismogenic coupling along the Hellenic subduction zone. The A.D. 365 M ˜8.4, the A.D. 1303 M ˜8 Crete suggest that portions of the plate interface must be locked. My primary focus in this study is to examine potential upper plate deformation resulting from a locked subduction interface, active hanging-wall extension, or both. I consider multiple model scenarios in an attempt to interpret the both the horizontal and vertical geodetic signals in the region and its implications for earthquake hazard assessment.

Chapter 2

Okhotsk Plate Motion

2.1 Abstract

Independent Okhotsk and Amurian microplate motions are tested using velocities from 123 GPS sites (80 from within the proposed OKH and AMU plate boundaries) used to constrain the plate kinematics of northeast Asia. A block modeling approach is used to incorporate both rigid block rotation and near-boundary elastic strain accumulation effects in a formal inversion of the GPS velocities. Models include scenarios with and without independent OKH and AMU plate motion. Our modeling favors scenarios with independent OKH and AMU motion, based on the application of F-test statistics. The independent OKH plate rotates 0.231 deg/Myr clockwise with respect to North America about a pole located north of Sakhalin. The modeled AMU plate rotates 0.298 deg/Myr counterclockwise with respect to NAM about a pole located west of the Magadan region. The plate-motion parameters of the independent plates are consistent with the kinematics inferred from earthquake focal mechanism solutions along their boundaries.

2.2 Introduction

Northeast Asia is one of the last plate tectonic frontiers in the world. Boundaries between the North American (NAM) and Eurasian (EUR) plates are uncertain, and remain enigmatic due to the possible independent rotation of smaller microplates (such as the proposed Okhotsk, Amurian, and Bering microplates) within the broader plate-boundary zone. Elucidating the current plate kinematics of the region is further complicated by subduction-dominated deformation in the east and little differential plate motion in the west resulting in diffuse and sparse seismicity obfuscating the plate boundaries.

The possible existence of independently rotating Okhotsk (OKH) and Amurian (AMU) microplates has been examined by many in an attempt to explain both seismological and geologic data in Northeast Asia [*Cook et al.*, 1986; *Riegel et al.*, 1993; *Seno et al.*, 1996]. Geodetic measurements can be used to fully characterize the motion of tectonic plates; however, because most GPS sites in this region are in such close proximity to plate boundaries, previous attempts to confirm or refute an independent OKH plate have been inconclusive [*Heki et al.*, 1999; *Takahashi et al.*, 1999; *Steblov et al.*, 2003]. Establishment of independent AMU plate motion has remained as elusive because of the uncertainty of the southwestern plate boundary and fewer plate-interior GPS sites [*Petit and Fournier*, 2005].

Horizontal surface velocities of 123 GPS sites (80 from within the proposed OKH and AMU plate boundaries) allow for a rigorous test of the possibility of independent OKH and AMU plate motion. We use a block modeling approach to incorporate both rigid block rotation and near-boundary elastic strain accumulation effects in a formal inversion of the GPS velocities. We consider models that include scenarios with and without independent microplates.

2.3 Plate Boundaries

The first challenge in establishing a plate tectonic model of northeast Asia lies in defining the boundaries of the major and minor plates in the region. While some boundaries are well defined by active fault traces, youthful geomorphology, and abundant localized seismicity, others appear diffuse and ambiguous. We draw on the distribution and kinematics of 20th century seismicity, local geology and mapped faults, and the GPS velocity field itself to define our model block boundaries.

Figure 2.1 shows the seismicity of northeast Asia, dominated by subduction of the Pacific plate along Kamchatka and southward along the Kurile Islands and Japan. Seismicity in the north (Chersky range) and the west (Magadan region) is sparse and diffuse. Sakhalin Island exhibits large magnitude events that reflect both contractional and right-lateral faulting [*Kogan et al.*, 2003]. North of Sakhalin in the northeast Okhotsk Sea, seismicity is notably absent. West of Sakhalin, earthquakes become more frequent but substantially more diffuse along the Stanovoy Mountains. Active rifting is distinct through the Baikal region, although the distribution of earthquakes becomes substantially more diffuse through central Mongolia and northern China. Seismicity, while useful for examining plate boundary geometry and general deformation styles, does not provide a complete picture of the plate kinematics of the region. In areas of diffuse seismicity we augmented earthquake data with active fault maps [*Greninger et al.*, 1999], and other published boundary models [*Bird*, 2002; *Petit and Fournier*, 2005].

Finally, we use the constraints provided by the GPS velocity field itself to test variable geometries where the seismicity does not paint a clear picture of the plate boundary geometry. This allows us to refine the model geometry along the Kamchatka and Japan subduction zones and to test different plate boundary scenarios along the Sakhalin deformation

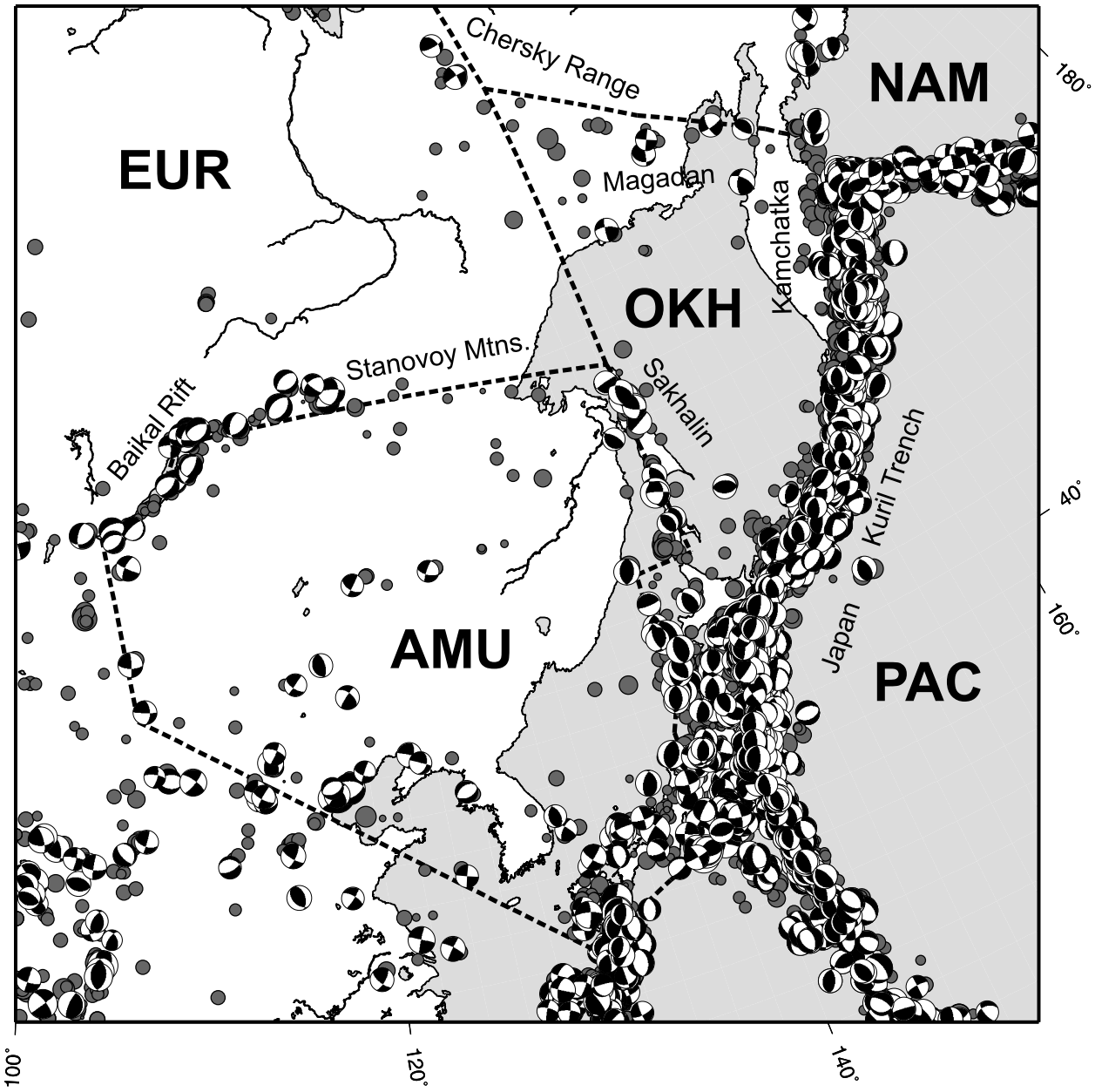

Figure 2.1. Seismicity of northeast Asia. Hypocenters (solid circles) are sized by magnitude and plotted to a depth of 35 km from the *Engdahl et al.* [1998] catalog. Focal mechanisms are from Harvard CMT catalog (http://www.seismology.harvard.edu/CMTsearch.html). Plate boundaries (dashed lines) are from this study.

zone. However, the lack of dense GPS coverage in Siberia and over the northeastern OKH crust precluded the boundaries in these regions from further improvement and from being significant in the block modeling.

2.4 GPS Velocities

The GPS velocities used in our inversion are from an updated velocity field of 151 global stations by *Steblov et al.* [2003]. We include observations from additional campaign stations from central Sakhalin [*Kogan et al.*, 2003] and the Kamchatka peninsula [*Bürgmann et al.*, 2005], and from 18 stations in northern Japan that are part of the continuous network (GEONET) operated by the Geographical Survey Institute. Details of the data analysis using GAMIT/GLOBK are given in *Steblov et al.* [2003].

In addition to our own analysis we included from published work GPS velocities that help to define the deformation patterns for the Baikal and central AMU regions [*Calais et al.*, 2003] and selected stations from *Zhang et al.* [2004] that fell within or near the boundaries of the proposed AMU microplate. We integrated these velocities into the reference frame of our own solutions by estimating translation and/or rotation parameters that minimized the differences in horizontal velocities for common sites. 123 sites were selected from the combined solution for our inversion including locations within the 'stable' plate interiors of the Pacific, North American, and Eurasian plates (Table A.1). Velocities in our area of interest are shown in Figure 2.2.

2.5 Block Modeling

Testing for independent plate rotation is accomplished by determining a best-fit pole of rotation on a spherical earth that matches surface velocities for sites that lie within a 'stable' plate interior [e.g., *Larson et al.*, 1997; *Sella et al.*, 2002]. However, regions like northeast Asia require a more sophisticated approach because many (if not all) of the measured velocities contain components of both rigid block motion and plate boundary strain. By modeling plate boundary deformation at block edges we can separate the velocity contribution from elastic strain accumulation from the rigid block motion and test for independent plate motion [e.g., *Matsu'ura et al.*, 1986; *McCaffrey et al.*, 2000a].

Our approach combines aspects from the above mentioned studies by defining our plates as rigid blocks in a spherical framework bounded by dislocations in an elastic halfspace [*Okada*, 1985]. We invert for poles and rates of rotation for each block using the block modeling code by *Meade and Hager* [2005] that implements our approach by minimizing the misfit to the GPS velocities. The segments that bound the blocks represent uniformly slipping elastic dislocations locked to some specified depth. Because our inversion combines rigid block rotation with elastic strain accumulation effects, the parameterization of the block

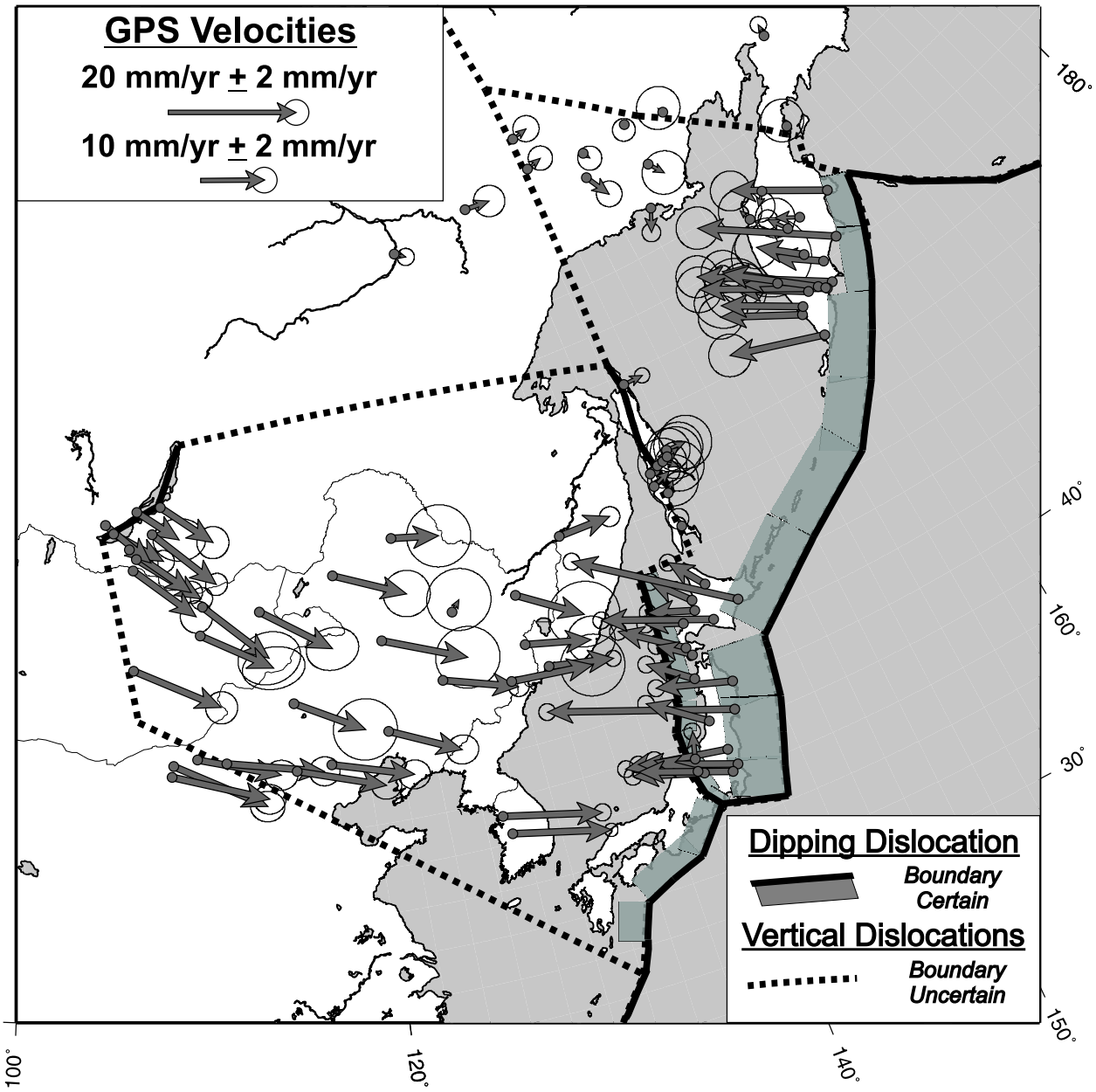

Figure 2.2. Combined GPS velocities from continuous, campaign, and published data. 90 of the 123 velocities are shown here in a fixed North American reference frame. The remaining far field sites are outside the range of the figure and can be seen in Figure 2.3. Plate boundaries shown in this figure reflect their geometry and certainty.

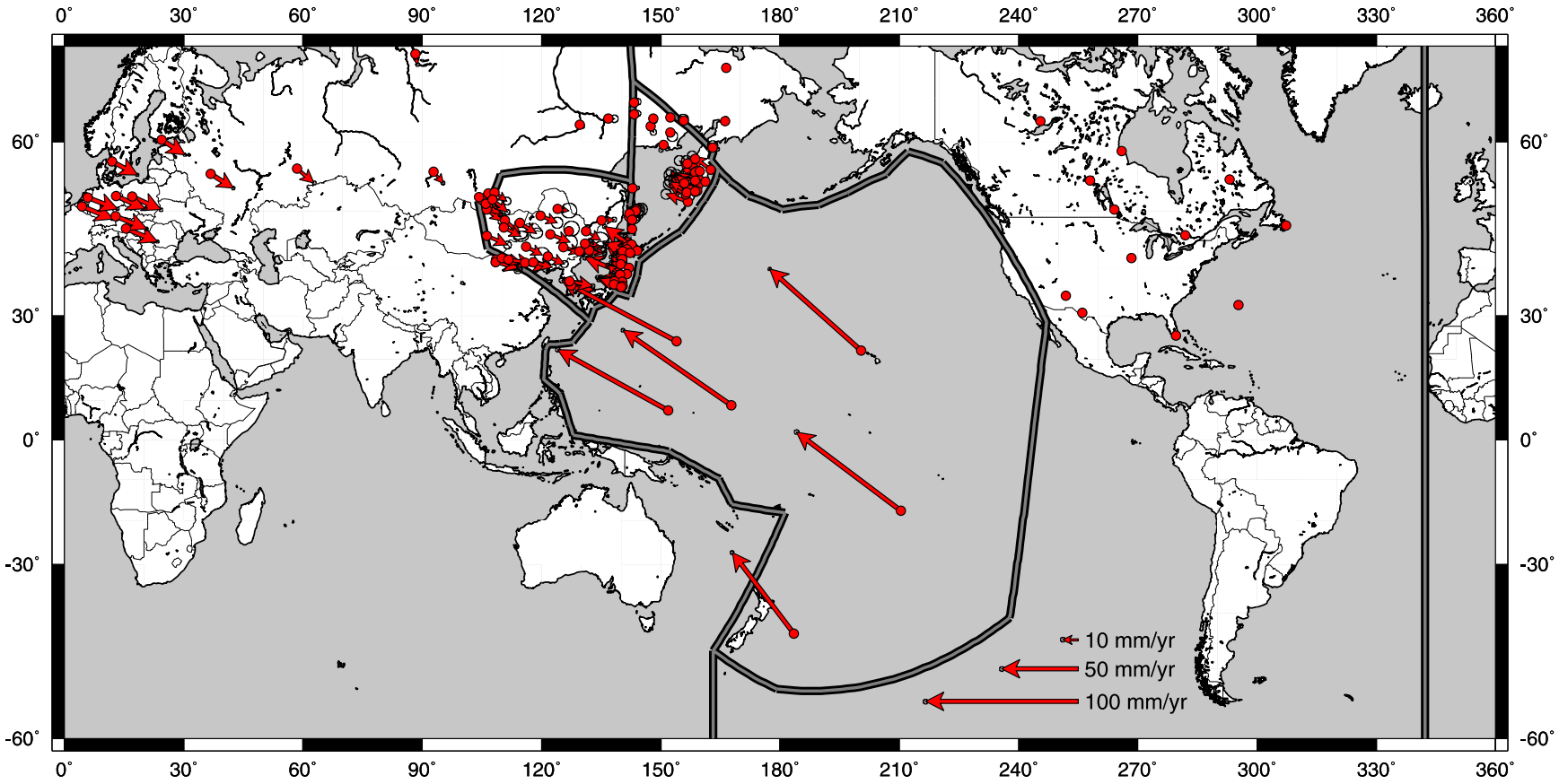

Figure 2.3. 123 global GPS velocities, shown in a fixed North American reference frame with 1 sigma uncertainty ellipses. Plate boundaries are from the 5-plate model and include the Pacific, North American, Eurasian, Amurian, and Okhotsk plates.

boundary geometry is critical for GPS measurements located within several locking depths of the block boundary. Geometry of the block boundaries is based heavily on seismicity (as discussed in section 2.3), adopted from prior analyses [*Mazzotti et al.*, 2000; *Bürgmann et al.*, 2005; *Toya and Kasahara*, 2005] or adjusted as indicated by the geodetic data [*Kogan et al.*, 2003].

Subduction zones are represented by discrete dipping dislocations locked to ˜40 km depth (see Table B.2 for complete individual block segment parameters) and allowed to accommodate both strike-slip and dip-slip motion. Diffuse boundaries surrounding the OKH region in the northern and western edges are not manifested as discrete fault zones. With the exception of the Baikal region, the AMU region is also bounded by zones of distributed and complex faulting. These plate boundary deformation zones are represented in our model by vertical dislocations locked to depths of 70 km that are allowed both strike-slip and opening motions. Seventy percent of the displacement gradient across such boundaries is distributed across a distance equivalent to two locking depths.

We invert the horizontal GPS velocities for poles of rotation constrained by the prescribed block geometry. Systematic patterns in the residual velocities (observed minus predicted) are used as an indicator of where and how the model matches the observed surface velocities. Misfit statistics are used to formally evaluate the statistical significance of the plate kinematic scenarios we test.

2.6 Results

Independent OKH plate motion is tested using three main block configurations. In our 3-plate model we include the NAM, EUR, and Pacific (PAC) blocks. We assume that the Okhotsk region is part of the NAM plate and Amuria belongs to Eurasia [*Steblov et al.*, 2003]. Our 4-plate model allows the OKH block to rotate independently while the 5-plate model includes an additional independently rotating AMU block. We then compare the misfit of each inversion to test for significance using F-statistics [*Stein and Gordon*, 1984]. The chi-squared statistics are summarized in 2.1.

Our 3-plate model shows a clear, systematic pattern of residual velocities that suggests independent OKH plate motion (Figure 2.4). In our 4-plate model the improvement in fit measured by the chi-squared misfit for the OKH sites is reduced from 786.2 to 476.7 (Table 2.1). The calculated F-statistic between the 3-plate and the 4-plate model is 51.97, well above the 99% confidence level of 3.87. Rotation vectors calculated from our optimized 4-plate inversion, suggest the OKH block rotates 0.231 ± 0.013 deg/Myr clockwise, with respect to NAM, about a pole located north of Sakhalin (Figure 2.5).

The addition of an independently rotating AMU block in our 5-plate inversion reduces the misfit by rotating counterclockwise about a pole of rotation west of the Magadan region at 0.289 ± 0.017 deg/Myr. Our 5-plate model shows a decrease in the chi-squared misfit from the 4-plate system by reducing the misfit of AMU sites from 105.1 to 53.9 (Table 2.1).

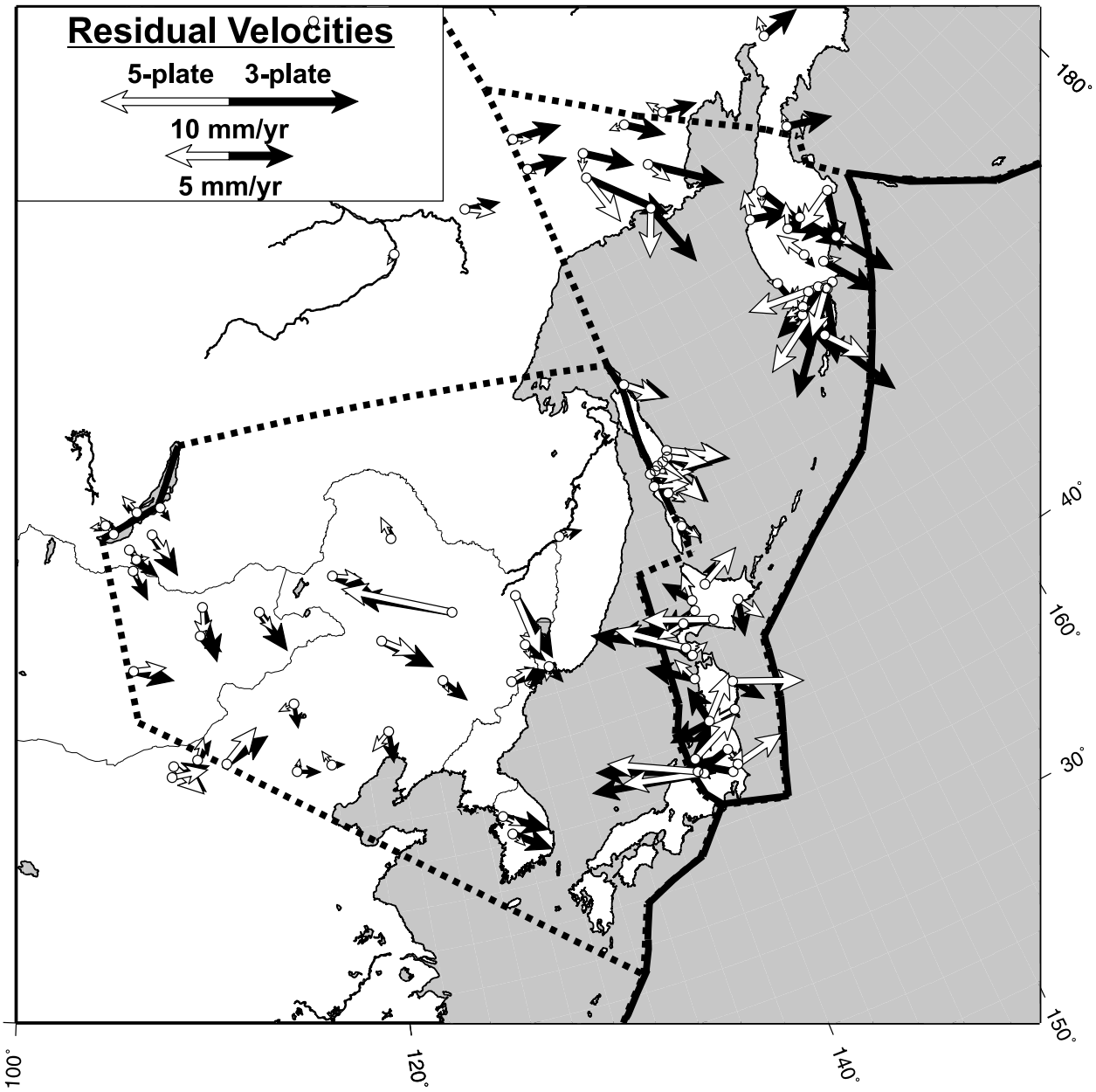

Figure 2.4. Residual velocities from the 3-plate model (NAM, EUR, and PAC) are shown in black; residuals from the 5-plate model are shown in white. Residuals are greatly reduced with additional independently rotating Okhotsk and Amurian plates.

Table 2.1. Statisitical Summary of block models

BLOCKS	**3**		**4**		**5**	
	n	χ^2	**n**	χ^2	**n**	χ^2
EUR	24	79.7	24	46.2	24	31.7
AMU	32[a]	115.7	32[a]	105.1	32	53.9
NAM	13	89.9	13	15.1	13	15.1
OKH	48[b]	786.2	48	476.7	48	499.7
PAC	6	14.3	6	8.5	6	8.4
Total	123	1086	123	652	123	609

[a] *In the 3 and 4-block model AMU sites are assumed to be on EUR.*

[b] *In the 3-block model OKH sites are assumed to be on NAM.*

The calculated F-statistic between the 4-plate and the 5-plate model is 30.17, above the 99% confidence level of 2.88.

Our inversions favor a scenario with both independent OKH and AMU plate motion, based on the application of F-test statistics. The improvement in the fit to the data is significant well above the 99% confidence limits for both plates.

2.7 Discussion and Conclusion

The plate-motion parameters of independently rotating OKH and AMU plates are consistent with the style of active deformation inferred from focal mechanism solutions. For example, our inversions predict right-lateral motion in northern Sakhalin, oblique contraction in southern Sakhalin, and little to no active deformation in the sub-marine crust north of Sakhalin. Predicted rifting in the Baikal region is also consistent with historical seismicity and active structures.

Calais et al. [2003] estimate opening in the Baikal rift zone at 4 ± 1 mm/yr, consistent with our estimate of 3 ± 1 mm/yr (Figure 2.5). Oblique contraction in southern Sakhalin is observed in the seismicity [*Kogan et al.*, 2003] and consistent with our estimates of right lateral (2 ± 1 mm/yr) oblique contraction (14 ± 2 mm/yr) in the same region (Figure 2.5). Further south, along the western Japanese backarc, the convergence rates increase from to ˜15-19 mm/yr (EUR-NAM) in our 3-plate model to ˜19-28 mm/yr (AMU-OKH) in the 5-plate model (Figure 2.5). Calculated slip rates from our model also suggest left-lateral slip along the northern boundary (Ulakhan fault) of the OKH plate at rate of 3 ± 1 mm/yr (Figure 2.5). *Hindle et al.* [2006] suggest left-lateral slip rates along this fault as high as

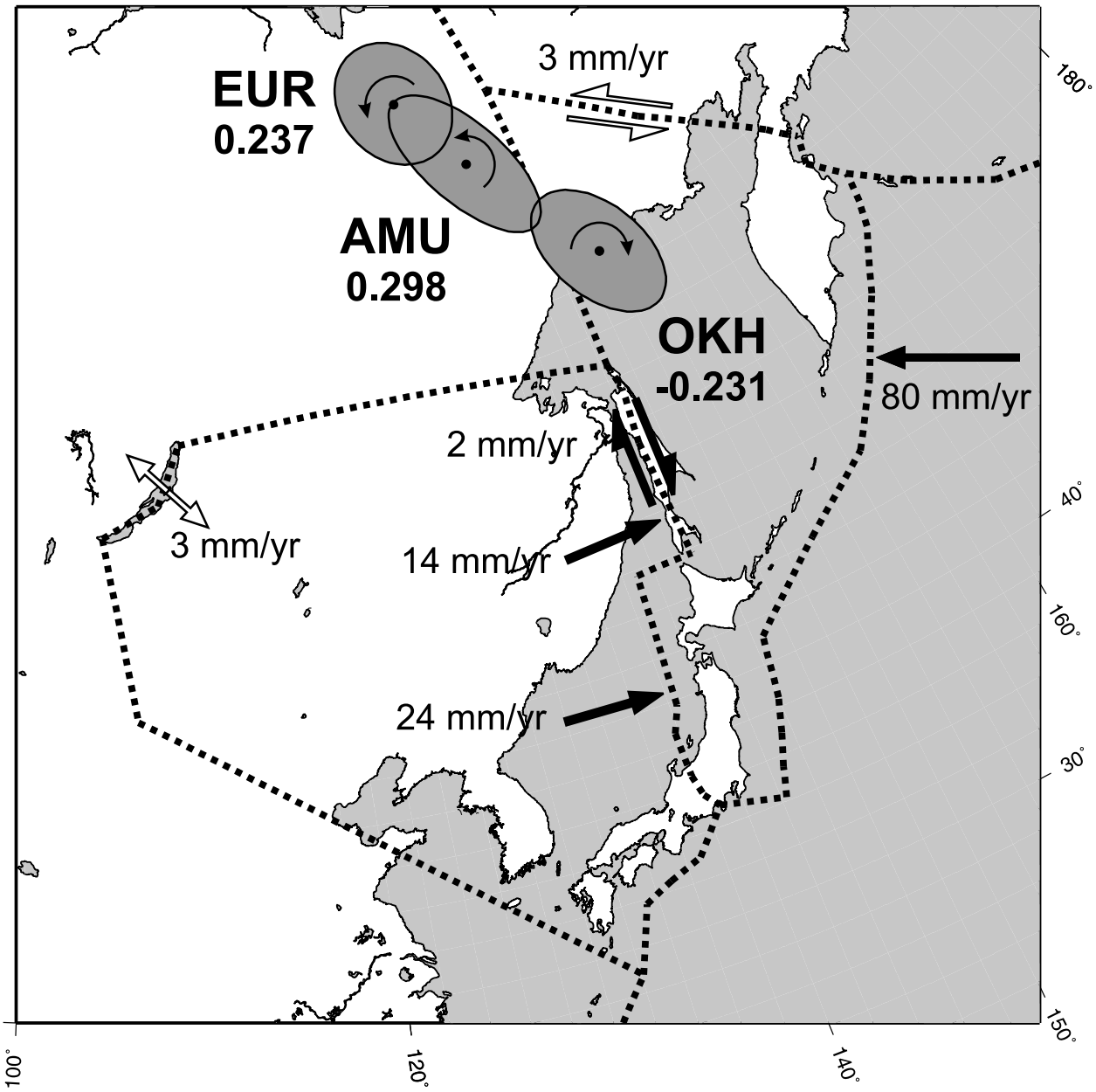

Figure 2.5. Rotation rates are in degrees per million years with a positive counterclockwise convention. Error ellipses show 95% confidence limits. Selected slip rates from the 5-plate model are consistent with previous studies.

5.5 mm/yr, similar to our estimates, although the complexities of continental deformation in this region may be under modeled.

Poles of rotation for the OKH plate derived from focal mechanisms [*Cook et al.*, 1986] predict a counter-clockwise rotation with respect to North America about a pole located in northern Siberia. *Seno et al.* [1996] predict a counter-clockwise rotation of 0.195 deg/Myr with respect to North America about a pole located east of Hokkaido. More recent geodetic global plate motion models [*Sella et al.*, 2002], using 5 GPS velocities from the plate interior, predict an OKH plate rotating counter-clockwise 0.305 deg/Myr about a pole of rotation in the Sea of Okhotsk just south of the Magadan region. These poles are consistent with the ones calculated in this study (see Figure 2.6 and Table 2.2 for a full summary of published poles.)

The systematic pattern of residual velocities in our 3-plate model is evident regardless of subtle changes made in each block model iteration (Figure 2.4). This pervasive systematic pattern is the most convincing evidence for an independently rotating OKH plate. In the absence of an independently rotating OKH block, residual velocities of 3-5 mm/yr show a clear rotational pattern about a point north of Sakhalin Island. Independently rotating OKH and AMU blocks are statistically significant above the 99% confidence level and consistent with the deformation types inferred from earthquake focal mechanism solutions along their boundaries.

2.8 Acknowledgments

We would like to thank Mikhail Kogan for his invaluable help in the collection and processing of the GPS data as well as insightful discussions. The manuscript benefited from helpful reviews and suggestions from Kaz Fujita and Kosuke Heki. Data collection and processing in east Asia was supported by following grants to Columbia University: NSF grants EAR-0106002, EAR-0408971, and EAR-0530965, JPL grant 1203235, and IRIS grant 311 as well as Berkeley Seismological Laboratory contribution 06-05.

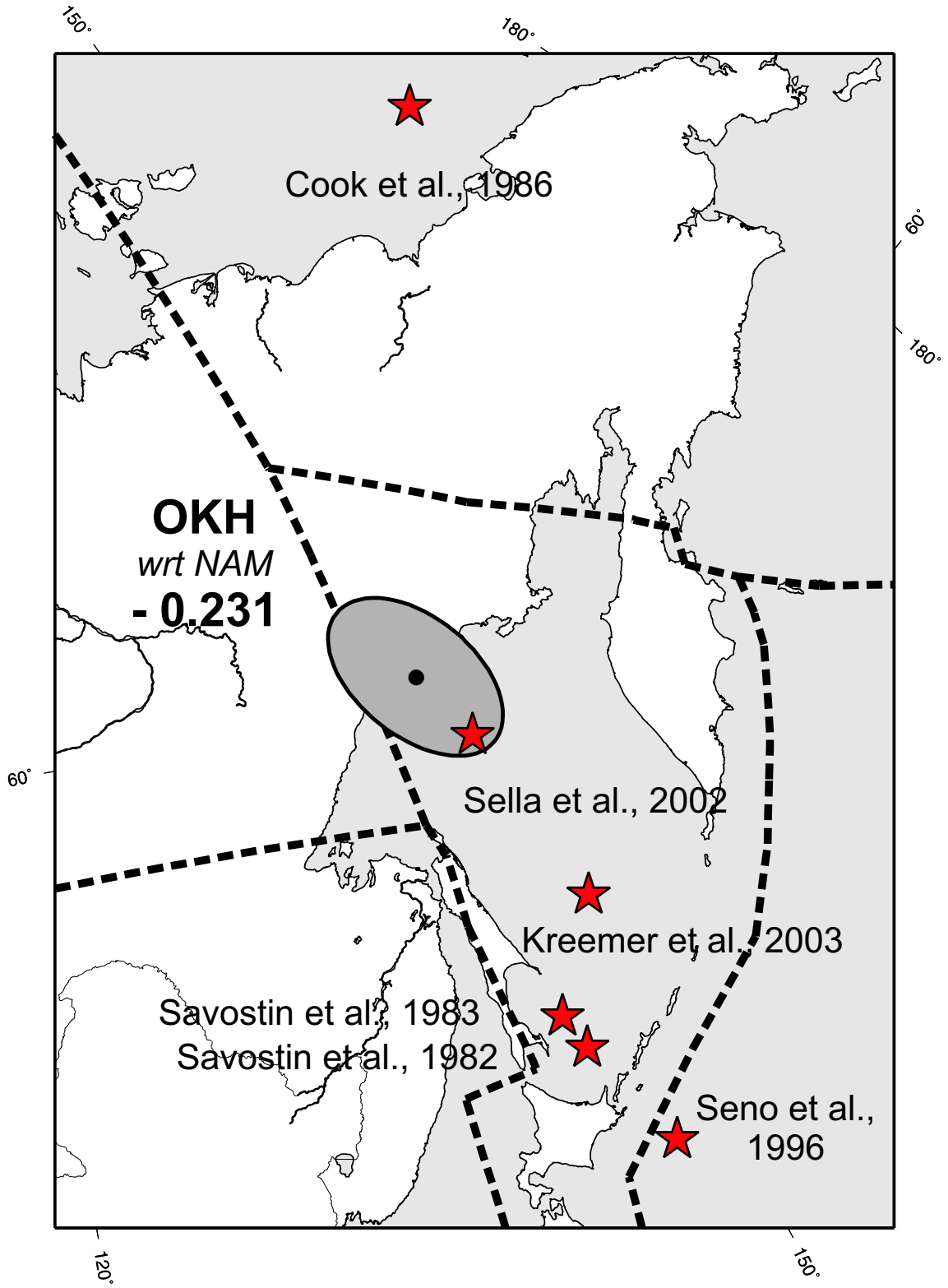

Figure 2.6. Pole of rotation for the Okhotsk plate shown with respect to North America with linearly propagated 2 sigma error ellipse. Stars show the locations of previously published Okhotsk poles.

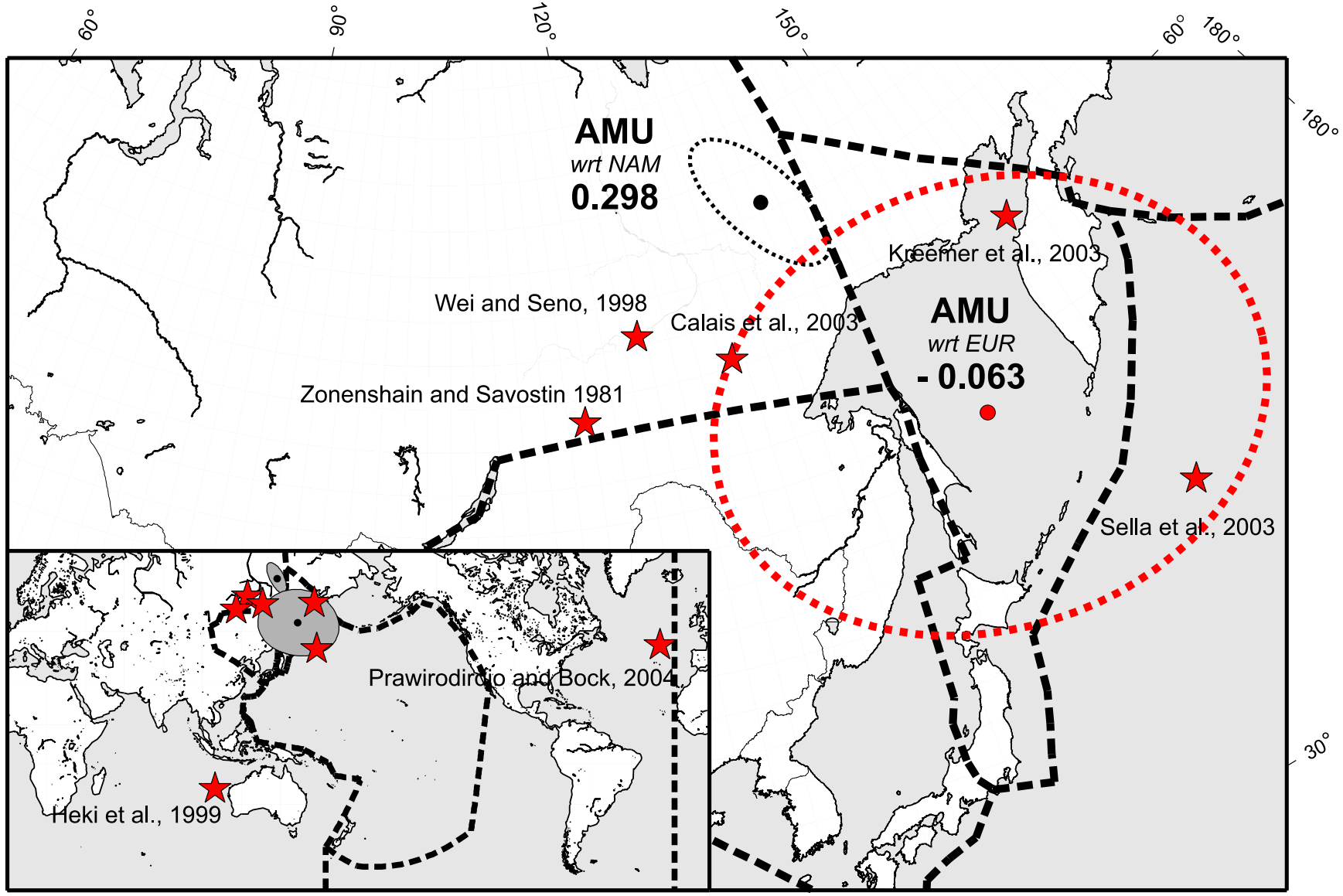

Figure 2.7. Poles of rotation from this study for the Amurian plate shown with respect to Eurasia and North America with linearly propagated 2 sigma error ellipses. Stars show the locations of previously published Amurian-Eurasian poles.

Table 2.2. Poles of rotation for the Okhotsk and Amurian plates from published work.

Pole	Lat	Long	deg/Myr	Error	Maj	Min	Azimuth	Source
NAM-OKH	45.8	145.3	0.41	**NR**	**NR**	**NR**	**NR**	Savostin et al., 1982
NAM-OKH	47.09	144.85	0.478	**NR**	**NR**	**NR**	**NR**	Savostin et al., 1983
NAM-OKH	72.4	169.8	**NR**	**NR**	**NR**	**NR**	**NR**	Cook et al., 1986
NAM-OKH	41.71	147.33	0.195	**NR**	39.93	13.37	81.8	Seno et al., 1996
NAM-OKH	56.65	147.01	0.305	0.121	11.8	1.7	18	Sella et al., 2002
NAM-OKH	50.36	148.7	-0.939	**NR**	**NR**	**NR**	**NR**	Kreemer et al., 2003[a]
NAM-OKH	59.04	344.4	-0.231	0.013	1.299	0.760	155.6	This Study
AMU-EUR	56.95	117.45	0.100	**NR**	**NR**	**NR**	**NR**	Zonenshain and Savostin, 1981
AMU-EUR	60.42	123.25	0.025	**NR**	**NR**	**NR**	**NR**	Wei and Seno, 1998
AMU-EUR	-22.3	106.6	-0.091	0.016	20.5	3.5	19.3	Heki et al., 1999
AMU-EUR	58.36	130.968	0.143	**NR**	**NR**	**NR**	**NR**	Calais et al., 2003
AMU-EUR	44.18	158.76	0.107	0.1	33.3	6.6	88	Sella et al., 2002
AMU-EUR	45.433	-25.253	0.093	0.023	43	4.4	171	Prawirodirdjo and Bock, 2004
AMU-EUR	58.8	157.5	0.034	0.013	5.5	3.4	-87	Kreemer et al., 2003
AMU-EUR	51.626	148.350	-0.063	0.017	5.311	4.201	99.1	This Study

NR = *Not Reported*

[a] *Not reported. This pole was calculated from other published poles.*

Chapter 3

Indian Plate motion, deformation, and plate boundary interactions

3.1 Abstract

We use 668 GPS-measured velocities to geodetically constrain India plate motion and intraplate strain, and we examine plate boundary deformation and plate interactions around the India plate. Our solution includes 15 GPS velocities from continuously recording stations from within the stable India plate interior that are used to estimate the angular velocity of the India plate with respect to its neighbors. We test a two-plate India system divided along the topographically prominent Narmada Son lineament and find this scenario predicting up to 4 mm/yr contraction across the lineament to be significant only to 89% confidence. Dense station coverage along the Himalayan range front allows us to rigorously test boundary parameterizations and develop a preferred plate boundary model with variable locking width along the arc, distributed block motions across Tibet, and considering an independent Shillong block. In our preferred model the Himalayan Range Front accumulates ˜50% of the India-Eurasia convergence with as much as 22 mm/yr of slip accumulation along some segments. We compare earthquake slip vector orientations with predicted divergence directions from our preferred model along the India-Somalia plate boundary. We see good agreement between predicted plate directions from our preferred model and the seismological data. Deviations between our model and the slip vectors highlight areas of diffuse oceanic deformation along the plate boundary. GPS measurements of India-Australia motions are consistent with geologic models that assume an independent Capricorn microplate. We estimate convergence vectors for the relative plate pairs along the Sumatra subduction zone. We test for the transition between Australia plate convergence and India plate convergence

along the Sumatra subduction zone and refine the estimated motion of the Burma sliver plate.

3.2 Introduction

The Middle and Far East (centered around India) are a complex region of actively deforming plate boundary zones. With the exception of some discrete mid-ocean ridges in the western Indian Ocean, the India plate is bounded by zones of broadly distributed active deformation. The most widely distributed plate boundary in the world is actively deforming as continental India continues to collide with Eurasia. Beginning at the India plates northern edge, along the Himalayan Range Front, active deformation extends through Tibet and into China, Mongolia, and as far north as Russia. Along Indias eastern flank the subduction of the India plate under the Burma plate in the Andaman-Nicobar Islands region was the source area of most of the 2004 M_W 9.2 Sumatra earthquake rupture. To the south the transition between the India plate and the Australia plate is uncertain as seismicity is dispersed over thousands of kilometers and shows no distinct trends that highlight an obviously distinct boundary. Along Indias western plate boundary, the Central Indian Ridge, the Carlsberg Ridge, and Owen Fracture zone discretely separate the India plate from the Somalia and Arabia plates through a series of spreading centers and transform faults manifested clearly in seismicity trends and bathymetry (Figure 3.1). It has been difficult to rigorously characterize the kinematics of many of these active boundaries due to the lack of robust angular velocity estimates for the India plate and the complex kinematics of smaller microplates involved in the deformation. Using a comprehensive GPS velocity field of 668 stations we determine the motion of India with respect to its neighbors, quantify deformation within the India plate, and explore the magnitude, nature, and distribution of deformation along the plate boundaries of the India plate. We focus on illuminating the pattern of brittle upper crustal deformation in these actively deforming plate boundary zones, within the context of simple block models that use measured interseismic GPS velocities to estimate the rotations of rigid blocks and elastic strain fields near locked block-boundary faults.

A number of models in recent years have attempted to explain the observed GPS velocities within the Eurasia-India collision zone. End member models include continuum interpretations or fluid-like models[*Zhang et al.*, 2004; *England and Molnar*, 2005, e.g.] and rigid block models [*Thatcher*, 2007; *Meade*, 2007; *Loveless and Meade*, 2011, e.g.], however discriminating one from the other still remains a challenge. We adopt the block modeling methods of the latter type of models to parameterize the Eurasia-India collision zone and the entire study area. Deformation in the upper crust is generally by brittle faults that often define crustal blocks and tectonic plates. Due to the tectonic size of the blocks defined in this study and the relatively dense station spacing this block model approach is appropriate. This is, in large part, due to the fact that the scope of this analysis and paper is focused on describing the deformation (rate and sense of fault slip) of the upper crust with respect to plate kinematics. We do not attempt to address the full problem of relating the inferred

kinematics of fault-bounded crustal blocks to the underlying dynamics and driving forces [*McCaffrey et al.*, 2000a; *Flesch et al.*, 2001; *Copley et al.*, 2010; *Loveless and Meade*, 2011].

3.2.1 Geologic Plate Motions

Conventionally, instantaneous India plate motion has been estimated using closed plate circuit models and summing motions across mid-ocean ridges constrained by magnetic lineations, transform fault strikes, and earthquake focal mechanisms [*DeMets et al.*, 1990, 1994]. In more recent revisions to the plate circuit models *DeMets et al.* [2005], *Royer et al.* [2006], and *DeMets et al.* [2010] separate Somalia from Nubia (formally the Africa plate) reducing the predicted India-Eurasia convergence rates by ˜12% from previous estimates that include Nubia and Somalia as one single plate. India plate motion slowed between 20 Ma to 10 Ma as the Himalayas and Tibetan Plateau grew and appears constant since ˜8 Ma [*DeMets et al.*, 2005; *Merkouriev and DeMets*, 2006]. The updated plate motion models more closely match geodetic plate motion estimates derived from GPS measurements (discussed in section 3.2.2).

Likely forces that drive India plate motion are edge forces (ridge push and slab pull) and basal tractions from relative motions with respect to the underlying mantle at the base of the plate [*Cloetingh and Wortel*, 1985; *Copley et al.*, 2010]. The gravitational potential of the Tibetan Plateau may also play an important resisting role to northward motion of India [*Flesch et al.*, 2001; *Copley et al.*, 2010, e.g.]. In this paper we examine plate boundaries where these forces act and rigorously characterize plate boundary processes and deformation. The style and magnitude of the deformation may have implications for potential plate tectonic driving forces, particularly in areas with complex plate interactions (e.g Capricorn plate boundaries) (Figure 3.2) or areas of diffuse continental deformation (Tibetan Plateau) where plate boundaries are not well characterized. However, we constrain the scope of this paper to the kinematic analyses of the tectonic plates and plate boundary interactions.

3.2.2 Geodetic Plate Motions

Recent geodetic estimates of India plate motion [*Paul et al.*, 2001; *Sella et al.*, 2002; *Prawirodirdjo and Bock*, 2004; *Socquet et al.*, 2006a; *Bettinelli et al.*, 2006; *Kogan and Steblov*, 2008, e.g.] used GPS velocity vectors to calculate a pole of rotation that suggests India-Eurasia convergence rates are ˜10% slower than geologic estimates spanning the last 3 Ma [*Royer et al.*, 2006] or the last 0.78 Ma [*DeMets et al.*, 2010]. The geodetic Euler pole location estimates vary (Table 3.1), in part because data from only two continuous India GPS sites (IISC, HYDE) were used. For example, *Socquet et al.* [2006a] estimate an India-Eurasia geodetic pole using these two sites in addition to four stations in southern Nepal (MAHE, NEPA, BHAI, and SIMR) which they assume record velocities representative of rigid India plate motion. Their predicted India-Eurasia convergence rates are ˜5 mm/yr slower along the Himalayan front than those presented in [*Paul et al.*, 2001], who also used data from 12 campaign GPS stations distributed across the southern subcontinent. [*Kogan and Steblov*,

2008] use DGAR, DHAK and MALD in addition to IISC and HYDE to define stable India plate motion. They assign DGAR, which is located close to the India-Capricorn plate boundary zone to the India plate, which does not change their angular velocity estimates within a significance level of 95%. Their estimates for IND-EUR plate motion are in good agreement with previously published geodetic poles (Figure 3.3). In this paper, we incorporate new data [*Banerjee et al.*, 2008] spanning a larger portion of the stable India plate than previous studies. Our solution includes data from 29 continuously recording stations in India, including 15 that are located well within the India plate. The new data provide robust constraints for estimating plate boundary motion between India and its neighboring plates.

3.2.3 India Intraplate Deformation

Intraplate seismicity exists across central India. It may be related to flexure of the plate as it is thrust below Tibet [*Bilham et al.*, 2003], high compressive stresses adjacent to the India-Eurasia collision zone, or, in the case of the Mw 7.7 Bhuj earthquake, an extension of diffuse plate boundary deformation (possibly involving an independent Sind microplate) that extends from the Ornach-Nal and Chaman faults through the eastern Sulaiman range front to Bhuj [*Stein et al.*, 2002].

A prominent topographic feature (Narmada-Son lineament) cuts through central India (Figure 3.2). This paleo-rift zone [*Jain et al.*, 1995] exhibits high heat flow levels and strain rates estimated from seismicity that are larger than many stable continental regions [*Rao*, 2000]. This suggests a potential concentration of intraplate deformation or the kinematic separation of India into two distinct plates. It is possible that the seismicity in the region is also enhanced by a thinned and weakened lithosphere due to passive-margin normal faulting in the Cretaceous [*Biswas et al.*, 2007] and by heating from the plume head responsible for the late Cretaceous Deccan flood basalts [*Kennett and Widiyantoro*, 1999; *Chandrasekhar et al.*, 2009]. Here we thoroughly evaluate geodetic evidence of active intraplate deformation within the India plate interior from the GPS data.

The Shillong plateau in Northeast India exhibits considerable north-south shortening supported by the existence of large earthquakes such as the great (M_W 8.1) Assam earthquake of 1897 [*Bilham and England*, 2001]. In addition detailed analysis of moderate earthquakes in the same region is also consistent with the north-south shortening [*Angelier and Baruah*, 2009]. Exhumation rates deduced from low-temperature chronometric data suggest a convergence rate of 13 mm/yr across the plateau, since 9 Ma [*Biswas et al.*, 2007; *Clark and Bilham*, 2008]. GPS data in the Shillong Plateau region also show contraction with respect to stable India [*Jade et al.*, 2007; *Banerjee et al.*, 2008]. We separate the Shillong Plateau from India as its own microplate and test its statistical significance using F-statistics. We use the Shillong blocks angular velocity to estimate slip rates along its boundaries.

3.2.4 Our Analysis

We present a robust tectonic India plate model that includes a high quality network of GPS stations from within the Indian continent and across its plate boundaries that is well distributed spatially [*Banerjee et al.*, 2008]. We model newly processed GPS velocities and velocities from published sources (see section refsec:pubsol) in a block modeling approach to incorporate both rigid block rotation and a first-order model of near-boundary elastic strain accumulation effects in a least squares inversion of the GPS velocities. We simplify boundary parameters (geometry and locking characteristics) along plate boundaries and within actively deforming zones in order to constrain large-scale motions on crustal-scale faults and other structures. The robust angular velocity estimates for Eurasia, Australia, Sunda, and India allow for the rigorous testing of variable plate boundary geometries and consideration of models that include smaller microplates within the plate boundary zones. These models allow us to test for independent microplate rotations and further illuminate patterns in the interseismic strain accumulation along Indias plate boundaries including the Sumatra subduction zone and the Himalayan range front.

3.3 India Plate Boundaries

Tectonic plates are often modeled as rigid blocks with discrete boundaries. Global plate models [*DeMets et al.*, 1990; *Sella et al.*, 2002; *DeMets et al.*, 2010, e.g] regardless of data source, explain crustal motions well within this simple paradigm. More complex models parameterize plate boundaries, marked by zones of deformation, using a series of rigid blocks with more distributed deformation (typically elastic) occurring along the edges that span the boundary zone [*Meade*, 2007, e.g.]. This increased complexity of bounding rigid blocks with elastic dislocations has been useful for interpreting geodetically measured, interseismic crustal deformation data by providing context for far field plate rates while simultaneously estimating slip rates along localized structures.

The India plate and its boundaries provide a unique opportunity to fully characterize plate boundary deformation around an entire plate. The collection of geologic slip rates and earthquake sources in and around the India plate allow us to compare our model derived from geodetic data with geologic and seismological data in the context of one plate tectonic construct. In the following sections, we will circumnavigate the India plate in a counterclockwise direction examining each of the plate boundary deformation zones in turn.

3.3.1 West: Ocean ridges and transforms

To the west, the Owen fracture zone separates India from the Arabia plate. This fracture zone marks the northernmost oceanic India plate boundary. The Owen fracture zone is a dextral transform fault zone [*Fournier et al.*, 2008] that connects with the Dalrymple Trough

[*Gordon and Demets*, 1989] which intersects the Makran subduction zone at the diffuse triple junction of the India, Arabia, and Eurasia plates. The southern extent of the Owen fracture zone terminates at the India-Arabia-Somalia triple junction. South of the Owen fracture zone, the India plate is separated from the Somalia plate along a mid-ocean ridge. This boundary is completely submarine defined by the Carlsberg Ridge and the Central Indian Ridge (Figure 3.2) highlighted by discrete seismicity (Figure 3.1), sea floor ridges, young crust, and rift-orthogonal transform faults. Here we compare the orientations of relative plate motions derived from slip vectors of transform and normal-faulting earthquakes with slip orientations predicted by our model in an effort to explore in more detail the transition from India to Australia plate motion.

3.3.2 South: Diffuse India-Australia deformation

Around 4° S, the Carlsberg Ridge meets the northern edge of a broad region of oceanic lithosphere that is actively deforming between the adjoining India and Australia plates [*Wiens et al.*, 1985; *Drolia and DeMets*, 2005] (Figure 3.1). *Delescluse and Chamot-Rooke* [2007] thoroughly analyzed this plate boundary zone by exploiting seismological data, far field GPS velocities and heat-flow data, and conclude that the region appears to be neither rigid India plate nor rigid Australia plate. They also conclude that while the Ninetyeast Ridge represents a clear strain discontinuity, the separation between the India and Australia plate is not discrete. The broad plate boundary zone (shaded region in Figure 3.2) may involve an independently rotating Capricorn plate identified from magnetic anomaly data [*DeMets et al.*, 2005, and references therein] and indirectly using geodetic data *Gordon et al.* [2008]. As a result of this diffuse deformation the Sumatra subduction zone, south of the Andamans, may mark the edge of either the India or Australia plate, as described in sections 3.3.1 and 3.3.3. We further explore the distribution of strain in this deformation zone where it interacts with the western plate boundaries and potential Capricorn plate motion.

3.3.3 East: Arakan-Andaman-Sumatra

Along the eastern boundary of the India plate, south of the Shillong Plateau, is the northwest-southeast striking Arakan Trench and sub-parallel right-lateral Sagaing [*Ledain et al.*, 1984; *Bertrand et al.*, 1998] fault zone. The active Andaman subduction zone is the southern extension of the Arakan Trench that separates the India plate from the Burma microplate. The small, narrow Burma microplate is sandwiched between the India plate and the Sunda plate (Figure 3.2). This sliver plate [*Jarrard*, 1986; *McCaffrey et al.*, 2000b] is bounded to the west by the Sumatra subduction zone and to the east by the strike-slip Great Sumatra Fault (GSF). The extension of the GSF north of Sumatra is a series of stepping transform and oceanic ridge segments in the Andaman Sea that connect to the Sagaing fault in Myanmar [*Curray*, 2005, and references therein]. The subduction of both the India and Australia plates under the Burma microplate is the cause for megathrust events like the M_W 9.2 Sumatra-Andaman Island earthquake of 2004. Accurate convergence

rates across the Sumatra subduction zone and displacement rates of the Burma microplate are important for recurrence rate estimates in light of the2004 earthquake. Previous studies have not always clearly defined which plate rate was (or should be) used for interseismic strain rate estimates along this boundary [*McCaffrey et al.*, 2000a; *Chlieh et al.*, 2008, e.g.]. We update the Sunda and Burma angular velocities and interseismic strain accumulation estimates across the Sumatra-Andaman subduction zone. We explore the possibility and implications of either India or Australia plate subduction beneath Sumatra and the effects of both on partitioning between the megathrust and the GSF.

3.3.4 North: Himalayan-Tibet

The most notable expression of the India-Eurasia plate boundary zone is the Main Frontal Thrust along the Himalayan Range Front. To the east, the frontal thrust appears to terminate in the Eastern Himalayan Syntaxis, north of the Shillong Plateau, as deformation becomes more distributed [*Avouac*, 2008] and the plate boundary between India and Eurasia becomes less distinct. North of the Main Frontal Thrust the India plates collision with Eurasia is manifested in the actively deforming Himalayan mountain range with most of the remaining deformation occurring along faults across the adjoining Tibetan Plateau [*Tapponnier and Molnar*, 1979; *Zhang et al.*, 2004, e.g.]. Estimates of India-Eurasia convergence rates range from 32 to 45 mm/yr from west to east [*Royer et al.*, 2006; *Paul et al.*, 2001; *Sella et al.*, 2002, e.g.] with potentially as much as 20 mm/yr accumulating at the range front itself [*Jade et al.*, 2004; *Lave and Avouac*, 2000; *Larson et al.*, 1999, e.g.]. The remainder is partitioned to the north across intracontinental faults (e.g. Kunlun Fault, Haiyuan fault, Altyn Tagh Fault) that cut the Tibetan Plateau [*Tapponnier et al.*, 2001; *Cowgill et al.*, 2003]. We evaluate the rates of underthrusting along the Himalayas in a block model that allows us to consider the roles of the geometry and locking width of the Himalayan megathrust and the complex kinematics of internal deformation of Tibet. In addition, we consider a Shillong microplate, bounded by the Dauki fault to the south and the Oldham fault to the north [*Biswas et al.*, 2007], providing the means to more rigorously determine geodetic fault slip rates along its major bounding fault zones and establish the nature and degree of partitioning that the Shillong block imparts on the Himalayan plate boundary.

3.3.5 Northwest: Transpressional Chaman plate boundary zone

The India-Arabia-Eurasia triple junction marks the transition from broad continental deformation to more localized submarine plate boundaries. Oblique active deformation is distributed over a ˜150km-wide zone accommodating transpressional plate boundary strain across multiple structures [*Mohadjer et al.*, 2010].The north-south striking, left-lateral Ornach-Nal and Chaman transform fault zones, and Kirthar thrust belt accommodate India-Eurasia plate motion near the coast. Further north the Sulaiman and Salt ranges [*Stein et al.*, 2002; *Ambraseys and Bilham*, 2003] exhibit similarly diffuse patterns of deformation as they intersect the Main Frontal Thrust in the Hindu Kush [*Pegler and Das*, 1998] region of the

westernmost Himalayan range. Little GPS data is currently available for this region; however, *Mohadjer et al.* [2010] constrain the upper bound on slip rates of the known faults using a new network of only 10 survey-style GPS stations which were not included in this velocity combination. We constrain far-field motions but do not address detailed motion and slip rates along individual small structures across this region.

3.4 GPS Velocities

The GPS data were processed using the GAMIT/GLOBK software package [*Herring*, 2005; *King and Bock*, 2005] to solve for station coordinates and velocities in the ITRF2000 reference frame. The primary data come from 106 survey-mode GPS (SGPS) stations and 29 continuous GPS (CGPS) stations from India [*Banerjee et al.*, 2008]. While the CGPS stations are located all over India including the Himalaya, the SGPS sites are mostly from the northwestern Himalaya. The earliest campaign data were collected in 1995, but most sites were first occupied in 2001. Occupations have been repeated annually through 2007 although some stations have been lost and have been measured for as little as 3 years. Each SGPS station was occupied for 4-6 days continuously, once a year. In addition to the Indian GPS data we also processed data from surrounding IGS stations (IISC, HYDE, KIT3, POL2, LHAS, BAHR, DGAR, MALD, NTUS) available from Scripps Orbital and Positioning Analysis Centre (SOPAC; http://sopac.ucsd.edu). Precise satellite orbits, earth orientation parameters and tightly constrained positions of the IGS sites in a self-consistent reference frame were used to produce daily solutions which include GPS station positions, satellite orbits, earth orientation parameters, and tropospheric delays. The loosely constrained, ambiguity-fixed daily solutions were combined with ambiguity-free quasi-solutions of 33 globally distributed IGS sites (igs1, igs2, igs3), available at SOPAC (http://sopac.ucsd.edu). The local and IGS daily solutions of the entire period were then combined to estimate position and velocities for each site. Selected, globally distributed IGS sites were used to define the ITRF2000 reference frame [*Altamimi et al.*, 2002], both for positions and velocities, with a residual RMS of 3.3 mm and 0.9 mm/yr respectively.

3.4.1 Published Solutions

In addition to our own analysis we considered over 2500 GPS-station velocities from published work along the Himalayas, throughout China, Southeast Asia, Australia, Africa and Middle East [*Bock et al.*, 2003; *Zhang et al.*, 2004; *Shen et al.*, 2005; *Reilinger et al.*, 2006; *Bettinelli et al.*, 2006; *Socquet et al.*, 2006a; *Calais et al.*, 2006; *Jade et al.*, 2007; *Simons et al.*, 2007; *Sol et al.*, 2007; *Gan et al.*, 2007; *Kogan and Steblov*, 2008]. Solutions were transformed into a consistent reference frame defined by our original processed solutions. We minimized the misfit (RMS) of collocated stations between networks using a six-parameter transformation (three translations, three rotations). All the transformed velocities remain within 95% confidence level of the original solutions assuring the robustness of the original

solution as well as the transformed one. Original velocities, site transformations, and misfits are summarized in the supplementary material (Table B.1). For collocated sites with velocities from multiple sources we used a single velocity for the site based on the following priorities: 1) GPS velocity solution was processed in this study. 2) GPS velocity was derived from the time series with the most observations, typically the most recent publication. 3) GPS velocity comes from the larger network. 4) GPS velocity with the smallest uncertainties. Selected velocities are plotted and colored by source in Figure 3.1.

3.4.2 Outlier Exclusion

All GPS velocities from the above-mentioned references were incorporated in our combined velocity solution, however some were excluded prior to the block model inversion. Sites were excluded for one of three reasons (see Table B.1 for site specific details): We exclude 1) sites outside our area of interest e.g. *Reilinger et al.* [2006] Aegean sites or *Gan et al.* [2007] sites north of the Tarim basin), 2) sites whose absolute 1σ uncertainty exceeds 4 mm/yr, and 3) redundant velocity estimates for collocated sites with a preferred velocity (see section 3.4.1). Following the block model inversion we also exclude sites because of extreme misfit to our model. If the residual velocity exceeds 3σ then the site was excluded from our preferred model and the summary statistics. These sites have misfits that deviate from the systematic pattern exhibited by surrounding sites. Some of these sites may have had hardware or site stability problems that did not manifest in the formal velocity uncertainties. The final velocity field we consider includes 688 horizontal station velocities across the region.

3.5 Methology: Plates and Blocks

We use a block modeling approach to incorporate both rigid block rotation and near-boundary elastic strain accumulation effects in a formal inversion of the GPS velocities [*McCaffrey et al.*, 2000a; *Meade and Hager*, 2005, e.g.]. We consider models that include scenarios with and without independent micro-blocks to constrain the plate rates along the India plate boundaries and elucidate the plate kinematics responsible for interseismic deformation and slip budget estimates.

Plate boundary locations are critical for characterizing GPS velocities and the plate boundary kinematics of a particular region. While some plate boundaries in the Indian region are well defined by active fault traces, youthful geomorphology and abundant local seismicity (Figure 3.1), others appear more diffuse or the distribution of active deformation may be ambiguous. We draw on the distribution and kinematics of 20^{th} century seismicity, local geology, mapped faults, and the GPS velocity field itself to define our block model boundaries. Most block boundary locations and geometry in our models are based heavily on seismicity trends (e.g. mid-ocean ridges, subduction zone dip) and well recognized plate boundaries (e.g. Himalayan range front). Additional boundary information is adopted or

supplemented from neotectonic structures [*Taylor and Yin*, 2009, and references therein], plate reconstructions [*Replumaz and Tapponnier*, 2003] coseismic studies [*Pollitz et al.*, 2006] and prior analyses [*Socquet et al.*, 2006a, b; *Reilinger et al.*, 2006; *Simons et al.*, 2007; *Meade*, 2007; *Thatcher*, 2007]. In some areas, however, geometry is adjusted as indicated by the geodetic data. For example in the Himalayan region we test multiple block boundary locations and variable geometry (i.e. dip). In the Sumatran region we test the location of the India-Australia-Burma triple junction for optimal fit to the data by exploring the parameter space (discussed in section 3.7). Within this paper the term plate (and microplate) refers to the rigid, coherent, lithospheric entity defined by bounding active fault zones. The term block is the specific implementation of these data into a parameterized set of variables within our block model [*Apel et al.*, 2006, e.g.].

We implement our blocks as rigid entities on a spherical earth bounded by dislocations and invert for poles and rates of rotation that minimize the misfit to the GPS velocities using the block modeling code by *Meade and Hager* [2005]. The segments that bound the blocks represent uniformly slipping dislocations in an elastic half-space locked to some specified depth (varies by segment, see Table **??** for details). Because our inversion combines rigid block rotation with elastic strain accumulation effects, the parameterization of the block boundary location and geometry is particularly important where the elastic strain field is broadly distributed (such as along subduction zones) and where a large number of stations are located near a boundary fault (such as along the Himalaya frontal thrust).

We invert the horizontal GPS velocities for poles of rotation constrained by the prescribed block locations and geometry defined above. Systematic patterns in the residual velocities (observed minus predicted) are used as an indicator of where and how the model matches the observed surface velocities. Misfit statistics are used to formally evaluate the statistical significance of the block kinematic scenarios we test using the F-test [*Stein and Gordon*, 1984]. For larger blocks (e.g. Eurasia, India, and Arabia) the motion of interior sites are unaffected by plate boundary deformation and effectively define the angular velocity. For smaller blocks, elastic strain along the boundaries more directly affects block motion angular velocity estimates.

3.5.1 Chi-Squared Statistics

We quantify the goodness of fit in terms of the χ^2 and χ^2/DOF statistics:

$$\chi^2 = \sum_{c=1}^{\#data} \left(\frac{v_c^{model} - v_c^{data}}{\sigma_c} \right)^2 \tag{3.1}$$

$$\chi^2/DOF = \frac{\chi^2}{\#data - \#model\ parameters} \tag{3.2}$$

where v_c^{model} and v_c^{data} are the predicted observed velocity components, and σ_c is the 1σ uncertainty for each component of the input GPS velocities. The number of degrees of

freedom (DOF) is defined by: $\#data$, the number of GPS components used as input data (east and north components for each station) and $\#modelparameters$, the number of model parameters that we solve for in the inversion (3 per block - pole of rotation latitude and longitude and rotation rate). The statistics indicate how well the model fit the data within their uncertainty bounds. Lower values of χ^2 indicate better fit to the data. χ^2 can be calculated for a single data component at a single station, for sites within an individual block, or for the entire model. Increasing the number of model parameters inevitably leads to better fits and lower total χ^2. Dividing by the number of degrees of freedom helps us to compare our model where we solve for a different number of parameters, but χ^2/DOF ignores all correlations between parameters. Because these correlations change as model geometry changes, caution should be exercised in making strictly quantitative comparisons of models using χ^2/DOF alone. Nonetheless, the statistics provide a basis for qualitative comparisons. For uncorrelated parameters, a χ^2/DOF of 1 indicates that on average all the predicted velocities are consistent with the 1σ standard deviation of the input data.

3.5.2 F-Test

Increasing the number of model parameters (i.e. more blocks) inevitably leads to better fits and lower χ^2 . Therefore we follow the approach of Stein and Gordon (1984) to test the statistical significance of additional microblocks. In our model we test the fit of N motion data (2-component GPS velocities) produced by a model with b + 1 blocks for significant improvement relative to a model with b blocks. The b block model has 3 (b - 1) parameters (N - 3b + 3 degrees of freedom) while the b + 1 block model has 3b parameters (N - 3b degrees of freedom) so the statistic F:

$$F = \frac{\chi^2(b\ blocks) - \chi^2(b+1\ blocks)/3}{\chi^2(b+1\ blocks)/(N-3b)} \tag{3.3}$$

The probability (or 1/significance level) is then calculated given the above mentioned degrees of freedom and the F-statistic. Statistically significant variations are commonly between $\geq$95%.

3.6 Results: Plate and Blocks

We evaluate different variations in fault geometry (i.e. location, locking depth, and dip), number of blocks and block configurations in an effort to develop a model that fits the data well while still maintaining geologically reasonable block boundary locations and geometry. For each variation we inverted the horizontal GPS velocities for poles of rotation and slip rates constrained by our prescribed block locations and plate boundary fault geometry as described in 3.3. To evaluate the misfit of each block model variation we compare the input GPS velocities with the models predicted velocities (Figures 3.4). Examining residual

velocities (difference between the data velocity and model velocity) allows for a more detailed comparison of the systematic differences between observations and predictions for the different model realizations.

Estimates of major blocks motions vary little between our model realizations and are relatively insensitive to variable block configurations and boundary geometry. The Eurasia block, Australia block, India block, and Sunda blocks angular velocities are defined primarily by the sites that lie within the stable interior and are affected very little by plate boundary strain. The inferred motion of smaller blocks, such as the Burma block and sub-blocks within the Himalaya-Tibet region changes based on the parameterization of the boundaries of these blocks. The stability of the major blocks provides robust constraints on far-field motions and allows us to test variable block configurations and deformation geometries along these boundaries to develop our preferred model.

Generally the major block motions are consistent with previous tectonic studies and we see good agreement with previously published Euler poles. Systematic misfits remain in some areas, such as the Tien Shan region north of the Tarim basin (Figure 3.4). This area is considered part of the Eurasia block in our model; however, the northerly residuals clearly show that this region is not part of stable Eurasia consistent with more detailed previous studies using GPS [*Abdrakhmatov et al.*, 1996; *Meade and Hager*, 2001] and geologic slip rate data [*Thompson et al.*, 2002].

3.6.1 India Motion and Deformation

Indias angular velocity is primarily defined by 19 stations; 3 IGS sites (IISC, HYDE, and MALD), 13 additional CGPS sites (TIR0, KODI, PUN2, BMBY, BHBN, NAGP, JBPR, RRLB, DHAN, JHAN, LUCK, BAN2 and DELH), and 3 sites from previous studies (DHAK from *Kogan and Steblov* [2008]; COLA and KRN2 from *Bettinelli et al.* [2006]). Previous studies constrained India plate motion using only the IGS sites and additional SGPS sites at various locations [*Paul et al.*, 2001; **?**; *Bettinelli et al.*, 2006, e.g.]. The determination of Indias angular velocity in earlier studies suffered from a lack of intraplate CGPS stations and narrow east-west aperture of networks within the Indian continent. Our network uses 16 CGPS sites and has good coverage both north-south and east-west providing robust block motion estimates.

Internal Deformation

Residual velocities across India from our inversion (black vectors in Figure 3.5) show systematic northward residuals in the south (1-3 mm/yr) and southward directed residuals in the north (2-4 mm/yr). This systematic pattern in the residual velocities suggests potential unmodeled contraction across central India [*Banerjee et al.*, 2008]. We test the significance of a two-block India model using only velocities from the 16 CGPS stations processed in our

GPS solution. We exclude the 3 sites from other sources (see section 3.6.1) in an attempt to exclude model velocity bias from solution combination errors.

We separate the India block along the Narmada Son lineament because of its strong topographic expression and high heat flow [*Rao*, 2000] suggesting weaker crust. In addition, recent earthquakes (Figure 3.1) and historical events (e.g. 1938 Satpura earthquake) have occurred along this lineament suggesting that it may be an actively deforming zone. Separation of the India block into northern (nIND) and southern (sIND) blocks along a boundary following the Narmada Son line reduces the chi-squared misfit for the 16 sites from 2.06 to 1.59. Our 2-block model predicts contraction that varies from 4 mm/yr in the east to 0 mm/yr in the west near the nIND-sIND pole (Figure 3.5). The calculated F-statistic [*Stein and Gordon*, 1984] between the 1-block and the 2-block model is 2.25, suggesting significantly distinct motions at the 89% confidence level. Because the confidence level is below 95% we chose not to separate India in our preferred model. Although the patterns in the residual velocities indicate an observable systematic change from north to south within the India plate, the data do not allow us to determine if the apparent N-S contraction represents broadly distributed intraplate deformation or fragmentation of India into two plates near the Narmada-Son lineament.

Shillong Block Motion

Eleven sites in our GPS solution lie within the boundaries of the Shillong Plateau (Figures 3.9 and 3.10). If the sites are included with the above mentioned 16 sites in our India plate motion estimates, the reduced chi-squared misfit statistic rises to 8.05. The reduced chi-squared statistic for those 27 sites decreases to 3.36 when the Shillong block is allowed to rotate independently of India. The calculated F-statistic [*Stein and Gordon*, 1984] between the two models is 7.23, equivalent to a 99.96% confidence level. Therefore we assume the Shillong block to be independently rotating counterclockwise with respect to India about a pole just north of the block (92.6°E, 26.9°N) and estimate slip rates along its boundaries (Figure 3.10). This rotation results in lower slip rates (18 mm/yr) along the Bhutan Himalayas and higher slip rates (25 mm/yr) further to the east (Figure 3.10). Slip rates predicted from our preferred model (6 mm/yr) along the southern edge of the Shillong block (Dauki fault) are about half of those found by *Banerjee et al.* [2008] at 11 mm/yr, but twice the rate suggested by geologic studies *Biswas et al.* [2007]; *Clark and Bilham* [2008]. Nonetheless, convergence rates along the Main Frontal Thrust along the northern Shillong boundary are higher than along the rest of the Himalayan Range Front where slip rates are between 15-18 mm/yr (Figure 3.10). Fit to our model is good (inset Figure 3.9) although lack of data along the most northeastern extent of the Himalayan range north of the Shillong Plateau leaves slip rates poorly constrained in this region.

3.6.2 Relative Block Motions

Eurasia

Eurasias angular velocity is defined by 19 IGS sites (ARTU, BOR1, BRUS, GLSV, GOPE, HERS, JOZE, KIRU, KOSG, LAMA, MDVO, MOBN, NRIL, NVSK, NYA1, POTS, TIXI, WTZR, and ZWEN.) Misfits are all less than 1.5 mm/yr with a mean misfit of 0.65 mm/yr (inset Figure 3.3). The EUR block angular velocity is very well constrained and consistent with previously published poles shown in Table **??**. The consistency of our EUR pole with previously published poles indicates that sites within our EUR block contain little bias and that the velocity combination did not introduce any significant shifts.

We compare IND-EUR poles from our one-plate and two-plate models with published poles (Figure 3.3). In our models it appears that Indias angular velocity is dominated by the southern sites as our sIND-EUR and IND-EUR poles are statistically indistinguishable. The published IND-EUR pole estimates (see references listed in Figure 3.3 and Table **??**) vary in their east-west location due to the primarily north-south distribution of GPS stations in India. Poles from this study also show larger uncertainties in the east-west direction due to the inherently narrower east-west aperture of the network. However, the magnitude of the uncertainties is 50-80% smaller in this study than in previous work.

Somalia and Arabia

Somalias angular velocity is defined by 7 sites from *Stamps et al.* [2008] and 6 sites from *Reilinger et al.* [2006]. Sites from *Stamps et al.* [2008] are concentrated mostly in the southern region of the block while sites from *Reilinger et al.* [2006] are mostly in the north. The Somalia block rotation is consistent with both *Stamps et al.* [2008] and *Reilinger et al.* [2006], although there is some variation resulting from the combination of the two solutions.

Arabias angular velocity is defined by 22 sites. All but one of these GPS velocities comes from *Reilinger et al.* [2006]. Misfits are all less than 4 mm/yr with a mean misfit of 1.6 mm/yr and a reduced chi-squared statistics equal to 1.5. The lack of systematic patterns in the residual velocities among the well distributed stations within the Arabia block suggest little to no measureable internal deformation.

Australia

Australias angular velocity is defined by 6 IGS sites (HOB2, JAB1, KARR, PERT, TIDB, and YAR1,) and 4 sites (DARW, CEDU, ALIC, and TOW2) from *Bock et al.* [2003]. The mean misfit of 2.0 mm/yr is shown in the inset of Figure 3.7. These Euler pole estimates differ from previously published poles [*Sella et al.*, 2002; *Bock et al.*, 2003; *Delescluse and Chamot-Rooke*, 2007, e.g.] in that our relative IND-AUS pole location lies further south than other geodetic poles (Figure 3.7).

Although India plate motion independent of the Australia plate is not a particularly new idea [*Le Pichon and Heirtzle.Jr*, 1968; *DeMets et al.*, 1994, e.g.], ten GPS velocities within the stable Australia plate precisely discriminate Australian motion with respect to India. Our new solution provides tight constraints on the relative far-field motion and provides context for the Capricorn plate (see section 3.6.3) and widely distributed deformation within Indias southern plate boundary zone [*Delescluse and Chamot-Rooke*, 2007].

Sunda

Sundas angular velocity is defined by 49 sites from Bock et al., 2003; Calais et al., 2006; Simons et al., 2007; and Socquet et al., 2006. Three sites from Thailand (Socquet et al., 2006) were excluded from angular velocity estimates and our preferred model (but shown on Figure 3.13) as extreme outliers (see section 3.3). Some sites from northern Borneo were excluded because these sites may move independently of the Sunda block (Simons et al., 2007). All sites east of 119°E were also excluded as we did not attempt to address the complexities in the Sulawesi region. The Sunda blocks angular velocity is compared with previously published poles in Table 3.5.

3.6.3 Plate Boundary Interactions

Eurasia

The deformation associated with Indias collision with Eurasia is manifested most famously along the Himalayan range front and broadly distributed deformation across the Tibetan Plateau. Along the Himalayan range front we estimate total IND-EUR convergence to vary from 33-39 mm/yr from ˜76°-91° east longitude. The amount of deformation accommodated on the main Himalayan thrust system depends on the nature and distribution of deformation in southern Tibet. Our Tibetan block geometry is simplified and modified from previous studies [*Meade*, 2007; *Thatcher*, 2007; *Loveless and Meade*, 2011, e.g.] as this paper does not attempt to address all the complexities of the entire India-Eurasia collision zone. We parameterize the Himalayan front with four main blocks defined by the major geologic features like the Indus-Zangbo suture, Gulu rift, and Karakorum fault (Figure 3.9).

Slip along the HRF varies from 15-22 mm/yr with the greatest amount in the NE, Bhutan Himalaya north of Shillong, and the least in central Tibet (Figure 3.9). Estimates of slip from our model are consistent but smaller than other published estimates from *Feldl and Bilham* [2006, and references therein] and *Bettinelli et al.* [2006, and references therein]. By separating Tibet into multiple blocks our model captures east-west extension evidenced by predicted slip rates along structures like the Gulu-Sangxung and Kung Co graben systems (Figure 3.9). Our extension rates (4-9 mm/yr) are quite consistent with other estimates of extension in southern Tibet [*Chen et al.*, 2004, e.g.] which use considerably fewer GPS data.

Differences between the two estimates are the result of block boundary choice and model parameterization.

Makran subduction is driven by the northly motion of the Arabia block with respect to Eurasia, or perhaps a separate Lut block [*Reilinger et al.*, 2006]. At the eastern end of the Makran subduction zone is the triple junction of Arabia-India-Eurasia where relative ARB-IND displacement along the Owen fracture zone is transferred along the Ornach Nal fault through the Chaman Transform zone and into the Sulaiman Range. However, poor GPS station density prevents us from making more precise estimates of slip, and our model does not try to capture the complexities of deformation in the zone.

Arabia

The Owen Fracture Zone separates the India plate from the Arabia plate and accommodates ˜5 mm/yr of dextral motion (see Table **??** for segment specific slip rates). This rate is slightly greater than 3 mm/yr predicted by **?***Fournier et al.* [2008] and slightly greater than the rate predicted by *Reilinger et al.* [2006]. The rotation of the Arabia block with respect to Eurasia is manifested, as convergence along the Makran subduction zone at 35-38 mm/yr. The rate of subduction may be as little as 23 mm/yr *Reilinger et al.* [2006] if an independent Lut block is considered (Figure 3.2). Unlike *Reilinger et al.* [2006] we did not include a separate Lut block in our preferred model as it is not required by the currently available data. Possible Lut block motion is only constrained, at present, by 2 GPS sites, both of which are within the zone of elastic strain accumulation of the Makran subduction zone.

Somalia

The eastern edge of the Somalia plate is adjacent to the Australia plate along the Central Indian Ridge in the south and the India plate along the Carlsberg Ridge in the north (Figures 3.2 and 3.8). These plate boundaries are marked by discrete, localized seismicity. We compare our predicted displacement directions (plate vectors) with earthquake slip vectors from events along the spreading centers. We derive slip vectors from focal mechanism solutions (www.globalcmt.org) south of the SOM-IND-ARB triple junction and north of the SOM-CAP-ANT triple junction. We selected only those events between these triple junctions that lie within 100 km of the mid-ocean ridge, which we assume are related to the divergence of the plates. 311 events from the catalog fit our selection criteria. We derive slip vectors for these events and compare them to the azimuth of plate motion calculated from our model at the location of each earthquake (inset rose diagrams in Figure 3.8).

Along the Somalia plate boundary the relative plate motion transitions from SOM-IND to SOM-CAP and/or SOM-AUS block motion through the diffuse India-Australia plate boundary zone [*Royer and Gordon*, 1997; *DeMets et al.*, 2010]. We attempt to elucidate the diffuse nature of the IND-AUS plate boundary along the mid-ocean ridges by comparing

both the predicted SOM-IND plate vectors and the SOM-AUS plate direction with the slip vectors in the central ridge region (12°S-2°N lat). The trend of the slip vectors in the north along the Carlsberg Ridge are consistent with SOM-IND block motion (top inset Figure 3.8).

Along the central section of the mid-ocean ridge, plate boundary slip vectors appear more consistent with SOM-IND block motion rather than with SOM-AUS plate motion (middle inset Figure 3.8). In the central section the orientation of SOM-IND, SOM-CAP, and SOM-AUS motion becomes sub parallel because of the close proximity to the CAP-IND and IND-AUS poles (Figure 3.7) making the distinction between them difficult.

South of 11°S lat nearly all of the slip vectors are exactly parallel with SOM-AUS plate motion with a small concentration of dip slip events that deviate from the plate motion direction. These events are not concentrated spatially and are scattered throughout the southern region from north to south. The correlation between the slip vector data in this region and the plate motion directions suggests that our SOM-AUS relative plate motion is robust. However, based on our analysis, the earthquake slip vectors do not provide detailed enough resolution to show measureable deviation of the AUS plate motion from the CAP plate motion.

Australia and Capricorn

GPS velocities within the interior of Australia and India clearly show that the two blocks move independently of each other (Figure 3.7), verified with F-statistics; however, the tectonic boundary between the two remains enigmatic and may be complicated by an independently rotating Capricorn plate [*DeMets et al.*, 2005, and references therein]. The boundary zone between the India and Australia plates is quite diffuse [*Delescluse and Chamot-Rooke*, 2007]. Within this zone our preferred model predicts 1-2 mm/yr N-S extension west of the IND-AUS pole between it and the Central Indian Ridge (Figure 3.7) and up to 12 mm/yr of N-S contraction in the vicinity of the 90°E ridge. The IND-AUS-SOM and the IND-AUS-SUN triple junctions remain somewhat enigmatic due to the diffuse nature of the IND-AUS plate boundary and the lack of geodetic data on the Capricorn plate.

The continuous GPS station on the island of Diego Garcia (DGAR) is included in our velocity combination but is not used to estimate India's angular velocity. The predicted velocity for DGAR is consistent with our initial estimates of India plate motion to within ˜1mm/yr (inset Figure 3.5) similar to *Kogan and Steblov* [2008]; however, based on the plate boundaries defined by *Royer and Gordon* [1997]; *DeMets et al.* [2005] the DGAR station likely lies on the Capricorn plate, not the India plate. We compare the DGAR station velocity in a fixed India reference frame (this study) to predicted Capricorn-India plate motion from *Gordon et al.* [2008]; *Bull et al.* [2010]; *DeMets et al.* [2010] (Figure 3.6). The DGAR GPS velocity is approximately 2±2 mm/yr east-southeast with respect to a fixed India plate. Predicted velocities from the above mentioned CAP-IND poles are very similar in both magnitude and direction (Figure 3.6) to the GPS velocity. However, due to the close proximity of the CAP-IND poles to the DGAR site the predicted velocities are statistically

close to zero and the velocity of the DGAR site does not provide statistically significant additional evidence for independent Capricorn plate motion.

Although little or no GPS data is available for the Capricorn plate, its motion is still testable using geodetic measurements. Following the methodology in *Gordon et al.* [2008] we show the velocity at the Bangalore station (IISC) in a fixed Australia reference frame (Figure 3.11). We also calculate Indias motion with respect to the Capricorn plate using published poles [*Gordon et al.*, 2008; *Bull et al.*, 2010; *DeMets et al.*, 2010]. Figure 3.11 shows the predicted velocity for IISC based on each one of these poles. If the Capricorn plate does not move with respect to Australia then predicted IND-CAP motion will be equal to IND-AUS motion. However, our GPS velocity (IND-AUS) is larger than any of the three IND-CAP plate motion vectors, suggesting that a significant amount of motion is accommodated between the Capricorn and Australia plates. Vector summation of IND-CAP and CAP-AUS motions yields IND-AUS motion which can directly be compared to the GPS velocity at the IISC site *Gordon et al.* [2008]. The IND-AUS GPS velocity at IISC, although larger than the GPS rate presented in *Gordon et al.* [2008], is still consistent with the IND-CAP plus CAP-AUS poles presented there. However, our results are not consistent at the 95% confidence level with *DeMets et al.* [2010]. Because *Gordon et al.* [2008] rely on more data and average motion over a longer time interval than *DeMets et al.* [2010] , their resolution of the IND-CAP plate pair is likely more robust [*C. DeMets, personal communication*, 2011].

Sunda

The interaction between the Sunda plate and the India plate is most significant along the Sumatra-Andaman subduction zone where IND-SUN motion is partitioned along the megathrust and the sub-parallel strike-slip Great Sumatra Fault [*McCaffrey et al.*, 2000b, e.g.]. We consider a separate Burma forearc block (sliver block) bounded by the Sumatra subduction zone and the Great Sumatra fault (Figure 3.2). Along the Sumatra subduction zone segment, the plate-boundary fault geometry is based on previous geometric constructions [*McCaffrey*, 2002; *Banerjee et al.*, 2007; *Chlieh et al.*, 2007, e.g.].

In an attempt to elucidate an optimal boundary location in the zone of diffuse deformation between the India and Australia blocks (Figure 3.2) we separate the India block from the Australia block along the Sumatra subduction zone through the segment endpoints (number 1-11 in Figure 3.13). We compute and compare the model misfit for models in which we place the eastern IND-AUS boundary at each of these segment intersections. We repeated this test while also varying the Sumatra segment geometry (locking depth and dip) to estimate best-fit parameters for the region. In this analysis, we assume homogenous segment parameters for the subduction zone (common dip and locking depth for all segments).We find that locking depth and dip are highly correlated. As dip increases, so does the locking depth that is required to minimize the misfit to the GPS velocities. We base our model segment geometry on the parameters that provide the minimum misfit; however, our preferred model geometry is modified from this somewhat and uses heterogeneous segment parameters. Figure 3.13 shows variable locking depths along strike of the Sumatra subduction zone. This variability

is more consistent with locked portions of the subduction that pre-date the 2004 M_W 9.2 earthquake. This segment configuration fits our data better than any of the homogenous segment geometry sets. Regardless of segment geometry, the segment location of the IND-AUS boundary with the minimum misfit was endpoint 8 (Figure 3.13) the approximate southern extent of the 1797 rupture and significant locking proposed by *Chlieh et al.* [2007]. Interseismic slip rates from our preferred model (18-22 mm/yr) are consistent with published geologic estimates of slip rates along the Great Sumatra fault [*Sieh and Natawidjaja*, 2000, e.g.] and backarc spreading ridges [*Curray*, 2005] and provide robust estimates of Burma block motion.

Residual velocities from the Sumatra region, while larger than in most other areas do not show any systematic patterns (Figure 3.13). The few large outliers that do exist [*Bock et al.*, 2003] are related to poorly resolved station velocities rather than model misfits and were excluded from our final analysis (see discussion in section 3.4.2).

3.7 Discussion

3.7.1 Internal Deformation of the India Plate

Systematic differences in the GPS velocities from southern and northern India may reflect internal deformation of the India plate. The predicted Euler poles from our 2-block India model suggest that northern India is moving slower with respect to Eurasia than the southern block, leading to contraction between the two blocks (Figure 3.3). Given the observed seismicity along the Narmada-Son (1938 Satpura earthquake and the 1997 Jabalpur earthquake), it is possible that India intraplate deformation is concentrated along this lineament. If deformation is focused along the Narmada Son lineament, our pole of rotation (Figure 3.3) predicts as much as 4-5 mm/yr of contraction in eastern India.

Rather than being concentrated along a linear zone, more distributed intraplate deformation in central India could also result from flexure of the India plate as it collides with Eurasia [*Bilham et al.*, 2003]. *Bilham et al.* [2003] demonstrate how flexural deformation may be reflected in the stress field and topography. the flexural model also predicts contractional deformation in central India approximately parallel to the Narmada-Son lineament. Estimates of deformation resulting from flexure are smaller in magnitude than those predicted from a two plate system, as the deformation is more distributed in a flexural model than in a block model.

While some systematic residual velocities are evident when assuming a single rigid India plate, they are not statistically significant (˜89

3.7.2 India-Australia Plate Boundary

Based on GPS data presented here we estimate a robust India-Australia angular velocity that constrain far-field motions between the plates. Most of the sites lie within the stable interiors of the two plates far away from the diffuse boundary between India and Australia. The data themselves do not elucidate the plate boundary or the locations of the IND-AUS-SOM or IND-AUS-BUR triple junctions. However, consideration of the GPS-constrained plate motions and sea floor spreading data supports assertions of independent Capricorn plate motion [*Gordon et al.*, 2008].

The eastern triple junction (IND-AUS-BUR) is somewhat difficult to constrain. *Delescluse and Chamot-Rooke* [2007] suggest that the 90°E Ridge is a major discontinuity for both strain and velocity. The intersection of this ridge with the Sumatra-Andaman subduction zone could be the northern most possibility of the triple-junction. However, our modeling suggests (section 3.6.3) that the interaction along Sumatra is much more likely to reflect India plate motion rather than Australian pushing the triple junction location much further south (Figures reffigi12 and 3.13). Implications of India plate motion driving convergence this far south include potential underestimation of long term plate convergence along the Sumatra subduction zone.

Magnetic anomaly analysis [*DeMets et al.*, 1994] and seismicity [*Royer and Gordon*, 1997] indicate a potential western triple junction (IND-AUS-SOM) between 2°-9°S, suggesting that the Diego Garcia island GPS site is on the Capricorn plate (Figure 3.15). We rigorously test the possibility that DGAR exhibits Capricorn plate motion, independent of India. We find that the site velocity is consistent with Capricorn plate motion however due to the close proximity of DGAR to both the IND-CAP poles and the IND-AUS poles, discriminating one from the other is statistically impossible given the current resolution of the GPS data.

3.7.3 Himalayan Range Front

Although modern GPS data provides robust measurements of displacements rates, interpretations of these data vary, especially in areas of distributed continental deformation like the broadly distributed India-Eurasia collision zone. With far field motions of the bounding India and Eurasia plates tightly constrained, differences in micro-block rotations and slip estimates along the Himalaya vary mostly as a result of variable data densities, model parameters, and assumptions. *Meade* [2007] uses a conceptually identical model with fewer GPS stations [*Zhang et al.*, 2004, only]. Estimates of slip from *Meade* [2007] along the Himalayan Range Front (HRF) vary from 17-22 mm/yr, 15-20% greater than our model. Differences in convergence rates along the HRF may partly be the result of different India plate angular velocity estimates, but these differences do not explain a reduction in convergence by 15-20%. Instead, we find that *Meade* [2007] higher slip rates are the result of a more steeply 10° north dipping HRF. In our preferred model, segments along the HRF dip between 6 and 8 degrees. We estimate range front segment dips by migrating the HRF boundary from north to south and varying the dip and locking depth exploring ranges of geometries that

minimize the misfit to the observed data while maintaining the projection of the bottom locking depth to correspond with the 3500 m topographic contour [*Avouac*, 2003]. Shallower dipping segments require less slip to produce similar magnitudes of horizontal deformation at the surface then more steeply dipping segments. As a result our preferred model requires lower slip rates than *Meade* [2007] to produce similar fits to the data.

Thatcher [2007] uses the same data [*Zhang et al.*, 2004] and after removing sites where effects of elastic strain accumulation are large estimates block rotation rates that are even larger than *Meade* [2007]. *Thatcher* [2007] assumption is that the remaining velocities only capture rigid block motion and that no component of the velocity is measuring elastic strain accumulation. It is not surprising then that the block rotation estimates (and fault slip estimates) from this method are larger than those for methods that consider elastic strain effects.

We note that differences in analyses within the same conceptual framework are largely the result of assumptions made within the analyses, whether it is the rigidity of the blocks or the parameters of the segments that bound them. First order results from our model, *Thatcher* [2007], and *Meade* [2007] all suggest that the paradigm of plate tectonics (i.e. rigid blocks controlling crustal deformation) holds true at large scales and may be appropriate to some degree for continental deformation. Although even in this family of models when the same data is used there still exist some discrepancies. These discrepancies have not yet been adequately addressed and may require a more complex analysis than simple rigid block models, particularly in areas of diffuse deformation like continents.

3.8 Conclusions

We present robust estimates for the India plates angular velocity using numerous GPS sites across India in the context of a block model. Angular velocities for other major tectonic plates (Eurasia, Australian, Somalia, and Sunda) are also derived using dense GPS data from in and around these plates. We refine relative motions between these plates and perform a detailed kinematic assessment of Indias plate boundary interactions with its adjacent tectonic plates not previously possible given the scarcity of geodetic data within India. The GPS network within India suggests that active contraction of up to ˜4 mm/yr may be occurring within the subcontinent. A 2-plate model with a discrete boundary following the Narmada Son lineament does provide a significantly better fit at greater than 89% confidence.

Using the data on the India block we estimate IND-EUR convergence vectors that are consistent but ˜10 % slower than most recent geologic estimates and ˜5 % slower than previous geodetic estimates. This results in estimated slip rates along the Himalayas that are also slower than previously estimated.

Table 3.1. Geodetically Derived Euler Pole Indian Plate Rotation Parameters

Reference	Year	Latitude °N	Longitude °E	Rate ω °/Myr	σ_{maj}	σ_{min}	Azimuth	# Sites Used
Sella	2002	-13.99	53.65	0.483±0.013	11.7	0.5	80	3
Prawirodirdjo	2004	-41.99	45.72	0.487±0.015	12.11	0.73	29	2
Bettinelli	2006	-10.92	51.41	0.483±0.015	NR	NR	NR	5
Socquet	2006	-12.1	50.9	0.486±0.010	5.11	0.61	108	6
THIS STUDY	2010	-1.572	53.27	0.503±0.001	3.144	0.96	86	19

NR - Parameters were not reported.

Table 3.2. Eurasia Euler Pole Parameters

Reference	Reference Frame	# Sites Used	Latitude °N	Longitude °E	Rate ω °/Myr	σ_{maj}	σ_{min}	Azimuth	σ_{lat}	σ_{long}
EURASIA										
Demets et al., 1994	NUVEL-1A	-	50.6	-112.3	0.234					
Sella et al., 2002	ITRF97	15	58.27	-102.21	0.257±0.003	1.5	0.4	34		
Altamimi et al., 2002	ITRF00	19	58.0	-99.4	0.260±0.005	1.2	2.7	NR		
Bock et al., 2003	ITRF00	18	58.3	-97.2	0.260±0.001	1.5	0.3	48		
Fernandes et al., 2003	ITRF00	58	54.6	-103.9	0.249±0.003	1.6	0.4	51		
Calais et al., 2003	ITRF00	15	52.3	-107.0	0.245±0.005	0.2	0.2	NR		
Prawirodirdjo et al., 2004	ITRF00	18	57.2	-99.7	0.260±0.002	0.8	0.2	52		
Shen et al., 2004	ITRF00	11	55.6	-102.4	0.252±0.010	1.8	0.9	56		
Altamimi et al., 2007	ITRF05	41	56.330	-95.979	0.261±0.003				0.549	0.969
THIS STUDY	ITRF00	19	55.339	-105.022	0.260±0.001				0.280	0.370

NR - Parameters were not reported.

Table 3.3. Relative India-Eurasia Euler Pole Parameters

Reference	Reference Frame	# Sites Used	Latitude °N	Longitude °E	Rate ω °/Myr	σ_{maj}	σ_{min}	Azimuth	σ_{lat}	σ_{long}
IND-EUR										
Demets, et al., 1994	NUVEL-1A		24.5	17.7	0.510				1.8	8.8
Holt et al., 2000			29.78	7.51	0.353±0.024					
Paul et al., 2001	ITRF96		25.6	11.1	0.440±0.026				˜1	˜9
Sella et al., 2002	ITRF00		28.56	11.62	0.357±0.033	14.4	1.1	-89		
Socquet et al., 2006	ITRF00		27.5	12.9	0.398					
Bettinelli et al., 2006	ITRF00		26.45	13.99	0.354±0.015				3.4	7.8
Banerjee et al., 2008	ITRF00		28.146	21.770	0.408±0.014				0.56	2.71
THIS STUDY	1-Plate		27.600	21.405	0.404±0.011	2.12	0.36	92.4	0.37	2.38
THIS STUDY	nIND-EUR		24.059	4.462	0.331±0.029	11.98	0.75	108.8	3.97	12.58
THIS STUDY	sIND-EUR		27.089	25.853	0.431±0.018	2.72	0.40	86.2	0.44	3.05

NR - Parameters were not reported.

Table 3.4. Relative India-Australia Euler Pole Parameters

Reference	Reference Frame	# Sites Used	Latitude °N	Longitude °E	Rate ω °/Myr	σ_{maj}	σ_{min}	Azimuth	σ_{lat}	σ_{long}
IND-AUS										
DeMets et al., 1994	NUVEL-1A		-3.2	75.1	0.305±0.028	2.5	1.2	43		
Tinnon et al., 1995			-10.1	81.5	0.100±0.060	9.1	5.4	0		
Kreemer et al., 2003			-5.2	70.5	0.398±0.019	0.8	0.8	25		
DeMets et al., 2005			-4.9	73.1	0.318±0.036	3.9	1.5	39		
Delescluse et al. 2006	EQ+GPS		-21.0	81.3	0.064±0.020	11.9	4.2	-3		
Delescluse et al. 2006	ITRF00		-11.27	72.80	0.310±0.012	3.2	0.8	11.5		
Socquetet al., 2006	ITRF00		-6.6	73.7	0.397±0.028	3.3	0.7	11.3		
THIS STUDY	ITRF00		-14.418	70.623	0.350±0.003	1.4	0.7	170.4		

NR - Parameters were not reported.

Table 3.5. Sundland Euler Pole Parameters

Reference	Reference Frame	# Sites Used	Latitude °N	Longitude °E	Rate ω °/Myr	σ_{maj}	σ_{min}	Azimuth	σ_{lat}	σ_{long}
SUN										
Wilson et al., 1998	ITRF94	31.80	-46.00	0.280	NR	NR	NR			
Simons et al., 1999	ITRF96	51.00	-113.00	0.230	NR	NR	NR			
Michel et al., 2000	ITRF97	59.70	-102.70	0.340±0.010	2.9	3.9	NR			
Michel et al., 2001	ITRF97	56.00	-102.70	0.339±0.007	NR	NR	NR			
Simons et al., 2007	ITRF00	49.00	-94.20	0.336±0.007	1.9	0.3	111			
Sella et al., 2002	ITRF97	38.90	-86.90	0.393±0.062	10.2	0.8	110			
Kreemer et al., 2003	NNR	47.30	-90.20	0.392±0.008	1.9	0.5	109			
Bock et al., 2003	ITRF00	49.80	-95.90	0.320±0.010	3.5	1	121			
Prawiro et al., 2004	ITRF00	32.60	-86.80	0.462±0.064	7	0.8	113			
THIS STUDY	ITRF00	44.50	-85.83	0.342±0.0042	1.4	0.1	149.5			

NR - Parameters were not reported.

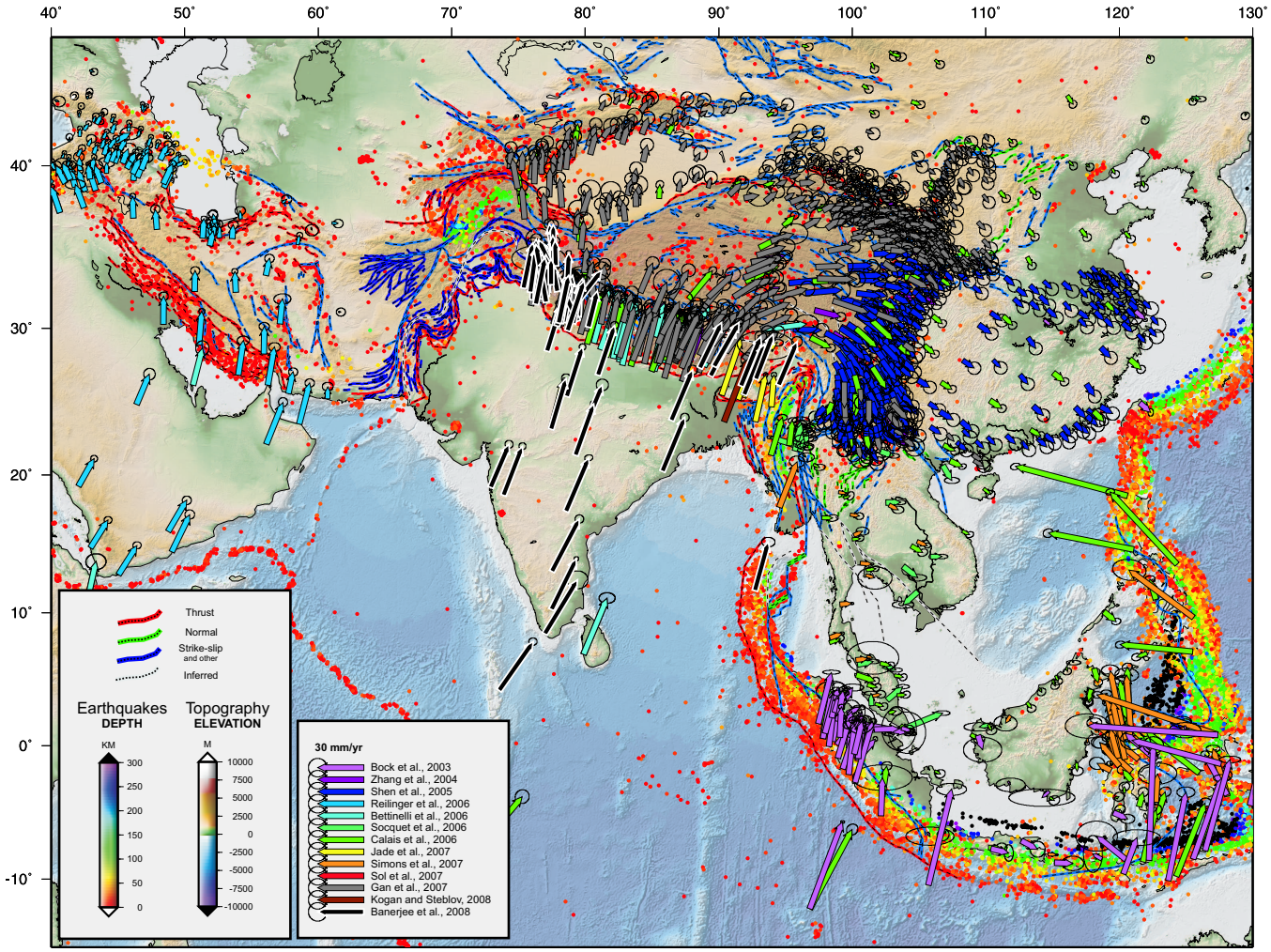

Figure 3.1. Observed GPS velocity field from our combined solution relative to a fixed Eurasia plate (see text for explanation). Velocity vectors are tipped with 95% error ellipses and colored by source (see legend). Earthquake hypocenters are from the updated (1964-2005) EHB catalog [*Engdahl et al.*, 1998] and are colored by depth. Crustal faults are from *Replumaz and Tapponnier* [2003] and colored by fault type.

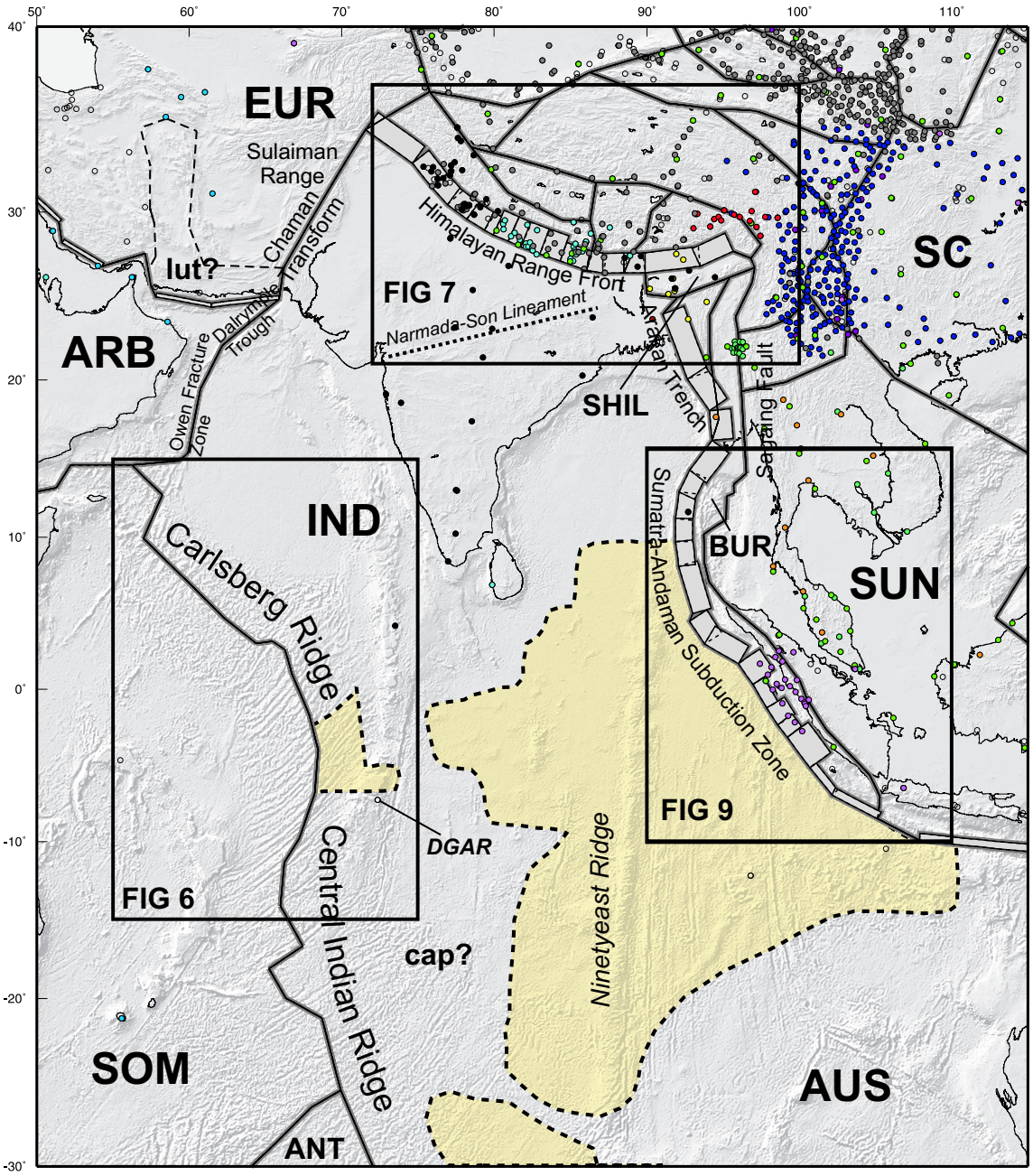

Figure 3.2. India block boundaries used in our block model inversion. Locked portions of dipping fault segments are shaded and shown projected into the horizontal. Circles show the locations of the GPS sites from our combined solution. Filled circles are sites colored by source (see legend in Figure 1) selected from our velocity combination (Figure 1) and used in our inversion (see text for explanation). Zones of diffuse deformation between the Indian and Australia plate are highlighted in yellow (modified from *Royer and Gordon* [1997]). Rectangular boxes enclose areas of more detailed study. Major blocks (uppercase) and geographic locations mentioned in the text are labeled.

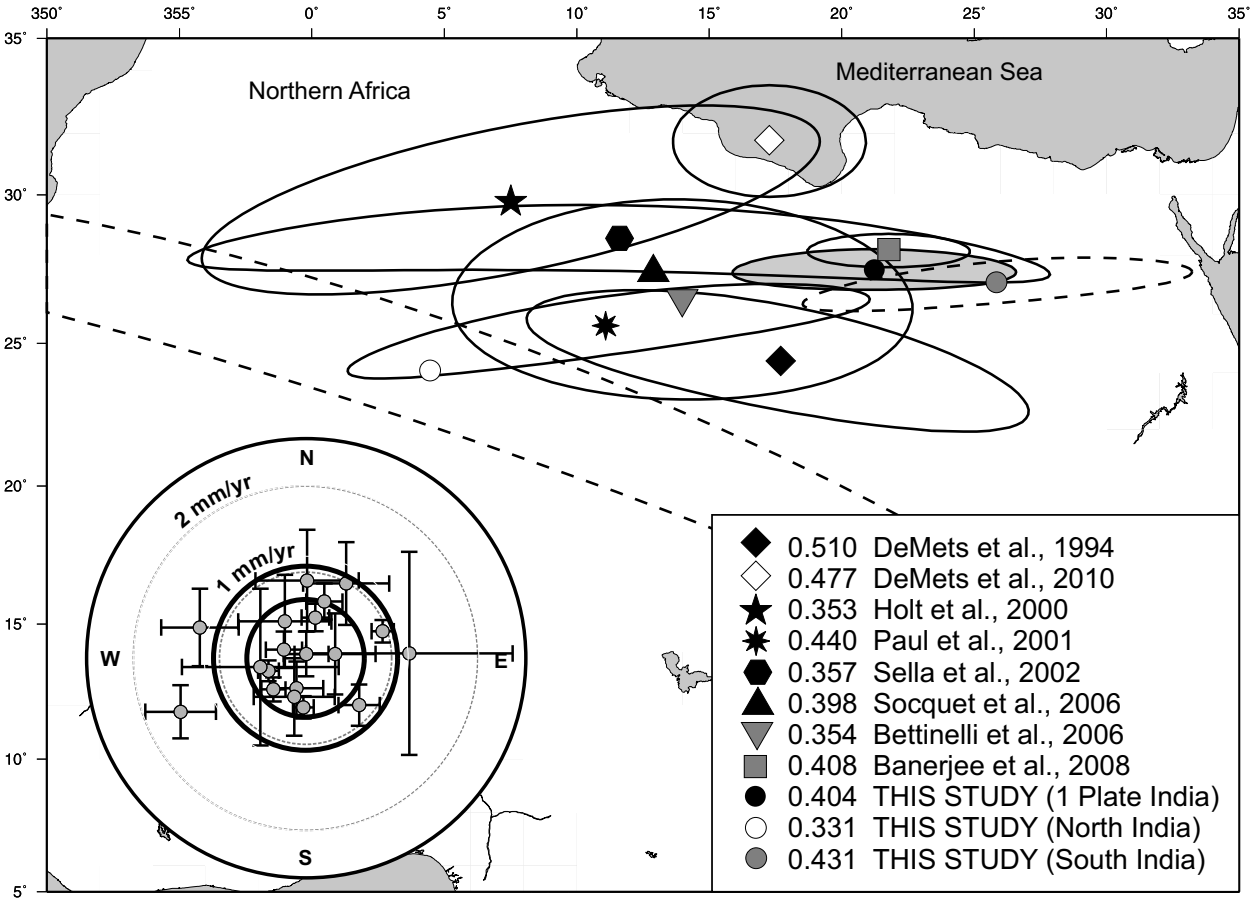

Figure 3.3. Relative India plate poles with respect to Eurasia (see Table 2 for pole details) with 95% error ellipses (uncertainties for *Socquet et al.* [2006a] were not reported). The rotation rate (counter-clockwise positive convention) of each pole is shown next to each poles source in the legend and reported in degrees per million years. We include the IND-EUR pole from our preferred model as well as the nIND-EUR and sIND-EUR poles from our 2-block India model (shaded ellipses). Inset figure shows vector components and 1-sigma error bars of the residual velocities for the stable interior sites of the Eurasia block. All Eurasian residuals are less than 2 mm/yr. Dark concentric circles represent the mean plus 1-sigma uncertainty bounds for misfit values.

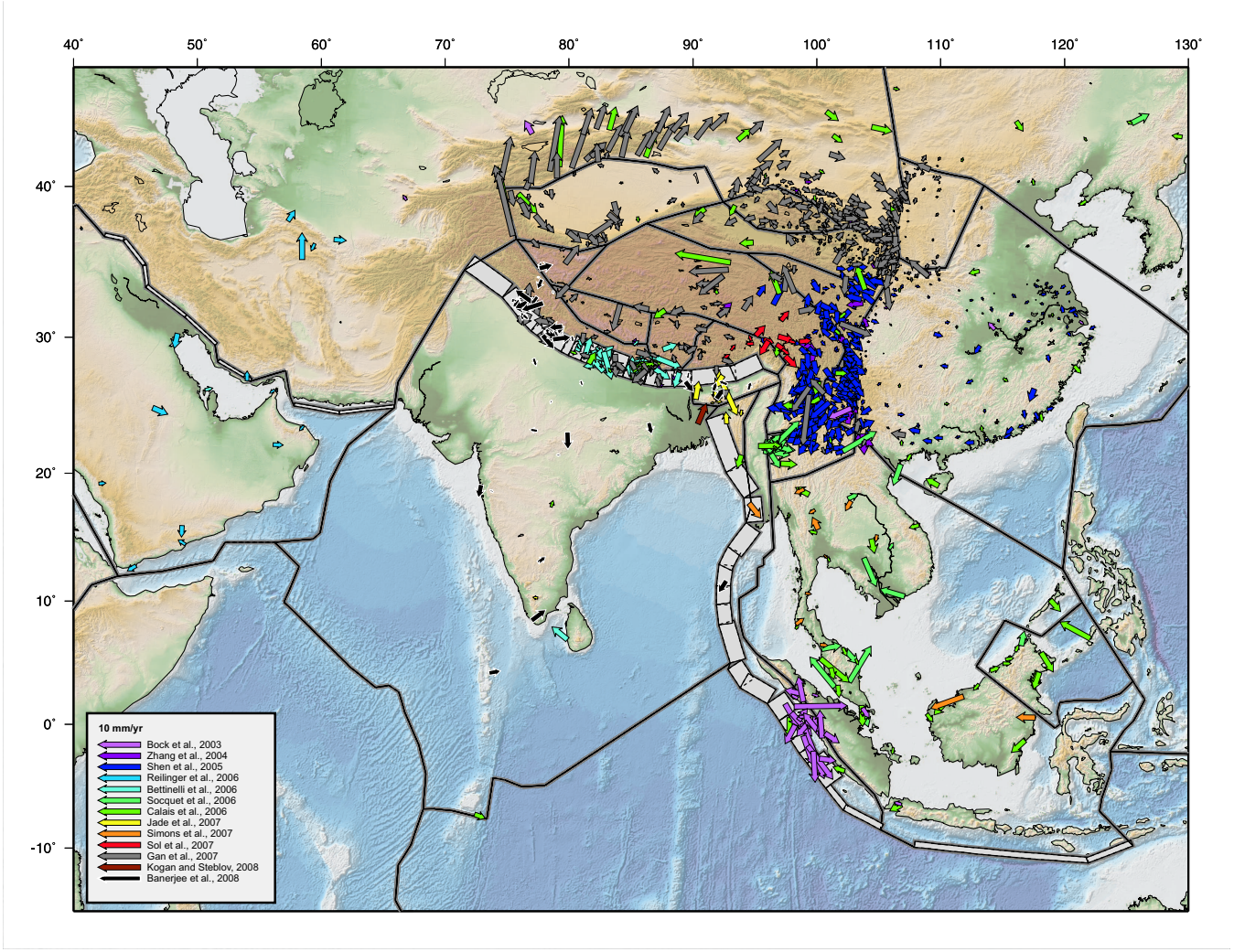

Figure 3.4. Residual Velocities and segment boundaries from preferred model. Locked portions of dipping fault segments are shaded and shown projected into the horizontal. Velocity vectors are colored by source (see legend).

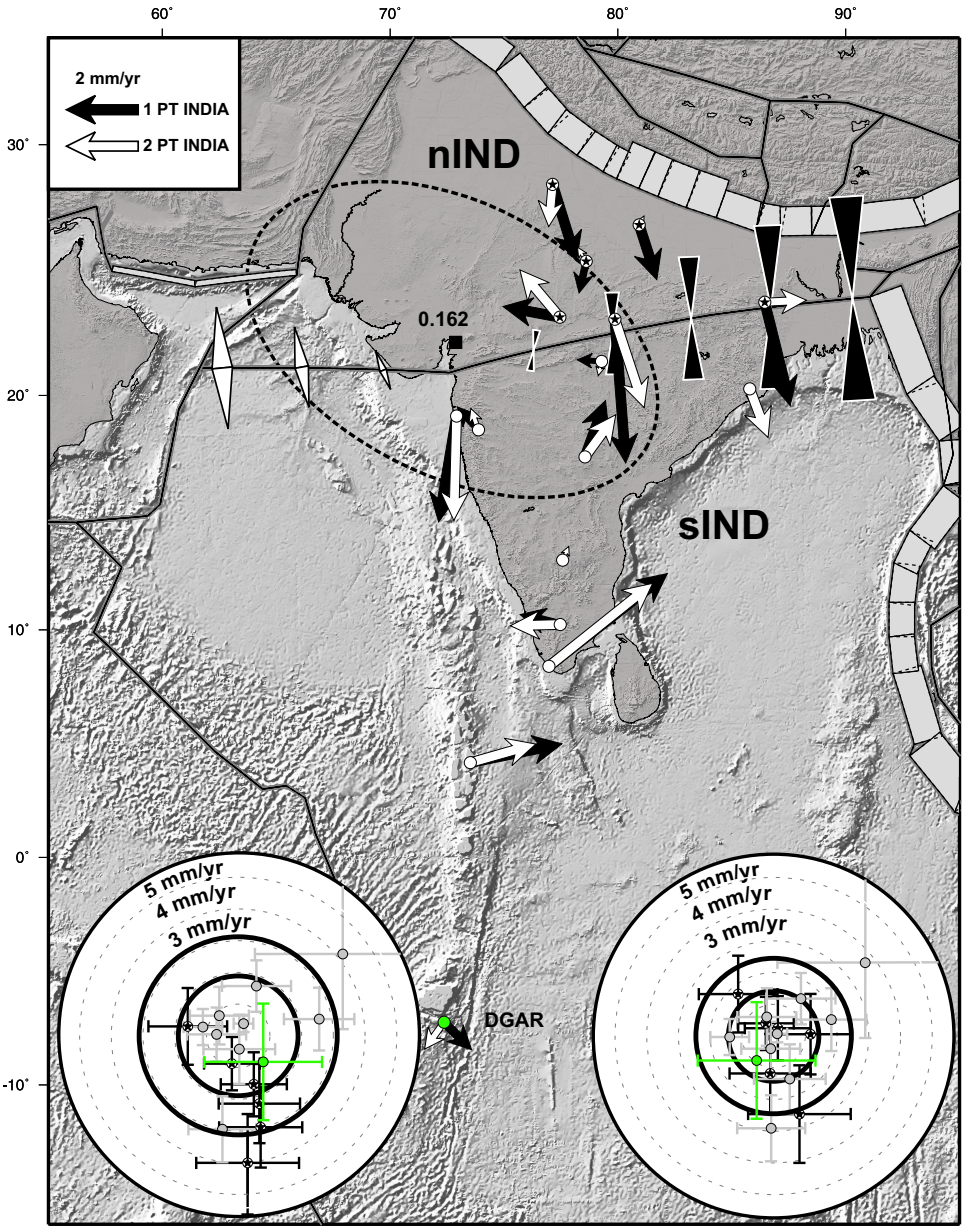

Figure 3.5. Indian GPS Residual Velocities. Residual velocities shown for the 1-block India model (black vectors) and the 2-block India model (grey vectors). Separation of the India block (grey line) is along the Narmada-Son lineament in central India. The relative pole of rotation for the 2-block India model is shown in the west with a 95% error ellipse. The rotation rate of 0.162 deg/My predicts contraction along the Narmada-Son line from 5 mm/yr in the east to 0 mm/yr near the pole in the west (black triangles). Inset figures show the residual components of the velocities. Residual velocities from DGAR are also shown on the map and in the inset plot (green) but are not used in the India plate angular velocity estimation. Dark concentric circles represent the mean plus 1-sigma uncertainty bounds for misfit values. Sites located north of the Narmada-Son line are marked with stars and southern sites are marked with grey circles.

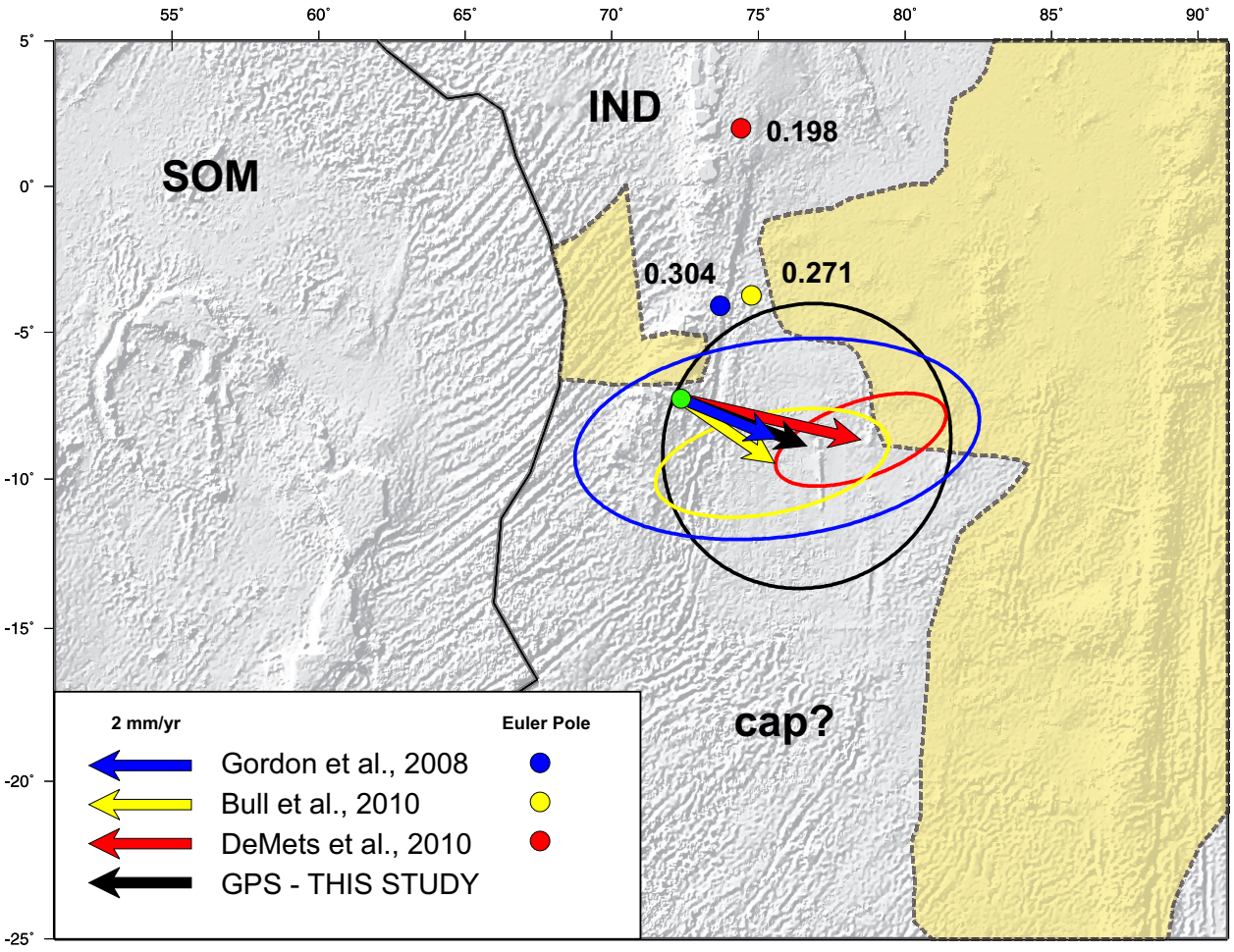

Figure 3.6. Capricorn velocities and Euler poles at the Diego Garcia station (DGAR) Somalia, India, and Capricorn plate boundaries are shown with zones of diffuse deformation (yellow) from *Royer and Gordon* [1997]. Relative CAP-IND Euler poles are also shown for three published poles [*Gordon et al.*, 2008; *Bull et al.*, 2010; *DeMets et al.*, 2010] with rotation rates in deg/My. Pole error ellipses are excluded for the sake of brevity. Predicted Capricorn plate velocities with respect to a fixed India plate and 68% error ellipses for the DGAR site are shown for the three poles. The DGAR velocity (black) is shown in a fixed India reference frame (this study) for comparison.

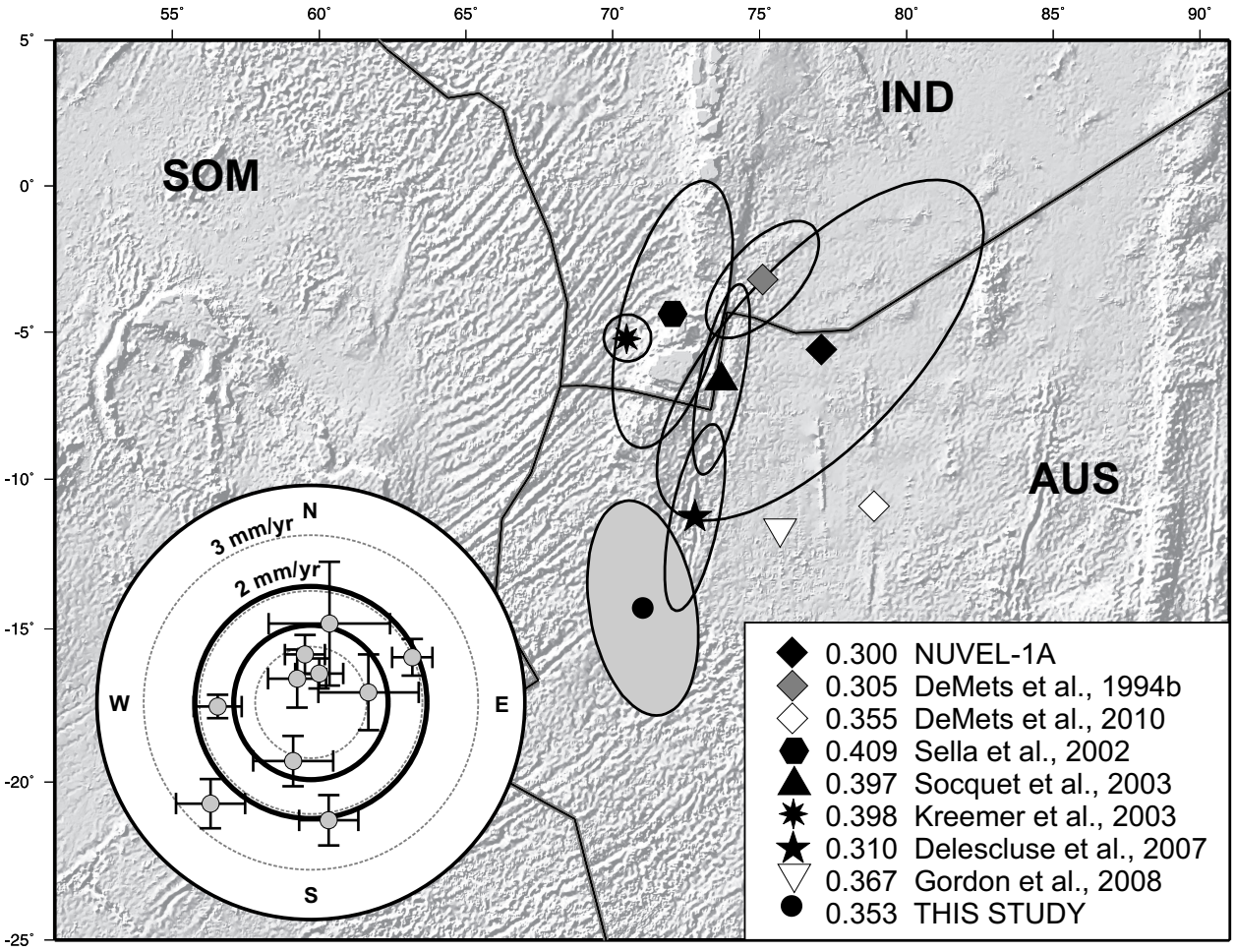

Figure 3.7. Relative Australian plate poles with respect to India (see Table 2 for pole details) with 95% error ellipses. The rotation rate (counter-clockwise positive convention) of each pole is shown next to each pole's source and reported in degrees per million years. Inset figure shows vector components and 1-sigma error bars of the residual velocities for the stable interior sites of the Australian block. DGAR is also shown in the inset plot (light grey) but is not used in the Australia plate angular velocity estimation. Dark concentric circles represent the mean plus 1-sigma uncertainty bounds for misfit values.

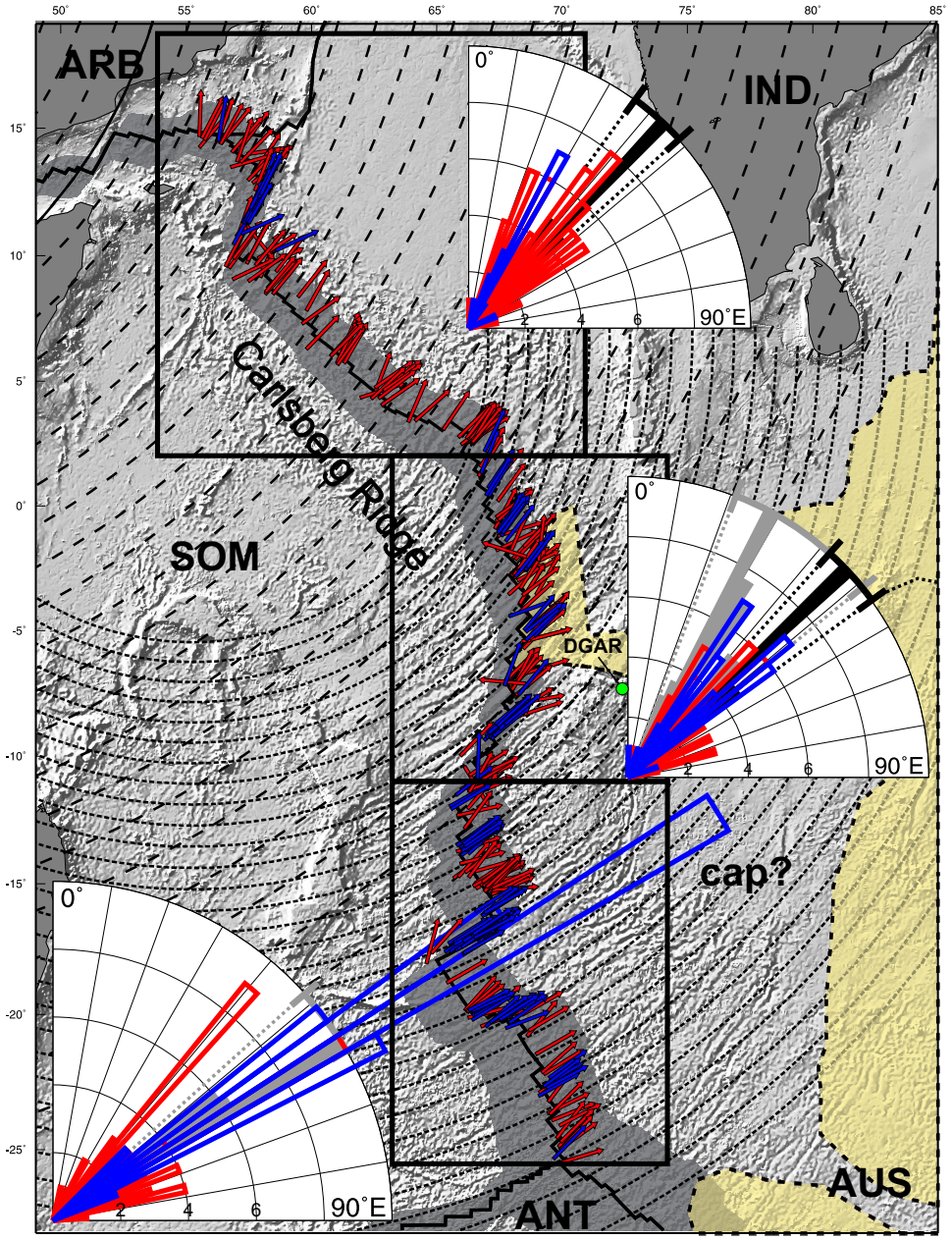

Figure 3.8. India-Somalia (Carlsberg Ridge) and Australia-Somalia (Central Indian Ridge) divergent plate boundaries. Oceanic crust from 0-10 Mya is highlighted in grey along the ridges. Small circles represent the predicted relative plate motion direction and displacement rates from our preferred model for both the IND-SOM and AUS-SOM block pairs. The small circles are generally perpendicular to the isochrons along the ridges and parallel to submarine transform faults (see text for explanation). Slip vectors (dip-slip in red, null axis plunge <45 degrees and strike-slip in blue, null axis plunge >45 degrees), calculated from historic moment tensors, (www.globalcmt.org) are shown at the focal mechanism location. Inset figures show slip vectors in 3 degree bins and are also generally parallel to the plate motion orientation. Azimuthal histograms compare slip vector orientation (dip slip in red and strike slip in blue) with predicted plate motion vectors (SOM-IND in black and SOM-AUS in grey). Zones of diffuse deformation are shown in yellow [*Royer and Gordon*, 1997, modified from].

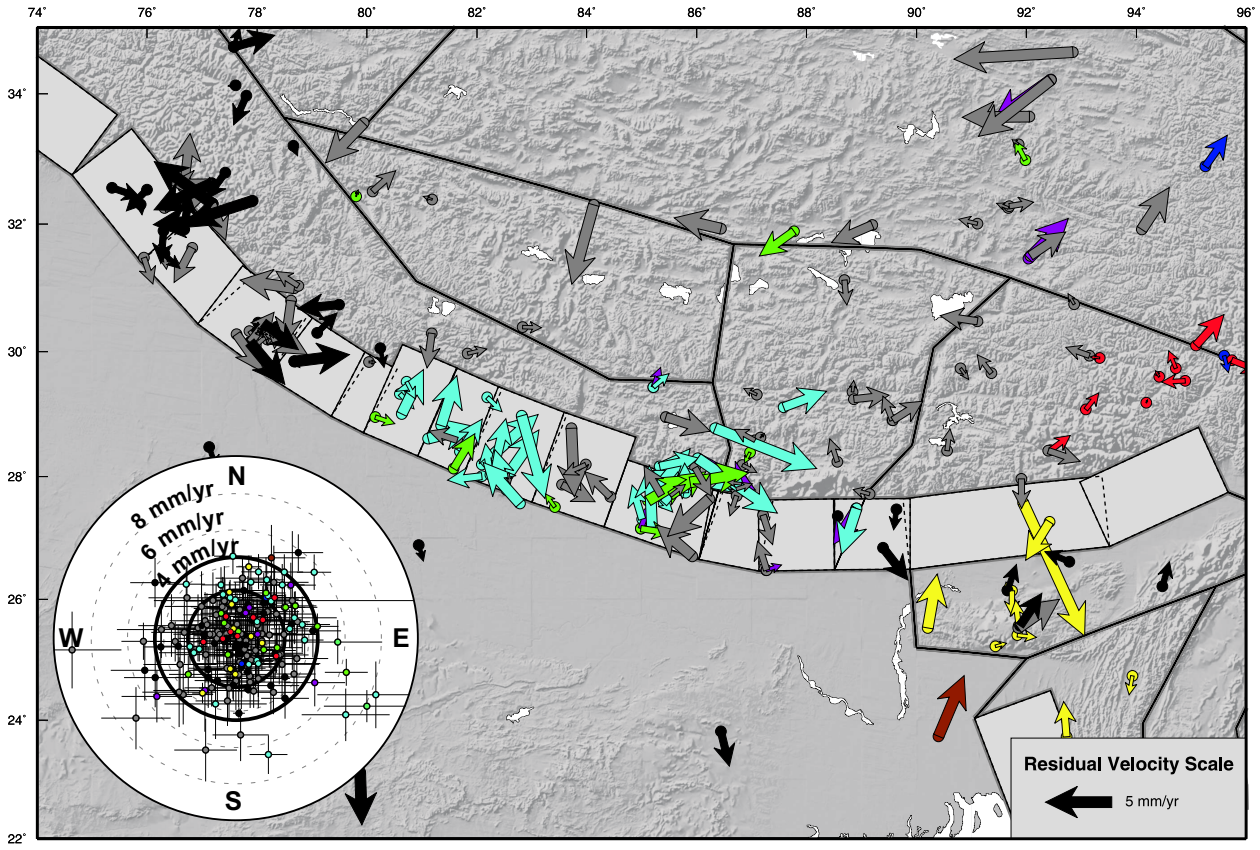

Figure 3.9. Residual velocities and GPS station locations along the Himalayan range front, sites are colored by source (see legend in Figure 1). Our preferred block model boundaries are shown with dipping segments of the locked portion of the Himalayan thrust faults projected into the horizontal. The 3500-m elevation contour line is also shown for reference. Along the Himalaya fault segments dip at 8 degrees and are locked to 18 km, with the exception of the central HRF. In the central section segment dip shallower at 6 degrees. Inset bull's-eye figure shows the residual velocities for the stations on the map. Dark concentric circles represent the mean plus 1-sigma uncertainty bounds for misfit values.

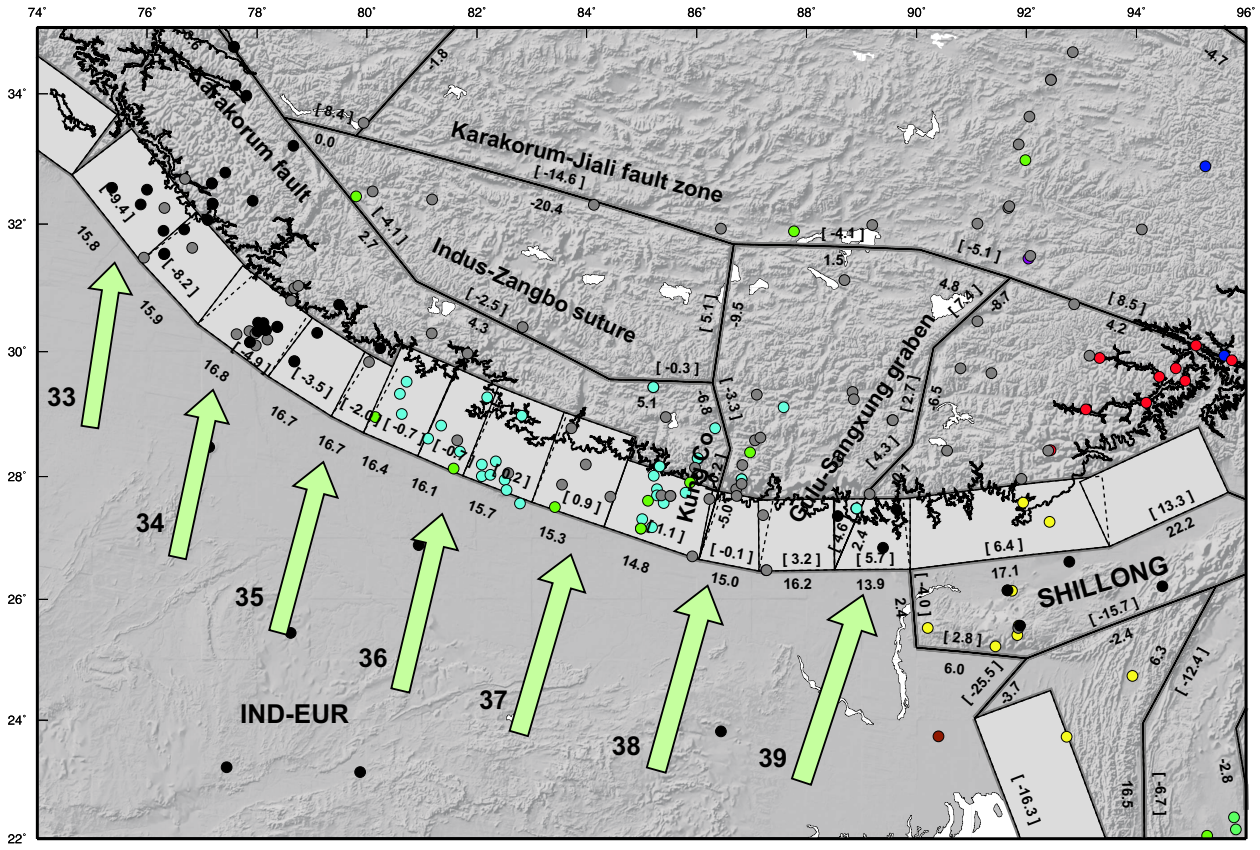

Figure 3.10. Slip rates and GPS station locations along the Himalayan range front. Our preferred block model boundaries are shown with dipping segments of the locked portion of the Himalayan thrust faults projected into the horizontal. Slip rates in brackets above the fault segments are the strike-slip component with a positive-left lateral convention, dip-slip rates are provided below each segment (thrust motion positive). The 3500-m elevation contour line is also shown for reference. Significant structures and blocks (mentioned in the text) are also labeled. Relative plate motion vectors (IND-EUR) from our preferred model are shown in green. The magnitude of each velocity is shown next to each vector.

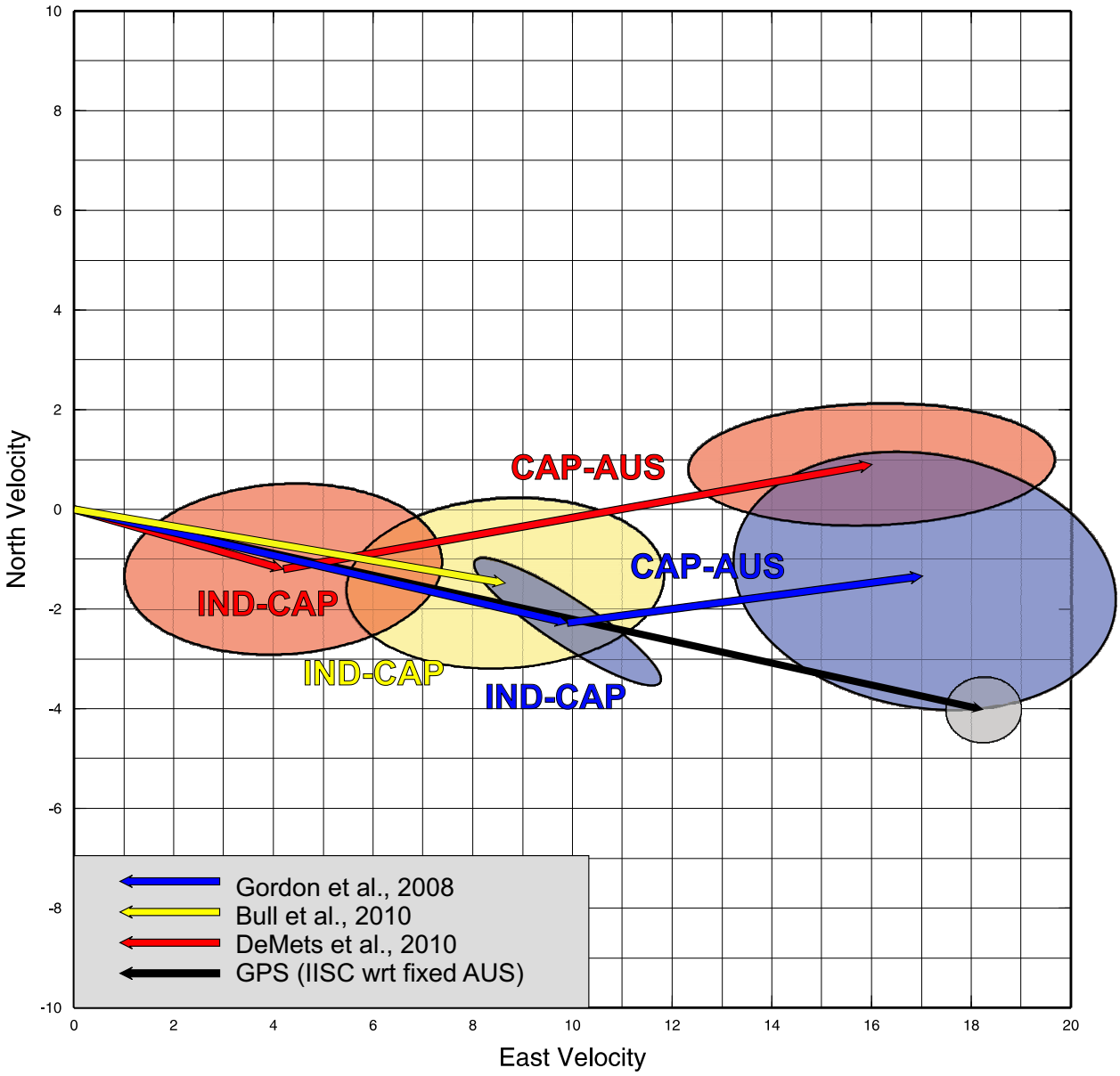

Figure 3.11. Predicted IND-CAP-AUS Velocities at the Bangalore (IISC) GPS station IND-CAP and CAP-AUS plate motions are shown in blue, yellow, and red for the three published poles of *Gordon et al.* [2008]; *Bull et al.* [2010]; *DeMets et al.* [2010], respectively(*Bull et al.* [2010] does not report a CAP-AUS pole).The GPS velocity of the IISC station is also shown with respect to a fixed Australia reference frame. All predicted IND-CAP vectors are significantly slower than the oversexed GPS velocity. Only the vector summation of the *Gordon et al.* [2008] IND-CAP and CAP-AUS plate motion vectors are consistent with the measured velocity at the IISC station.

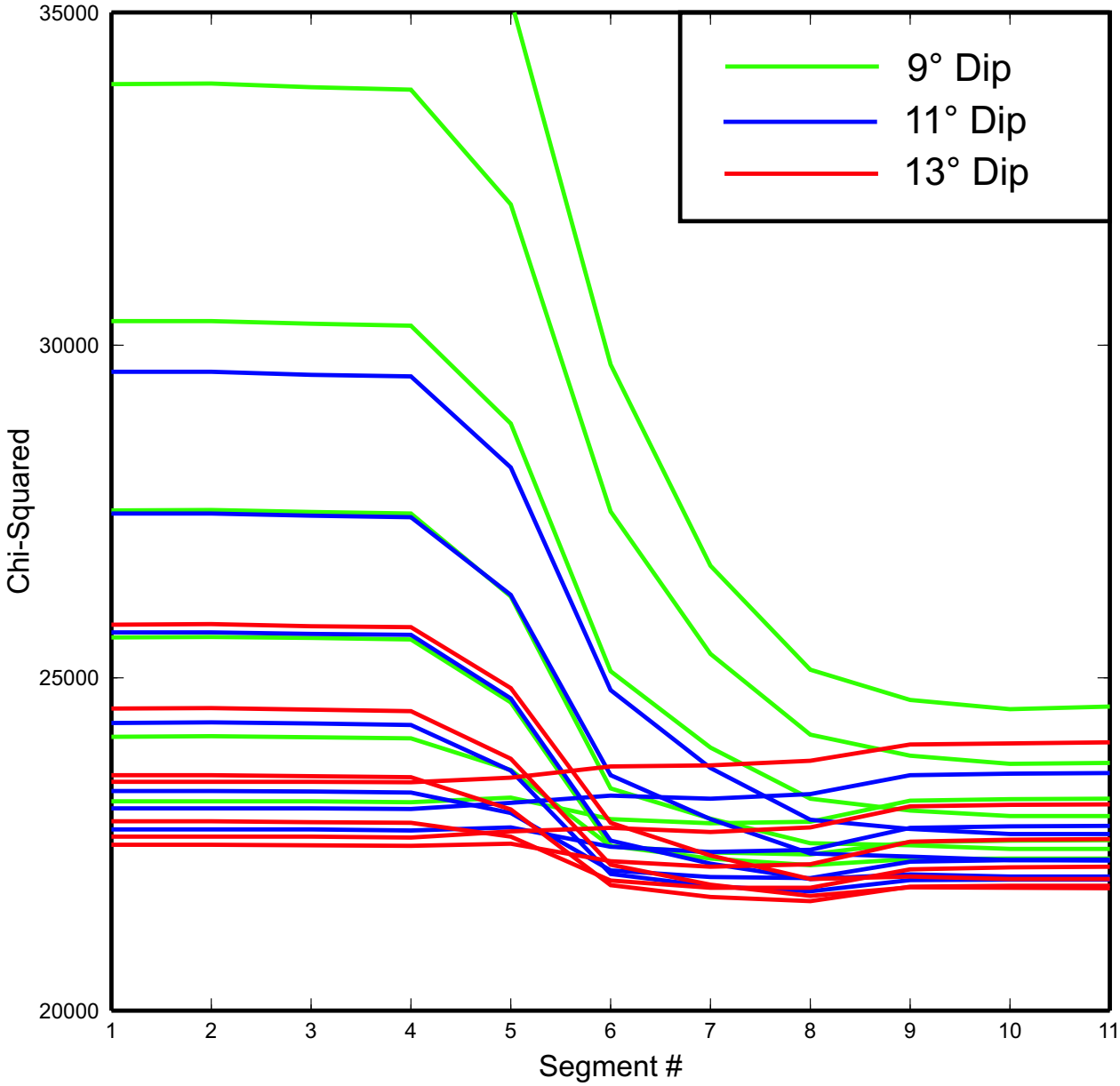

Figure 3.12. Lines show the value of the misfit statistic (chi-squared) at each segment location (Figure 9) for constant locking depths (20-50 km). Lines are colored by depth.

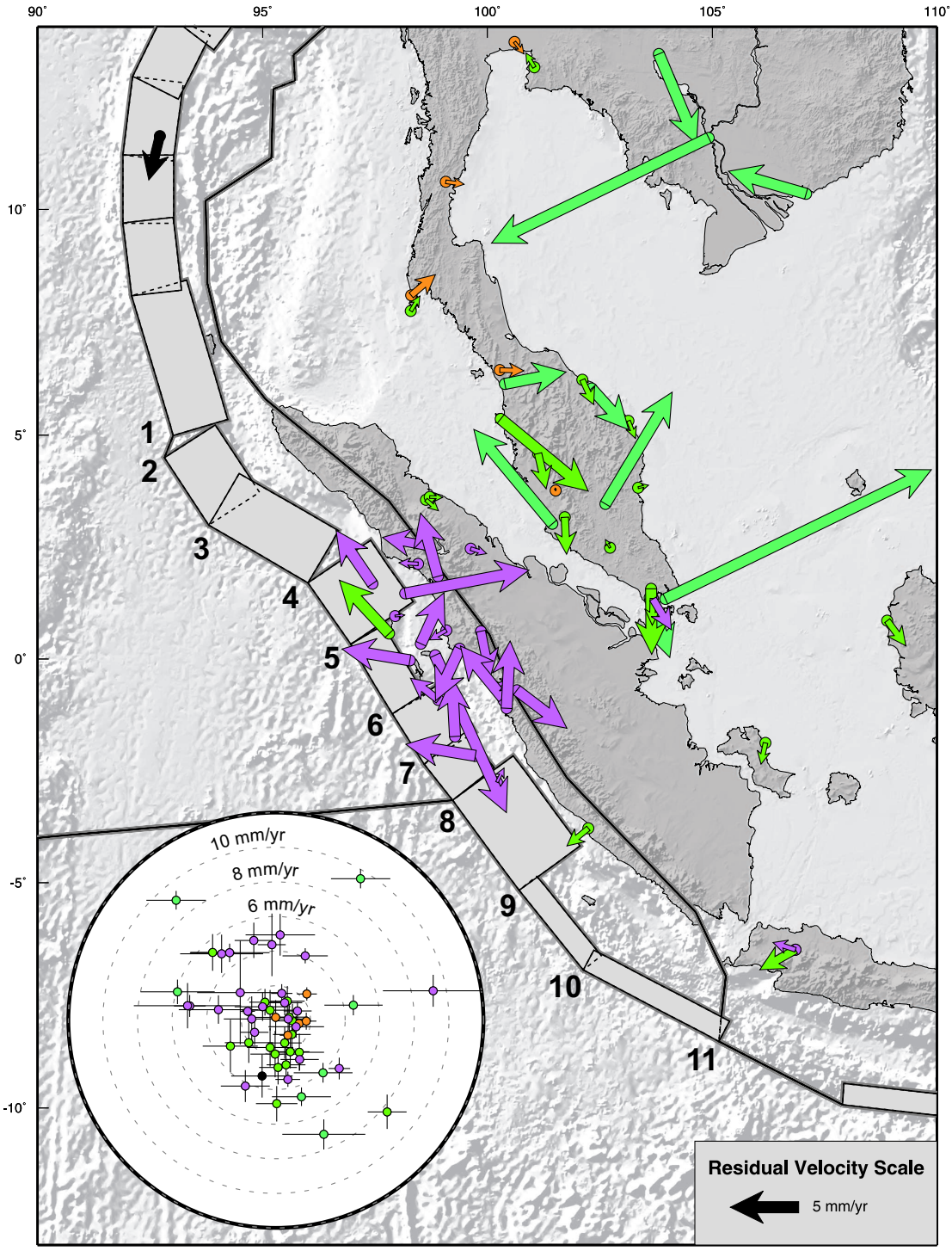

Figure 3.13. Residual Velocities and GPS station locations along the Sumatra subduction zone and backarc, sites are colored by source (see legend in Figure 1). Our preferred block model boundaries are shown with dipping segments projected to the surface. Slip rates in brackets above the fault segments are the strike-slip component with a positive-left lateral convention, dip-slip rates are provided below each segment (thrust motion positive). Inset bull's-eye figure shows the residual velocities for the stations on the map. Dark concentric circles represent the mean plus 1-sigma uncertainty bounds for misfit values. Segment intersection locations are numbered from north to south (see text for discussion).

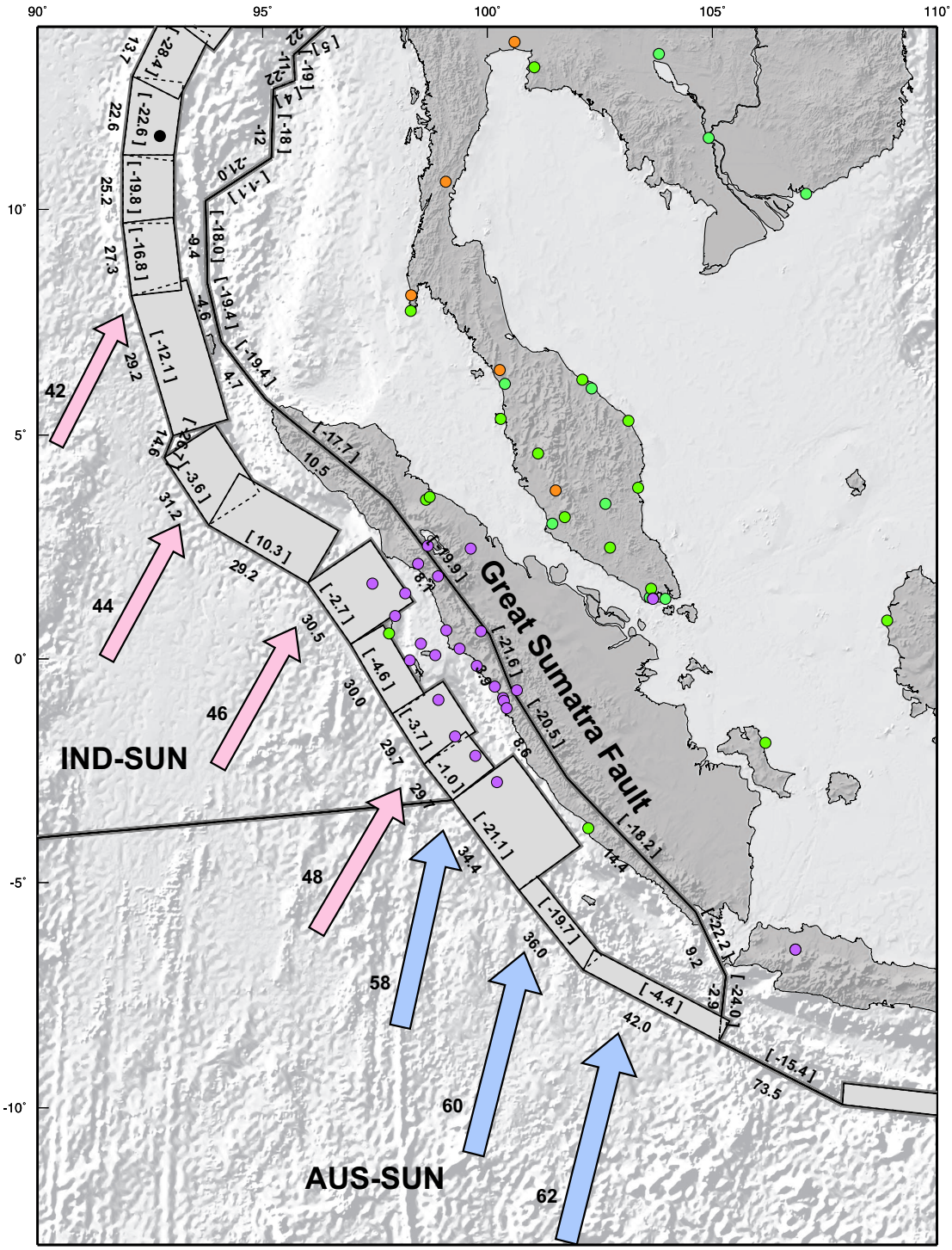

Figure 3.14. Slip rates and GPS station locations along the Sumatra subduction zone and backarc, sites are colored by source (see legend in Figure 1). Our preferred block model boundaries are shown with dipping segments projected to the surface. Slip rates in brackets above the fault segments are the strike-slip component with a positive-left lateral convention, dip-slip rates are provided below each segment (thrust motion positive). Significant structures and blocks (mentioned in the text) are also labeled. Relative plate motion vectors (IND-SUN and AUS-SUN) from our preferred model are shown in red and blue, respectively. The magnitude of each velocity is shown next to each vector.

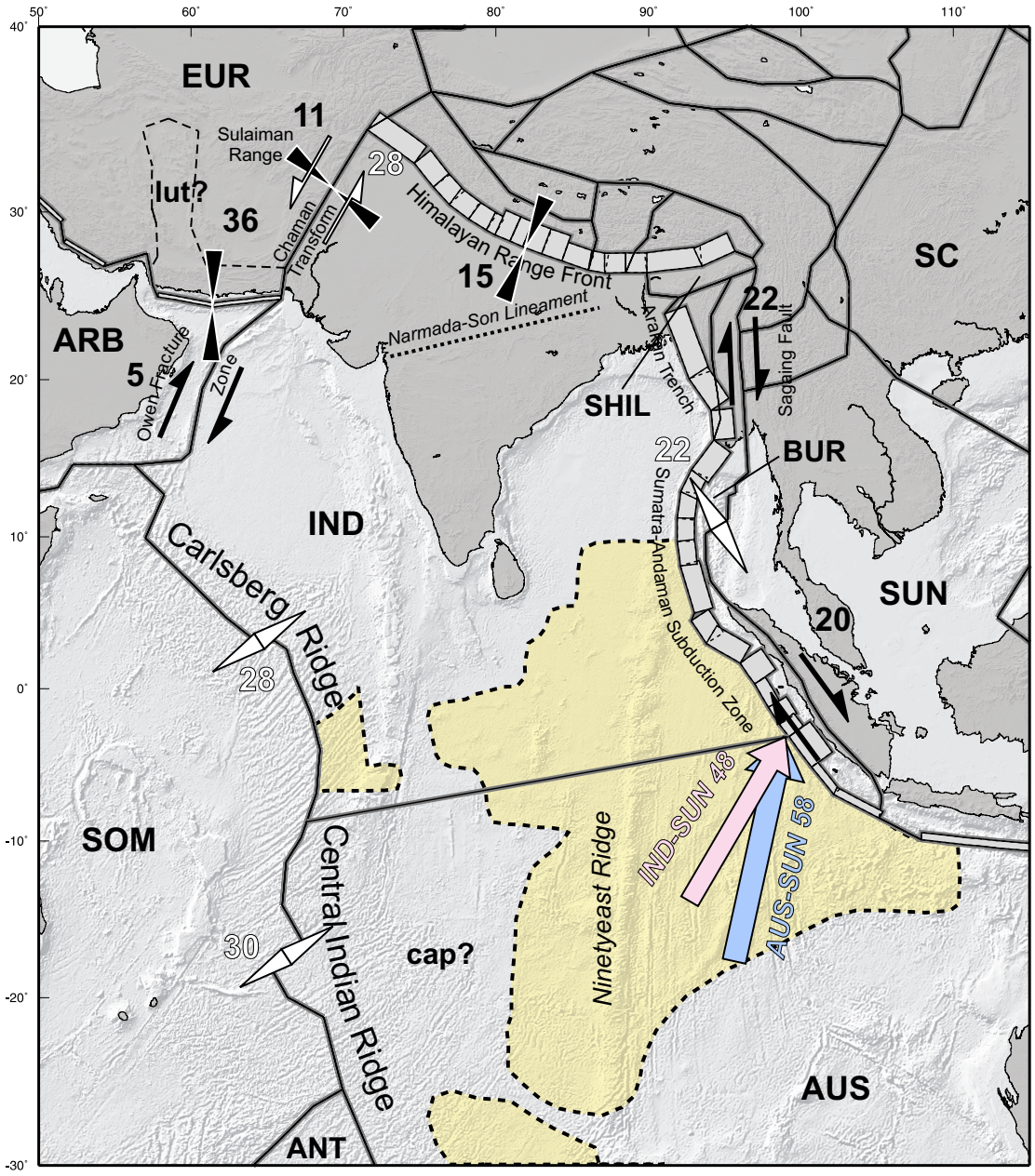

Figure 3.15. Selected slip rates from our preferred model. Contractional rates are shown by black triangles and extensional rates in white. Dextral rates are shown in black and sinistral rates are shown in white. India block boundaries used in our block model inversion are shown with locked portions of dipping fault segments shaded and shown projected into the horizontal. Zones of diffuse deformation between the India and Australia plates are highlighted in yellow (modified from Royer and Gordon, 1997). Major blocks (uppercase) and geographic locations mentioned in the text are labeled.

Chapter 4

Hellenic Subduction

4.1 Abstract

We combine available GPS data in and around the Aegean region to evaluate models of plate motions and elastic plate boundary deformation and seismogenic coupling constrained by the observed velocity field. Previously, GPS data in the region have been used as evidence that a southern Aegean block behaves rigidly with little to no coupling along the Hellenic subduction zone. These first-order models match the observed GPS data quite well, suggesting little intra-plate or plate-boundary deformation. However, the A.D. 365 M ˜8.4, the A.D. 1303 M ˜8 Crete and other large historic earthquakes that occurred along the Hellenic subduction zone suggest that portions of the plate interface or some portion of the subduction system (synthetic splay faults) must be locked. Depending on the elastic locking required to generate earthquakes of this magnitude, a measureable elastic arc-normal contraction of the overriding plate should be evident in the surface velocity field. However, it is possible that the surface deformation generated by convergence at a locked subduction zone is masked by simultaneous extension in the hangingwall of the southward retreating subduction zone, creating the illusion of rigid block motion. The primary focus of this study is to examine potential upper plate deformation resulting from a locked subduction interface, active hanging-wall extension, or both. We consider multiple model scenarios in an attempt to interpret the current geodetic signal in the region and its implications for earthquake hazard assessment. We use a block modeling approach that considers both rigid rotations of plates and elastic strain fields along plate boundary faults to examine the possible trade-off between these components. We parameterize the geometry of the subduction thrust based on seismic studies, but also consider the impact of variations in dip on the model results. We generate multiple models to explore the solution space of all reasonable parameters. Our modeling suggests that it is not possible for contemporaneous extension and convergence to occur across a micro-plate masquerading as rigid block motion. The horizontal GPS data

alone do not unambiguously document that the Hellenic subduction zone is effectively uncoupled. We use parameters from the solution space to test predicted vertical rates across the Aegean from these models and compare them to measured GPS vertical rates in attempt to reconcile the recurrence of large earthquakes along the Hellenic arc with apparent block-like (aseismic) motion of the Aegean.

4.2 Introduction

The Aegean plate is nestled in between the converging Nubia and Eurasia plates in the Eastern Mediterranean. The Aegean plate is composed mostly of thinned continental crust resulting from Cenozoic extension which opened the Aegean Basin north of the retreating Hellenic subduction zone. [*Faccenna et al.*, 2003; *Ring et al.*, 2010]. GPS measurements suggest that the Aegean plate moves approximately 34 mm/yr south-southwest with respect to a fixed Nubian plate [e.g. *McClusky et al.*, 2000; *Reilinger et al.*, 2006; *Floyd et al.*, 2010] as the oceanic crust, south of the Hellenic trench subducts beneath the Aegean plate along the Hellenic subduction zone (Figure 4.1).

The Hellenic subduction zone is outlined well by small to moderate earthquakes from the instrumental record (Figures 4.1 and 4.2) with no events M>7. However, in A.D. 365 a M_W ~8.4 [*Shaw et al.*, 2008] earthquake ruptured offshore of western Crete. This event generated static uplift in western Crete as large as 9 to 11 meters and caused a tsunami that reached as far south as the Nile Delta [*Ambraseys et al.*, 1994]. In addition, a M ~8 in A.D. 1303 [*Hamouda*, 2006] was also thought to have ruptured along the Hellenic subudction zone east of Crete causing a tsunami. While the smaller events outline a typical Benioff zone subduction geometry (Figure 4.2). Focal mechanisms along the trench for most these events are also consistent with the subduction in the region.

Several geodetic studies of the Aegean region suggest that the region is behaving coherently as a rigid block with very little to no elastic strain accumulation occurring along the Hellenic subduction zone [*McClusky et al.*, 2000; *Nyst and Thatcher*, 2004; *Reilinger et al.*, 2006, 2010]. *McClusky et al.* [2000]; *Nyst and Thatcher* [2004] see good agreement between measured GPS velocities and modeled velocities from rigid Aegean block inversions and do not attempt to explicitly examine the subduction zone coupling. Other studies [*Jackson and Mckenzie*, 1988; *Shaw and Jackson*, 2010] state that 10-20% of the convergence is stored as elastic strain based on the moment release from the last one hundred years of seismicity. Likewise, *Reilinger et al.* [2010] model the interseismic elastic strains and suggest that the Hellenic subduction zone is not locked shallowly and less than 20% coupled at depths between 20 and 40 km. On the other hand *Ganas and Parsons* [2009] suggest that the interface is fully coupled.

Here, we use GPS data in the region to construct a kinematic model to examine the potential amount of locking and seismogenic coupling along the Hellenic subduction zone. We processed new data from continuously operating stations in the area and integrate additional published GPS velocities to construct a comprehensive solution in a fixed Nubia reference

frame. We invert this GPS data in a simple block model in order to estimate the amount of strain contributed to each velocity by rigid block motion and elastic strain accumulation along block boundaries.

We consider the possibility that an interseismic contractional signal associated with a (partially) locked subduction thrust could be masked by concurrent extension of the southernmost Aegean in the hanging wall creating a pattern in the GPS velocities that appears as rigid block motion. We test this hypothesis in an effort to estimate the magnitude of seismogenic coupling along the Hellenic subduction zone and estimate maximum probable earthquakes for the region. We show that some locking may exist along the Hellenic subduction zone. We also show that contemporaneous extension and contraction is not likely as it requires unreasonably deep locking depths and contraction along the hanging-wall structures.

A locked subduction zone produces vertical deformation patterns that can be used to independently evaluate the degree and width of locking across the Hellenic subduction thrust [e.g. *Matsu'ura and Sato*, 1989; *Aoki and Scholz*, 2003; *Chlieh et al.*, 2008]. At present we have few vertical data, which can be used to further validate potential coupling scenarios. However, detailed paleo-shoreline studies, repeating earthquakes, episodic slow slip, and seafloor geodesy may be better suited to ultimately constrain the amount of coupling along the Hellenic trench.

4.2.1 Seismicity

The southern Aegean is one of the most seismically active regions in Europe. Seismicity in the region is dominated by the subduction of Nubia plate under the Aegean plate (Figures 4.1 and 4.2). In the instrumental record a Wadati-Benioff zone, extending to depths over 100 km is plainly identified [*Papazachos et al.*, 2000; *Meier et al.*, 2004]. However, complexities in the seismicity patterns show lateral variations [e.g. *Bohnhoff et al.*, 2005], variable seismogenic thicknesses, and some aseismic regions [*Meier et al.*, 2004]. In addition, historic and ancient seismicity patterns suggest potential temporal clustering [*Stiros*, 2001]. Along the Hellenic subduction zone no earthquake larger than magnitude 6.9 has been recorded in instrumental history nor has an earthquake larger than magnitude 7.3 been inferred in the last 400 years [*Stiros and Papageorgiou*, 2001].

Historic Seismicity

Evidence of large earthquakes (M 7+) can be seen in the historic (e.g. M_S 7.3 in 1903 - *Ambraseys* [2001] and ancient records (e.g. M ˜8 1303 *Hamouda* [2006]; M 8.4 365 A.D. *Shaw et al.* [2008] Historical accounts, sedimentological and geomorphic data, and archeological evidence have all contributed to a catalogue of earthquakes that predate the instrumental record 550 BC 1899 AD [*Papazachos and Papazachou*, 1997]. A number of large events in this region suggest that the subduction zone has generated large ruptures within the last 4000 years. Of particular note is the A.D. 365 earthquake that occurred in Western

Crete. This M>8 event is considered to be the largest earthquake recorded in ancient or instrumental times in this region [*Burton et al.*, 2004]. The earthquake generated 9-11 m of uplift along the southwestern coast of Crete [*Thommeret et al.*, 1981; *Pirazzoli et al.*, 1996; *Stiros*, 2001]. *Shaw et al.* [2008] attempt to model the displacements of the 365 A.D. earthquake using shallowly dipping planes (approximately 20°) that are parallel with the subduction interface. A subduction zone rupture from the surface to a depth of 45 km would require 40 m of slip for that event to generate the observed amount of uplift. Instead, *Shaw et al.* [2008] conclude that the 365 A.D. earthquake likely ruptured a steeper dipping thrust (approximately 30°). *Stiros* [2010] presents an alternative fault model that dips 40° and ruptures to a depth of 70 km with only 16 meters of slip. *Stiros* [2010] suggests that the strike of the fault need not necessarily be constrained, a priori, by the strike of the Aegean Arc.

Subduction Zone Geometry and Slip

The instrumental seismic record for this region is relatively complete for large magnitude events and contains earthquakes down to approximately magnitude 4.0 since 1900 [*Burton et al.*, 2004]. Instrumental seismicity clearly outlines distinct tectonic boundaries such as the Hellenic subduction zone, the Corinth rift and the north Anatolian fault in northern Turkey. In cross section (Figure 4.2) it is quite clear that these events outline a Benioff zone consistent with a subducting slab. Along the Hellenic arc between the Ionian Sea and Rhodes, *Bohnhoff et al.* [2005] find events with shallowly N-NNE dipping nodal planes consistent with N12°±15°E directed slip on the subduction interface. In the Aegean region shallow upper crustal seismicity is substantially more defuse likely related to an actively extending Aegean crust. *Bohnhoff et al.* [2005] showed active east-west extension in Crete via stress-tensor inversions from focal mechanisms. The extension becomes oriented more ENE-WSW in the central Aegean, north of Crete. Focal mechanisms along the Gulf of Corinth, in the central Aegean, and western Turkey (Figure 4.1) outline the active N-S extension in this region approximately parallel with the volcanic arc (Figure 4.2).

Focal mechanisms along the Hellenic subduction zone are consistent with active contraction, however lack of large megathrust events along the Hellenic subduction zone may suggest that the subduction is largely aseismic or uncoupled, or that recurrence times between large megathrust events is significantly longer than our observations. It is also possible that the deformation in the region is partly accommodated on secondary structures within the hanging wall or upper crust of the Aegean plate. Such splay faults are not uncommon and have been imaged in other subduction zones around the world [e.g. *Park et al.*, 2002; *Mountjoy and Barnes*, 2011]. The fault models of the A.D. 365 earthquake from *Stiros et al.* [2006]; *Papadimitriou and Karakostas* [2008]; *Shaw et al.* [2008]; *Stiros* [2010] are also consistent with a steeper dipping plane then the megathrust interface. Although the rupture did not occur along the interface, this region of the Aegean clearly has the potential for generating large tsunamigenic earthquakes.

Along the Hellenic subduction the most active region appears to be the western edge where the largest and most frequent earthquakes have occurred (Figure 4.1). *Laigle et al.*

[2002] suggest that in the Ionian Islands region the subduction zone is fully coupled. They see strong a reflector in seismic reflection data and collocated hypocenters to suggest that this reflector is the plate interface and has strong seismogenic character to depths of 15 km. They see evidence for a deeper downdip limit and suggest that the slab has broken off [*Laigle et al.*, 2004]. In addition, micro-earthquakes recorded from their temporary array show focal mechanism solutions consistent with a downgoing slab. Using the narrow seismically imaged interface locked to 15 km *Laigle et al.* [2002] show that predicted moment release along this zone is consistent with the recorded seismicity along the western Hellenic subduction zone. However, farther south a deeper downdip limit of the interface appears to be deeper indicated by deeper thrust events (Figure 4.1) and suggested by *Laigle et al.* [2004]; *Bohnhoff et al.* [2005]; *Shaw and Jackson* [2010]. A larger downdip rupture area is consistent with possible large magnitude earthquakes [*Shaw et al.*, 2008; *Stiros*, 2010, e.g.]. However, the seismic moment release rate does not seem to support regular recurrence of such large (M>8) events [*Jackson and Mckenzie*, 1988; *Laigle et al.*, 2004; *Shaw and Jackson*, 2010] and consequently suggest that the subduction interface is largely uncoupled.

4.3 GPS Velocities

4.3.1 GPS Data Processing

We process and combine epoch GPS data collected from 1991 to 2004 [*Serpelloni et al.*, 2005] and references therein for details on the networks used) and CGPS data from publicly available networks in the Euro-Mediterranean region for the 1996-2011.2 period, in order to determine a uniform velocity solution.

We analyze GPS observations following a distributed processing approach, using the GAMIT/GLOBK software [*Herring*, 2005; *King and Bock*, 2005]. Position time-series are analyzed by means of the QOCA software [*Dong et al.*, 2002], estimating velocities in the ITRF08 reference frame [*Altamimi and Collilieux*, 2010], which have been subsequently rotated into the fixed Eurasian frame computed by *Serpelloni et al.* [2007]. For the CGPS stations we simultaneously estimate, and remove, seasonal terms (annual and semi-annual) and offsets in the time-series. Uncertainties are obtained following *Mao et al.* [1999]; *Dixon et al.* [2000].

4.3.2 Combination with Published Solutions

In addition to our own analysis we integrated over 2000 GPS-station velocities from published work in the Mediterranean and Aegean region and [*Burchfiel et al.*, 2006; *Reilinger et al.*, 2006; *Hollenstein et al.*, 2008; *Floyd et al.*, 2010]. Solutions were transformed into a consistent reference frame defined by our original processed solutions. In order to align

the published velocities to our solution we apply a seven-parameter Helmert transformation that minimizes the root-mean-square (RMS) differences between the velocities of common to the networks. After alignment, the RMS of velocity misfit is less than 1mm/yr for all solutions with most less than 0.5 mm/yr assuring the robustness of the original solution as well as the transformed one. The combined velocity field (in the IGS08, fixed Nubian, and fixed Eurasian frames) is given in Table C.1 of the auxiliary material.

All the transformed velocities remain within 95

All GPS velocities from the above-mentioned references were incorporated in our combined velocity solution, however some stations were excluded prior to the block model inversion. Sites were excluded for one of three reasons (see Table C.1 for site specific details): We exclude 1) sites outside our area of interest *Reilinger et al.* [2006, e.g.], Middle East sites or *Burchfiel et al.* [2006] sites in northern Greece sites), 2) sites whose absolute uncertainty exceeds 4 mm/yr, and 3) redundant velocity estimates for collocated sites with a preferred velocity (see above section).

4.4 Aegean Block Motion

4.4.1 Methodology

We use a block modeling approach to incorporate both rigid block rotation and near-boundary elastic strain accumulation effects in a formal inversion of the GPS velocities [e.g. *McCaffrey et al.*, 2000a; *Meade and Hager*, 2005]. We implement our blocks as rigid entities on a spherical earth bounded by dislocations and invert (using a least squares approach) for poles and rates of rotation that minimize the misfit to the GPS velocities using the block modeling code by *Meade and Hager* [2005]. We further explore the characteristics of the Hellenic arc by varying both the dip and the locking depth of the subduction plate interface. In addition, we the test amount of extension along hanging-wall structures required mask the signal of a locked subduction zone in a multi-parameter search for minimum misfit.

Within this paper the term plate (and microplate) refers to the rigid, coherent, lithospheric entity defined by bounding active fault zones. The term block is the specific implementation of these data into a parameterized set of variables within our block model [e.g. *Apel et al.*, 2006]. Correctly specifying the location and geometry of block-bounding faults is critical for modeling GPS velocities and the plate boundary kinematics of a particular region. While some plate boundaries in the Aegean region are well defined by mapped active fault traces, youthful geomorphology and abundant local seismicity, others appear more diffuse or the distribution of active deformation may be ambiguous.

We separate the Aegean region into 6 blocks (Figure 4.5). Generally, our block model boundaries are consistent with the models of *Nyst and Thatcher* [2004]; *Reilinger et al.* [2006, 2010]; *Floyd et al.* [2010] in the far field (e.g. Marmara and Anatolian blocks) and along the Hellenic arc. We include some smaller subdivisions of the Aegean block. We include

a northern Greece block assuming that the Gulf of Corinth is a major plate boundary feature. We also separate the region between the western coast of Greece and the Kephalonia fault zone as a separate block, including the islands of Kephalonia and Zakynthos where the GPS velocity field itself suggest separation of the Kephalonia block as independent from the Aegean using boundaries similar to *Hollenstein et al.* [2008]; *Floyd et al.* [2010]; *Vassilakis et al.* [2011]. The southern Aegean is also separated from the northern Aegean along a backarc boundary that corresponds to the active extension observed in the seismicity (Figure 4.1) and is approximately parallel to the volcanic arc (Figure 4.2). Unlike the Kephalonia, the GPS velocity field itself do not suggest (or require) the separation of the northern Aegean from the south Aegean. However, we place slip along this boundary in order to evaluate the required amount of extension required to compensate the shortening associated Hellenic subduction.

We do not further subdivide the southern Aegean region into smaller blocks similar to *Reilinger et al.* [2006]; *Floyd et al.* [2010]. While more blocks may improve the model fit, we attempt to explore the likelihood that the residuals from a simple block model may be related to elastic strain accumulation along the Hellenic subduction zone or in the backarc region as a result of active extension.

The block boundaries (dip and locking depth) are modeled as vertical dislocations in an elastic half-space, with both fault-normal and fault-parallel displacement-discontinuity components, except along the Hellenic subduction zone where boundaries are non-vertical. Along the Hellenic arc we test variable dips and locking depths that minimize the misfit to the GPS data. We assume the simple backslip model *Savage* [1983] is adequate for this subduction zone and does not require a more complex model such as those developed by *Kanda and Simons* [2010].

4.4.2 Misfit Statistics

We quantify the goodness of fit in terms of the χ^2 and χ^2/DOF statistics:

$$\chi^2 = \sum_{c=1}^{\#data} \left(\frac{v_c^{model} - v_c^{data}}{\sigma_c} \right)^2 \tag{4.1}$$

$$\chi^2/DOF = \frac{\chi^2}{\#data - \#model\ parameters} \tag{4.2}$$

where v_c^{model} and v_c^{data} are the predicted observed velocity components, and σ_c is the 1σ uncertainty for each component of the input GPS velocities. The number of degrees of freedom (DOF) is defined by: $\#data$, the number of GPS components used as input data (east and north components for each station) and $\#modelparameters$, the number of model parameters that we solve for in the inversion (3 per block - pole of rotation latitude and longitude and rotation rate). The statistics indicate how well the model fit the data within their uncertainty bounds. Lower values of χ^2 indicate better fit to the data. χ^2 can be

calculated for a single data component at a single station, for sites within an individual block, or for the entire model. Increasing the number model parameters inevitably leads to better fits and lower total χ^2. Dividing by the number of degrees of freedom helps us to compare our model where we solve for a different number of parameters, but χ^2/DOF ignores all correlations between parameters. Because these correlations change as model geometry changes, caution should be exercised in making strictly quantitative comparisons of models using χ^2/DOF alone. Nonetheless, the statistics provide a basis for qualitative comparisons. For uncorrelated parameters, a χ^2/DOF of 1 indicates that on average all the predicted velocities are consistent with the 1σ standard deviation of the input data.

4.5 Results

We invert the GPS velocities, using a least squares approach, and derive Euler poles for the major blocks (Eurasia, Nubia, and Anatolia) which are based primarily on sites far from major tectonic boundaries and generally represent rigid block motion without influence of elastic deformation. Poles for these major blocks are consistent with previously published solutions. Using the Euler poles derived from this inversion we calculate the block velocity at each site. Systematic patterns in the residual velocities (observed minus predicted) are used as an indicator of where and how the poles predicted velocities match the observed surface velocities. Large residual velocities can be indicative of deformation not captured by simple block rotation.

4.5.1 Rigid block rotation models

We first examine a 4-block model of the region with one Aegean block, without consideration of elastic boundary effects. The RMS misfit for all of the stations on the Aegean block is ˜7.5 mm/yr with a reduced chi-squared χ^2/DOF statistic of 128. Systematic misfits are evident in a number of locations (Figure 4.5a). In the Ionian Islands (Kephalonia and Zakynthos) sites with strong northward residuals are separated from the Aegean block onto the Kephalornia block and the North Aegean is separated from the south Aegean to form our 6-block model (described above and shown in Figure 4.5b).

Using this 6-block configuration we again invert the velocities for rigid block rotations without elastic block boundary strain and see substantial improvement in the fit with an RMS misfit of ˜4.5 mm/yr with a reduced chi-squared χ^2/DOF statistic of 31. The misfit is somewhat higher than previous studies [e.g. *Nyst and Thatcher*, 2004; *Reilinger et al.*, 2006; *Floyd et al.*, 2010] primarily because we include data substantially more data. But patterns in the residual velocities (Figure 4.5b) and estimated Euler poles are consistent. We estimate the Aegean plate motion parameters to be statistically indistinguishable from previous geodetic studies [e.g. *Kreemer and Chamot-Rooke*, 2004; *Hollenstein et al.*, 2008; *Floyd et al.*, 2010]. Minimal differences in our Aegeans plate motion parameters compared

to others suggest that minimal errors (if any) were introduced in the GPS velocity solution combination process.

The good agreement between predicted velocities from our simple block models and the GPS data suggests that the Aegean region is behaving rigidly to first order, which is consistent with previous studies [*Nyst and Thatcher*, 2004; *Reilinger et al.*, 2006, 2010]. There are no clear patterns in the residual velocity field that indicate that the Hellenic subduction zone is locked.

4.5.2 Consideration of Elastic Block Boundary Strain

Predicted residual velocities from a forward model considering elastic strain accumulation along the Hellenic trench are shown in Figure 4.6 where we assume the rigid Aegean block motion parameters as in Figure 4.5b, although we do not separate the Aegean into two blocks. The dipping subduction zone (20°) is locked to a depth of 30 km and projected into the horizontal. Interestingly the GPS velocities in the central Aegean north of Crete (Figures 4.5a and 4.5b) are directed southerly with respect to near zero velocities on Crete. These southerly directed velocities indicate contraction between Crete and the volcanic arc rather than extension. The velocity profile through the subduction zone (Figure **??**, discussed below) also show small amounts of contraction (˜3 mm/yr).

Figure 4.6 shows the elastic effects from a coupled Hellenic subduction zone are as large as 25 mm/yr near the trench and extend a few hundred of kilometers north into the Aegean block. Block models that do not use elastic boundaries along subduction zones will over predict velocities resulting in residuals directed away from the boundary. In addition, effects of a locked subduction zone will extend into the upper plate (Aegean) hundreds of kilometers away. These patterns are not evident in the residuals to the block model without elastic strain considered in the previous section (Figure 4.5). Most residual velocities from this model are actually oriented towards the trench, suggesting that hanging wall extension, not subduction-related contraction, is a larger contributor to the deformation field.

Considering a single Aegean block and a dipping subduction zone (20°) locked to a depth of 30 km we invert the GPS velocities. Residual velocities are shown in Figure 4.7. The strong trenchward directed residuals indicate that the model is underpredicting the GPS velocities along the subduction zone. Coeval backarc extension may mask this subduction signal so we explore coeval extension and contraction by testing various locking depths along the volcanic arc boundary. We parameterize the boundary as vertical elastic dislocation locked from 10 to 200 km. The reduced chi-squared χ^2/DOF statistic from the dipping subduction zone (20°) locked to a depth of 30 km is 113, shown in Figure 4.6 and 4.7. As locking increases the chi-squared misfit increases to a depth of 80 km (Figure 4.9). That is, no amount of slip along the volcanic arc boundary fit to the data better that rigid block model. For locking depths greater 80 km the misfit decreases, however slip required along boundary is contractional.

Although first order patterns are not immediately visible in the residual velocities we

explicitly test various geometric subduction zone configurations to test for improved fit of the GPS data. Along the subduction zone the downdip geometry is constrained by catalog seismicity (Figure 4.2) that outlines a Wadati-Benioff zone consistent with previous studies [*Bohnhoff et al.*, 2001] and refined by surface wave seismic studies [*Meier et al.*, 2004] and detailed analysis of focal mechanisms [*Bohnhoff et al.*, 2005]. However, the scatter in the event data and uncertain trench location suggest potential variability in the actual subduction geometry. We test a reasonable set of subduction zone parameters which include dips from 0 to 50 degrees and a locking depth of 0 to 50 km in a parameter search to test the optimal subduction zone geometry favored by the horizontal GPS data. In these models, the other regional block boundaries are locked to 15 km, although we do not consider the east-west extensional boundary dividing the Aegean region.

The reduced chi-squared values from the models in this parameter search are contoured and shown in Figure 4.7. The model that best fits the GPS data is a model with subduction zone parameters that produce the least amount of elastic horizontal deformation (i.e. minimal locking depth). This confirms the first-order observations that the measured horizontal velocities capture little to no interseismic elastic strain accumulation. However, it is possible that convergence at a locked subduction zone could be masked by simultaneous back-arc extension.

4.6 Discussion and Conclusions

Convergence along a locked subduction zone produces a very predictable deformation signal in the upper crust that we further explore with forward models using elastic dislocations (Figures 4.6 and 4.10b). Figure 4.10c shows the elastic rates produced by locked dipping faults given a plate rate of 36 mm/yr. Rates were calculated along a profile parallel to the relative Aegean-Nubia block motion vector (see Figure 4.2 for profile location). We compare predicted velocities from both a 30 degree dipping splay fault [*Shaw et al.*, 2008] and a 20 degree dipping interface (Figure 4.10b). Faults are locked from the surface to various depths in 5 km increments. As the locking depth increases, the misfit of the predicted elastic signal compared to the GPS data increases. No configuration of either the shallowly dipping subduction zone, or the steeply dipping splay fault in the upper plate improve the fit to the GPS data.

The abovementioned models assume the full plate rate is resolved onto the fault and predict uplift rates of ˜5 mm/yr with respect to the Aegean block interior. However GPS uplift rates along the Hellenic subduction are small (1-2 mm/yr) and slightly positive (Figures 4.4 and 4.10d). The magnitude of these velocities suggests that any elastic strain accumulation along either the subduction zone or a synthetic splay fault must be at a rate far below the full plate rate. Assuming partial coupling (˜10%) we estimate the maximum resolved slip rate to be ˜4 mm/yr with an uplift rate of about ˜2 mm/yr on either the shallowing dipping subduction zone or a steeply dipping splay fault (Figure 4.10). Predicted uplift rates from the splay fault loaded at 4 mm/yr are show in Figure 4.10d.

Reilinger et al. [2010] model horizontal elastic deformation across the Hellenic subduction zone also dipping at 20 degrees, although they model the upper 20 km as aseismic only locking the subduction zone from depths of 20-40 km. They conclude that the coupling along the subduction zone is likely to be $\leq$20%. *Ganas and Parsons* [2009] use a finite element model, GPS data, and use similar, but very detailed Hellenic subduction geometry and suggest that coupling approaches 100%. The model of *Ganas and Parsons* [2009] greatly overpredicts the uplift measured by GPS velocities. Recent seismic moment calculations [*Shaw and Jackson*, 2010] also show that the seismic moment release predicted by *Ganas and Parsons* [2009] is too large given the record of earthquakes in last one hundred years.

First order block models based on available horizontal GPS data in and around the Aegean region match the observed GPS data quite well, suggesting little intra-plate or plate-boundary deformation. The GPS data dont show measureable elastic arc-normal contraction of the overriding plate. We show that it is not possible for surface deformation generated by convergence at a locked subduction zone to be masked by simultaneous extension in the hangingwall of the southward retreating subduction zone, creating the illusion of rigid block motion. Any active extension is minimal and may does mask the accumulation of strain along the Hellenic subduction zone. We test multiple model scenarios showing that while coeval extension and contraction could be occurring, uplift rates and expected locking depths and slip rates are unreasonable.

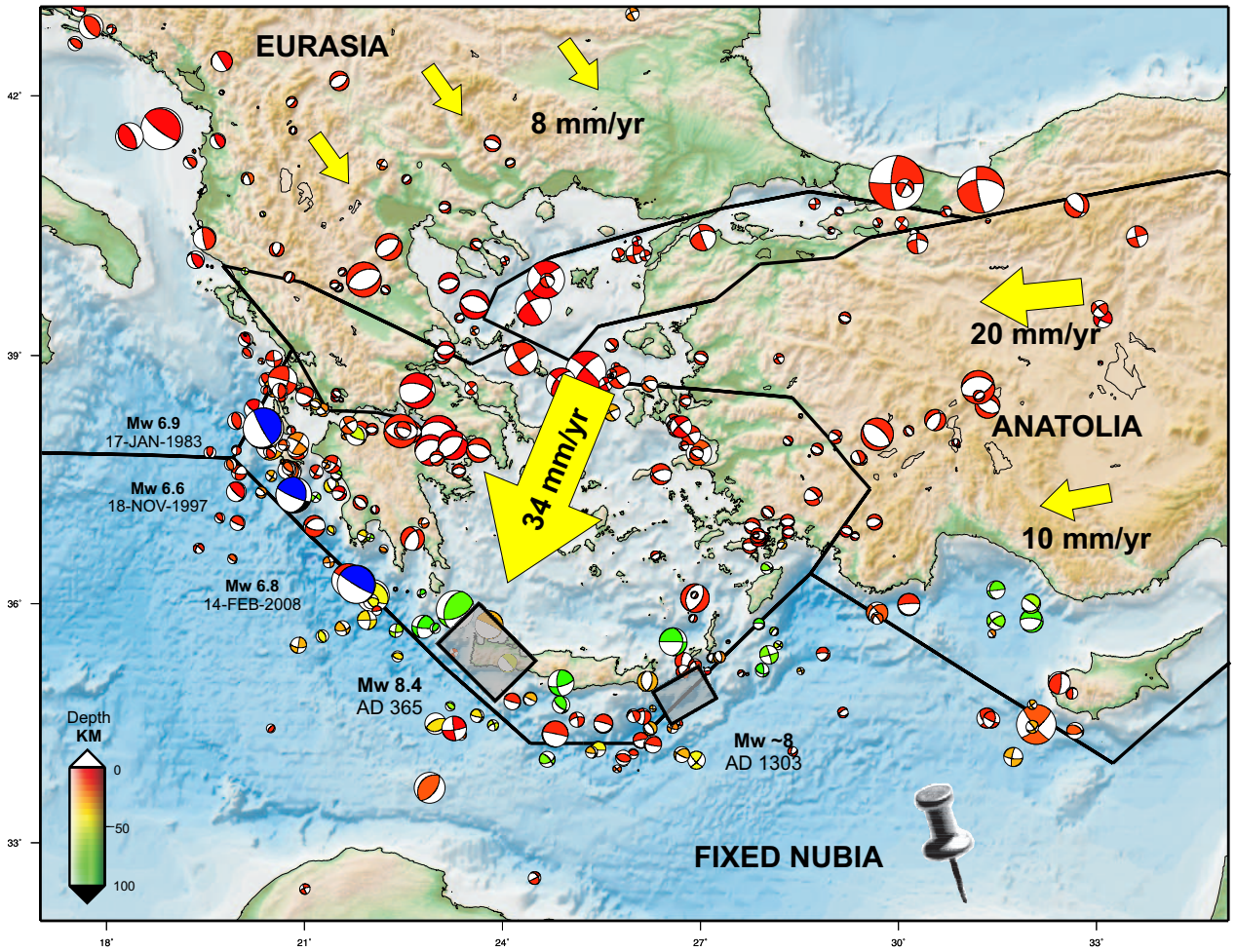

Figure 4.1. Tectonic setting and instrumental seismicity of the Aegean region. Focal mechanisms (1973- 2009) shown are from Global CMT catalog (www.globalcmt.org) and sized by magnitude. The only three earthquakes along the western Hellenic subduction zone greater than M_W 6.5 are shown in blue and labeled. Rectangles highlight the approximate rupture areas of the M_W 8.4 A.D. 365 earthquake [*Shaw et al.*, 2008] and the M˜8 1303 A.D. earthquake [*Hamouda*, 2006, modified from]. Arrows represent general block motions with respect to a fixed Nubia reference frame. Block boundaries shown are from our simplified 4-block model.

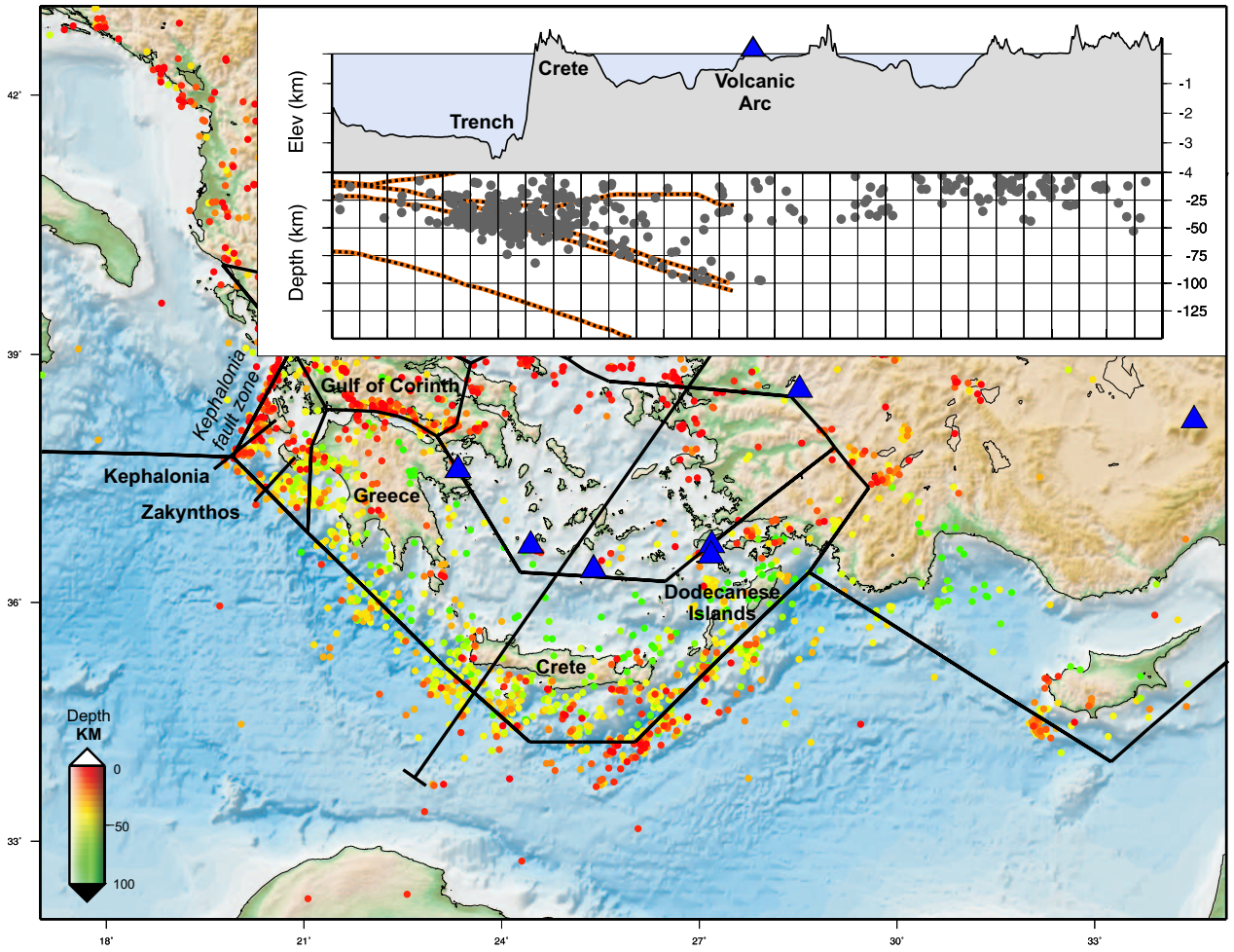

Figure 4.2. Historical seismicity of the Aegean region from 0 to 100 km depth. Earthquake hypocenters are from the updated (1964-2007) EHB Centennial catalog [*Engdahl et al.*, 1998] and are colored by depth. Blue triangles show the locations of volcanoes in the region. Block boundaries shown are from our simplified 6-block model. Cross section of seismicity and lithospheric structure based on seismic refraction [modified from *Meier et al.*, 2004] from the central Aegean region (inset) and is parallel to the relative Aegean-Nubian motion.

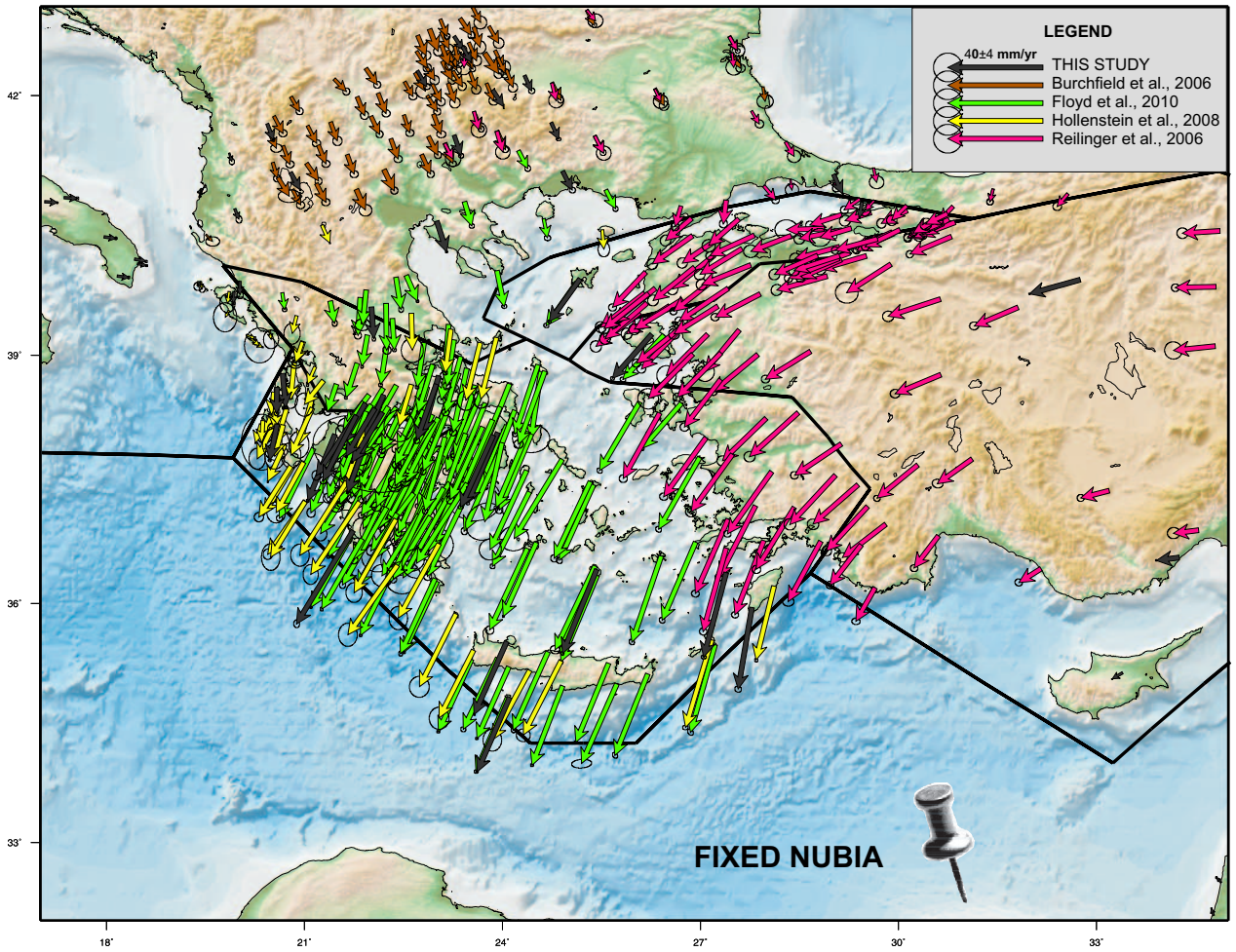

Figure 4.3. Observed GPS velocity field from our combined solution relative to a fixed Nubia plate (see text for explanation). Velocity vectors are tipped with 95% error ellipses and colored by source (see legend). Not all velocities shown were used in the analysis (see text for explanation).

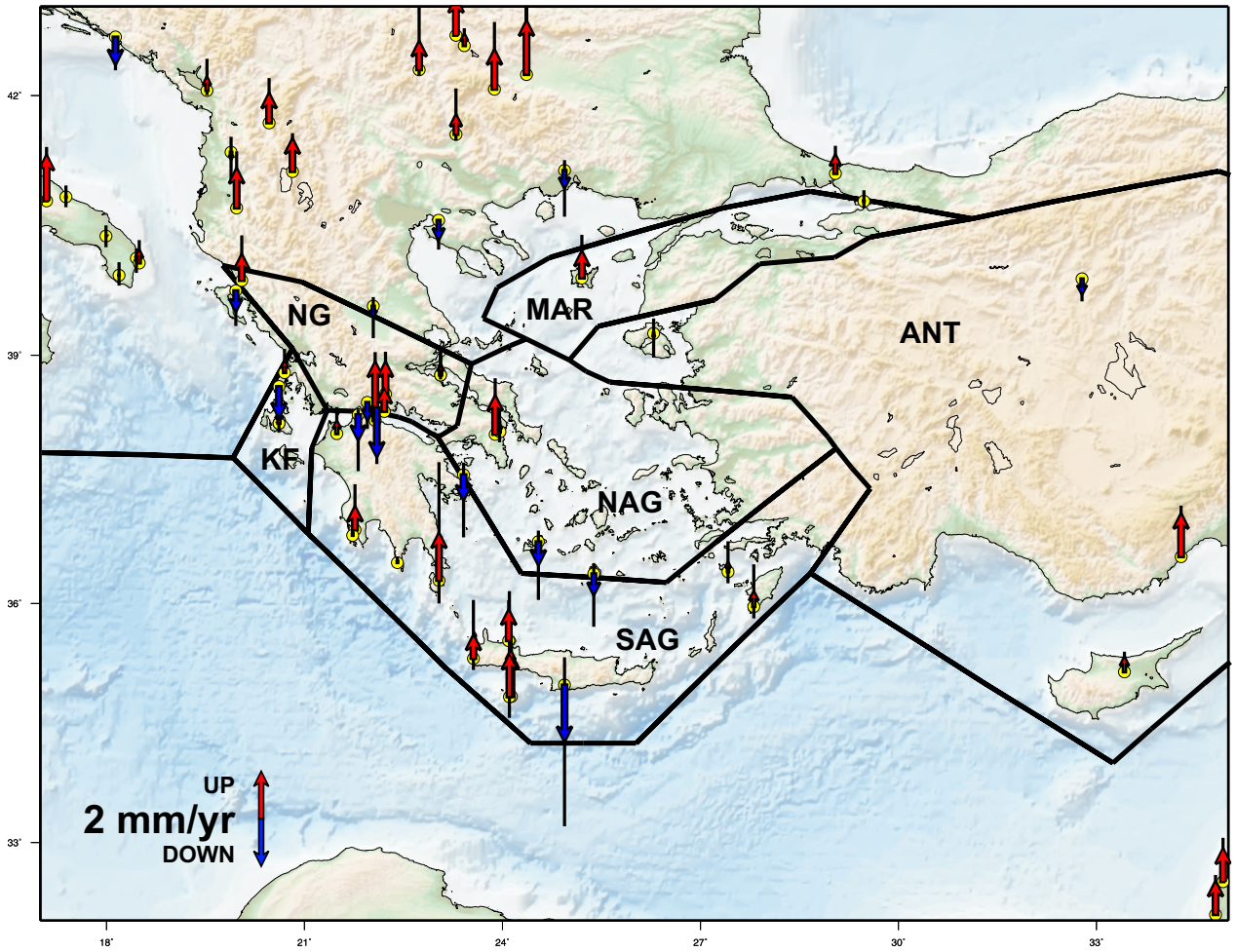

Figure 4.4. Observed vertical rates from continuous GPS measurements in the Aegean region. Velocity vectors are tipped with one-sigma error bars and colored by direction (red up, blue down). Aegean block boundaries are also shown (Northern Greece (NG), Kephalonia (KF), Marmara (MAR), Anatolia (ANT), Northern Aegean (NAG) and Southern Aegean (SAG)).

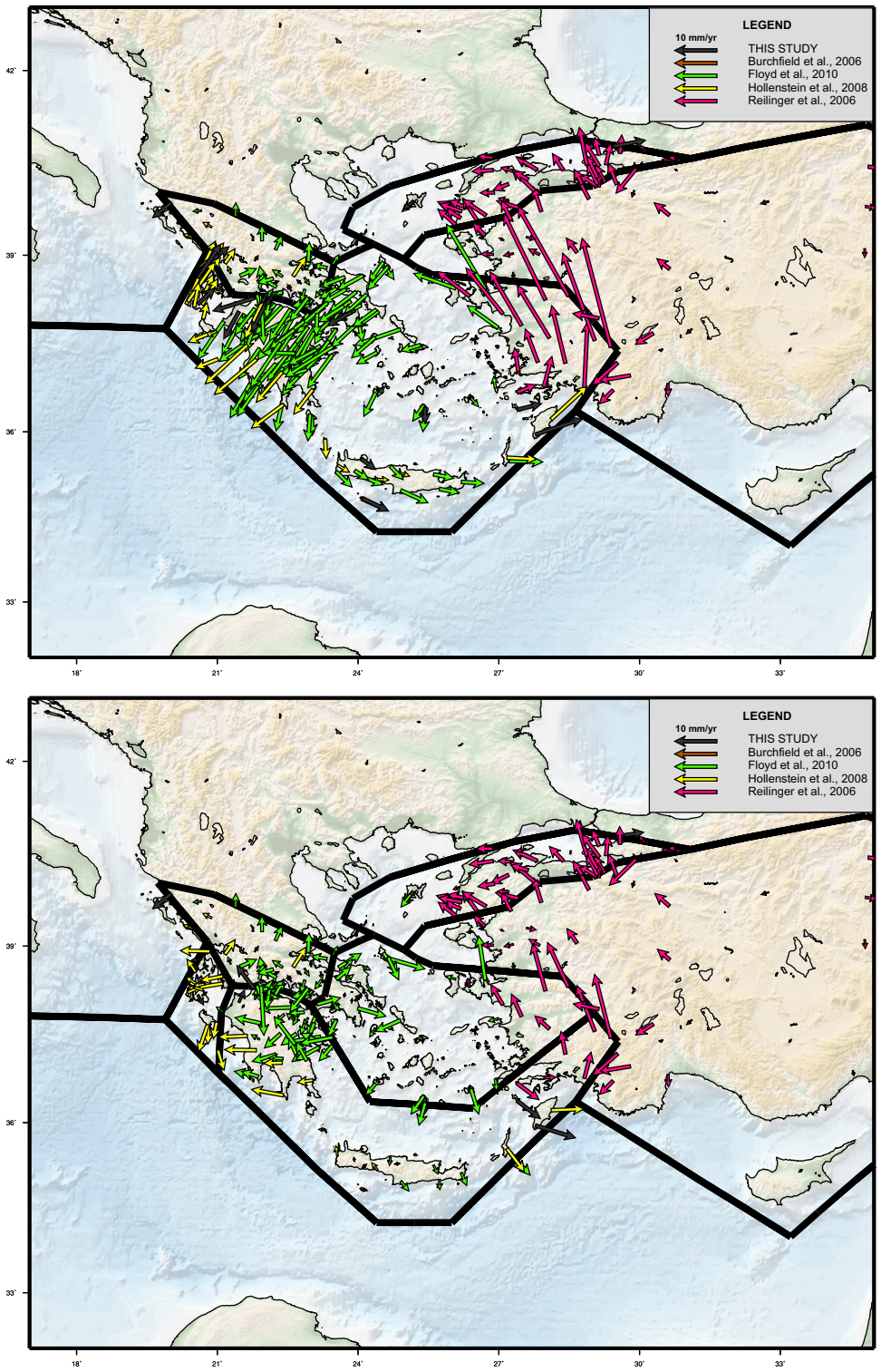

Figure 4.5. Residual (measured minus modeled) velocity vectors from purely rigid 4-block and 6-block model inversions without consideration of elastic strain about block boundaries. A significant improvement in fit to the data is achieved by adding two additional blocks in the Aegean region. In the 6-block model systematic patterns of oppositely directed residual velocities in southern Greece and the Dodecanese Islands suggest active along-arc extension of the southern Aegean region. Residual velocities from our 6-block model around Crete are statistically indistinguishable from zero.

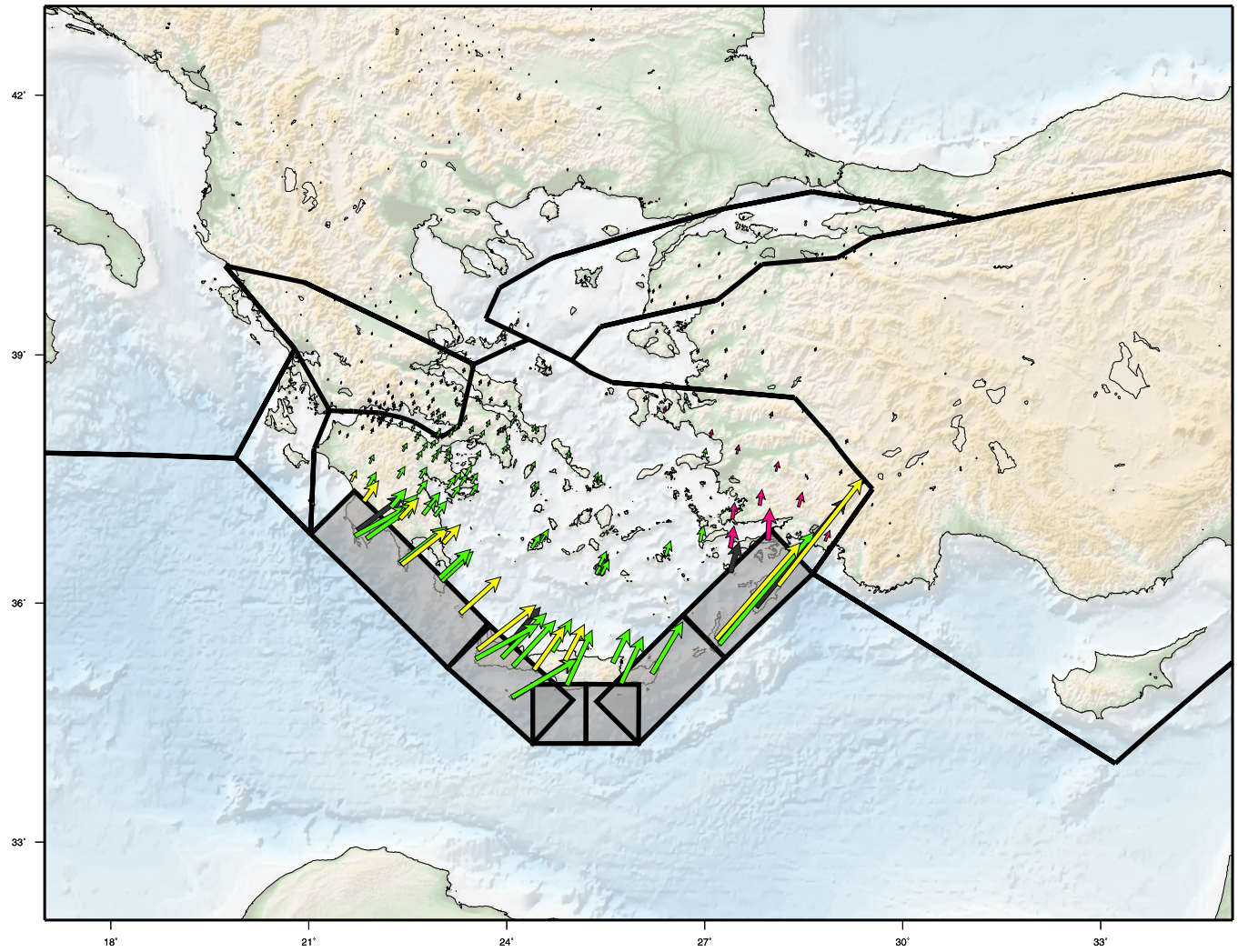

Figure 4.6. Predicted residual velocities from a forward model considering elastic strain accumulation along the Hellenic trench. Elastic strain accumulation estimates are based on a dipping (20°) subduction zone locked to 30 km depth. Elastic effects from Hellenic subduction and Aegean block motion are as large as 25 mm/yr and extend hundreds of kilometers north of the trench into the Aegean block.

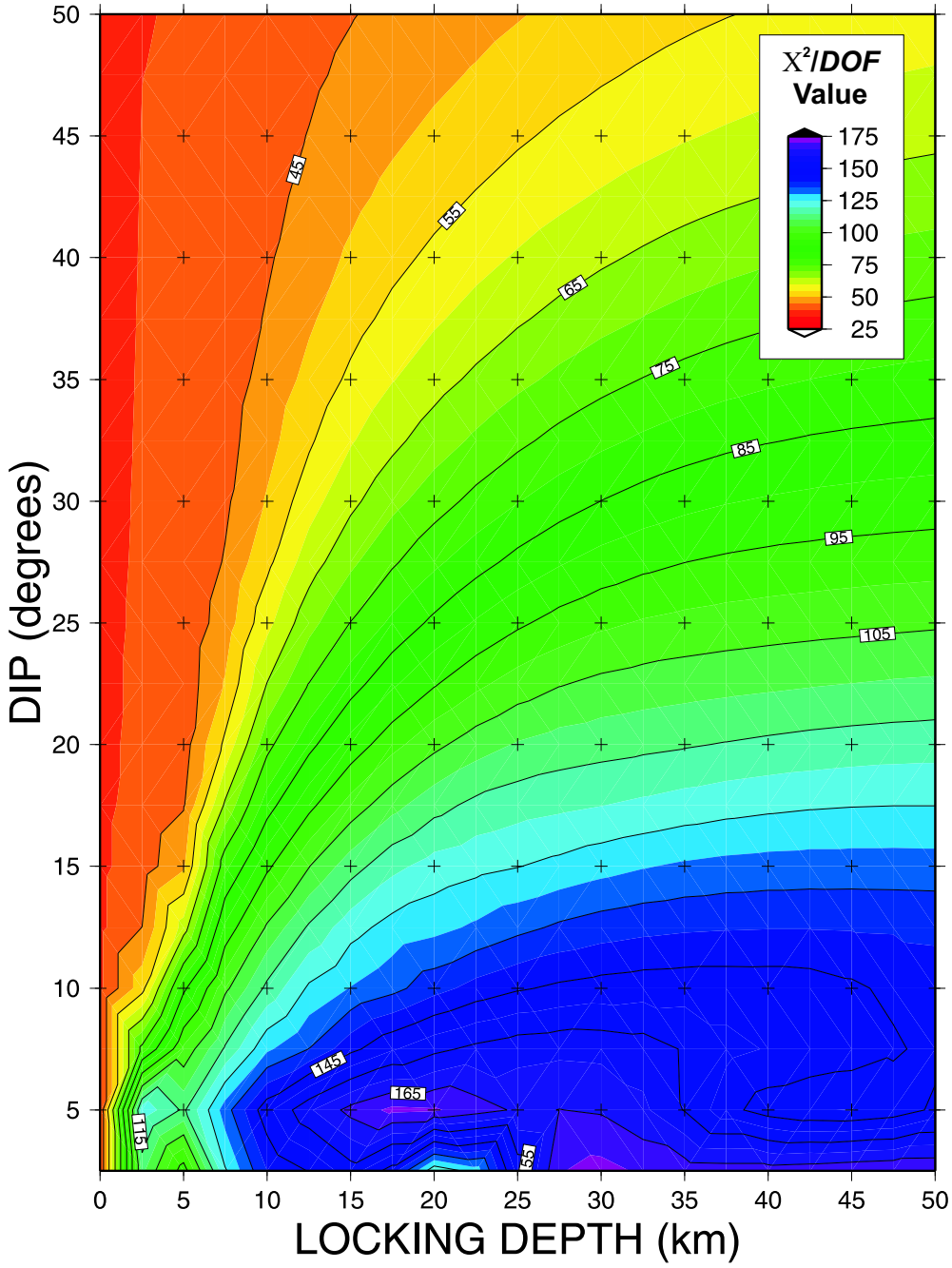

Figure 4.7. Reduced chi-squared misfit statistic for Aegean blocks sites given variable subduction zones parameters. The reduced chi-squared statistic is shown as a function of the Hellenic subduction zone dip and locking depth. Best fitting models are ones with the smallest reduced chi squared statistic. These models generate the least amount of plate boundary elastic strain (i.e. minimal locking depth).

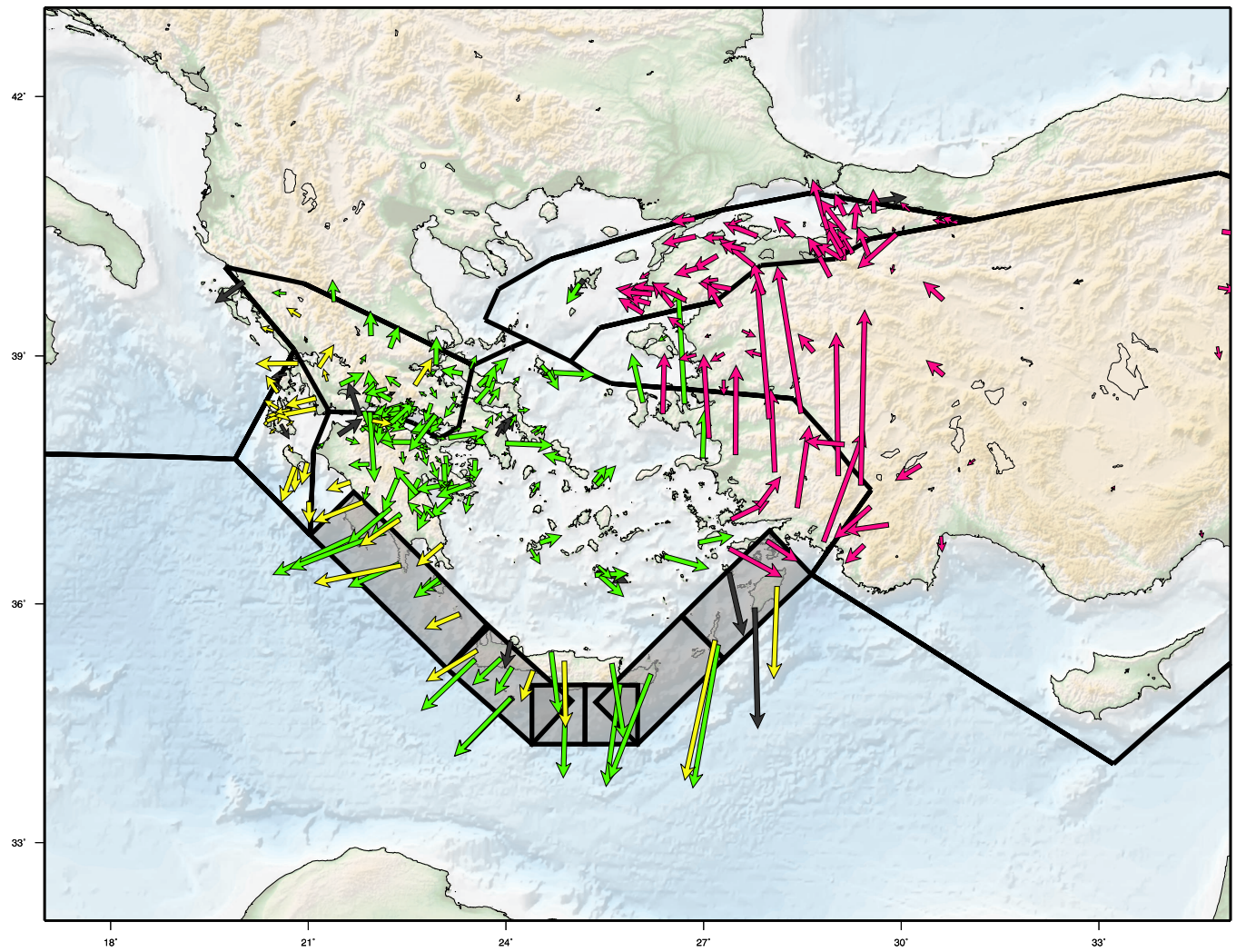

Figure 4.8. Residual (measured minus modeled) velocity vectors from a 5-block model inversion with consideration of elastic strain about block boundaries. Elastic strain accumulation estimates are based on a dipping (20°) subduction zone locked to 30 km depth.

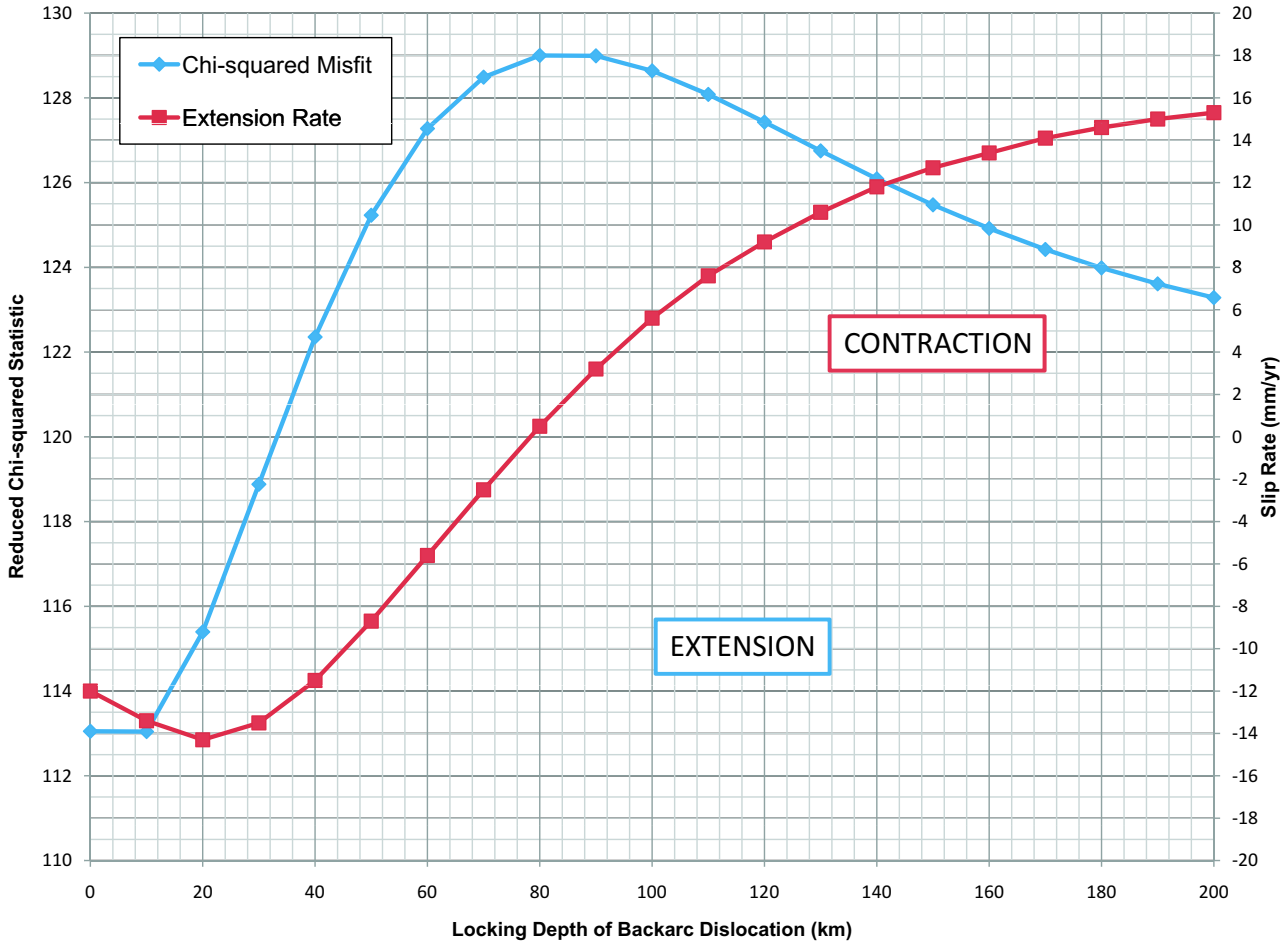

Figure 4.9. Chi-squared misfit (blue) and backarc slip (red) as a function of backarc locking depth in the central Aegean. A 0 km locking depth is equivalent to rigid block motion between the southern and north Aegean.

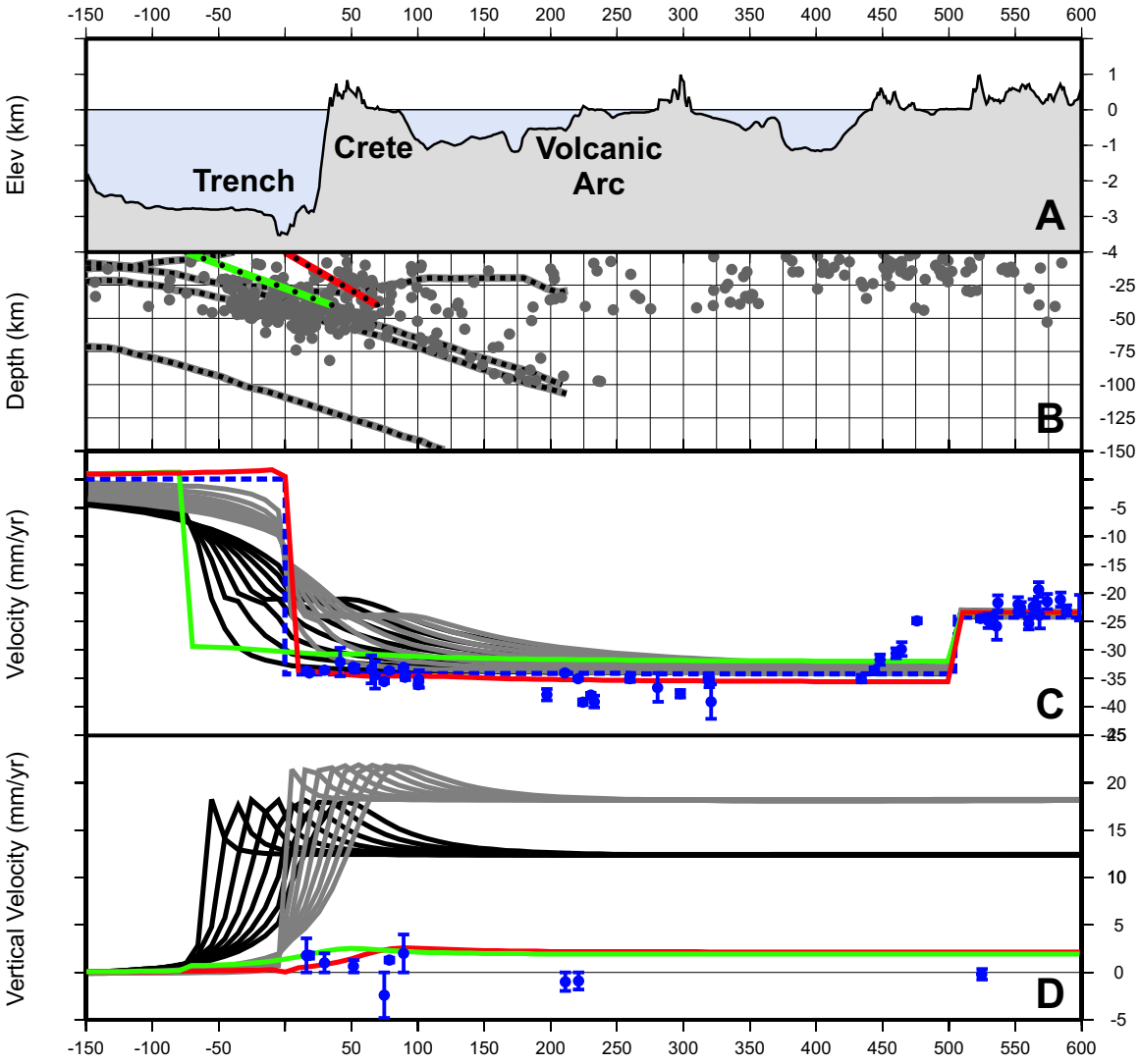

Figure 4.10. Profile through the Hellenic subduction zone parallel to relative to a fixed Nubia plate(N 36°E). A) sea-floor bathymetry, B) Earthquake hypocenters and model of crust beneath the Aegean [*Meier et al.*, 2004]. Steeply dipping (30°) splay fault and gently dipping (20°) subduction zone are shown in green and red, respectively. C) observed horizontal GPS velocities with one-sigma error bars (blue) through the Aegean subduction zone. Predicted velocity profiles from the shallow subduction zone (20° dip) are shown in black and the splay fault (30°) dip) are show in grey for various locking depths (see text for explanation). Rigid block motion is shown in blue. D) Modeled vertical velocities from the shallow subduction zone (20°) dip) are shown in black and the splay fault (30°) dip) are show in grey for various locking depths (see text for explanation). Predicted vertical velocities for partially coupled (10%) subduction zone and splay fault at an approximate loading rate of 4 mm/yr are shown in green and red, respectively. Observed vertical GPS velocities with one-sigma error bars are show in blue.

Bibliography

Abdrakhmatov, K. Y., et al., Relatively recent construction of the Tien Shan inferred from GPS measurements of present-day crustal deformation rates, *Nature*, *384*(6608), 450–453, 1996.

Altamimi, Z., and X. Collilieux, Quality Assessment of the IDS Contribution to ITRF2008, *Advances in Space Research*, *45*(12), 1500–1509, 2010.

Altamimi, Z., P. Sillard, and C. Boucher, ITRF2000: A new release of the International Terrestrial Reference frame for earth science applications, *Journal of Geophysical Research-Solid Earth*, *107*(B10), 19, 2002.

Ambraseys, N., and R. Bilham, Earthquakes and associated deformation in northern Baluchistan 1892-2001, *Bulletin of the Seismological Society of America*, *93*(4), 1573–1605, 2003.

Ambraseys, N., C. P. Melville, and R. D. Adams, *The Seismicity of Egypt, Arabia and the Red Sea: A Historical Review*, Cambridge University Press, Cambridge, 1994.

Ambraseys, N. N., Far-field effects of Eastern Mediterranean earthquakes in Lower Egypt, *Journal of Seismology*, *5*(2), 263–268, 2001.

Angelier, J., and S. Baruah, Seismotectonics in Northeast India: a stress analysis of focal mechanism solutions of earthquakes and its kinematic implications, *Geophysical Journal International*, *178*(1), 303–326, 2009.

Aoki, Y., and C. H. Scholz, Interseismic deformation at the Nankai subduction zone and the Median Tectonic Line, southwest Japan, *Journal of Geophysical Research-Solid Earth*, *108*(B10), 2003.

Apel, E. V., R. Bürgmann, G. Steblov, N. Vasilenko, R. King, and A. Prytkov, Independent active microplate tectonics of northeast Asia from GPS velocities and block modeling, *Geophysical Research Letters*, *33*(11), 5, 2006.

Avouac, J., Dynamic Processes in Extensional and Compressional Settings - Mountain Building: From Earthquakes to Geological Deformation, in *Treatise on Geophysics*, vol. 6, edited by A. Watts, pp. 377 – 439, University of California, Los Angeles, Los Angeles, CA, 2008.

Avouac, J. P., Mountain building, erosion, and the seismic cycle in the Nepal Himalaya, in *Advances in Geophysics, Vol 46*, *Advances in Geophysics*, vol. 46, pp. 1–80, Academic Press Inc, San Diego, 2003.

Banerjee, P., F. Pollitz, B. Nagarajan, and R. Bürgmann, Coseismic slip distributions of the 26 December 2004 Sumatra-Andaman and 28 March 2005 Nias earthquakes from GPS static offsets, *Bulletin of the Seismological Society of America*, *97*(1), S86–S102, 2007.

Banerjee, P., R. Bürgmann, B. Nagarajan, and E. Apel, Intraplate deformation of the Indian subcontinent, *Geophysical Research Letters*, *35*(18), 5, 2008.

Bertrand, G., C. Rangin, R. C. Maury, H. M. Htun, H. Bellon, and J. P. Guillaud, The Singu basalts (Myanmar): new constraints for the amount of recent offset on the Sagaing Fault, *Comptes Rendus De L Academie Des Sciences Serie Ii Fascicule a-Sciences De La Terre Et Des Planetes*, *327*(7), 479–484, 1998.

Bettinelli, P., J. P. Avouac, M. Flouzat, F. Jouanne, L. Bollinger, P. Willis, and G. R. Chitrakar, Plate motion of India and interseismic strain in the Nepal Himalaya from GPS and DORIS measurements, *Journal of Geodesy*, *80*(8-11), 567–589, 2006.

Bilham, R., and P. England, Plateau 'pop-up' in the great 1897 Assam earthquake, *Nature*, *410*(6830), 806–809, 2001.

Bilham, R., R. Bendick, and K. Wallace, Flexure of the Indian plate and intraplate earthquakes, pp. 315–329, Indian Academy Sciences, 2003.

Bird, P., An updated digital model of plate boundaries, *Geochemistry Geophysics Geosystems*, *4(3)*, 2002.

Biswas, S., I. Coutand, D. Grujic, C. Hager, D. Stockli, and B. Grasemann, Exhumation and uplift of the Shillong plateau and its influence on the eastern Himalayas: New constraints from apatite and zircon (U-Th-[Sm])/He and apatite fission track analyses, *Tectonics*, *26*(6), 22, 2007.

Bock, Y., L. Prawirodirdjo, J. F. Genrich, C. W. Stevens, R. McCaffrey, C. Subarya, S. S. O. Puntodewo, and E. Calais, Crustal motion in Indonesia from Global Positioning System measurements, *Journal of Geophysical Research-Solid Earth*, *108*(B8), 22, 2003.

Bohnhoff, M., J. Makris, D. Papanikolaou, and G. Stavrakakis, Crustal investigation of the Hellenic subduction zone using wide aperture seismic data, *Tectonophysics*, *343*(3-4), 239–262, 2001.

Bohnhoff, M., H. P. Harjes, and T. Meier, Deformation and stress regimes in the Hellenic subduction zone from focal mechanisms, *Journal of Seismology*, *9*(3), 341–366, 2005.

Bull, J. M., C. DeMets, K. S. Krishna, D. J. Sanderson, and S. Merkouriev, Reconciling plate kinematic and seismic estimates of lithospheric convergence in the central Indian Ocean, *Geology*, *38*(4), 307–310, 2010.

Burchfiel, B. C., R. W. King, A. Todosov, V. Kotzev, N. Durmurdzanov, T. Serafimovski, and B. Nurce, GPS results for Macedonia and its importance for the tectonics of the Southern Balkan extensional regime, *Tectonophysics*, *413*(3-4), 239–248, 2006.

Bürgmann, R., M. G. Kogan, G. M. Steblov, G. Hilley, V. E. Levin, and E. Apel, Interseismic coupling and asperity distribution along the Kamchatka subduction zone, *Journal of Geophysical Research-Solid Earth*, *110*(B7), 2005.

Burton, P. W., Y. B. Xu, C. Y. Qin, G. A. Tselentis, and E. Sokos, A catalogue of seismicity in Greece and the adjacent areas for the twentieth century, *Tectonophysics*, *390*(1-4), 117–127, 2004.

Calais, E., M. Vergnolle, V. San'kov, A. Lukhnev, A. Miroshnitchenko, S. Amarjargal, and J. Deverchere, GPS measurements of crustal deformation in the Baikal-Mongolia area (1994-2002): Implications for current kinematics of Asia, *Journal of Geophysical Research-Solid Earth*, *108*(B10), –, 2003.

Calais, E., L. Dong, M. Wang, Z. Shen, and M. Vergnolle, Continental deformation in Asia from a combined GPS solution, *Geophysical Research Letters*, *33*(24), –, 2006.

Chandrasekhar, D. V., R. Bürgmann, C. D. Reddy, P. S. Sunil, and D. A. Schmidt, Weak mantle in NW India probed by geodetic measurements following the 2001 Bhuj earthquake, *Earth and Planetary Science Letters*, *280*(1-4), 229–235, 2009.

Chase, C. G., Plate Kinematics - Americas, East-Africa, and Rest of World, *Earth and Planetary Science Letters*, *37*(3), 355–368, 1978.

Chen, Q. Z., J. T. Freymueller, Z. Q. Yang, C. J. Xu, W. P. Jiang, Q. Wang, and J. N. Liu, Spatially variable extension in southern Tibet based on GPS measurements, *Journal of Geophysical Research-Solid Earth*, *109*(B9), 2004.

Chlieh, M., J. P. Avouac, K. Sieh, D. H. Natawidjaja, and J. Galetzka, Heterogeneous coupling of the Sumatran megathrust constrained by geodetic and paleogeodetic measurements, *Journal of Geophysical Research-Solid Earth*, *113*(B5), 2008.

Chlieh, M., et al., Coseismic slip and afterslip of the great M-w 9.15 Sumatra-Andaman earthquake of 2004, *Bulletin of the Seismological Society of America*, *97*(1), S152–S173, 2007.

Clark, M. K., and R. Bilham, Miocene rise of the Shillong Plateau and the beginning of the end for the Eastern Himalaya, *Earth and Planetary Science Letters*, *269*(3-4), 336–350, 2008.

Cloetingh, S., and R. Wortel, Regional Stress-Field of the Indian Plate, *Geophysical Research Letters*, *12*(2), 77–80, 1985.

Cook, D. B., K. Fujita, and C. A. Mcmullen, Present-Day Plate Interactions in Northeast Asia - North-American, Eurasian, and Okhotsk Plates, *Journal of Geodynamics*, *6*(1-4), 33–51, 1986.

Copley, A., J. P. Avouac, and J. Y. Royer, India-Asia collision and the Cenozoic slowdown of the Indian plate: Implications for the forces driving plate motions, *Journal of Geophysical Research-Solid Earth*, *115*, 2010.

Cowgill, E., A. Yin, T. M. Harrison, and X. F. Wang, Reconstruction of the Altyn Tagh fault based on U-Pb geochronology: Role of back thrusts, mantle sutures, and heterogeneous crustal strength in forming the Tibetan Plateau, *Journal of Geophysical Research-Solid Earth*, *108*(B7), 2003.

Curray, J. R., Tectonics and history of the Andaman Sea region, *Journal of Asian Earth Sciences*, *25*(1), 187–228, 2005.

Delescluse, M., and N. Chamot-Rooke, Instantaneous deformation and kinematics of the India-Australia Plate, *Geophysical Journal International*, *168*(2), 818–842, 2007.

DeMets, C., R. G. Gordon, D. F. Argus, and S. Stein, Current Plate Motions, *Geophysical Journal International*, *101*(2), 425–478, 1990.

DeMets, C., R. G. Gordon, D. F. Argus, and S. Stein, Effect of Recent Revisions to the Geomagnetic Reversal Time-Scale on Estimates of Current Plate Motions, *Geophysical Research Letters*, *21*(20), 2191–2194, 1994.

DeMets, C., R. G. Gordon, and J. Y. Royer, Motion between the Indian, Capricorn and Somalian plates since 20 Ma: implications for the timing and magnitude of distributed lithospheric deformation in the equatorial Indian ocean, *Geophysical Journal International*, *161*(2), 445–468, 2005.

DeMets, C., R. G. Gordon, and D. F. Argus, Geologically current plate motions, *Geophysical Journal International*, *181*(1), 1–80, 2010.

Dixon, T., F. Farina, C. DeMets, F. Suarez-Vidal, J. Fletcher, B. Marquez-Azua, M. Miller, O. Sanchez, and P. Umhoefer, New kinematic models for Pacific-North America motion from 3 ma to present, II: Evidence for a "Baja California shear zone", *Geophysical Research Letters*, *27*(23), 3961–3964, 2000.

Dong, D., P. Fang, Y. Bock, M. K. Cheng, and S. Miyazaki, Anatomy of apparent seasonal variations from GPS-derived site position time series, *Journal of Geophysical Research-Solid Earth*, *107*(B4), 2002.

Drolia, R. K., and C. DeMets, Deformation in the diffuse India-Capricorn-Somalia triple junction from a multibeam and magnetic survey of the northern Central Indian ridge, 3 degrees S-10 degrees S, *Geochemistry Geophysics Geosystems*, *6*, 2005.

Engdahl, E. R., R. van der Hilst, and R. Buland, Global teleseismic earthquake relocation with improved travel times and procedures for depth determination, *Bulletin of the Seismological Society of America*, *88*(3), 722–743, 1998.

England, P., and P. Molnar, Late Quaternary to decadal velocity fields in Asia, *Journal of Geophysical Research-Solid Earth*, *110*(B12), 27, 2005.

Faccenna, C., L. Jolivet, C. Piromallo, and A. Morelli, Subduction and the depth of convection in the Mediterranean mantle, *Journal of Geophysical Research-Solid Earth*, *108*(B2), 2003.

Feldl, N., and R. Bilham, Great Himalayan earthquakes and the Tibetan plateau, *Nature*, *444*(7116), 165–170, 2006.

Flesch, L. M., A. J. Haines, and W. E. Holt, Dynamics of the India-Eurasia collision zone, *Journal of Geophysical Research-Solid Earth*, *106*(B8), 16,435–16,460, 2001.

Floyd, M. A., et al., A new velocity field for Greece: Implications for the kinematics and dynamics of the Aegean, *Journal of Geophysical Research-Solid Earth*, *115*, 2010.

Fournier, M., N. Chamotrooke, C. Petit, O. Fabbri, P. Huchon, B. Maillot, and C. Lepvrier, In situ evidence for dextral active motion at the Arabia-India plate boundary, *Nature Geoscience*, *1*(1), 54–58, 2008.

Gan, W. J., P. Z. Zhang, Z. K. Shen, Z. J. Niu, M. Wang, Y. G. Wan, D. M. Zhou, and J. Cheng, Present-day crustal motion within the Tibetan Plateau inferred from GPS measurements, *Journal of Geophysical Research-Solid Earth*, *112*(B8), 2007.

Ganas, A., and T. Parsons, Three-dimensional model of Hellenic Arc deformation and origin of the Cretan uplift, *Journal of Geophysical Research-Solid Earth*, *114*, 2009.

Gordon, R. G., and C. Demets, Present-Day Motion Along the Owen Fracture-Zone and Dalrymple Trough in the Arabian Sea, *Journal of Geophysical Research-Solid Earth and Planets*, *94*(B5), 5560–5570, 1989.

Gordon, R. G., D. F. Argus, and J. Y. Royer, Space geodetic test of kinematic models for the Indo-Australian composite plate, *Geology*, *36*(10), 827–830, 2008.

Greninger, M., S. Klemperer, and W. Nokleberg, Geographic Information Systems (GIS) Compilation of Geophysical, Geologic, and Tectonic Data for the Circum-North Pacific, *USGS Open File Report*, *99*(422), 1999.

Hamouda, A. Z., Numerical computations of 1303 tsunamigenic propagation towards Alexandria, Egyptian Coast, *Journal of African Earth Sciences*, *44*(1), 37–44, 2006.

Heki, K., S. Miyazaki, H. Takahashi, M. Kasahara, F. Kimata, S. Miura, N. F. Vasilenko, A. Ivashchenko, and K. D. An, The Amurian Plate motion and current plate kinematics in eastern Asia, *Journal of Geophysical Research-Solid Earth*, *104*(B12), 29,147–29,155, 1999.

Herring, T. A., *GLOBK, Global Kalman filter VLBI and GPS analysis program, Version 10.2*, vol. Release 10.2, Mass. Instit. of Tech., 2005.

Hindle, D., K. Fujita, and K. Mackey, Current deformation rates and extrusion of the northwestern Okhotsk plate, northeast Russia, *Geophysical Research Letters*, *33*(2), 2006.

Hollenstein, C., M. D. Muller, A. Geiger, and H. G. Kahle, GPS-derived coseismic displacements associated with the 2001 Skyros and 2003 Lefkada earthquakes in Greece, *Bulletin of the Seismological Society of America*, *98*(1), 149–161, 2008.

Jackson, J., and D. Mckenzie, The Relationship between Plate Motions and Seismic Moment Tensors, and the Rates of Active Deformation in the Mediterranean and Middle-East, *Geophysical Journal-Oxford*, *93*(1), 45–73, 1988.

Jade, S., B. C. Bhatt, Z. Yang, R. Bendick, V. K. Gaur, P. Molnar, M. B. Anand, and D. Kumar, GPS measurements from the Ladakh Himalaya, India: Preliminary tests of plate-like or continuous deformation in Tibet, *Geological Society of America Bulletin*, *116*(11-12), 1385–1391, 2004.

Jade, S., et al., Estimates of interseismic deformation in Northeast India from GPS measurements, *Earth and Planetary Science Letters*, *263*(3-4), 221–234, 2007.

Jain, S., K. Nair, and D. Yedekar, *Geology of the Son-Narmada-Tapti lineament zone in Central India*, *CRUMANSONATA - Special Publication*, vol. 10, Geologic Survey of India, 1995.

Jarrard, R. D., Terrane Motion by Strike-Slip Faulting of Fore-Arc Slivers, *Geology*, *14*(9), 780–783, 1986.

Kanda, R. V. S., and M. Simons, An elastic plate model for interseismic deformation in subduction zones, *Journal of Geophysical Research-Solid Earth*, *115*, 2010.

Kennett, B. L. N., and S. Widiyantoro, A low seismic wavespeed anomaly beneath northwestern India: a seismic signature of the Deccan plume?, *Earth and Planetary Science Letters*, *165*(1), 145–155, 1999.

King, R., and Y. Bock, *Documentation for the GAMIT GPS Analysis software*, vol. Release 10.2, Mass. Instit. of Tech. Scripps Inst. Oceanogr., 2005.

Kogan, M. G., and G. M. Steblov, Current global plate kinematics from GPS (1995-2007) with the plate-consistent reference frame, *Journal of Geophysical Research-Solid Earth*, *113*(B4), 17, 2008.

Kogan, M. G., et al., The 2000 M-w 6.8 Uglegorsk earthquake and regional plate boundary deformation of Sakhalin from geodetic data, *Geophysical Research Letters*, *30*(3), –, 2003.

Kreemer, C., and N. Chamot-Rooke, Contemporary kinematics of the southern Aegean and the Mediterranean Ridge, *Geophysical Journal International*, *157*(3), 1377–1392, 2004.

Laigle, M., A. Hirn, M. Sachpazi, and C. Clement, Seismic coupling and structure of the Hellenic subduction zone in the Ionian Islands region, *Earth and Planetary Science Letters*, *200*(3-4), 243–253, 2002.

Laigle, M., M. Sachpazi, and A. Hirn, Variation of seismic coupling with slab detachment and upper plate structure along the western Hellenic subduction zone, *Tectonophysics*, *391*(1-4), 85–95, 2004.

Larson, K. M., J. T. Freymueller, and S. Philipsen, Global plate velocities from the Global Positioning System, *Journal of Geophysical Research-Solid Earth*, *102*(B5), 9961–9981, 1997.

Larson, K. M., R. Bürgmann, R. Bilham, and J. T. Freymueller, Kinematics of the India-Eurasia collision zone from GPS measurements, *Journal of Geophysical Research-Solid Earth*, *104*(B1), 1077–1093, 1999.

Lave, J., and J. P. Avouac, Active folding of fluvial terraces across the Siwaliks Hills, Himalayas of central Nepal, *Journal of Geophysical Research-Solid Earth*, *105*(B3), 5735–5770, 2000.

Le Pichon, X., Sea-Floor Spreading and Continental Drift, *Journal of Geophysical Research*, *73*(12), 3661, 1968.

Le Pichon, X., and Heirtzle.Jr, Magnetic Anomalies in Indian Ocean and Sea-Floor Spreading, *Journal of Geophysical Research*, *73*(6), 2101, 1968.

Ledain, A. Y., P. Tapponnier, and P. Molnar, Active Faulting and Tectonics of Burma and Surrounding Regions, *Journal of Geophysical Research*, *89*(Nb1), 453–472, 1984.

Loveless, J. P., and B. J. Meade, Partitioning of localized and diffuse deformation in the Tibetan Plateau from joint inversions of geologic and geodetic observations, *Earth and Planetary Science Letters*, *303*(1-2), 11–24, 2011.

Mao, A. L., C. G. A. Harrison, and T. H. Dixon, Noise in GPS coordinate time series, *Journal of Geophysical Research-Solid Earth*, *104*(B2), 2797–2816, 1999.

Matsu'ura, M., and T. Sato, A dislocation model for the earthquake cycle at convergent plate boundaries, *Geophysical Journal International*, *96*(1), 23–32, 1989.

Matsu'ura, M., D. D. Jackson, and A. Cheng, Dislocation Model for Aseismic Crustal Deformation at Hollister, California, *Journal of Geophysical Research-Solid Earth and Planets*, *91*(B12), 2661–2674, 1986.

Mazzotti, S., X. Le Pichon, P. Henry, and S. Miyazaki, Full interseismic locking of the Nankai and Japan-west Kurile subduction zones: An analysis of uniform elastic strain accumulation in Japan constrained by permanent GPS, *Journal of Geophysical Research-Solid Earth*, *105*(B6), 13,159–13,177, 2000.

McCaffrey, R., *Crustal block rotations and plate coupling, in Plate Boundary Zones*, *Geodynamic Series*, vol. 30, AGU, Washington, D.C., 2002.

McCaffrey, R., M. D. Long, C. Goldfinger, P. C. Zwick, J. L. Nabelek, C. K. Johnson, and C. Smith, Rotation and plate locking at the southern Cascadia subduction zone, *Geophysical Research Letters*, *27*(19), 3117–3120, 2000a.

McCaffrey, R., P. C. Zwick, Y. Bock, L. Prawirodirdjo, J. F. Genrich, C. W. Stevens, S. S. O. Puntodewo, and C. Subarya, Strain partitioning during oblique plate convergence in northern Sumatra: Geodetic and seismologic constraints and numerical modeling, *Journal of Geophysical Research-Solid Earth*, *105*(B12), 28,363–28,376, 2000b.

McClusky, S., et al., Global Positioning System constraints on plate kinematics and dynamics in the eastern Mediterranean and Caucasus, *Journal of Geophysical Research-Solid Earth*, *105*(B3), 5695–5719, 2000.

McKenzie, D. P., and R. L. Parker, North Pacific - an Example of Tectonics on a Sphere, *Nature*, *216*(5122), 1476, 1967.

Meade, B. J., Present-day kinematics at the India-Asia collision zone, *Geology*, *35*(1), 81–84, 2007.

Meade, B. J., and B. H. Hager, The current distribution of deformation in the western Tien Shan from block models constrained by geodetic data, *Geologiya I Geofizika*, *42*(10), 1622–1633, 2001.

Meade, B. J., and B. H. Hager, Block models of crustal motion in southern California constrained by GPS measurements, *Journal of Geophysical Research-Solid Earth*, *110*(B3), –, 2005.

Meier, T., M. Rische, B. Endrun, A. Vafidis, and H. P. Harjes, Seismicity of the Hellenic subduction zone in the area of western and central Crete observed by temporary local seismic networks, *Tectonophysics*, *383*(3-4), 149–169, 2004.

Merkouriev, S., and C. DeMets, Constraints on Indian plate motion since 20 Ma from dense Russian magnetic data: Implications for Indian plate dynamics, *Geochemistry Geophysics Geosystems*, *7*, 25, 2006.

Minster, J. B., and T. H. Jordan, Present-Day Plate Motions, *Journal of Geophysical Research*, *83*(Nb11), 5331–5354, 1978.

Mohadjer, S., et al., Partitioning of India-Eurasia convergence in the Pamir-Hindu Kush from GPS measurements, *Geophysical Research Letters*, *37*, 2010.

Mountjoy, J. J., and P. M. Barnes, Active upper plate thrust faulting in regions of low plate interface coupling, repeated slow slip events, and coastal uplift: Example from the Hikurangi Margin, New Zealand, *Geochemistry Geophysics Geosystems*, *12*, 2011.

Nyst, M., and W. Thatcher, New constraints on the active tectonic deformation of the Aegean, *Journal of Geophysical Research-Solid Earth*, *109*(B11), 2004.

Okada, Y., Surface Deformation Due to Shear and Tensile Faults in a Half-Space, *Bulletin of the Seismological Society of America*, *75*(4), 1135–1154, 1985.

Papadimitriou, E. E., and V. G. Karakostas, Rupture model of the great AD 365 Crete earthquake in the southwestern part of the Hellenic Arc, *Acta Geophysica*, *56*(2), 293–312, 2008.

Papazachos, B., and C. Papazachou, *The Earthquakes of Greece*, P. Ziti and Co., Thessaloniki, Greece, 1997.

Papazachos, B. C., V. G. Karakostas, C. B. Papazachos, and E. M. Scordilis, The geometry of the Wadati-Benioff zone and lithospheric kinematics in the Hellenic arc, *Tectonophysics*, *319*(4), 275–300, 2000.

Park, J. O., T. Tsuru, S. Kodaira, P. R. Cummins, and Y. Kaneda, Splay fault branching along the Nankai subduction zone, *Science*, *297*(5584), 1157–1160, 2002.

Paul, J., et al., The motion and active deformation of India, *Geophysical Research Letters*, *28*(4), 647–650, 2001.

Pegler, G., and S. Das, An enhanced image of the Pamir Hindu Kush seismic zone from relocated earthquake hypocentres, *Geophysical Journal International*, *134*(2), 573–595, 1998.

Petit, C., and M. Fournier, Present-day velocity and stress fields of the Amurian Plate from thin-shell finite-element modelling, *Geophysical Journal International*, *160*(1), 357–369, 2005.

Pirazzoli, P. A., J. Laborel, and S. C. Stiros, Earthquake clustering in the Eastern Mediterranean during historical times, *Journal of Geophysical Research-Solid Earth*, *101*(B3), 6083–6097, 1996.

Pollitz, F. F., R. Bürgmann, and P. Banerjee, Post-seismic relaxation following the great 2004 Sumatra-Andaman earthquake on a compressible self-gravitating Earth, *Geophysical Journal International*, *167*(1), 397–420, 2006.

Prawirodirdjo, L., and Y. Bock, Instantaneous global plate motion model from 12 years of continuous GPS observations, *Journal of Geophysical Research-Solid Earth*, *109*(B8), –, 2004.

Rao, B. R., Historical seismicity and deformation rates in the Indian Peninsular Shield, *Journal of Seismology*, *4*(3), 247–258, 2000.

Reilinger, R., S. McClusky, D. Paradissis, S. Ergintav, and P. Vernant, Geodetic constraints on the tectonic evolution of the Aegean region and strain accumulation along the Hellenic subduction zone, *Tectonophysics*, *488*(1-4), 22–30, 2010.

Reilinger, R., et al., GPS constraints on continental deformation in the Africa-Arabia-Eurasia continental collision zone and implications for the dynamics of plate interactions, *Journal of Geophysical Research-Solid Earth*, *111*(B5), 2006.

Replumaz, A., and P. Tapponnier, Reconstruction of the deformed collision zone between India and Asia by backward motion of lithospheric blocks, *Journal of Geophysical Research-Solid Earth*, *108*(B6), 24, 2003.

Riegel, S. A., K. Fujita, B. M. Kozmin, V. S. Imaev, and D. B. Cook, Extrusion Tectonics of the Okhotsk Plate, Northeast Asia, *Geophysical Research Letters*, *20*(7), 607–610, 1993.

Ring, U., J. Glodny, T. Will, and S. Thomson, The Hellenic Subduction System: High-Pressure Metamorphism, Exhumation, Normal Faulting, and Large-Scale Extension, *Annual Review of Earth and Planetary Sciences, Vol 38*, *38*, 45–76, 2010.

Royer, J. Y., and R. G. Gordon, The motion and boundary between the Capricorn and Australian plates, *Science*, *277*(5330), 1268–1274, 1997.

Royer, J. Y., R. G. Gordon, and B. C. Horner-Johnson, Motion of nubia relative to antarctica since 11 Ma: Implications for Nubia-Somalia, Pacific-North America, and India-Eurasia motion, *Geology*, *34*(6), 501–504, 2006.

Savage, J. C., A Dislocation Model of Strain Accumulation and Release at a Subduction Zone, *Journal of Geophysical Research*, *88*(Nb6), 4984–4996, 1983.

Sella, G. F., T. H. Dixon, and A. L. Mao, REVEL: A model for Recent plate velocities from space geodesy, *Journal of Geophysical Research-Solid Earth*, *107*(B4), –, 2002.

Seno, T., T. Sakurai, and S. Stein, Can the Okhotsk plate be discriminated from the North American plate?, *Journal of Geophysical Research-Solid Earth*, *101*(B5), 11,305–11,315, 1996.

Serpelloni, E., M. Anzidei, P. Baldi, G. Casula, and A. Galvani, Crustal velocity and strain-rate fields in Italy and surrounding regions: new results from the analysis of permanent and non-permanent GPS networks, *Geophysical Journal International*, *161*(3), 861–880, 2005.

Serpelloni, E., G. Vannucci, S. Pondrelli, A. Argnani, G. Casula, M. Anzidei, P. Baldi, and P. Gasperini, Kinematics of the Western Africa-Eurasia plate boundary from focal mechanisms and GPS data, *Geophysical Journal International*, *169*(3), 1180–1200, 2007.

Shaw, B., and J. Jackson, Earthquake mechanisms and active tectonics of the Hellenic subduction zone, *Geophysical Journal International*, *181*(2), 966–984, 2010.

Shaw, B., et al., Eastern Mediterranean tectonics and tsunami hazard inferred from the AD 365 earthquake, *Nature Geoscience*, *1*(4), 268–276, 2008.

Shen, Z. K., J. N. Lu, M. Wang, and R. Bürgmann, Contemporary crustal deformation around the southeast borderland of the Tibetan Plateau, *Journal of Geophysical Research-Solid Earth*, *110*(B11), 17, 2005.

Sieh, K., and D. Natawidjaja, Neotectonics of the Sumatran fault, Indonesia, *Journal of Geophysical Research-Solid Earth*, *105*(B12), 28,295–28,326, 2000.

Simons, W. J. F., et al., A decade of GPS in Southeast Asia: Resolving Sundaland motion and boundaries, *Journal of Geophysical Research-Solid Earth*, *112*(B6), 2007.

Socquet, A., C. Vigny, N. Chamot-Rooke, W. Simons, C. Rangin, and B. Ambrosius, India and Sunda plates motion and deformation along their boundary in Myanmar determined by GPS, *Journal of Geophysical Research-Solid Earth*, *111*(B5), 2006a.

Socquet, A., W. Simons, C. Vigny, R. McCaffrey, C. Subarya, D. Sarsito, B. Ambrosius, and W. Spakman, Microblock rotations and fault coupling in SE Asia triple junction (Sulawesi, Indonesia) from GPS and earthquake slip vector data, *Journal of Geophysical Research-Solid Earth*, *111*(B8), 2006b.

Sol, S., et al., Geodynamics of the southeastern Tibetan Plateau from seismic anisotropy and geodesy, *Geology*, *35*(6), 563–566, 2007.

Stamps, D. S., E. Calais, E. Saria, C. Hartnady, J. M. Nocquet, C. J. Ebinger, and R. M. Fernandes, A kinematic model for the east African rift, *Geophysical Research Letters*, *35*(5), 6, 2008.

Steblov, G. M., M. G. Kogan, R. W. King, C. H. Scholz, R. Bürgmann, and D. I. Frolov, Imprint of the North American plate in Siberia revealed by GPS, *Geophysical Research Letters*, *30*(18), –, 2003.

Stein, S., and R. G. Gordon, Statistical Tests of Additional Plate Boundaries from Plate Motion Inversions, *Earth and Planetary Science Letters*, *69*(2), 401–412, 1984.

Stein, S., G. Sella, and E. Okal, *The January 26, 2001 Bhuj earthquake and the diffuse western boundary of the Indian plate, in Plate Boundary Zones*, *Geodynamic Series*, vol. 30, AGU, Washington, D.C., 2002.

Stiros, S., S. Papageorgiou, V. Kontogianni, and P. Psimoulis, Church repair swarms and earthquakes in Rhodes Island, Greece, *Journal of Seismology*, *10*(4), 527–537, 2006.

Stiros, S. C., The AD 365 Crete earthquake and possible seismic clustering during the fourth to sixth centuries AD in the Eastern Mediterranean: a review of historical and archaeological data, *Journal of Structural Geology*, *23*(2-3), 545–562, 2001.

Stiros, S. C., The 8.5+magnitude, AD365 earthquake in Crete: Coastal uplift, topography changes, archaeological and historical signature, *Quaternary International*, *216*(1-2), 54–63, 2010.

Stiros, S. C., and S. Papageorgiou, Seismicity of Western Crete and the destruction of the town of Kisamos at AD 365: Archaeological evidence, *Journal of Seismology*, *5*(3), 381–397, 2001.

Takahashi, H., et al., Velocity field of around the Sea of Okhotsk and Sea of Japan regions determined from a new continuous GPS network data, *Geophysical Research Letters*, *26*(16), 2533–2536, 1999.

Tapponnier, P., and P. Molnar, Active Faulting and Cenozoic Tectonics of the Tien Shan, Mongolia, and Baykal Regions, *Journal of Geophysical Research*, *84*(NB7), 3425, 1979.

Tapponnier, P., Z. Q. Xu, F. Roger, B. Meyer, N. Arnaud, G. Wittlinger, and J. S. Yang, Geology - Oblique stepwise rise and growth of the Tibet plateau, *Science*, *294*(5547), 1671–1677, 2001.

Taylor, M., and A. Yin, Active structures of the Himalayan-Tibetan orogen and their relationships to earthquake distribution, contemporary strain field, and Cenozoic volcanism, *Geosphere*, *5*(3), 199–214, 2009.

Thatcher, W., Microplate model for the present-day deformation of Tibet, *Journal of Geophysical Research-Solid Earth*, *112*(B1), 13, 2007.

Thommeret, Y., J. Laborel, L. Montaggioni, and P. A. Pirazzoli, *Late Holocene shoreline changes and seismotectonic displacements in western Crete (Greece)*, *Zeitung fur Geomorphologie, Neue Folge (Supplement)*, vol. 40, 1981.

Thompson, S. C., R. J. Weldon, C. M. Rubin, K. Abdrakhmatov, P. Molnar, and G. W. Berger, Late Quaternary slip rates across the central Tien Shan, Kyrgyzstan, central Asia, *Journal of Geophysical Research-Solid Earth*, *107*(B9), 2002.

Toya, Y., and M. Kasahara, Robust and exploratory analysis of active mesoscale tectonic zones in Japan utilizing the nationwide GPS array, *Tectonophysics*, *400*(1-4), 27–53, 2005.

Vassilakis, E., L. Royden, and D. Papanikolaou, Kinematic links between subduction along the Hellenic trench and extension in the Gulf of Corinth, Greece: A multidisciplinary analysis, *Earth and Planetary Science Letters*, *303*(1-2), 108–120, 2011.

Vine, F. J., and D. H. Matthews, Magnetic Anomalies over Oceanic Ridges, *Nature*, *199*(489), 947, 1963.

Vine, F. J., and J. T. Wilson, Magnetic Anomalies over a Young Oceanic Ridge Off Vancouver Island, *Science*, *150*(3695), 485, 1965.

Wiens, D. A., et al., A Diffuse Plate Boundary Model for Indian-Ocean Tectonics, *Geophysical Research Letters*, *12*(7), 429–432, 1985.

Zhang, P. Z., Z. Shen, M. Wang, W. J. Gan, R. Bürgmann, and P. Molnar, Continuous deformation of the Tibetan Plateau from global positioning system data, *Geology*, *32*(9), 809–812, 2004.

Appendix A

GPS velocities and segment geometry used in the Okhotsk Plate model

Table A.1: GPS Velocities Used in Okhotsk Plate Inversion - Fixed North American Reference Frame

Long	**Lat**	**Velocity (mm/yr)**				**Corr**	**Site**	**Plate**
°E	**°N**	**East**	**North**	σ **E**	σ **N**			
142.543	49.690	4.09	1.30	2.65	2.67	0.007	AIVA	AMU
110.850	48.520	9.90	-8.65	3.26	2.73	0.093	BATS	AMU
142.157	49.637	2.41	0.85	2.55	2.56	0.006	BOSH	AMU
125.444	43.791	11.34	-3.61	1.06	1.02	0.002	CHAN	AMU
114.580	48.090	10.77	-6.92	2.73	2.20	0.068	CHOI	AMU
127.374	36.399	15.08	-3.12	0.70	0.69	0.000	DAEJ	AMU
109.966	41.755	12.98	-3.12	1.72	1.55	-0.008	HB04	AMU
111.709	41.515	15.18	-2.37	1.59	1.50	-0.002	HB08	AMU
115.846	40.870	13.61	-3.85	1.56	1.43	-0.002	HB34	AMU
117.914	40.961	12.59	-3.31	1.65	1.49	0.001	HB58	AMU
121.599	42.053	10.84	-4.94	1.66	1.50	0.006	HB76	AMU
119.741	49.270	10.98	-4.69	2.44	2.40	-0.002	HLAR	AMU
124.103	50.390	7.38	-1.18	3.33	3.21	-0.004	JAGD	AMU
135.046	48.521	8.46	0.37	1.06	1.02	0.001	KHAJ	AMU
106.490	50.740	10.07	-6.35	1.14	1.15	0.015	KIAT	AMU
104.890	51.850	7.81	-4.28	1.14	1.15	-0.004	LIST	AMU
106.220	45.800	13.65	-5.92	1.66	1.67	0.003	MAND	AMU
142.759	48.573	1.45	1.57	2.64	2.65	0.004	PORE	AMU
131.170	46.650	9.49	-5.92	3.72	3.38	-0.012	SHUA	AMU

Continued on next page...

Table A.1 – Continued from previous page

Long	Lat	Velocity (mm/yr)				Corr	Site	Plate
°E	°N	East	North	σ E	σ N			
126.969	46.650	1.50	1.64	3.34	3.20	-0.005	SUIH	AMU
130.908	44.433	10.15	-2.15	2.46	2.41	-0.003	SUIY	AMU
106.250	50.230	9.79	-7.34	1.66	1.67	-0.019	SUKG	AMU
127.054	37.276	15.30	-3.14	0.89	0.89	-0.001	SUWN	AMU
108.240	52.970	8.06	-5.78	1.66	1.67	0.005	TURK	AMU
106.010	51.170	9.63	-6.83	1.14	1.15	0.000	UDUN	AMU
142.065	49.076	3.13	1.29	1.11	1.10	0.002	UGLE	AMU
122.172	46.062	12.75	-5.09	3.34	3.19	-0.004	UHOT	AMU
107.620	51.810	9.83	-8.11	1.14	1.15	0.040	ULAN	AMU
110.590	47.260	11.13	-5.74	3.26	2.20	0.081	UNDE	AMU
131.926	43.197	10.00	-1.70	0.82	0.82	0.000	VLAD	AMU
116.104	43.903	10.64	-5.41	3.32	3.17	0.000	XHOT	AMU
129.489	43.003	12.93	-0.85	3.34	3.19	-0.005	YANJ	AMU
166.211	62.456	0.44	1.88	0.85	0.85	0.001	KMS	EUR
106.580	52.790	6.53	-4.43	2.72	2.20	0.002	ANGA	EUR
58.560	56.430	11.21	-9.51	0.79	0.79	0.000	ARTU	EUR
166.438	68.076	1.03	-0.64	0.81	0.81	0.000	BILI	EUR
17.073	52.277	18.85	-8.55	0.77	0.77	0.000	BOR1	EUR
4.359	50.798	20.31	-8.27	0.77	0.77	0.000	BRUS	EUR
108.518	41.511	14.50	-6.85	1.78	1.58	-0.013	GI02	EUR
15.493	47.067	20.58	-8.51	0.69	0.69	-0.001	GRAZ	EUR
108.400	41.030	15.18	-4.04	1.67	1.53	-0.006	HB03	EUR
104.316	52.219	7.15	-5.81	0.76	0.75	-0.002	IRKT	EUR
5.810	52.178	19.62	-7.51	0.71	0.71	-0.001	KOSG	EUR
92.794	55.993	6.32	-7.45	0.86	0.86	0.001	KSTU	EUR
24.395	60.217	15.30	-9.82	0.72	0.72	0.000	METS	EUR
88.360	69.362	1.23	-7.10	0.82	0.82	0.000	NRIL	EUR
11.865	78.930	9.21	-8.71	0.55	0.55	0.000	NYA1	EUR
155.770	62.518	-0.28	0.93	2.27	2.21	-0.003	OMS1	EUR
11.926	57.395	16.71	-8.86	0.69	0.68	-0.001	ONSA	EUR
163.067	59.243	-0.01	1.14	2.23	2.20	0.000	OSSO	EUR
13.066	52.379	18.99	-8.34	0.74	0.73	-0.001	POTS	EUR
128.866	71.634	-1.85	-1.08	0.81	0.81	0.000	TIXI	EUR
136.812	62.784	3.99	-0.17	1.63	1.62	-0.002	TKL1	EUR
12.879	49.144	20.27	-8.18	0.71	0.71	0.000	WTZR	EUR
129.680	62.031	1.63	-0.98	0.89	0.89	0.000	YAKT	EUR
36.759	55.699	14.94	-9.46	0.72	0.72	0.000	ZWEN	EUR
281.929	45.956	-0.05	-1.01	0.69	0.69	0.000	ALGO	NAM
295.304	32.370	-0.49	0.24	0.69	0.68	0.000	BRMU	NAM
265.911	58.759	0.91	0.07	0.78	0.77	0.000	CHUR	NAM
264.134	50.259	0.25	0.53	0.87	0.87	0.000	DUBO	NAM

Continued on next page...

Table A.1 – Continued from previous page

Long	Lat	Velocity (mm/yr)				Corr	Site	Plate
°E	°N	East	North	σ E	σ N			
258.022	54.726	0.24	-0.87	0.78	0.77	0.000	FLIN	NAM
255.985	30.681	-0.16	0.50	0.69	0.68	0.000	MDO1	NAM
268.425	41.772	0.14	0.40	0.69	0.68	0.000	NLIB	NAM
251.881	34.302	-0.43	0.16	0.69	0.68	0.000	PIE1	NAM
279.616	25.614	0.41	-0.12	1.60	1.52	-0.005	RCM6	NAM
293.167	54.832	-0.04	1.44	0.92	0.91	0.000	SCH2	NAM
307.322	47.595	-0.31	0.61	0.75	0.75	0.001	STJO	NAM
291.212	76.537	-1.13	-0.83	0.77	0.77	-0.001	THU1	NAM
245.519	62.481	0.54	0.36	0.69	0.68	0.000	YELL	NAM
158.697	55.930	-1.82	2.94	1.01	1.02	0.000	_ES1	OKH
158.686	57.759	-1.78	-1.67	1.67	1.65	0.001	_TIG	OKH
141.510	43.854	-5.02	5.18	0.87	0.87	0.001	0008	OKH
140.107	42.008	-8.95	6.26	0.88	0.88	0.001	0021	OKH
142.626	44.295	-4.04	5.37	0.87	0.87	0.001	0107	OKH
141.431	43.405	-6.94	2.45	0.87	0.87	0.001	0117	OKH
144.127	43.121	-21.49	15.89	0.87	0.87	0.001	0124	OKH
140.499	43.057	-5.57	2.04	0.87	0.87	0.001	0126	OKH
142.296	42.727	-16.28	6.63	0.87	0.87	0.001	0133	OKH
140.316	41.599	-4.71	3.43	0.87	0.87	0.000	0149	OKH
139.928	40.578	-6.24	4.85	0.87	0.87	0.000	0154	OKH
141.951	39.869	-11.53	3.54	0.87	0.87	0.000	0162	OKH
141.449	38.683	-27.38	10.63	0.87	0.87	0.000	0175	OKH
139.832	38.594	-8.24	6.09	0.87	0.87	0.000	0196	OKH
140.260	37.126	-16.00	2.92	0.87	0.87	0.000	0210	OKH
140.476	36.344	-14.56	5.64	0.87	0.87	0.000	0216	OKH
138.553	36.508	-10.65	3.39	0.91	0.91	0.000	0221	OKH
138.334	37.231	1.07	4.18	0.87	0.87	0.000	0241	OKH
138.247	36.665	-5.84	3.99	0.91	0.90	0.001	0267	OKH
158.213	53.280	-11.25	10.24	2.21	2.18	0.001	KORC	OKH
159.865	56.042	-3.23	2.12	2.05	2.05	0.000	KOZY	OKH
159.481	54.025	-6.37	5.11	4.15	4.10	-0.006	KRM9	OKH
161.194	54.585	-16.96	13.61	2.20	2.18	-0.002	KRON	OKH
147.431	61.883	1.87	-3.95	1.33	1.33	-0.001	KUL1	OKH
150.770	59.576	-1.85	-3.37	0.96	0.96	0.000	MAG0	OKH
157.474	53.333	-9.45	6.50	3.22	3.23	-0.004	MALK	OKH
158.623	54.693	-5.58	5.13	2.25	2.18	-0.003	MILK	OKH
159.197	53.142	-17.15	12.45	2.18	2.16	0.000	NALY	OKH
142.946	53.602	3.21	0.11	0.79	0.78	0.001	OKHA	OKH
143.804	50.292	3.21	-0.01	2.73	2.75	0.006	OKRG	OKH
156.810	51.466	-14.24	5.15	2.21	2.20	0.004	PAUZ	OKH
142.817	49.838	2.57	1.63	2.24	2.22	0.002	PBDN	OKH

Continued on next page...

Table A.1 – Continued from previous page

Long	**Lat**	**Velocity (mm/yr)**				**Corr**	**Site**	**Plate**
°E	**°N**	**East**	**North**	σ **E**	σ **N**			
143.270	49.922	2.03	-1.69	2.57	2.58	0.006	PERV	OKH
158.607	53.067	-12.26	10.76	0.88	0.87	-0.001	PETP	OKH
158.650	53.023	-16.81	10.92	2.36	2.35	0.002	PETS	OKH
143.646	50.049	2.23	0.62	2.55	2.56	0.008	PILG	OKH
152.422	62.925	-0.45	-0.65	1.19	1.17	0.001	SEY2	OKH
155.962	54.304	-4.70	2.74	2.25	2.22	0.000	SOBL	OKH
148.168	62.779	0.53	-1.15	1.25	1.25	0.000	SUS1	OKH
152.392	61.130	1.43	-2.47	2.30	2.23	-0.001	TAL1	OKH
143.246	63.260	2.57	0.61	1.26	1.26	-0.004	TOM1	OKH
140.087	36.106	-13.79	5.26	0.68	0.68	0.001	TSKB	OKH
156.244	52.661	-11.05	6.46	2.30	2.25	-0.016	UBR1	OKH
156.575	52.928	-10.76	6.99	2.53	2.58	-0.206	UBR2	OKH
156.738	57.091	-0.54	1.93	2.26	2.23	0.002	UHAZ	OKH
162.593	56.265	-12.22	9.04	2.07	2.06	0.002	UKAM	OKH
143.242	64.566	2.60	0.52	1.36	1.35	-0.001	UNR1	OKH
142.717	47.030	-0.03	1.27	1.07	1.06	0.000	YSSK	OKH
183.434	-43.956	-40.37	53.26	0.82	0.81	0.004	CHAT	PAC
200.335	22.126	-59.74	53.36	0.73	0.71	0.002	KOKB	PAC
167.730	8.722	-70.96	49.35	0.79	0.76	-0.003	KWJ1	PAC
153.979	24.290	-75.18	39.87	1.13	1.05	-0.001	MARC	PAC
210.394	-17.577	-68.34	51.45	1.03	0.98	0.004	THTI	PAC
151.887	7.447	-72.43	39.91	1.03	0.96	0.000	TRUK	PAC

Table A.2: Detailed segment geometry of the elastic dislocations that bound the Okhotsk, Amurian, Eurasian, Pacific and North American blocks.

Segment	Start Point		End Point		Locking Depth	Dip
Number	Long °E	Lat °N	Long °E	Lat °N	(km)	°
1	78.708	88.878	341.129	89.129	0	90
2	78.708	88.878	114.668	88.552	0	90
3	104.092	51.633	106.480	43.525	70	90
4	104.092	51.633	108.107	53.034	70	90
5	106.480	43.525	132.119	28.812	70	90
6	108.107	53.034	109.768	55.595	70	90
7	109.768	55.595	142.406	54.636	70	90
8	114.668	88.552	128.880	85.068	0	90
9	120.552	15.205	121.027	22.400	0	90
10	120.552	15.205	124.722	11.645	0	90
11	121.027	22.400	121.715	23.522	0	90
12	121.715	23.522	124.740	23.642	0	90
13	124.722	11.645	127.104	4.015	0	90
14	124.740	23.642	127.811	24.043	0	90
15	127.104	4.015	127.998	1.218	0	90
16	127.811	24.043	132.119	28.812	0	90
17	127.998	1.218	152.121	-2.852	0	90
18	128.880	85.068	143.016	66.751	70	90
19	132.119	28.812	133.353	31.774	0	90
20	133.353	31.774	134.945	32.435	25	10
21	134.945	32.435	136.817	33.007	30	20
22	136.817	33.007	138.765	34.904	30	25
23	137.776	38.591	137.838	36.577	20	20
24	137.776	38.591	138.436	39.770	30	20
25	137.838	36.577	138.107	35.608	25	25
26	138.107	35.608	138.765	34.904	25	25
27	138.436	39.770	138.662	42.758	30	20
28	138.662	42.758	138.910	45.745	50	20
29	138.765	34.904	142.289	34.176	15	90
30	138.910	45.745	142.642	45.791	70	90
31	142.284	51.077	142.642	45.791	70	90
32	142.284	51.077	142.745	53.474	70	90
33	142.289	34.176	142.764	35.480	25	20
34	142.406	54.636	142.744	60.650	70	90
35	142.406	54.636	142.745	53.474	70	90
36	142.744	60.650	142.962	63.864	70	90
37	142.764	35.480	143.396	36.905	25	10
38	142.962	63.864	143.016	66.751	70	90

Continued on next page...

Table A.2 – Continued from previous page

Segment	Start		End		Locking Depth	Dip
Number	Long °E	Lat °N	Long °E	Lat °N	KM	°
39	143.016	66.751	153.821	62.924	70	90
40	143.396	36.905	144.026	38.408	30	10
41	144.026	38.408	144.598	41.187	25	15
42	144.598	41.187	149.796	44.197	25	10
43	149.796	44.197	154.971	46.488	40	20
44	152.121	-2.852	164.629	-9.718	0	90
45	153.821	62.924	161.678	59.626	70	90
46	154.971	46.488	157.773	48.882	30	20
47	157.773	48.882	159.582	50.613	40	20
48	159.387	-89.710	163.250	-46.913	0	90
49	159.387	-89.710	342.871	-88.548	0	90
50	159.582	50.613	160.956	51.834	50	15
51	160.956	51.834	163.339	54.192	30	15
52	161.678	59.626	162.454	59.141	70	90
53	162.454	59.141	163.259	58.687	70	90
54	162.509	57.615	164.437	56.330	70	90
55	162.509	57.615	163.259	58.687	70	90
56	163.250	-46.913	181.306	-18.111	0	90
57	163.250	-46.913	179.129	-53.129	0	90
58	163.339	54.192	163.941	55.157	30	15
59	163.941	55.157	164.437	56.330	20	15
60	164.437	56.330	167.552	54.576	40	90
61	164.629	-9.718	167.905	-16.076	0	90
62	167.552	54.576	172.011	52.410	40	90
63	167.905	-16.076	181.306	-18.111	0	90
64	172.011	52.410	180.482	50.266	0	90
65	179.129	-53.129	237.774	-40.935	0	90
66	180.482	50.266	189.753	51.003	0	90
67	189.753	51.003	196.984	52.970	0	90
68	196.984	52.970	206.621	55.643	0	90
69	206.621	55.643	212.279	58.694	0	90
70	212.279	58.694	220.916	57.169	0	90
71	220.916	57.169	247.124	28.684	0	90
72	237.774	-40.935	247.124	28.684	0	90
73	341.129	89.129	342.871	-88.548	0	90

Appendix B

GPS velocities and segment geometry used in the India Plate model

Table B.1: GPS Velocities Used in India Plate Inversion
- ITRF 2000 Reference Frame

Long	**Lat**	**Velocity (mm/yr)**				**Corr**	**Site**	**Source**[†]	**EXC**[‡]
°E	**°N**	**East**	**North**	σ **E**	σ **N**				
0.336	50.867	19.43	15.79	0.13	0.13	0.13	HERS	a	U
4.359	50.798	19.01	14.76	0.14	0.14	0.14	BRUS	m	U
5.81	52.178	18.89	14.83	0.12	0.12	0.12	KOSG	m	U
6.605	52.915	19.05	15.32	0.54	0.54	0.54	WSRT	d	U
11.865	78.93	11.44	14.16	0.91	0.91	0.91	NYA1	m	U
12.879	49.144	21.56	14.6	0.16	0.16	0.16	WTZR	m	U
13.066	52.379	20.7	13.53	0.12	0.13	0.13	POTS	a	U
14.786	49.914	21.97	13.91	0.47	0.47	0.47	GOPE	d	U
17.073	52.277	21.26	13.62	0.21	0.21	0.21	BOR1	m	U
20.67	53.892	20.57	13.3	0.45	0.45	0.45	LAMA	d	U
21.032	52.097	22.49	13.54	0.21	0.21	0.21	JOZE	m	U
30.497	50.364	22.72	10.49	0.41	0.31	0.31	GLSV	a	U
36.57	55.115	25.31	9.87	1.2	1.18	1.18	MOBN	d	U
37.224	56.027	24.02	10.57	0.6	0.59	0.59	MDVO	d	U
58.56	56.43	26.11	4.36	0.26	0.26	0.26	ARTU	m	U
72.37	-7.27	46.12	30.93	1.86	1.84	1.84	DGAR	g	U
72.916	19.133	38.72	28.88	1.07	1.04	1.04	BMBY	m	U
73.526	4.189	46.27	32.44	1.11	0.99	0.99	MALD	m	U
73.882	18.558	39.02	32.6	0.93	0.91	0.91	PUN2	m	U
75.363	32.565	33.83	29.91	1.54	1.37	1.37	HIRA	m	U
75.881	32.304	31.78	29.8	0.78	0.77	0.77	NURP	m	U
75.94	31.48	33.89	30.48	1.39	0.95	0.95	BOHA	k	U
75.993	32.536	29.36	27.88	0.78	0.76	0.76	DALH	m	U
76.294	31.897	31.95	28.89	0.89	0.88	0.88	JWLM	m	U
76.307	31.538	33.67	30.47	1.02	0.98	0.98	UNAN	m	U
76.31	32.25	34.29	30.58	0.69	0.63	0.63	NADI	k	U
76.31	31.54	32.61	30.36	1.3	0.94	0.94	UNA0	k	U
76.673	31.919	32.27	33.37	1.36	1.29	1.29	CHBG	m	U
76.69	32.7	31.04	25.16	1.48	1.2	1.2	UDAI	k	U
76.82	31.63	30.23	27.48	1.48	1.02	1.02	REWL	k	U
76.969	8.423	46.34	34.93	2.77	2.37	2.37	TIR0	m	U
77.108	32.067	27	23.45	0.91	0.89	0.89	KULU	m	U
77.126	28.482	36.84	30.23	1.28	1.25	1.25	DELH	m	U
77.175	32.634	25.35	17.31	1.71	1.63	1.63	JISP	m	U
77.18	32.63	26.45	19.29	1.38	1.1	1.1	JIPA	k	U
77.19	32.32	31.82	18.18	1.28	0.92	0.92	KOTH	k	U
77.192	32.317	26.41	24.14	1.36	1.35	1.35	KOT1	m	U
77.425	32.798	27.66	16.38	1.8	1.67	1.67	SRCH	m	U
77.447	23.209	36.93	32.7	1.24	1.21	1.21	RRLB	m	U

Continued on next page...

Table B.1 – Continued from previous page

Long	Lat	Velocity (mm/yr)				Corr	Site	Source†	EXC‡
°E	°N	East	North	σ E	σ N				
77.47	10.23	41.56	32.68	0.61	0.57	0.57	KODI	h	U
77.512	13.034	43.69	33.87	1.15	1.1	1.1	BAN2	m	U
77.57	13.021	42.14	32.8	0.31	0.27	0.27	IISC	m	U
77.613	34.13	27.2	17.89	0.68	0.65	0.65	SABU	m	U
77.63	30.28	35.9	28.56	1.47	1.2	1.2	QASI	k	U
77.808	33.972	27.11	15.93	1.25	1.12	1.12	SHAK	m	U
77.86	30.33	34.51	30.08	1.01	0.76	0.76	SABA	k	U
77.868	30.147	36.71	28.23	1.31	1.12	1.12	MOHA	m	U
77.87	30.15	35.89	33.67	1.57	1.29	1.29	MOND	k	U
77.921	32.364	24.49	16.91	1.86	1.66	1.66	KAZA	m	U
77.97	30.29	33.91	31.14	1.01	0.84	0.84	WILD	k	U
77.98	30.1	35.39	32.53	1.38	1.01	1.01	RAJA	k	U
78.01	30.33	36.11	30.23	0.67	0.55	0.55	WIH2	k	U
78.012	30.329	34.17	30.73	1.19	1.13	1.13	WIHG	m	U
78.021	30.459	33.34	30.44	0.73	0.71	0.71	HATI	m	U
78.115	30.452	35.94	28.43	1.38	1.28	1.28	BATA	m	U
78.155	30.342	33.01	30.87	1.14	1.09	1.09	DHAU	m	U
78.16	30.34	36.72	28.88	1.19	1.01	1.01	DHOU	k	U
78.19	30.19	33.5	31.76	1	0.83	0.83	DOIW	k	U
78.368	30.394	33.45	29.86	0.88	0.84	0.84	CHMB	m	U
78.37	30.4	33.03	28.41	2.44	1.56	1.56	CHAM	k	U
78.55	17.42	41.39	34.08	1.09	0.81	0.81	HYDE	g	U
78.608	25.452	37.68	31.64	0.88	0.84	0.84	JHAN	m	U
78.62	30.81	31.28	21.34	1.75	1.37	1.37	BHAT	k	U
78.66	33.209	28.55	15.79	0.7	0.65	0.65	NYOM	m	U
78.68	29.848	38.43	31.79	1.55	1.45	1.45	LAN2	m	U
78.68	29.85	34.67	30.78	1.56	1	1	LANS	k	U
78.68	31	27.7	23.12	2.44	1.56	1.56	SUKI	k	U
78.75	31.04	29.81	22.8	1.95	1.56	1.56	HARS	k	U
79.09	30.298	33.74	28.33	1.29	1.12	1.12	GHOL	m	U
79.276	21.394	38.92	32.62	0.93	0.85	0.85	NAGP	m	U
79.493	30.743	28.25	20.52	1.26	1.11	1.11	BADR	m	U
79.8	32.43	30.18	16.28	1.07	1.07	1.07	JB56	g	U
79.874	6.892	39.98	35.63	2.14	1.42	1.42	COLA	e	U
79.876	23.129	39.39	28.62	1.62	1.54	1.54	JBPR	m	U
79.94	33.56	29.37	15.16	1.64	1.64	1.64	J049	k	U
80.04	29.84	34.1	26.72	2.73	1.65	1.65	CHAU	k	U
80.1	32.51	31.98	16.68	1.74	1.35	1.35	SHIQ	k	U
80.15	28.96	37.35	32.87	1.08	0.73	0.73	MAHE	g	U
80.24	30.06	33.51	22.52	2.35	2.31	2.31	MUNS	m	U
80.602	29.334	36.6	30.15	0.94	0.87	0.87	DAD2	e	U

Continued on next page...

Table B.1 – Continued from previous page

Long	Lat	Velocity (mm/yr)				Corr	Site	Source†	EXC‡
°E	°N	East	North	σ E	σ N				
80.636	29.012	37.48	35.06	0.94	0.97	0.97	SHP0	e	U
80.721	29.527	36.21	28.94	0.94	0.87	0.87	SHB0	e	U
80.943	26.891	38.36	31.18	1.04	1.01	1.01	LUCK	m	U
81.116	28.613	39.95	32.75	1.53	1.54	1.54	LMK1	e	U
81.18	30.29	31.36	19.05	1.64	1.64	1.64	J045	k	U
81.19	32.38	29.97	16	1.64	1.64	1.64	J044	k	U
81.353	28.824	37.35	35.33	0.94	0.97	0.97	GUT0	e	U
81.58	28.13	38.52	34.85	1.08	0.73	0.73	NEPA	g	U
81.64	28.59	34.37	32.55	2.04	1.84	1.84	SURK	k	U
81.691	28.407	38.42	34.53	0.94	0.97	0.97	SPS2	e	U
81.83	29.97	33.93	22.93	1.74	1.54	1.54	GPpI	k	U
82.094	28.196	41.2	35.72	0.94	0.97	0.97	BBP0	e	U
82.095	28.01	34.59	31.72	0.94	0.97	0.97	KUS0	e	U
82.191	29.277	36.15	27.78	0.94	0.96	0.96	JML0	e	U
82.247	28.03	36.79	34.41	0.94	0.97	0.97	AMP0	e	U
82.346	28.249	37.7	35.1	0.94	0.97	0.97	MUL0	e	U
82.504	27.951	39.88	35.9	1.04	0.97	0.97	CHP0	e	U
82.54	27.786	36.57	35.31	1.04	0.97	0.97	BMT0	e	U
82.57	28.06	37.32	31.22	2.03	1.94	1.94	RANJ	k	U
82.785	27.568	35.35	35.2	1.04	0.97	0.97	KRN2	e	U
82.818	28.983	37.22	22.66	1.04	1.06	1.06	DLP0	e	U
82.83	30.39	33.28	17.71	1.73	1.63	1.63	J046	k	U
83.235	54.841	26.58	-3.02	0.47	0.45	0.45	NVSK	m	U
83.42	27.51	37.18	33.11	1.17	0.73	0.73	BHAI	g	U
83.55	27.87	40	30.6	2.03	1.93	1.93	TANS	k	U
83.72	28.78	35.91	22.97	1.54	1.44	1.44	JOMO	k	U
83.98	28.2	35.34	30.47	1.63	1.54	1.54	POKH	k	U
84.13	32.3	35.55	17.02	1.72	1.72	1.72	J043	k	U
84.43	27.68	36.18	34.31	2.03	1.93	1.93	BHAR	k	U
84.98	27.16	40.67	31.34	1.36	0.81	0.81	GPpR	g	U
84.982	27.163	39.13	33.54	2.38	1.47	1.47	GPpA	b	U
85.008	27.316	37.49	34	1.04	0.97	0.97	HET0	e	U
85.11	27.61	40.91	32.49	1.16	0.8	0.8	DAMA	g	U
85.187	27.183	38.28	36.3	1.04	0.97	0.97	NIJ0	e	U
85.21	29.44	34.18	20.15	2.32	1.25	1.25	WT12	e	U
85.214	29.441	33.55	20.63	1.36	1.11	1.11	SAGA	b	U
85.222	28.015	39.52	26.48	1.04	0.96	0.96	RAM0	e	U
85.279	27.8	39.51	32.08	1.23	1.15	1.15	KKN0	e	U
85.28	27.7	38.6	28.59	3.41	1.83	1.83	AIRP	e	U
85.329	28.171	38.13	26.37	1.04	1.06	1.06	SYA0	e	U
85.36	27.7	36.09	31.91	1.63	1.53	1.53	AIRP	k	U

Continued on next page...

Table B.1 – Continued from previous page

Long	Lat	Velocity (mm/yr)				Corr	Site	Source†	EXC‡
°E	°N	East	North	σ E	σ N				
85.398	27.575	39.7	32.58	1.04	0.97	0.97	PKI0	e	U
85.44	28.96	36.92	20.12	1.73	1.73	1.73	J040	k	U
85.52	27.69	40.09	31.26	1.07	0.72	0.72	NAGA	g	U
85.52	27.69	38.53	30.29	1.41	1.32	1.32	NAGD	k	U
85.792	20.263	41.32	32.51	1.13	1.09	1.09	BHBN	m	U
85.795	27.745	36.9	30.26	1.04	0.97	0.97	BAL0	e	U
85.88	27.91	40.39	26.95	1.16	0.71	0.71	GUMB	g	U
85.92	26.71	37.47	34.6	2.12	1.93	1.93	JANK	k	U
85.97	28.15	36.23	22.43	1.73	1.63	1.63	J041	k	U
86.02	28.3	40.62	19.14	2.42	1.44	1.44	WT16	e	U
86.023	28.294	38.94	20.94	1.67	1.3	1.3	NYLM	b	U
86.23	27.64	35.07	26.83	2.02	1.92	1.92	JIRI	k	U
86.34	28.78	43.33	18.62	3.21	1.83	1.83	GUCO	e	U
86.44	31.93	38.78	15.55	1.82	1.72	1.72	J036	k	U
86.444	23.815	41.05	30.06	1.31	1.27	1.27	DHAN	m	U
86.72	27.8	40.09	26.38	2.12	1.43	1.43	NAMC	k	U
86.73	27.69	38.38	24.47	2.12	1.92	1.92	LUKL	k	U
86.813	27.958	36.49	23.42	1.23	0.69	0.69	EVE1	e	U
86.813	27.958	36.19	23.22	1.92	1.35	1.35	EVEB	e	U
86.82	27.89	37.6	24.75	2.12	1.23	1.23	PHER	k	U
86.83	28.19	39.23	21.46	2.22	2.02	2.02	RONG	k	U
86.97	28.39	37.88	20.01	1.16	1.07	1.07	JB54	g	U
87.06	28.59	36.97	20.89	1.72	1.72	1.72	J030	k	U
87.09	29.32	38.34	19.6	1.72	1.72	1.72	J038	k	U
87.16	28.63	39.07	20.16	2.22	1.92	1.92	TING	k	U
87.21	27.38	41.04	30.52	2.22	1.43	1.43	KHAN	k	U
87.264	26.484	40.87	32.96	2.95	1.74	1.74	BIRA	b	U
87.27	26.48	39.04	34.77	2.12	1.92	1.92	BIRP	k	U
87.58	29.12	42.82	19.87	2.32	1.44	1.44	LAZE	e	U
87.77	31.89	42.95	15.4	1.05	1.05	1.05	JB53	g	U
88.36	69.362	22.92	-4.33	0.31	0.31	0.31	NRIL	m	U
88.56	28.24	38.81	20.61	1.72	1.62	1.62	J029	k	U
88.569	27.365	41.57	26.2	2.41	2.31	2.31	GBSK	m	U
88.69	31.13	42.26	14.32	1.81	1.81	1.81	J026	k	U
88.84	29.36	40.5	17.75	1.72	1.72	1.72	J037	k	U
88.86	29.25	42.99	17.24	1.82	1.52	1.52	XIGA	k	U
88.906	27.489	40.15	22.57	2.83	2.26	2.26	YADO	b	U
88.91	27.49	40.74	21.84	2.81	1.93	1.93	WT15	e	U
89.15	27.72	40.24	24.12	1.62	1.62	1.62	J042	k	U
89.2	31.99	43.61	11.67	2.01	1.91	1.91	J035	k	U
89.392	26.849	43.92	27.78	1.56	1.48	1.48	RBIT	m	U

Continued on next page...

Table B.1 – Continued from previous page

Long	Lat	Velocity (mm/yr)				Corr	Site	Source[†]	EXC[‡]
°E	°N	East	North	σ E	σ N				
89.56	28.91	40.15	18.32	1.72	1.62	1.62	J039	k	U
89.57	28.91	43.15	17.91	2.01	1.81	1.81	JIAN	k	U
89.635	27.472	43.49	25	1.13	1.11	1.11	TIMP	m	U
90.21	25.53	39.72	33.21	0.7	0.61	0.61	TURA	h	U
90.401	23.727	42.48	36.64	1.86	1.81	1.81	DHAK	l	U
90.56	28.42	42.78	18	1.62	1.62	1.62	J033	k	U
90.8	29.74	47.88	12.95	1.71	1.61	1.61	BALA	k	U
91.104	29.657	46.19	12.37	0.89	0.88	0.88	LHAS	m	U
91.11	30.48	45.53	13.46	1.81	1.71	1.71	J021	k	U
91.11	32.01	45.93	7.87	2.01	1.81	1.81	J025	k	U
91.36	29.66	46.45	12.87	1.81	1.71	1.71	DAGZ	k	U
91.44	25.23	39.44	28.51	0.89	0.71	0.71	NOPE	h	U
91.66	26.15	39.31	26.65	0.55	0.55	0.55	GHTU	h	U
91.661	26.153	40.1	27.97	1.6	1.56	1.56	GAUH	m	U
91.67	32.25	47.22	6	2.11	1.81	1.81	J018	k	U
91.69	32.28	50.03	5.89	1.91	1.81	1.81	ANDU	k	U
91.74	26.14	39.41	24.04	0.89	0.71	0.71	GHTY	h	U
91.84	25.41	39.97	26.29	0.89	0.71	0.71	MUNN	h	U
91.86	25.57	38.48	28.19	0.54	0.52	0.52	CSOS	h	U
91.86	33.23	50.37	5.24	1.91	1.71	1.71	TANG	k	U
91.885	25.566	40.35	28.63	0.98	0.96	0.96	SHLN	m	U
91.91	27.97	42.4	13.59	1.61	1.61	1.61	J034	k	U
91.94	27.58	48.6	10.31	1.55	0.88	0.88	TAWA	h	U
91.98	32.99	49.41	6.05	1.14	1.05	1.05	JB52	g	U
92.036	31.469	49.12	7.93	1.38	1.23	1.23	NAGQ	b	U
92.06	33.65	46.99	4.18	1.21	1.02	1.02	YANS	k	U
92.07	31.51	48.86	6.57	1.81	1.71	1.71	J020	k	U
92.4	28.42	45.29	8.97	1.61	1.61	1.61	J032	k	U
92.42	27.27	41.4	18.26	0.56	0.56	0.56	BOMD	h	U
92.439	28.432	43.81	10.7	2.13	1.86	1.86	LOZ2	j	U
92.447	34.214	49.25	-0.04	1.94	1.42	1.42	TUOT	b	U
92.45	34.21	48.09	-1.24	1.91	1.71	1.71	TTHE	k	U
92.719	11.613	34.18	27.35	1.78	1.25	1.25	CARI	m	U
92.73	23.72	33.8	26.23	0.57	0.58	0.58	AIWL	h	U
92.78	26.618	38.42	24.87	1.14	1.13	1.13	TZPR	m	U
92.85	34.63	45.59	1.33	2.71	2.11	2.11	ERDA	k	U
92.87	30.75	48.67	4.72	1.81	1.71	1.71	J028	k	U
93.05	35.09	42.78	3.41	1.13	1.04	1.04	JB51	g	U
93.082	29.082	46.47	6.74	1.11	0.92	0.92	LAC1	m	U
93.15	29.94	47.1	4.54	1.71	1.71	1.71	J022	k	U
93.784	31.89	50.65	4.34	1.36	1.01	1.01	SOXI	a	U

Continued on next page...

Table B.1 – Continued from previous page

Long	Lat	Velocity (mm/yr)				Corr	Site	Source[†]	EXC[‡]
°E	°N	East	North	σ E	σ N				
93.9	21.38	34.15	19.9	1.37	0.83	0.83	MIND	g	U
93.93	24.74	28.81	16.2	0.74	0.66	0.66	IMPH	h	U
94.1	31.92	49.38	1.76	1.91	2.01	2.01	J019	k	U
94.184	29.189	46.04	1.76	0.99	0.84	0.84	MLX1	a	U
94.184	29.189	46.04	1.76	0.99	0.84	0.84	MLX1	m	U
94.418	29.601	47.31	-0.26	0.93	0.82	0.82	LZX1	a	U
94.418	29.601	47.31	-0.26	0.93	0.82	0.82	LZX1	m	U
94.475	26.22	39.13	23.52	1.41	1.35	1.35	LUMA	m	U
94.537	17.692	37.89	24.88	2.04	1.49	1.49	LAUN	i	U
94.724	29.737	47.41	-1.14	0.96	0.84	0.84	LLZ1	m	U
95.067	30.099	47.7	-0.94	1.88	1.66	1.66	TOM3	j	U
95.257	32.894	51.57	-2.65	2.2	2.2	2.2	J008	c	U
95.29	22.05	28.76	11.58	1.18	0.74	0.74	KWEH	g	U
95.595	21.962	31.32	9.77	1.9	0.88	0.88	HTIS	f	U
95.601	29.939	45.63	-5.83	1.86	1.86	1.86	J011	c	U
95.716	21.691	30.31	8.78	2.03	0.88	0.88	MYOT	f	U
95.757	21.986	28.1	8.39	1.8	0.91	0.91	LEGY	f	U
95.778	22.367	30.89	6.44	2.36	0.88	0.88	WETL	f	U
95.809	22.162	29.58	9.7	2.44	1.21	1.21	THIT	f	U
95.919	21.672	30.18	9.11	2.44	1.09	1.09	CHAU	f	U
95.919	21.991	28.82	7.78	1.65	0.88	0.88	SAYE	f	U
95.981	21.934	29.18	4.94	2.99	1.15	1.15	TNYO	f	U
96.011	22.003	31.3	6.76	2.57	1.11	1.11	LEPA	f	U
96.081	21.636	32.45	7.42	3.15	1.23	1.23	NYAN	f	U
96.097	22.009	7.18	0.76	0.85	0.4	0.4	MDPG	f	U
96.111	22.36	28.92	-0.58	3.13	1.2	1.2	BODA	f	U
96.172	21.989	28.83	0.2	2.55	0.99	0.99	YANG	f	U
96.317	22.324	29.59	-2.99	2.61	0.95	0.95	KUNT	f	U
96.323	21.473	28.72	-7.34	2.13	1.18	1.18	KINV	f	U
96.501	32.27	50.87	-3.3	2.24	2.33	2.33	Y226	c	U
96.53	22.06	28.49	-6.68	1.18	0.74	0.74	YWEN	g	U
96.87	29.39	40.31	-12.18	1.24	1.05	1.05	JB50	g	U
96.886	30.055	45.63	-10.69	0.34	0.28	0.28	BMZ1	m	U
96.99	33	47.84	-4.47	1.23	1.04	1.04	JB49	g	U
97.076	32.858	50.34	-4.03	0.48	0.41	0.41	BTX4	m	U
97.09	20.75	30.69	-7.42	1.47	0.83	0.83	TAUN	g	U
97.122	31.164	46.66	-8.26	0.96	0.83	0.83	CAD1	m	U
97.169	31.162	44.15	-9.76	1.35	1.19	1.19	J010	b	U
97.217	29.153	41.39	-11.9	1.03	0.85	0.85	GYX1	a	U
97.217	29.153	41.39	-11.9	1.03	0.85	0.85	GYX1	m	U
97.447	1.686	32.04	27.83	2.3	0.53	0.53	D962	a	U

Continued on next page...

Table B.1 – Continued from previous page

Long	Lat	Velocity (mm/yr)				Corr	Site	Source†	EXC‡
°E	°N	East	North	σ E	σ N				
97.456	28.65	41.28	-13.88	1.08	0.85	0.85	CHY1	a	U
97.456	28.65	41.28	-13.88	1.08	0.85	0.85	CHY1	m	U
97.72	16.94	33.2	-5.75	1.49	0.87	0.87	HPAA	g	U
97.82	0.57	27.01	28.03	1.29	1.06	1.06	TEDA	g	U
97.856	24.013	22.46	-10.91	1.83	1.74	1.74	H218	c	U
97.943	24.712	20.62	-12.34	1.72	1.72	1.72	H213	c	U
97.946	0.958	30.62	22.64	0.91	0.63	0.63	D953	a	U
97.997	29.709	42.46	-13.8	1.79	1.79	1.79	J012	c	U
98.178	1.469	39.52	19.53	2.9	0.92	0.92	BINT	a	U
98.274	-0.035	26.4	22.26	0.91	0.63	0.63	D949	a	U
98.287	24.256	23.46	-11.83	1.81	1.72	1.72	H217	c	U
98.3	7.76	31.72	-3.1	1	0.88	0.88	PHUK	g	U
98.303	24.808	21.41	-12.94	1.8	1.71	1.71	H212	c	U
98.308	8.105	32.93	-2.77	0.58	0.39	0.39	PHKT	i	U
98.436	25.04	23.51	-13.83	0.56	0.41	0.41	OLZ3	m	U
98.459	2.122	27.72	14.01	1.61	1.31	1.31	JULU	a	U
98.498	25.018	27.56	-12.41	2.83	2.43	2.43	TENG	a	U
98.5	25.02	23.18	-14.47	1.16	1.07	1.07	JB41	g	U
98.526	0.341	29.1	21.55	1.31	0.44	0.44	D944	a	U
98.56	31.77	49.98	-13.54	3.1	2.4	2.4	DS11	k	U
98.599	29.671	44.11	-16.83	1.35	1.19	1.19	H186	b	U
98.64	3.56	31.84	-1.45	1.09	0.98	0.98	MEDA	g	U
98.668	27.759	34.1	-17.67	1.77	1.77	1.77	H194	c	U
98.675	24.577	24.46	-14.74	1.8	1.7	1.7	H211	c	U
98.682	2.524	27.52	6.7	2.3	0.82	0.82	MART	a	U
98.687	29.244	40.99	-16.89	1.77	1.77	1.77	H187	c	U
98.72	3.62	31.76	-1.18	1.09	0.98	0.98	SAMP	g	U
98.815	25.987	29.07	-18.69	1.77	1.68	1.68	H203	c	U
98.84	23.801	23.98	-13.68	1.81	1.72	1.72	H216	c	U
98.846	0.085	31.89	5.95	2.8	1.51	1.51	D947	a	U
98.878	26.909	29.73	-19.62	1.77	1.67	1.67	H197	c	U
98.907	1.852	26.91	14.01	1.11	1.02	1.02	PISA	a	U
98.909	-0.915	31.83	24.38	2.5	3	3	NSIB	a	U
98.915	28.442	36.53	-19.64	1.76	1.77	1.77	H191	c	U
98.923	26.548	27.9	-17.93	1.77	1.67	1.67	H200	c	U
98.973	18.771	31.44	-6.9	0.45	0.33	0.33	CHMI	i	U
99.027	27.611	34.47	-20.26	1.76	1.76	1.76	H193	c	U
99.076	10.61	33.07	-5.37	0.48	0.3	0.3	BANH	i	U
99.084	0.638	24.19	13.84	0.81	0.72	0.72	SIKA	a	U
99.087	24.928	25.13	-18.13	0.6	0.42	0.42	QLQ1	m	U
99.108	30.011	42.49	-16.51	1.48	1.48	1.48	Y273	c	U

Continued on next page...

Table B.1 – Continued from previous page

Long	Lat	Velocity (mm/yr)				Corr	Site	Source†	EXC‡
°E	°N	East	North	σ E	σ N				
99.11	25.652	24.72	-19.07	1.68	1.68	1.68	H206	c	U
99.14	27.311	32.04	-19.79	1.57	1.57	1.57	Y293	c	U
99.148	25.07	24.47	-18.87	1.68	1.69	1.69	H207	c	U
99.16	25.1	26.55	-15.35	2.97	2.55	2.55	BAOS	a	U
99.16	25.1	28.28	-17.28	2.16	1.97	1.97	Y308	c	U
99.168	30.094	42.29	-16.22	1.77	1.77	1.77	H069	c	U
99.17	23.62	24.75	-13.07	1.8	1.71	1.71	H221	c	U
99.249	24.002	24.08	-13.39	1.79	1.7	1.7	H215	c	U
99.254	28.844	37.92	-20.54	1.76	1.76	1.76	H188	c	U
99.26	23.135	24.2	-13.38	1.72	1.72	1.72	H223	c	U
99.278	-1.735	35.16	31.2	0.81	1.81	1.81	D937	a	U
99.293	27.18	32.52	-19.23	1.76	1.76	1.76	H196	c	U
99.37	25.89	28.05	-28.96	2.11	2.01	2.01	H202	k	U
99.37	18.34	30.53	-4.43	1.02	1.11	1.11	OTRI	g	U
99.377	25.88	25.52	-19.64	2.15	1.96	1.96	Y298	c	U
99.377	25.88	29.41	-18.69	2.72	2.46	2.46	YUNL	a	U
99.384	29.258	40.84	-19.18	1.47	1.47	1.47	Y276	c	U
99.388	0.221	23.78	11.55	1.41	0.92	0.92	AIRB	a	U
99.404	23.536	24.82	-13.73	1.8	1.71	1.71	H220	c	U
99.41	26.44	26.97	-23.04	2.91	2.61	2.61	H999	k	U
99.436	26.468	27.26	-18.57	2.05	2.05	2.05	H199	c	U
99.454	22.738	25.94	-15.33	1.82	1.73	1.73	H225	c	U
99.535	25.463	24.88	-19.68	1.77	1.67	1.67	H205	c	U
99.592	22.312	25.39	-11.27	1.74	1.74	1.74	H227	c	U
99.618	24.241	25.67	-15.29	1.78	1.69	1.69	H214	c	U
99.626	26.421	27.75	-22.02	2.15	1.95	1.95	Y296	c	U
99.629	2.462	31.5	-2.41	1.61	0.63	0.63	DEMU	a	U
99.643	24.838	27.02	-17.21	1.68	1.68	1.68	H210	c	U
99.645	27.313	32.61	-21.43	1.75	1.76	1.76	H195	c	U
99.667	30.294	43.06	-17.06	1.76	1.76	1.76	H184	c	U
99.708	27.829	33.43	-22.15	1.65	1.75	1.75	H192	c	U
99.712	26.526	29.41	-21.76	3.19	1.69	1.69	SZS2	m	U
99.73	27.684	36.17	-21.65	0.53	0.34	0.34	TAC3	m	U
99.732	-2.171	26.25	26.2	3.1	1.31	1.31	SIOB	a	U
99.745	29	37.02	-22.82	1.54	1.19	1.19	H189	b	U
99.757	28.32	36.76	-21.47	1.75	1.75	1.75	H190	c	U
99.766	-0.157	25.47	16.25	1.61	0.82	0.82	AJUN	a	U
99.768	28.973	40.89	-22.57	2.12	1.65	1.65	XAC1	m	U
99.812	22.712	26.38	-13.38	1.43	1.19	1.19	H224	b	U
99.827	23.47	24.29	-15.74	1.7	1.7	1.7	H219	c	U
99.834	23.045	27.95	-16.84	1.9	1.81	1.81	H222	c	U

Continued on next page...

Table B.1 – Continued from previous page

Long	Lat	Velocity (mm/yr)				Corr	Site	Source†	EXC‡
°E	°N	East	North	σ E	σ N				
99.859	0.62	27.27	4.73	0.71	0.44	0.44	P37E	a	U
99.862	17.161	31.94	-7.04	1.16	0.9	0.9	SISM	i	U
99.89	26.461	28.23	-23.29	1.85	1.76	1.76	DIAN	c	U
99.89	26.461	33.28	-24.23	2.57	1.62	1.62	DINA	a	U
99.907	24.628	27.89	-18.17	1.68	1.68	1.68	H209	c	U
99.92	22.55	27.44	-12.24	1.17	1.08	1.08	JB42	g	U
99.924	25.716	26.17	-20.49	1.66	1.67	1.67	H204	c	U
99.933	26.45	29.13	-21.6	1.66	1.66	1.66	H198	c	U
99.937	26.618	28.82	-20.01	1.62	1.09	1.09	JIAC	a	U
99.938	26.617	29.14	-22	1.46	1.47	1.47	Y295	c	U
99.95	25.69	27.47	-19.5	1.47	1.47	1.47	Y299	c	U
99.987	26.144	28.5	-21.21	1.66	1.66	1.66	H201	c	U
99.991	26.125	27.8	-22.21	2.14	1.95	1.95	Y297	c	U
99.995	26.783	27.95	-24.5	3.88	0.95	0.95	BHC2	m	U
100.01	15.38	31.12	-5.68	0.96	0.74	0.74	UTHA	g	U
100.065	27.109	30.96	-23.54	1.65	1.65	1.65	H107	c	U
100.09	23.881	25.01	-15.72	1.78	1.69	1.69	H162	c	U
100.094	25.979	28.68	-21.04	1.66	1.66	1.66	H124	c	U
100.109	22.222	26.55	-14	1.73	1.73	1.73	H178	c	U
100.111	23.598	23.39	-17.02	1.88	1.7	1.7	H163	c	U
100.121	29.175	38.98	-21.18	1.75	1.75	1.75	H080	c	U
100.122	15.673	31.66	-3.46	1.7	1.05	1.05	NAKH	i	U
100.136	24.445	27.16	-18.23	1.77	1.68	1.68	H148	c	U
100.148	24.446	28.56	-16.84	1.49	1.49	1.49	Y314	c	U
100.148	24.446	31.9	-13.65	2.87	2.54	2.54	YUNX	a	U
100.161	26.514	29.62	-20.96	1.75	1.66	1.66	H118	c	U
100.163	-0.621	27.95	15.26	0.81	0.53	0.53	TOBO	a	U
100.17	26.88	31.11	-22.56	1.15	1.06	1.06	JB38	g	U
100.17	26.883	30.8	-20.92	2.51	2.39	2.39	LIJI	a	U
100.214	29.994	39.9	-18.11	0.52	0.38	0.38	LTZ1	m	U
100.215	-2.758	33.73	33.51	1.01	0.72	0.72	PAGA	a	U
100.237	29.986	41.27	-17.49	2.61	2.41	2.41	LITN	a	U
100.237	29.986	40.72	-19.22	1.49	1.51	1.51	Y274	c	U
100.25	25.61	27.11	-21.07	1.16	1.07	1.07	XIAG	g	U
100.255	25.608	29.17	-17.72	0.9	0.85	0.85	DALI	a	U
100.255	25.608	28.31	-19.62	1.47	1.51	1.51	Y304	c	U
100.28	6.45	32.1	-5.38	0.58	0.49	0.49	ARAU	i	U
100.28	29.99	40.58	-18.73	1.14	1.05	1.05	JB40	g	U
100.3	5.36	36.48	-10.36	1.12	0.99	0.99	USMP	g	U
100.314	24.837	28.78	-19.19	1.76	1.67	1.67	H147	c	U
100.319	29.03	44.1	-22.73	2.15	1.66	1.66	DAC1	m	U

Continued on next page...

Table B.1 – Continued from previous page

Long	Lat	Velocity (mm/yr)				Corr	Site	Source†	EXC‡
°E	°N	East	North	σ E	σ N				
100.353	-0.878	23.34	18.06	2.4	1.11	1.11	PADU	a	U
100.369	-0.944	26.84	16.07	0.62	0.53	0.53	PADA	a	U
100.369	25.437	27.12	-21.11	1.56	1.47	1.47	Y302	c	U
100.385	6.14	34.72	-4.46	1.68	0.59	0.59	DOP5	f	U
100.39	29.695	40.58	-20.76	1.75	1.75	1.75	H075	c	U
100.429	-1.109	26.84	20.07	2.01	1.21	1.21	P003	a	U
100.45	21.95	28.24	-14.04	2.61	2.41	2.41	H179	k	U
100.456	25.432	31.72	-17.54	1.68	0.97	0.97	SXD3	m	U
100.496	25.341	27.71	-19.14	1.66	1.66	1.66	H140	c	U
100.522	25.037	27.48	-19.74	1.66	1.67	1.67	H141	c	U
100.548	25.482	29.91	-19.46	1.66	1.66	1.66	H138	c	U
100.56	25.797	30.74	-19.86	1.65	1.66	1.66	H131	c	U
100.567	25.44	26.91	-16.2	1.25	0.9	0.9	XIAY	a	U
100.567	25.44	29.61	-18.86	1.47	1.47	1.47	Y307	c	U
100.584	24.788	28.65	-14.26	1.49	0.98	0.98	NANJ	a	U
100.584	24.788	27.86	-17.56	1.47	1.48	1.48	Y313	c	U
100.59	25.95	27.53	-15.16	1.81	1.71	1.71	BINC	k	U
100.597	26.212	29.46	-20.58	1.65	1.65	1.65	H123	c	U
100.607	13.668	33.17	-7.16	0.47	0.32	0.32	BNKK	i	U
100.653	27.748	36.56	-23.71	1.64	1.65	1.65	H097	c	U
100.653	-0.701	32.14	4.26	0.62	0.63	0.63	KACA	a	U
100.671	21.588	29.55	-11.34	1.74	1.74	1.74	H181	c	U
100.728	26.706	30.42	-22.47	1.72	1.26	1.26	YOSH	a	U
100.757	26.665	32.58	-22.42	1.65	1.65	1.65	H117	c	U
100.786	22.013	29.39	-13.28	1.72	1.73	1.73	H177	c	U
100.876	24.417	27.51	-18.13	1.76	1.67	1.67	H153	c	U
100.895	23.868	28.86	-16.03	1.77	1.68	1.68	H160	c	U
100.914	24.283	28.69	-13.7	2.09	1.24	1.24	JIND	a	U
100.934	27.138	34.6	-21.28	1.64	1.65	1.65	H106	c	U
101.012	30.029	39.63	-18.51	0.52	0.38	0.38	HKZ1	m	U
101.023	30.106	38.45	-19.23	1.75	1.75	1.75	H068	c	U
101.023	25.313	27.27	-20.98	1.46	1.47	1.47	Y310	c	U
101.05	13.12	31.67	-5.45	0.91	0.77	0.77	CHON	g	U
101.05	22.741	29.27	-14.05	2.54	2.39	2.39	GPpO	a	U
101.05	22.74	28.49	-15.45	1.17	1.08	1.08	JB39	g	U
101.058	23.074	27.08	-16.46	1.79	1.7	1.7	H168	c	U
101.063	22.507	28.22	-15.86	1.8	1.71	1.71	H175	c	U
101.074	23.008	28.28	-18.83	1.16	0.86	0.86	XSJ1	m	U
101.093	24.023	28.66	-17.99	1.77	1.68	1.68	H152	c	U
101.13	4.59	30.27	-8.09	1.13	1	1	IPOH	g	U
101.238	27.656	36.71	-21.46	1.74	1.64	1.64	H096	c	U

Continued on next page...

Table B.1 – Continued from previous page

Long	Lat	Velocity (mm/yr)				Corr	Site	Source†	EXC‡
°E	°N	East	North	σ E	σ N				
101.245	26.677	34.85	-21.16	1.64	1.64	1.64	H114	c	U
101.272	25.739	37.08	-18.37	2.85	2.53	2.53	DAYA	a	U
101.272	25.739	33.88	-19.75	2.14	1.94	1.94	Y300	c	U
101.313	27.592	36.71	-22.2	1.42	1.07	1.07	MIAN	a	U
101.313	27.592	37.3	-22.28	1.44	1.45	1.45	Y319	c	U
101.32	25.732	31.28	-17.97	1.65	1.65	1.65	H130	c	U
101.35	21.888	30.44	-13.63	1.81	1.72	1.72	H176	c	U
101.389	23.29	27.07	-18.36	1.78	1.69	1.69	H159	c	U
101.446	3.025	23.42	1.58	1.72	0.54	0.54	DOP1	f	U
101.483	25.077	36.66	-20.64	2.79	2.51	2.51	CHUX	a	U
101.483	25.077	30.22	-17	1.46	1.46	1.46	Y311	c	U
101.51	27.42	35.84	-20.53	1.15	1.06	1.06	JB37	g	U
101.512	28.996	37.56	-21.25	1.44	1.45	1.45	Y277	c	U
101.514	27.42	35.41	-18.81	2.5	2.38	2.38	YANY	a	U
101.517	3.765	29.35	-5.45	1.28	0.99	0.99	BEHR	i	U
101.518	28.964	37.86	-21.85	1.64	1.74	1.74	H083	c	U
101.55	21.493	29.49	-12.88	2.01	1.83	1.83	H180	c	U
101.558	29.846	37.2	-21.37	1.74	1.74	1.74	H074	c	U
101.573	24.985	29.1	-20.52	1.65	1.66	1.66	H136	c	U
101.583	24.924	30.38	-18.83	0.75	0.47	0.47	DLH3	m	U
101.633	24.688	29.58	-18.94	2.14	1.76	1.76	H146	c	U
101.683	26.05	36.28	-22.87	1.64	1.65	1.65	H122	c	U
101.685	23.434	29.27	-19.74	1.77	1.68	1.68	H158	c	U
101.688	23.517	29.57	-17.72	1.16	0.75	0.75	BSC2	m	U
101.71	27.539	35.87	-20.29	1.73	1.74	1.74	H104	c	U
101.72	3.17	29.28	-8.35	1.09	0.98	0.98	KTPK	g	U
101.749	26.504	34.3	-22.19	1.64	1.64	1.64	H116	c	U
101.855	26.689	34.61	-21.92	1.64	1.64	1.64	H113	c	U
101.86	22.59	28.72	-15.49	2.71	2.51	2.51	H174	k	U
101.902	25.642	32.63	-19.72	1.64	1.65	1.65	H129	c	U
101.959	27.049	35.72	-21.65	1.64	1.64	1.64	H112	c	U
101.975	24.07	27.4	-19.42	1.66	1.67	1.67	H151	c	U
101.994	23.597	29.96	-18.32	1.67	1.67	1.67	H157	c	U
102.071	25.155	31.38	-20.26	1.65	1.65	1.65	H135	c	U
102.097	27.874	39.34	-20.47	1.09	0.41	0.41	THZ4	m	U
102.1	26.826	34.2	-21.49	1.73	1.64	1.64	H111	c	U
102.101	21.684	35.42	-9.8	1.44	0.62	0.62	PHON	f	U
102.11	6.23	30.85	-8.29	1.1	0.96	0.96	GETI	g	U
102.126	28.515	36.89	-21.11	1.73	1.74	1.74	H092	c	U
102.135	23.882	30.49	-20.48	1.72	1.33	1.33	DSM1	m	U
102.153	24.676	29.14	-19.97	1.65	1.66	1.66	H145	c	U

Continued on next page...

Table B.1 – Continued from previous page

Long	Lat	Velocity (mm/yr)				Corr	Site	Source†	EXC‡
°E	°N	East	North	σ E	σ N				
102.188	27.454	36.23	-21.52	1.73	1.64	1.64	H103	c	U
102.219	27.902	36.35	-20.23	1.44	1.44	1.44	Y318	c	U
102.232	27.875	35.35	-21.13	1.73	1.64	1.64	H095	c	U
102.25	-3.79	24.85	12.84	1.39	1.17	1.17	BENG	g	U
102.263	26.69	34.58	-20.93	1.64	1.64	1.64	H110	c	U
102.303	28.903	43.95	-14.05	2.86	2.55	2.55	PUSH	a	U
102.303	28.903	37.3	-17.86	1.44	1.44	1.44	Y285	c	U
102.321	6.039	32.66	-9.61	1.7	0.57	0.57	DOP4	f	U
102.401	22.996	32.88	-14.62	1.78	1.68	1.68	H167	c	U
102.415	23.326	32.99	-15.04	1.17	0.97	0.97	MSA3	m	U
102.437	28.3	36.46	-17.49	1.73	1.73	1.73	H091	c	U
102.439	29.263	35.2	-15.8	1.73	1.74	1.74	H082	c	U
102.439	24.188	28.28	-19.44	1.66	1.66	1.66	H150	c	U
102.496	23.719	30.48	-14.26	1.24	1.1	1.1	H156	b	U
102.505	25.577	32.58	-21.98	1.64	1.65	1.65	H128	c	U
102.513	23.721	32.96	-15.79	1.14	0.94	0.94	PTS2	m	U
102.516	18.026	35.67	-6.62	1.44	0.58	0.58	VIEN	f	U
102.517	25.237	31.66	-21.08	1.65	1.65	1.65	H134	c	U
102.532	28.672	35.97	-16.32	1.73	1.64	1.64	H090	c	U
102.532	26.002	34.21	-21.69	1.64	1.64	1.64	H121	c	U
102.549	27.37	35.9	-20.11	1.73	1.64	1.64	H102	c	U
102.577	24.375	29.08	-19.28	1.75	1.66	1.66	H149	c	U
102.611	26.62	34.84	-21.62	1.64	1.64	1.64	H109	c	U
102.622	3.464	33.95	1.81	1.72	0.55	0.55	DOP3	f	U
102.655	29.348	34.49	-13.46	1.63	1.64	1.64	H077	c	U
102.73	2.49	28.39	-5.64	1.64	1.17	1.17	SEGA	g	U
102.747	17.865	32.08	-10.01	1.53	0.97	0.97	NNKI	i	U
102.751	24.118	31.45	-17.62	1.66	1.66	1.66	H155	c	U
102.757	24.073	33.31	-15.16	0.48	0.33	0.33	LSC1	m	U
102.767	28.955	34.86	-14.59	1.73	1.73	1.73	H087	c	U
102.79	27.693	35.09	-15.88	1.73	1.73	1.73	H100	c	U
102.797	25.03	30.2	-21.72	0.83	0.8	0.8	KUNM	m	U
102.797	24.882	25.97	-21.85	0.81	0.82	0.82	KUNM	a	U
102.798	25.029	32.72	-21.25	1.05	1.01	1.01	KMIN	b	U
102.814	23.59	32.53	-12.11	1.17	0.96	0.96	WBS1	m	U
102.833	27.999	36.91	-15.49	2.03	2.03	2.03	H094	c	U
102.836	23.224	34.87	-15.04	1.77	1.68	1.68	H166	c	U
102.907	26.931	34.84	-18	1.73	1.64	1.64	H108	c	U
102.923	24.679	31.98	-17.98	1.65	1.65	1.65	H144	c	U
102.941	25.798	32.86	-20.6	1.64	1.64	1.64	H127	c	U
103.015	25.17	32.31	-17.08	0.7	0.5	0.5	XSX1	m	U

Continued on next page...

Table B.1 – Continued from previous page

Long	Lat	Velocity (mm/yr)				Corr	Site	Source†	EXC‡
°E	°N	East	North	σ E	σ N				
103.043	28.847	32.33	-13.26	1.63	1.64	1.64	H086	c	U
103.121	28.312	33	-14.47	1.63	1.63	1.63	H089	c	U
103.135	28.328	30.43	-15.7	1.71	1.21	1.21	MEIG	a	U
103.14	5.32	30.11	-8.28	0.98	0.92	0.92	KUAL	g	U
103.151	23.292	33.11	-11.89	0.52	0.4	0.4	KFZ2	m	U
103.166	26.105	33.47	-17.26	1.64	1.64	1.64	H120	c	U
103.17	23.14	32.59	-10.61	2.71	2.41	2.41	H171	k	U
103.222	22.771	35.46	-14.13	1.62	1.19	1.19	H173	b	U
103.227	26.405	34.38	-16.08	1.63	1.64	1.64	H119	c	U
103.228	22.808	34.19	-12.56	1.24	0.9	0.9	DBC1	m	U
103.241	25.608	31.43	-15.37	1.74	1.64	1.64	H126	c	U
103.261	24.769	32.27	-13.37	1.75	1.65	1.65	H143	c	U
103.269	27.684	31.76	-13.3	1.63	1.63	1.63	H099	c	U
103.284	23.712	33.48	-13.66	2.05	1.76	1.76	H165	c	U
103.35	3.83	29.83	-6.73	1.08	0.96	0.96	KUAN	g	U
103.404	23.466	34.05	-11.79	1.76	1.67	1.67	H164	c	U
103.42	24.108	34.1	-14.7	1.75	1.66	1.66	H154	c	U
103.53	28.84	33.96	-13.28	1.15	1.05	1.05	JB36	g	U
103.569	27.109	33.22	-13.92	0.38	0.27	0.27	SWB1	m	U
103.608	1.377	29.71	-11.02	1.71	0.54	0.54	DOP2	f	U
103.64	28.25	33.96	-12.71	1.63	1.63	1.63	H093	c	U
103.64	1.57	28.33	-11.5	1.2	1.02	1.02	UTMJ	g	U
103.656	25.022	33.65	-13.87	1.74	1.65	1.65	H132	c	U
103.68	1.35	28.16	-8.61	1.42	1.34	1.34	NTUS	g	U
103.68	1.346	29.58	-8.92	1.11	0.63	0.63	NTUS	a	U
103.687	27.356	33.4	-13.01	1.73	1.63	1.63	H101	c	U
103.693	22.982	34.04	-15.85	1.62	1.28	1.28	H170	b	U
103.708	23.02	34.55	-9.21	1.38	0.93	0.93	DWY2	m	U
103.769	25.495	33.18	-13.71	1.74	1.64	1.64	H125	c	U
103.815	13.409	34.96	-14.49	2.4	0.87	0.87	SIEM	f	U
103.89	28.96	34.13	-12.64	2.6	2.6	2.6	H084	k	U
103.892	27.769	33.91	-13.77	1.63	1.63	1.63	H098	c	U
103.93	22.53	32.9	-12.39	2.61	2.41	2.41	H172	k	U
103.959	1.342	47.68	2.62	1.96	0.63	0.63	CCBS	f	U
103.978	28.605	33.64	-12.5	1.73	1.63	1.63	H088	c	U
104.272	23.353	33.08	-12.91	1.76	1.67	1.67	F081	c	U
104.311	24.879	31.69	-13.84	1.74	1.65	1.65	F076	c	U
104.42	14.9	33.24	-11.6	1.32	0.97	0.97	SRIS	g	U
104.871	15.245	32.3	-10.14	0.88	0.65	0.65	UBRT	i	U
104.918	11.574	15.62	-16.06	2.9	0.96	0.96	PENH	f	U
104.921	26.567	34.36	-12.22	1.73	1.64	1.64	F080	c	U

Continued on next page...

Table B.1 – Continued from previous page

Long	Lat	Velocity (mm/yr)				Corr	Site	Source†	EXC‡
°E	°N	East	North	σ E	σ N				
105.766	24.99	32.99	-12.02	1.74	1.74	1.74	F074	c	U
105.837	23.366	33.26	-12.31	1.76	1.76	1.76	F077	c	U
105.852	14.119	33.21	-7.51	1.51	0.58	0.58	KHON	f	U
106.18	-1.88	26.14	-9.6	1.34	1.11	1.11	TANJ	g	U
106.581	24.406	35.08	-13.11	1.75	1.75	1.75	F075	c	U
106.67	26.41	33.58	-12.38	1.15	1.06	1.06	JB25	g	U
106.69	26.724	33.86	-12.79	1.2	0.97	0.97	GUIY	a	U
106.791	20.696	32.08	-17.74	2.02	0.81	0.81	QT02	f	U
106.83	22.11	33.83	-11.79	1.17	1.08	1.08	JB26	g	U
106.849	-6.491	21.93	-7.67	0.42	0.27	0.27	BAKO	a	U
106.85	-6.49	20.93	-9.68	1.59	1.52	1.52	BAKO	g	U
107.087	10.353	25.35	-7.66	2.15	0.71	0.71	QT04	f	U
107.14	22.86	30.5	-12.64	1.72	1.73	1.73	F078	k	U
107.31	21	34.49	-11.71	1	0.74	0.74	CAMP	g	U
107.82	22.326	32.72	-13.69	1.78	1.69	1.69	F062	c	U
108.169	23.75	33.6	-14.6	1.76	1.76	1.76	F059	c	U
108.26	16	30.41	-10.63	1.04	0.8	0.8	NONN	g	U
108.295	27.875	33.83	-13.2	1.74	1.64	1.64	F058	c	U
108.296	23.149	30.94	-13.02	1.87	1.77	1.77	F060	c	U
108.89	0.86	28.7	-11.56	1.43	1.08	1.08	TABA	g	U
109.06	21.46	32.49	-13.84	1.74	1.65	1.65	F064	k	U
109.12	21.03	32.36	-12.15	1.75	1.65	1.65	F065	k	U
109.26	22.411	31.31	-13.45	1.79	1.69	1.69	F063	c	U
109.48	30.232	34.69	-14.43	1.74	1.65	1.65	F056	c	U
109.84	19.03	30.41	-12.35	1.2	1.11	1.11	QION	g	U
110.141	22.688	31.25	-13.97	1.78	1.69	1.69	F049	c	U
110.19	1.63	25.49	-12.7	1.42	1.07	1.07	KUCH	g	U
110.31	25.19	34.11	-13.98	1.16	1.07	1.07	JB21	g	U
110.35	31.049	34.76	-14.53	2.81	2.76	2.76	BADN	a	U
110.367	31.017	33.51	-13.86	1.75	1.65	1.65	F031	c	U
110.555	27.911	31.21	-13.86	1.74	1.65	1.65	F057	c	U
110.748	31.341	35.99	-13.76	2.81	2.76	2.76	GUFU	a	U
111.31	30.79	32.3	-14.94	1.14	1.05	1.05	JB20	g	U
111.475	33.28	32.1	-14.57	1.77	1.68	1.68	C060	c	U
111.563	22.786	32.04	-14.61	1.79	1.69	1.69	F047	c	U
111.843	2.27	20.3	-13.84	3.09	2.07	2.07	SIBU	i	U
112.108	31.905	32.12	-14.7	1.66	1.67	1.67	F029	c	U
112.351	32.538	32.7	-14.27	1.67	1.68	1.68	C063	c	U
112.563	26.911	31.26	-15.22	1.75	1.65	1.65	F034	c	U
112.688	22.338	30.8	-14.66	1.81	1.71	1.71	F044	c	U
113.07	3.26	26.86	-13.15	1.17	0.98	0.98	BINT	g	U

Continued on next page...

Table B.1 – Continued from previous page

Long	Lat	Velocity (mm/yr)				Corr	Site	Source†	EXC‡
°E	°N	East	North	σ E	σ N				
113.11	34.52	29.06	-14.97	1.13	1.04	1.04	JB06	g	U
113.168	29.386	31.07	-16.41	1.75	1.66	1.66	F033	c	U
113.18	36.23	30.28	-14.4	1.13	1.04	1.04	JB05	g	U
113.312	32.751	32.08	-15.2	1.68	1.68	1.68	C059	c	U
113.34	23.18	32.64	-13.31	1.17	1.08	1.08	GUAN	g	U
113.348	31.694	32.18	-14.89	1.67	1.67	1.67	C065	c	U
113.563	24.814	32.67	-15.52	1.68	1.68	1.68	F037	c	U
113.896	22.587	31.81	-15.25	1.81	1.72	1.72	F042	c	U
114	4.37	25.4	-12.08	1.15	1.01	1.01	MIRI	g	U
114.074	32.099	31.99	-15.77	1.68	1.68	1.68	C062	c	U
114.345	33.026	31.36	-14.75	1.69	1.7	1.7	C056	c	U
114.357	30.532	30.35	-12.2	0.46	0.43	0.43	WUHN	m	U
114.357	30.532	30.46	-13.19	0.52	0.53	0.53	WUHN	a	U
114.453	22.83	32.17	-15.28	1.72	1.72	1.72	F041	c	U
114.635	31.251	32.03	-15.49	1.67	1.68	1.68	C064	c	U
114.79	-3.87	25.15	-11.61	1.42	1.22	1.22	BATU	g	U
115.03	4.97	25.42	-13.54	1.14	0.94	0.94	BRUN	g	U
115.05	27.06	33.37	-15.61	1.16	1.07	1.07	JB22	g	U
115.25	5.28	25.58	-13.39	1.14	0.93	0.93	LABU	g	U
115.347	-29.047	37.28	56.03	0.9	0.68	0.68	YAR1	m	U
115.347	-29.047	37.29	56.2	0.19	0.22	0.22	YAR1	a	U
115.347	-29.047	38.44	55.91	1.06	1.03	1.03	YAR2	m	U
115.631	22.976	31.06	-16.15	1.73	1.73	1.73	F028	c	U
115.791	32.943	32.18	-15.69	1.71	1.71	1.71	C058	c	U
115.801	23.431	30.97	-16.6	1.72	1.72	1.72	F027	c	U
115.878	31.689	30.67	-15.68	1.79	1.69	1.69	C061	c	U
115.885	-31.802	37.45	56.77	0.36	0.33	0.33	PERT	m	U
115.885	-31.802	37.67	57.25	0.26	0.22	0.22	PERT	a	U
116.04	5.91	24.69	-12.58	1.13	0.92	0.92	KINA	g	U
116.128	37.378	31.41	-15.54	1.78	1.55	1.55	GI80	a	U
116.486	6.394	24.96	-11.04	1.92	0.61	0.61	D005	f	U
116.687	23.654	31.19	-15.9	1.74	1.74	1.74	F026	c	U
116.717	24.726	32.64	-17.13	1.71	1.72	1.72	F024	c	U
116.718	24.725	33.5	-14.31	1.79	1.56	1.56	YDIN	a	U
116.81	-1.27	23.17	-15.6	1.57	1.15	1.15	BLKP	g	U
116.971	31.085	32.44	-15.12	1.79	1.7	1.7	B072	c	U
116.984	33.646	31.01	-15.37	1.74	1.75	1.75	B058	c	U
117.015	23.423	32.15	-15.07	1.75	1.75	1.75	F025	c	U
117.018	30.583	30.73	-15.42	1.79	1.7	1.7	F010	c	U
117.097	-20.981	37.46	56.07	0.29	0.23	0.23	KARR	i	U
117.097	-20.981	36.3	56.71	0.43	0.27	0.27	KARR	a	U

Continued on next page...

Table B.1 – Continued from previous page

Long	Lat	Velocity (mm/yr)				Corr	Site	Source†	EXC‡
°E	°N	East	North	σ E	σ N				
117.108	32.498	30.41	-15.78	1.72	1.73	1.73	B065	c	U
117.12	36.22	29.6	-15.36	1.13	1.04	1.04	TAIN	g	U
117.427	23.708	31.93	-16.68	1.64	1.52	1.52	DSHA	a	U
117.558	33.554	31.14	-14.7	1.75	1.76	1.76	B057	c	U
117.564	26.291	31	-18.25	1.71	1.71	1.71	F014	c	U
117.589	24.13	32.72	-16.31	1.74	1.75	1.75	F023	c	U
117.608	24.557	33.24	-17.12	1.74	1.74	1.74	F022	c	U
117.641	0.558	22.64	-13.3	0.69	0.45	0.45	TNJB	i	U
117.708	32.562	31.03	-15.21	1.74	1.74	1.74	B062	c	U
117.793	34.482	33.03	-14.96	2.21	1.72	1.72	HB55	a	U
117.815	31.657	31.23	-15.32	1.72	1.73	1.73	B070	c	U
117.88	4.26	21.93	-18.73	1.1	0.97	0.97	MTAW	g	U
117.88	4.26	21.93	-18.23	1.32	1.02	1.02	TAWX	g	U
117.899	33.483	29.89	-15.07	1.76	1.76	1.76	B056	c	U
117.926	33.904	30.18	-15.39	1.77	1.78	1.78	B047	c	U
117.98	4.25	21.83	-18.85	1.11	0.97	0.97	TAWA	g	U
118.08	24.45	32.51	-17.18	1.17	1.08	1.08	XIAM	g	U
118.12	5.84	26.64	-19.57	1.21	0.99	0.99	SAND	g	U
118.121	24.618	40.6	-15.94	1.86	1.6	1.6	XMEN	a	U
118.166	26.633	33.43	-15.05	1.77	1.56	1.56	NANP	a	U
118.186	35.1	30.78	-19.72	2.21	1.71	1.71	HB61	a	U
118.19	33.481	30.35	-15.34	1.77	1.77	1.77	B055	c	U
118.221	31.085	31.18	-16.1	1.72	1.73	1.73	B073	c	U
118.242	25.49	34.28	-13.87	1.8	1.57	1.57	DEHU	a	U
118.3	32.284	30.26	-15.24	1.74	1.75	1.75	B066	c	U
118.335	31.72	30.56	-16.04	1.74	1.74	1.74	B069	c	U
118.477	32.971	29.72	-15.59	1.76	1.77	1.77	B061	c	U
118.48	35.837	31.14	-12.87	2.04	1.66	1.66	HB64	a	U
118.595	24.775	34.67	-14.65	1.35	1.21	1.21	QUAN	a	U
118.596	24.775	33.64	-15.04	1.76	1.76	1.76	F020	c	U
118.637	34.486	32.05	-13.76	2.23	1.72	1.72	HB65	a	U
118.643	28.734	32.02	-17.14	1.72	1.72	1.72	F012	c	U
118.672	33.761	29.98	-15.95	1.79	1.79	1.79	B054	c	U
118.74	26.575	32.24	-13.07	1.85	1.59	1.59	GUTI	a	U
118.813	26.297	41.03	-13.93	1.8	1.59	1.59	MQIN	a	U
118.85	10.09	32.66	-17.02	1.22	0.84	0.84	PUER	g	U
118.93	30.611	31.19	-16.34	1.83	1.74	1.74	F011	c	U
119.012	33.507	29.84	-16.02	1.88	1.79	1.79	B053	c	U
119.03	31.65	31.17	-16.36	1.14	1.05	1.05	JB04	g	U
119.037	32.734	30.65	-15.41	1.77	1.78	1.78	B060	c	U
119.149	25.1	35.66	-15.65	1.62	1.51	1.51	PUTI	a	U

Continued on next page...

Table B.1 – Continued from previous page

Long	Lat	Velocity (mm/yr)				Corr	Site	Source†	EXC‡
°E	°N	East	North	σ E	σ N				
119.424	33.176	30.59	-16.6	1.89	1.8	1.8	B059	c	U
119.463	31.381	31.62	-16.18	1.76	1.76	1.76	B074	c	U
119.49	32.402	30.5	-15.7	1.78	1.78	1.78	B067	c	U
119.894	31.738	30.55	-14.08	1.78	1.78	1.78	B012	c	U
120.038	33.55	29.5	-16.24	1.83	1.83	1.83	B052	c	U
120.205	30.838	31.02	-16.62	1.87	1.78	1.78	B017	c	U
120.236	30.328	31.92	-16.62	1.86	1.78	1.78	F001	c	U
120.366	32.513	30.78	-15.99	1.81	1.82	1.82	B010	c	U
120.464	33.165	29.55	-16.43	1.83	1.84	1.84	B009	c	U
120.569	31.247	31.07	-16.41	1.89	1.8	1.8	B015	c	U
120.774	31.668	31.74	-16.76	1.9	1.82	1.82	B013	c	U
120.78	27.97	32.93	-17.54	1.16	1.07	1.07	JB19	g	U
120.889	31.953	29.12	-16.59	2	1.91	1.91	B011	c	U
121.2	31.1	30.61	-15.98	0.19	0.17	0.17	SHAO	m	U
121.2	31.1	31.82	-16.49	0.62	0.44	0.44	SHAO	a	U
121.377	29.599	30.38	-16.44	1.9	1.82	1.82	F003	c	U
121.801	31.733	30.19	-15.88	2.03	1.86	1.86	B014	c	U
122.07	6.97	17.38	-13.55	1.28	0.98	0.98	ZAMB	g	U
122.269	29.977	29.86	-16.33	1.95	1.86	1.86	F002	c	U
122.434	30.741	29.52	-16.69	1.96	1.88	1.88	B019	c	U
128.866	71.634	16.96	-13.72	0.24	0.24	0.24	TIXI	m	U
131.133	-12.844	31.42	56.95	0.43	0.21	0.21	DARW	a	U
132.894	-12.659	33.08	58.3	1.09	1.11	1.11	JAB1	i	U
133.81	-31.867	26.6	54.68	0.53	0.45	0.45	CEDU	a	U
133.885	-23.67	27.53	54.97	0.62	0.44	0.44	ALIC	a	U
147.056	-19.269	26.24	52.8	0.72	0.45	0.45	TOW2	a	U
147.439	-42.805	12.15	54.15	0.52	0.52	0.52	HOB2	m	U
147.439	-42.805	12.3	53.89	0.3	0.26	0.26	HOB2	a	U
147.44	-42.804	12.91	53.82	1.19	1.19	1.19	HOB1	i	U
148.98	-35.399	17.58	52.38	0.99	0.98	0.98	TID2	m	U
148.98	-35.399	16.23	54.04	0.36	0.35	0.35	TIDB	m	U
148.98	-35.399	16.8	53.6	0.23	0.25	0.25	TIDB	a	U
166.41	-22.27	15.83	44.03	0.74	0.55	0.55	NOUM	a	U
350.581	38.693	19.13	16.91	0.92	0.87	0.87	CASC	d	U
0.336	50.867	17.76	16.93	2.8	2.8	2.8	HERS	m	1
1.481	43.561	19.95	15.59	0.7	0.7	0.7	TLSE	d	1
1.481	43.561	20.59	16.01	0.64	0.63	0.63	TOUL	m	1
6.921	43.755	21.48	14.85	0.23	0.23	0.23	GRAS	m	1
7.465	46.877	21.11	15.16	0.48	0.48	0.48	ZIMM	d	1
8.97	39.14	23.79	14.03	0.74	0.72	0.72	CAGL	g	1
9.672	0.354	23.43	18.69	0.72	0.71	0.71	NKLG	d	1

Continued on next page...

Table B.1 – Continued from previous page

Long	Lat	Velocity (mm/yr)				Corr	Site	Source†	EXC‡
°E	°N	East	North	σ E	σ N				
11.113	44.122	22.03	14.96	1.05	1.05	1.05	BRAS	d	1
11.28	48.086	21.45	14.79	0.74	0.74	0.74	OBER	d	1
11.647	44.52	24.93	15.61	0.52	0.52	0.52	MEDI	d	1
11.865	78.93	11.69	13.84	0.11	0.11	0.11	NYAL	m	1
11.865	78.93	11.5	14.59	0.23	0.23	0.23	NYAL	a	1
11.911	45.385	22.01	15.83	0.8	0.8	0.8	VOLT	d	1
11.925	57.395	17.94	14.03	0.12	0.12	0.12	ONSA	a	1
11.926	57.395	18.65	13.59	0.21	0.2	0.2	ONSA	m	1
12.291	45.23	20.93	15.63	0.8	0.8	0.8	SFEL	d	1
12.332	45.437	17.98	18.4	1.15	1.16	1.16	VENE	d	1
12.583	45.479	22.05	16.35	0.81	0.81	0.81	CAVA	d	1
12.879	49.144	21.28	13.75	0.13	0.13	0.13	WTZR	a	1
13.35	42.368	23.48	16.78	0.63	0.63	0.63	AQUI	d	1
13.552	-1.632	22.48	19.69	0.8	0.8	0.8	MSKU	d	1
14.99	36.876	21.63	17.9	0.63	0.62	0.62	NOT1	d	1
14.99	36.876	21.63	17.9	0.63	0.62	0.62	NOTO	d	1
15.493	47.067	23.32	14.22	0.3	0.29	0.29	GRAZ	m	1
15.493	47.067	22.05	16.01	0.31	0.31	0.31	GRAZ	a	1
16.31	39.201	25.58	16.8	0.83	0.82	0.82	COSE	d	1
16.704	40.649	24.62	17.93	0.22	0.22	0.22	MATE	m	1
17.879	-29.669	18.26	18.99	0.49	0.45	0.45	SBOK	a	1
18.158	-32.972	19.12	18.41	0.43	0.54	0.54	LGBN	a	1
18.414	43.868	26.41	13.45	0.69	0.69	0.69	SRJV	d	1
18.44	-34.188	16.18	18.72	1	1.01	1.01	GPpO	d	1
18.44	-34.188	16.51	18.17	1.44	1.16	1.16	SIMO	a	1
18.469	-33.951	18.19	18.46	0.51	0.55	0.55	MBRY	a	1
18.938	69.663	16.27	14.71	0.12	0.12	0.12	TROM	m	1
18.938	69.663	16.09	14.42	0.22	0.22	0.22	TROM	a	1
18.94	69.663	16.31	14.71	0.12	0.12	0.12	TRO1	m	1
19.282	47.79	25.28	12.86	0.67	0.65	0.65	PENC	d	1
19.762	-31.482	18.33	18.82	0.49	0.52	0.52	CALV	a	1
20.665	39.734	22.94	10.55	0.76	0.67	0.67	KRTS	d	1
20.794	41.127	24.44	10.21	0.7	0.69	0.69	ORID	d	1
20.81	-32.38	18.16	19.77	0.63	0.62	0.62	SUTH	d	1
20.811	-32.381	18.15	19.77	0.63	0.62	0.62	SUTM	d	1
20.968	67.857	17	14.42	0.86	0.85	0.85	KIRU	m	1
21.878	36.791	6	-12.25	0.46	0.44	0.44	XRIS	d	1
21.928	38.427	12.59	1.4	0.82	0.82	0.82	EYPA	d	1
22.046	38.209	10.13	-11.79	0.91	0.91	0.91	KOUN	d	1
22.073	38.365	9.95	-1.33	0.91	0.91	0.91	TRIZ	d	1
22.184	38.322	10.65	-2.02	0.82	0.82	0.82	PSAR	d	1

Continued on next page...

Table B.1 – Continued from previous page

Long	Lat	Velocity (mm/yr)				Corr	Site	Source†	EXC‡
°E	°N	East	North	σ E	σ N				
22.201	38.529	13.16	-0.68	0.85	0.85	0.85	LIDO	d	1
22.544	39.937	26.8	5.95	0.49	0.48	0.48	KRNA	d	1
22.823	37.184	7.33	-14.77	0.47	0.44	0.44	LEON	d	1
22.945	38.888	16.18	-2.6	0.47	0.45	0.45	NEVA	d	1
22.984	36.307	9.51	-13.15	0.77	0.65	0.65	KYRA	d	1
23.125	41.459	25.19	11.06	1.32	1.27	1.27	PETB	d	1
23.138	43.11	22.16	11.48	1.32	1.23	1.23	BERK	d	1
23.395	42.556	25.19	10.34	0.55	0.55	0.55	SOFI	d	1
23.425	42.477	21.25	11.37	1.23	1.14	1.14	PLA1	d	1
23.428	40.789	24.32	7.2	0.81	0.69	0.69	SOXO	d	1
23.569	41.823	23.72	9.78	1.34	1.3	1.3	DOBR	d	1
23.916	41.597	24.3	8.81	1.25	1.21	1.21	SAT1	d	1
23.919	39.994	25.65	2.44	0.74	0.67	0.67	STHN	d	1
23.932	38.079	8.85	-13.33	0.42	0.42	0.42	DIOA	d	1
23.932	35.325	9.58	-11.66	0.77	0.64	0.64	OMAL	d	1
23.933	38.079	8.85	-13.33	0.42	0.42	0.42	DION	d	1
23.993	-30.665	17.64	19.09	0.41	0.38	0.38	DEAR	a	1
24.392	38.086	9.66	-13.45	0.67	0.62	0.62	SEVA	d	1
24.395	60.217	21.28	11.65	0.14	0.14	0.14	METS	m	1
24.395	60.217	19.67	9.34	0.6	0.5	0.5	METS	a	1
24.41	37.363	7.69	-13.36	0.7	0.62	0.62	KYNS	d	1
24.521	36.747	8.7	-12.22	0.68	0.61	0.61	MILO	d	1
24.543	38.887	12.67	-11.43	0.75	0.67	0.67	NSKR	d	1
24.627	40.593	23.74	9.49	0.82	0.72	0.72	THAS	d	1
24.634	43.362	24.95	12.89	1.42	1.27	1.27	KAIL	d	1
24.694	35.404	9.16	-14.53	0.66	0.61	0.61	ROML	d	1
24.753	42.146	23.58	10.01	1.29	1.26	1.26	PLO2	d	1
25.126	39.851	9.95	-0.31	0.73	0.66	0.66	LIMN	d	1
25.277	42.963	25.49	12.84	1.29	1.19	1.19	GABR	d	1
25.379	37.449	8.87	-14.14	0.86	0.81	0.81	MKN2	d	1
25.402	41.545	25.84	10.12	1.27	1.22	1.22	MOMC	d	1
25.439	36.346	8.45	-18.35	0.45	0.44	0.44	THIR	d	1
25.513	40.466	22.31	8.5	0.83	0.81	0.81	SMTK	d	1
25.54	-25.805	19.85	20.9	0.49	0.86	0.86	MFKG	a	1
25.566	40.928	25.32	10.13	0.79	0.76	0.76	ASKT	d	1
25.611	-33.985	15.94	20.99	0.52	0.88	0.88	PELB	a	1
26.082	39.501	4.12	3.03	0.98	0.99	0.99	AMAN	d	1
26.085	38.443	5.99	-10.84	0.74	0.67	0.67	HIOS	d	1
26.126	44.464	24.96	10.7	0.61	0.61	0.61	BUCU	d	1
26.157	39.731	4.05	2.95	0.95	0.97	0.97	KEST	d	1
26.174	39.973	8.51	2.48	0.69	0.63	0.63	SUBA	d	1

Continued on next page...

Table B.1 – Continued from previous page

Long	Lat	Velocity (mm/yr)				Corr	Site	Source†	EXC‡
°E	°N	East	North	σ E	σ N				
26.189	39.614	5	2.25	0.95	0.97	0.97	BDER	d	1
26.206	35.129	10.03	-15.94	0.46	0.45	0.45	ZAKR	d	1
26.216	39.726	3.82	2.46	0.97	0.98	0.98	KRKE	d	1
26.268	43.599	24.04	11.57	1.33	1.25	1.25	TSAR	d	1
26.298	-29.104	19.87	18.53	0.85	0.6	0.6	BFTN	a	1
26.309	42.075	24.64	12.06	1.24	1.19	1.19	TOPO	d	1
26.317	39.785	4.88	2.87	0.97	1.01	1.01	EZIN	d	1
26.385	38.311	7.48	-10.32	0.71	0.69	0.69	CEIL	d	1
26.406	36.586	11.08	-17.94	0.7	0.62	0.62	ASTP	d	1
26.451	39.234	5.54	-0.64	0.76	0.67	0.67	LESV	d	1
26.535	39.58	4.54	5.53	0.96	0.98	0.98	HOBS	d	1
26.7	39.311	6.23	0.28	0.78	0.72	0.72	AYKA	d	1
26.706	40.739	20.01	8.65	0.73	0.73	0.73	DOKU	d	1
26.707	39.326	3.97	2.2	0.75	0.73	0.73	AYVA	d	1
26.725	43.488	23.79	11.59	1.34	1.27	1.27	SHUM	d	1
26.732	39.653	2.34	4.73	0.96	0.95	0.95	KCAM	d	1
26.871	40.601	11.47	7.82	0.93	0.96	0.96	KVAK	d	1
26.88	40.396	5.72	5.39	0.92	0.94	0.94	SEVK	d	1
26.885	39.01	4.04	-1.54	1.78	1.75	1.75	ESEN	d	1
26.91	40.029	5.27	3.31	0.95	0.95	0.95	BAH1	d	1
26.929	36.752	9.46	-14.54	0.74	0.64	0.64	KOSI	d	1
26.989	37.78	6.28	-11.93	0.72	0.63	0.63	SAMO	d	1
27.085	38.019	5.22	-7.73	0.71	0.63	0.63	OZDE	d	1
27.112	39.244	5.46	-0.18	1.67	1.72	1.72	D5DU	d	1
27.214	40.171	5.02	2.86	0.94	0.95	0.95	ARAK	d	1
27.217	39.897	5.4	3.51	0.63	0.62	0.62	KIRE	d	1
27.224	35.493	13.5	-18.48	0.46	0.44	0.44	KRPT	d	1
27.231	31.346	23.29	16.46	0.9	0.79	0.79	MATR	d	1
27.269	39.577	4.3	5.5	0.97	0.96	0.96	EGMI	d	1
27.301	40.381	6.74	6.33	0.91	0.91	0.91	KABI	d	1
27.308	38.711	7.75	-2.85	0.79	0.74	0.74	BAYO	d	1
27.316	39.024	4.52	-1.42	0.78	0.73	0.73	YAYA	d	1
27.393	40.811	21.4	7.1	0.73	0.7	0.7	YENB	d	1
27.394	36.681	13.56	-18	0.66	0.62	0.62	KNID	d	1
27.423	37.032	9.41	-14.19	0.69	0.6	0.6	BODR	d	1
27.424	39.785	2.12	3.35	0.75	0.74	0.74	ALAN	d	1
27.442	42.666	25.61	11.39	1.26	1.22	1.22	BURG	d	1
27.483	42.484	23.01	10.95	1.35	1.3	1.3	BUTG	d	1
27.486	37.818	5.64	-7.11	0.93	0.89	0.89	SOKE	d	1
27.586	40.588	9.95	6.02	1.14	1.08	1.08	MISL	d	1
27.59	39.295	8.4	-0.41	1.64	1.66	1.66	D7DU	d	1

Continued on next page...

Table B.1 – Continued from previous page

Long	Lat	Velocity (mm/yr)				Corr	Site	Source†	EXC‡
°E	°N	East	North	σ E	σ N				
27.629	40.245	5.03	6.34	0.94	0.95	0.95	UKIR	d	1
27.687	-25.89	19.36	17.37	0.53	0.52	0.52	HRAO	m	1
27.696	-23.687	19.54	17.45	0.68	0.68	0.68	ERAS	a	1
27.707	-25.887	17.56	15.43	1.87	1.8	1.8	HARB	m	1
27.708	-25.887	18.43	17.74	0.39	0.37	0.37	HART	m	1
27.763	40.059	2.17	8.86	0.96	0.96	0.96	KOCB	d	1
27.779	41.827	25.76	11.68	0.75	0.71	0.71	DEMI	d	1
27.781	35.952	17.31	-16.98	0.47	0.45	0.45	KATV	d	1
27.816	40.4	4.09	8.56	0.71	0.7	0.7	ERDE	d	1
27.836	37.196	7.82	-13.17	0.65	0.6	0.6	CAMK	d	1
27.873	39.006	4.2	1.48	0.7	0.68	0.68	AKGA	d	1
27.96	40.971	27.71	11.16	0.67	0.64	0.64	MAER	d	1
27.963	36.772	11.23	-14.18	0.61	0.55	0.55	MARM	d	1
28	38.248	4.69	-0.85	0.95	0.89	0.89	ODME	d	1
28.081	37.609	4.63	-9.18	0.65	0.56	0.56	CINE	d	1
28.283	-25.732	18.06	19.12	0.51	0.68	0.68	PRET	a	1
28.293	41.475	26.23	11.01	1.16	1.07	1.07	YALI	d	1
28.334	-28.25	17.56	18.87	0.43	0.45	0.45	BETH	a	1
28.365	41.052	23.43	12.46	1.15	1.08	1.08	SELP	d	1
28.373	40.398	5.93	10.43	1.23	1.08	1.08	YENI	d	1
28.427	37.175	7.36	-9.07	0.76	0.71	0.71	MULA	d	1
28.483	38.315	2.75	-1.5	0.98	0.91	0.91	ALSE	d	1
28.671	39.046	4.16	5.24	0.73	0.69	0.69	DMIR	d	1
28.673	-31.549	17.12	18.88	0.51	0.62	0.62	UMTA	a	1
28.779	40.167	4.79	9.05	0.95	0.95	0.95	HAGA	d	1
28.826	36.762	9.82	-8.39	1	0.81	0.81	DLMN	d	1
28.882	40.481	6.96	16.5	1.99	1.68	1.68	FIST	d	1
28.923	39.93	1.81	11.04	0.98	0.97	0.97	GIRE	d	1
29.02	41.104	23.09	11.61	0.7	0.7	0.7	ITAY	d	1
29.048	37.566	4.24	-3.78	1.04	0.99	0.99	TAVA	d	1
29.064	41.064	22.69	12.48	0.63	0.6	0.6	IKAN	d	1
29.102	40.136	1.8	8.5	0.73	0.72	0.72	ULUD	d	1
29.106	40.27	4.38	11.98	0.94	0.94	0.94	DTAS	d	1
29.111	40.165	3.97	10.79	0.95	0.95	0.95	ZEYA	d	1
29.136	37.941	3.68	3.73	0.69	0.65	0.65	PAMU	d	1
29.141	40.122	5.8	9.21	0.81	0.78	0.78	ULDA	d	1
29.143	40.639	9.55	12.62	0.73	0.71	0.71	CINA	d	1
29.146	40.46	5.1	13.37	0.94	0.94	0.94	GEML	d	1
29.261	40.2	4.14	10.18	0.95	0.95	0.95	CATA	d	1
29.288	40.485	9.81	12.98	1.81	1.55	1.55	KUTE	d	1
29.392	37.448	4.53	0.32	1.01	0.91	0.91	GKPN	d	1

Continued on next page...

Table B.1 – Continued from previous page

Long	Lat	Velocity (mm/yr)				Corr	Site	Source†	EXC‡
°E	°N	East	North	σ E	σ N				
29.423	40.821	16.33	12.31	0.7	0.7	0.7	GATE	d	1
29.439	36.72	10.51	-0.05	0.7	0.64	0.64	SIRA	d	1
29.451	40.787	17.69	7.49	1.4	1.37	1.37	TUBI	d	1
29.514	40.164	3.87	11.28	0.99	0.97	0.97	HMZA	d	1
29.535	37.185	6.35	-1.82	0.85	0.83	0.83	YSFC	d	1
29.585	40.667	12.14	13.4	0.96	0.95	0.95	OLUK	d	1
29.623	41.179	24.33	10.85	1.25	1.12	1.12	SILE	d	1
29.635	40.803	19.16	12.67	0.96	0.94	0.94	YUHE	d	1
29.648	36.194	15.68	2.72	0.73	0.56	0.56	KASO	d	1
29.681	40.362	5.4	12.05	0.67	0.59	0.59	DERB	d	1
29.81	36.971	5.48	2.89	0.84	0.83	0.83	KYBS	d	1
29.889	40.066	4.62	4.85	1.95	1.8	1.8	KPKL	d	1
29.908	40.438	7.6	9.64	0.61	0.61	0.61	IGAZ	d	1
29.929	40.425	7.6	9.64	0.61	0.61	0.61	IUCK	d	1
30.026	40.465	8.54	9.68	0.68	0.63	0.63	MEKE	d	1
30.13	40.745	16.81	10.69	0.91	0.94	0.94	SISL	d	1
30.134	40.69	12.35	11.36	0.81	0.83	0.83	SMAS	d	1
30.297	37.689	6.43	2.71	0.58	0.53	0.53	BURD	d	1
30.384	-23.08	18.59	17.22	0.7	0.69	0.69	TDOU	a	1
30.609	36.829	13.56	3.13	0.65	0.6	0.6	ANTG	d	1
30.637	39.658	1.46	9.51	0.99	0.92	0.92	ESKI	d	1
30.638	40.614	11.78	10.03	0.59	0.6	0.6	KTOP	d	1
30.644	38.769	4.33	8.71	0.86	0.76	0.76	AFYO	d	1
30.655	40.628	11.84	9.97	0.59	0.6	0.6	KKAP	d	1
30.679	40.552	8.36	10.61	0.69	0.72	0.72	BOZS	d	1
30.68	40.538	8.37	10.61	0.69	0.72	0.72	AGUZ	d	1
30.738	-0.601	25.58	16.19	0.81	0.81	0.81	MBAR	d	1
30.745	40.652	14.2	12.32	1.01	1.03	1.03	KMAL	d	1
30.761	40.589	12.32	10.06	0.8	0.81	0.81	AGOK	d	1
30.804	40.386	5.84	9.37	0.65	0.65	0.65	TEBA	d	1
30.827	40.735	17.43	10.68	0.75	0.76	0.76	KDER	d	1
30.862	40.555	8.19	11.04	0.98	0.99	0.99	PINA	d	1
30.888	29.514	23.61	16.82	0.84	0.8	0.8	MEST	d	1
30.947	-29.965	17.01	18.31	0.52	0.55	0.55	DRBN	a	1
30.975	-25.475	18.03	18.03	0.53	0.54	0.54	NSPT	a	1
31.121	37.762	9.17	6.22	0.94	0.76	0.76	AKSU	d	1
31.134	-23.952	17	17.64	0.47	0.47	0.47	PBWA	a	1
31.344	29.862	24.01	16.8	0.57	0.54	0.54	HELW	d	1
31.344	29.862	24.01	16.8	0.57	0.54	0.54	PHLW	d	1
31.421	-28.293	19.83	12.15	0.69	0.79	0.79	ULDI	a	1
31.438	40.937	22.04	11.2	0.57	0.55	0.55	YIG2	d	1

Continued on next page...

Table B.1 – Continued from previous page

Long	Lat	Velocity (mm/yr)				Corr	Site	Source†	EXC‡
°E	°N	East	North	σ E	σ N				
31.439	40.937	22.04	11.2	0.57	0.55	0.55	YIGI	d	1
31.814	39.564	5.18	8.7	0.81	0.7	0.7	SIVR	d	1
32.078	-28.796	17.67	17.66	0.77	0.78	0.78	RBAY	d	1
32.16	36.431	14.82	10.61	0.65	0.61	0.61	SEKI	d	1
32.226	41.52	25.94	9.94	0.89	0.88	0.88	HALI	d	1
32.566	29.379	24.86	17.98	0.61	0.6	0.6	FANA	d	1
32.57	40.881	19.09	11.11	0.77	0.71	0.71	ISME	d	1
32.758	39.887	1.58	10.52	0.86	0.85	0.85	ANKR	m	1
32.758	39.887	4.43	10.15	1.12	1.1	1.1	ANKR	m	1
32.759	39.886	4.3	9.33	0.57	0.56	0.56	ANKM	d	1
33.102	29.141	25.31	17.66	0.71	0.67	0.67	ABOZ	d	1
33.191	37.378	12.34	13.3	0.62	0.61	0.61	MELE	d	1
33.228	28.163	24.43	18.05	0.68	0.67	0.67	GARB	d	1
33.391	27.919	24.53	18.1	0.67	0.66	0.66	ZEIT	d	1
33.396	35.141	19.92	13.85	0.55	0.55	0.55	NICO	d	1
33.494	27.686	24.76	15.94	0.67	0.66	0.66	GEMS	d	1
33.596	28.269	23.28	17.11	0.6	0.6	0.6	TOUR	d	1
33.832	27.244	23.13	16.63	0.84	0.79	0.79	HURG	d	1
33.883	27.961	21.87	19.53	1.03	1.03	1.03	KENS	d	1
33.991	44.413	25.31	11.57	0.68	0.68	0.68	CRAO	d	1
33.995	28.639	25.61	17.12	1.05	1.06	1.06	CATH	d	1
34.184	27.846	23.1	17.97	0.6	0.6	0.6	SHAM	d	1
34.256	36.566	14.56	15.49	0.71	0.71	0.71	MERS	d	1
34.314	28.178	24.33	18.74	0.89	0.82	0.82	NABQ	d	1
34.47	28.529	23.48	18.07	0.65	0.65	0.65	DAHA	d	1
34.552	36.9	13.95	14.85	1.1	0.98	0.98	MER0	d	1
34.763	30.598	26.96	19.18	0.57	0.57	0.57	RAMO	d	1
34.781	32.068	24.71	17.97	0.53	0.54	0.54	TELA	d	1
34.803	39.106	6.63	14.29	1.5	1.49	1.49	ABDI	d	1
34.813	39.801	7.08	15.77	0.68	0.66	0.66	YOZG	d	1
34.866	31.378	23.51	18.21	0.76	0.76	0.76	LHAV	d	1
34.875	40.453	8.25	15.14	0.96	0.93	0.93	KKIR	d	1
34.921	29.509	26.08	19.4	0.55	0.56	0.56	ELAT	d	1
35.023	32.779	22.9	19.01	0.51	0.52	0.52	BSHM	d	1
35.089	31.723	24.88	17.72	1.2	1.14	1.14	BARG	d	1
35.145	33.023	22.67	18.6	0.59	0.59	0.59	KABR	d	1
35.202	31.771	23.63	19.02	0.97	0.95	0.95	JSLM	d	1
35.205	42.02	25.16	12	0.89	0.79	0.79	SINO	d	1
35.392	31.593	24.2	19.29	0.66	0.65	0.65	DRAG	d	1
35.416	32.479	22.9	20.02	0.59	0.59	0.59	GILB	d	1
35.674	34.115	19.56	18.67	0.97	0.97	0.97	LAUG	d	1

Continued on next page...

Table B.1 – Continued from previous page

Long	Lat	Velocity (mm/yr)				Corr	Site	Source†	EXC‡
°E	°N	East	North	σ E	σ N				
35.688	32.995	24.8	22.27	0.54	0.54	0.54	KATZ	d	1
35.771	33.182	23.8	21.55	0.68	0.68	0.68	ELRO	d	1
35.87	36.397	20.91	19.72	1.7	1.62	1.62	ULCN	d	1
35.94	36.456	16.72	19.9	1.06	1.02	1.02	ULUC	d	1
36.1	29.139	28.19	22.84	0.89	0.87	0.87	HALY	d	1
36.131	36.05	21.24	20.35	0.67	0.65	0.65	SENK	d	1
36.137	36.899	15.2	19.73	0.52	0.52	0.52	DORT	d	1
36.18	36.54	16.44	22.31	1.73	1.75	1.75	ISKE	d	1
36.245	38.231	12.39	18.49	1.59	1.44	1.44	PNLR	d	1
36.285	33.51	24.25	22.05	0.97	0.97	0.97	UDMC	d	1
36.33	37.572	12.15	19	1.66	1.6	1.6	ANDR	d	1
36.336	41.299	26.22	12.81	1	1.01	1.01	SAMS	d	1
36.378	26.458	29.88	24.37	1.77	1.77	1.77	ALWJ	d	1
36.524	36.788	18.54	20.18	0.69	0.69	0.69	HASA	d	1
36.643	37.088	18.89	21	0.78	0.74	0.74	FEVZ	d	1
36.758	55.699	24.29	8.76	0.47	0.47	0.47	ZWE2	d	1
36.972	37.19	18.19	21.58	0.51	0.52	0.52	SAKZ	d	1
36.996	37.522	16.95	20.54	0.57	0.59	0.59	KMAR	d	1
37.106	36.685	18.46	20.46	1.77	1.74	1.74	KILI	d	1
37.113	37.747	14.36	18.22	0.71	0.7	0.7	ABEY	d	1
37.22	38.179	13.07	19.26	0.68	0.69	0.69	ELBI	d	1
37.436	37.518	18.97	21.34	0.7	0.72	0.72	ALAR	d	1
37.574	36.901	19.7	23.52	0.58	0.55	0.55	GAZI	d	1
37.869	38.05	13.05	19.48	0.7	0.69	0.69	ALTP	d	1
37.886	37.541	19.31	22.32	0.76	0.75	0.75	CKRH	d	1
37.902	37.237	19.62	23.36	0.7	0.7	0.7	ARGA	d	1
37.958	39.454	9.25	19.7	0.46	0.46	0.46	SINC	d	1
38.049	44.552	25.59	8.61	1.5	1.32	1.32	GELE	d	1
38.215	38.456	14.9	20.58	0.76	0.74	0.74	MLT1	d	1
38.215	38.456	14.9	20.58	0.76	0.74	0.74	MLTY	d	1
38.231	37.747	18.87	23.73	0.85	0.82	0.82	ADYI	d	1
38.584	9.081	26.33	16.99	1.01	0.81	0.81	KOLO	d	1
38.766	9.035	26.31	16.81	0.56	0.49	0.49	ADD0	d	1
39.164	39.613	7.66	19.16	0.95	0.89	0.89	KMAH	d	1
39.242	44.704	25.63	9.39	1.27	1.13	1.13	GKL_	d	1
39.254	38.64	12.82	20.3	1.24	1.2	1.2	GMKV	d	1
39.282	8.472	28.48	16.52	0.67	0.59	0.59	BOKU	d	1
39.438	8.292	29.25	16.19	0.73	0.6	0.6	SELA	d	1
39.52	8.258	29.53	15.67	0.61	0.56	0.56	BOLO	d	1
39.524	39.071	9.48	21.3	1.45	1.3	1.3	TUNC	d	1
39.531	8.266	29.53	15.67	0.61	0.56	0.56	REDG	d	1

Continued on next page...

Table B.1 – Continued from previous page

Long	Lat	Velocity (mm/yr)				Corr	Site	Source[†]	EXC[‡]
°E	°N	East	North	σ E	σ N				
39.631	21.369	34.21	25.23	1.79	1.78	1.78	JEDD	d	1
39.702	40.974	26.99	11.83	0.49	0.47	0.47	AKTO	d	1
39.776	40.995	26.98	11.81	0.49	0.47	0.47	TRAB	d	1
39.805	37.847	17.66	24.41	0.77	0.76	0.76	KRCD	d	1
40.052	38.963	12.98	19.1	1.58	1.36	1.36	KAKO	d	1
40.254	39.731	23.67	14.98	0.77	0.7	0.7	MERC	d	1
40.272	43.681	27.92	8.03	1.68	1.41	1.41	KRPO	d	1
40.65	37.246	20.25	25.76	0.82	0.77	0.77	KIZ2	d	1
40.651	37.247	20.25	25.76	0.82	0.77	0.77	KIZI	d	1
40.809	40.437	27.18	12.34	0.58	0.53	0.53	ISPI	d	1
41.057	38.959	19.85	20.47	1.43	1.2	1.2	SOLH	d	1
41.3	39.973	25.89	14.81	0.68	0.66	0.66	ERZU	d	1
41.339	41.371	25.88	11.73	0.92	0.91	0.91	HOPA	d	1
41.454	39.186	20.74	19.64	2.01	1.29	1.29	VART	d	1
41.512	39.643	24.49	13.26	1.78	1.22	1.22	TKMN	d	1
41.565	43.788	26.95	10.07	1.06	1.05	1.05	ZECK	m	1
41.565	43.788	26.99	10.05	0.46	0.45	0.45	ZELB	d	1
41.794	38.754	21.99	23.58	0.86	0.71	0.71	KRKT	d	1
41.99	40.548	28.51	13.82	0.95	0.92	0.92	OLTU	d	1
42.045	19.211	36.05	26.59	0.92	0.89	0.89	NAMA	d	1
42.062	42.721	25.94	12.07	0.51	0.51	0.51	INGU	d	1
42.133	41.648	25.94	13.89	0.68	0.68	0.68	SHUA	d	1
42.149	39.714	25.22	17.54	1.4	1.24	1.24	KRYZ	d	1
42.195	43.349	26.01	8.57	0.87	0.85	0.85	ULKA	d	1
42.457	37.528	20.36	23.79	2.72	1.24	1.24	SRNK	d	1
42.471	42.022	28.65	12.8	0.77	0.71	0.71	VANI	d	1
42.547	38.488	21.14	22.65	1.52	1.21	1.21	RESD	d	1
42.667	43.743	26.82	10.71	0.83	0.84	0.84	SHAT	d	1
42.755	41.126	27.96	13.2	1.35	1.08	1.08	ARDA	d	1
42.787	44.011	26.31	9.84	0.87	0.87	0.87	BEUG	d	1
42.847	11.526	29.45	28.23	2.68	2.13	2.13	DJIA	e	1
42.847	11.526	29.45	28.23	2.68	2.13	2.13	DJIB	e	1
42.873	45.267	28.28	7.44	0.98	0.95	0.95	SVT1	d	1
42.91	39.232	24.71	18.01	0.63	0.54	0.54	PTNS	d	1
42.954	14.769	36.83	26.58	1.05	0.93	0.93	HODE	d	1
43.026	39.719	27.55	17.18	0.7	0.67	0.67	ARGI	d	1
43.135	42.468	27.51	12.44	0.88	0.73	0.73	KHOT	d	1
43.17	40.685	28.2	14.39	0.61	0.52	0.52	KARS	d	1
43.341	38.549	21.78	21.59	0.88	0.86	0.86	KAL2	d	1
43.382	42.578	26.81	7.9	0.75	0.68	0.68	KHUR	d	1
43.4	42.349	29.08	14.39	0.71	0.62	0.62	SACC	d	1

Continued on next page...

Table B.1 – Continued from previous page

Long	Lat	Velocity (mm/yr)				Corr	Site	Source†	EXC‡
°E	°N	East	North	σ E	σ N				
43.54	42.485	27.36	8.26	0.77	0.73	0.73	LESO	d	1
43.753	42.978	27.74	8.87	0.89	0.89	0.89	MATS	d	1
43.759	38.997	21.83	19.85	2.09	1.42	1.42	MRAD	d	1
43.768	40.972	28.07	14.94	0.94	0.86	0.86	AMAS	d	1
43.891	41.537	28.14	12.93	0.65	0.61	0.61	NINO	d	1
43.954	40.609	28.71	16.45	0.85	0.84	0.84	ARTI	d	1
44.114	40.178	29.2	16.11	0.85	0.84	0.84	MMOR	d	1
44.145	39.556	26.12	15.35	2.12	1.29	1.29	DBYZ	d	1
44.364	41.031	30.35	14.29	0.86	0.81	0.81	STEP	d	1
44.486	42.447	27.38	12.11	0.61	0.6	0.6	KRES	d	1
44.503	40.226	29.51	16.45	0.53	0.52	0.52	NSSP	d	1
44.526	41.831	28.17	14.71	0.6	0.57	0.57	NICH	d	1
44.742	40.149	29.68	17.86	0.64	0.56	0.56	GARN	d	1
44.826	41.377	35.49	13.34	2.69	1.7	1.7	SHUL	d	1
44.859	40.526	28.19	13.48	1.13	0.86	0.86	GAGA	d	1
45.04	12.812	37.39	27.04	1.1	0.94	0.94	ADEN	d	1
45.139	40.907	30.64	15.62	0.65	0.62	0.62	IJEV	d	1
45.341	40.124	29.84	17.51	2.1	1.45	1.45	ASTG	d	1
45.661	39.837	31.94	18.35	0.88	0.83	0.83	JERM	d	1
45.795	41.951	26.52	13.3	0.74	0.7	0.7	KUDI	d	1
46.093	39.536	31.17	17.88	1.01	0.9	0.9	NORA	d	1
46.162	39.126	28.25	22.34	2.11	1.39	1.39	KAJR	d	1
46.162	36.908	25.88	21.92	0.81	0.78	0.78	MIAN	d	1
46.367	39.511	31.71	19.19	0.85	0.83	0.83	GORI	d	1
46.401	24.911	34.8	27.44	1.53	1.53	1.53	SOLA	d	1
46.459	39.315	31.25	20.32	2.09	1.35	1.35	KARM	d	1
46.511	41.652	27.94	12.91	0.65	0.65	0.65	KATE	d	1
46.758	40.184	31.16	18.89	0.99	0.87	0.87	KASP	d	1
46.76	39.753	30.7	18.95	0.95	0.82	0.82	SHOU	d	1
46.842	43.026	28.59	11.35	0.57	0.57	0.57	DUBK	d	1
46.847	43.125	25.95	11.53	0.57	0.57	0.57	ZURA	d	1
47.25	41.132	28.14	13.2	0.66	0.66	0.66	SHEK	d	1
47.863	40.975	27.7	11.49	0.68	0.66	0.66	KEBE	d	1
47.93	36.232	25.46	20.36	1.26	1.14	1.14	BIJA	d	1
48.148	40.333	31.47	17.34	1.01	0.87	0.87	KURD	d	1
48.388	38.952	32.47	20.23	0.95	0.87	0.87	YARD	d	1
48.409	30.246	26.85	25.58	1.24	1.11	1.11	KHOS	d	1
48.419	38.706	32.26	19.43	0.93	0.82	0.82	GOSM	d	1
48.529	41.595	27.79	8.53	0.98	0.88	0.88	SAMU	d	1
48.551	40.614	29.83	8.99	0.9	0.81	0.81	MEDR	d	1
48.717	39.497	33.58	19.79	0.68	0.66	0.66	BILE	d	1

Continued on next page...

Table B.1 – Continued from previous page

Long	Lat	Velocity (mm/yr)				Corr	Site	Source[†]	EXC[‡]
°E	°N	East	North	σ E	σ N				
48.773	15.947	37.88	27.49	1.2	1.13	1.13	SYON	d	1
49.038	14.486	37.34	31.3	1.29	1.21	1.21	MKLA	d	1
49.12	41.066	28.14	9.11	0.9	0.81	0.81	SIYE	d	1
49.426	40.025	31.26	8.95	0.7	0.67	0.67	SHIK	d	1
50.608	26.209	32.93	30.84	1.76	1.97	1.97	BAHR	e	1
50.748	32.367	27.2	20.12	1.22	1.1	1.1	SHAH	d	1
51.082	28.919	28.65	28.3	0.83	0.77	0.77	ALIS	d	1
51.334	35.697	27.68	19.14	0.72	0.71	0.71	TEHN	d	1
51.812	35.73	27.12	16.22	0.73	0.7	0.7	BOOM	d	1
51.885	35.223	29.02	15.94	1.28	1.26	1.26	PISH	d	1
51.986	35.793	27.34	15.93	1.34	1.31	1.31	ABAL	d	1
52.157	35.868	27.73	13.71	1.33	1.31	1.31	MEHR	d	1
52.285	36.588	25.57	12.43	1.14	1.12	1.12	MAHM	d	1
52.305	36.206	24.94	15.5	1.41	1.3	1.3	HELI	d	1
52.586	35.701	26.08	15.15	1.24	1.21	1.21	AMIN	d	1
53.564	35.662	27.56	15.05	1.33	1.15	1.15	SEMN	d	1
53.822	32.313	26.4	19.53	0.8	0.76	0.76	ARD1	d	1
54.004	26.883	30.32	28.5	1.64	1.19	1.19	LAMB	d	1
54.199	36.86	26.6	11.11	1.37	1.14	1.14	KORD	d	1
55.572	-21.208	17.8	11.16	1.23	1.22	1.22	REUN	d	1
55.918	28.302	27.42	23.34	1.38	1.06	1.06	HAJI	d	1
56.07	33.369	29.55	16.48	1.27	1.11	1.11	ROBA	d	1
56.112	22.186	37.63	32.51	1.21	1.2	1.2	YIBL	d	1
56.233	26.208	31.29	30.22	1.55	1.17	1.17	KHAS	d	1
57.119	30.277	28.88	21.36	2.28	1.37	1.37	KERM	d	1
57.308	37.814	29.97	7.42	1.39	1.12	1.12	SHIR	d	1
57.767	25.636	30.14	19.11	1.22	1.08	1.08	JASK	d	1
58.464	35.293	28.51	10.84	0.83	0.77	0.77	KASH	d	1
58.56	56.43	26.11	4.36	0.26	0.26	0.26	ARTU	m	1
58.569	23.564	33.82	31.45	1.26	1.09	1.09	MUSC	d	1
59.48	36.335	27.71	2.78	1.76	1.54	1.54	MASH	d	1
60.694	25.3	27.25	12.08	1.43	1.14	1.14	CHAC	d	1
61.034	36.601	31.36	3.81	1.3	1.13	1.13	YAZT	d	1
61.517	31.049	28.96	3.94	1.21	1.08	1.08	ZABO	d	1
66.885	39.135	28.8	3.22	0.14	0.13	0.13	KIT3	m	1
66.885	39.135	27.88	3.61	0.42	0.24	0.24	KIT3	a	1
70.256	-49.351	4.96	-3.49	0.37	0.33	0.33	KERG	i	1
74.34	39.84	28.39	13.96	1.6	1.6	1.6	I089	k	1
74.694	42.68	28.68	2.83	0.15	0.14	0.14	POL2	m	1
74.694	42.68	29.03	1.77	0.51	0.33	0.33	POL2	a	1
74.95	38.66	23.92	19.92	1.68	1.68	1.68	I090	k	1

Continued on next page...

Table B.1 – Continued from previous page

Long	Lat	Velocity (mm/yr)				Corr	Site	Source†	EXC‡
°E	°N	East	North	σ E	σ N				
75.124	39.697	28.38	12.74	1.88	1.35	1.35	WUQO	a	1
75.211	37.847	24.13	21.71	1.88	1.35	1.35	TAXK	a	1
75.23	37.77	25.07	21.02	1.07	1.07	1.07	TASH	g	1
75.25	39.72	28	12.43	1.59	1.59	1.59	I078	k	1
75.45	36.85	25.7	21.61	1.67	1.58	1.58	I088	k	1
75.67	32.49	39.3	31.51	1.58	1.12	1.12	MANU	k	1
75.9	39.2	29.97	18.49	1.58	1.58	1.58	I081	k	1
75.92	39.52	31.63	14.96	1.07	1.07	1.07	JB48	g	1
75.92	39.517	32.38	17.32	1.53	1.2	1.2	KASH	a	1
76.068	31.842	29.95	39.56	1.44	1.38	1.38	CHIT	m	1
76.17	38.94	28.26	18.49	1.58	1.58	1.58	I083	k	1
76.51	39.81	29.72	15.48	1.67	1.67	1.67	I077	k	1
76.73	39.5	27.9	17.29	1.67	1.67	1.67	I079	k	1
76.89	40.2	29.84	12.74	1.67	1.67	1.67	I074	k	1
77.01	36.58	26.4	19.55	1.66	1.66	1.66	J047	k	1
77.017	43.179	28.94	1.57	0.2	0.19	0.19	SELE	m	1
77.017	43.179	26.97	2.84	0.71	0.52	0.52	SELE	a	1
77.085	31.683	20.89	37.55	0.93	0.91	0.91	PAND	m	1
77.17	28.54	36.47	30.55	1.49	0.87	0.87	JNUC	k	1
77.248	38.412	26.12	19.21	1.68	1.36	1.36	SHAC	a	1
77.28	38.17	28.22	18.28	1.56	1.56	1.56	I084	k	1
77.45	23.21	35.56	32.11	0.48	0.4	0.4	BHOP	h	1
77.57	13.021	41.87	32.38	1.15	1.13	1.13	IIS1	a	1
77.575	34.711	25.17	19.38	1.3	1.29	1.29	PAN2	m	1
77.576	34.71	27.82	18.82	1.45	1.32	1.32	PANA	m	1
77.62	38.9	27.87	19.57	1.66	1.56	1.56	I082	k	1
77.973	-68.577	-2.91	-4.88	0.61	0.6	0.6	DAV1	m	1
78.04	39.71	29.51	15.53	1.56	1.56	1.56	I075	k	1
78.19	41.864	35.94	6.47	2.46	2.43	2.43	KUMT	a	1
78.25	37.56	26.18	18.52	1.56	1.56	1.56	I086	k	1
78.436	39.95	27.87	16.34	1.69	1.39	1.39	SANC	a	1
78.45	40.94	31.08	13.69	1.56	1.56	1.56	I072	k	1
78.54	39.78	29.12	14.75	1.56	1.56	1.56	I076	k	1
78.612	30.82	50.31	28.65	2.33	2.31	2.31	BHTW	m	1
79.04	40.5	29.55	12.57	1.56	1.56	1.56	I073	k	1
79.21	41.2	29.45	12.52	1.05	1.05	1.05	WUSH	g	1
79.214	41.201	30.98	9.68	1.26	1.21	1.21	WUSO	a	1
79.26	35.94	29.37	15.44	2.53	2.33	2.33	G0BL	k	1
79.58	35.46	27.59	13.56	1.06	1.06	1.06	JB55	g	1
79.69	35.03	29.5	17.28	2.53	2.33	2.33	Y198	k	1
79.77	37.14	33.15	15.48	2.53	2.33	2.33	Y035	k	1

Continued on next page...

Table B.1 – Continued from previous page

Long	Lat	Velocity (mm/yr)				Corr	Site	Source†	EXC‡
°E	°N	East	North	σ E	σ N				
79.874	6.892	39.98	35.63	2.14	1.42	1.42	COL1	e	1
79.926	37.121	26.07	13.99	1.86	1.59	1.59	HOTA	a	1
79.96	37.1	27.25	14.92	1.54	1.54	1.54	I087	k	1
80.24	41.14	32.26	13.05	1.65	1.55	1.55	I061	k	1
80.39	40.64	31.24	12.99	1.55	1.55	1.55	I062	k	1
80.781	41.38	33.53	12.4	1.99	1.51	1.51	KARA	a	1
80.885	44.12	27.52	4.29	1.91	1.58	1.58	KORG	a	1
81.13	43.14	30.61	4.93	1.66	1.66	1.66	I052	k	1
81.325	40.61	28.15	14.41	2.03	1.51	1.51	ARAL	a	1
81.34	41.6	32.86	6.06	2.14	2.04	2.04	I059	k	1
81.48	36.46	24.5	12.58	1.54	1.54	1.54	I070	k	1
81.58	36.77	30.52	18.05	2.62	2.32	2.32	G0BC	k	1
81.66	36.84	26.72	11.72	1.63	1.63	1.63	I068	k	1
81.8	41.81	32.06	4.89	1.65	1.65	1.65	I055	k	1
82.22	43.47	30.59	4.04	1.65	1.65	1.65	I050	k	1
82.35	41.49	31.63	9.6	1.64	1.64	1.64	I058	k	1
82.446	41.79	30.36	12.63	2.01	1.58	1.58	KEZI	a	1
82.7	37.05	26.22	10.67	1.53	1.53	1.53	I067	k	1
82.79	41.22	31.01	10.15	1.64	1.64	1.64	I060	k	1
82.97	41.71	31.22	7.88	1.74	1.74	1.74	I057	k	1
82.99	36.74	26.09	10.86	1.53	1.53	1.53	I069	k	1
83.13	42.14	32.23	6.02	2.03	2.03	2.03	I054	k	1
83.16	38.26	30.08	8.92	1.73	1.63	1.63	I065	k	1
83.26	43.4	30.04	3.47	1.05	1.05	1.05	JB47	g	1
83.49	49.54	25.5	-1.54	1.34	1.25	1.25	SLP4	g	1
83.61	39.02	29.3	7.16	1.73	1.73	1.73	I064	k	1
83.81	37.59	27.22	9.09	1.72	1.63	1.63	I066	k	1
83.95	37.7	27.93	11.04	2.42	2.32	2.32	G0BP	k	1
84.16	43.03	32.11	4.76	1.64	1.64	1.64	I053	k	1
84.25	41.78	31.38	8.54	1.73	1.73	1.73	I056	k	1
84.294	43.268	28.02	5.87	2.01	1.71	1.71	NANA	a	1
84.34	40.22	29.93	8.81	1.73	1.73	1.73	I063	k	1
84.54	43.27	31.4	3.92	1.64	1.74	1.74	I051	k	1
84.77	50.94	25.64	-3.84	1.54	1.34	1.34	USTK	g	1
84.85	37.242	22.51	11.82	2.52	2.38	2.38	Y348	l	1
84.946	44.385	31.25	6.36	2.15	1.68	1.68	KUYT	a	1
84.984	27.165	35.6	29.41	1.75	1.65	1.65	GPpP	a	1
85.143	37.124	28.1	7.63	1.96	2.1	2.1	SLUB	l	1
85.144	37.057	26	10.13	1.87	1.93	1.93	ATUB	l	1
85.156	36.986	27.9	10.93	1.96	2.02	2.02	GRUB	l	1
85.427	37.582	25.39	8.42	1.87	1.93	1.93	QUIS	l	1

Continued on next page...

Table B.1 – Continued from previous page

Long	Lat	Velocity (mm/yr)				Corr	Site	Source†	EXC‡
°E	°N	East	North	σ E	σ N				
85.44	50.15	26.39	-4.12	1.44	1.44	1.44	KAIT	g	1
85.456	37.387	26.79	8.02	1.87	1.93	1.93	AQIN	l	1
85.52	41.91	32.53	5.29	1.73	1.73	1.73	I030	k	1
85.54	38.08	27.89	6.52	1.04	1.04	1.04	JB46	g	1
86.169	41.708	32.58	5.31	1.03	0.95	0.95	KORL	a	1
86.19	41.79	31.45	5.25	1.04	1.04	1.04	JB45	g	1
86.251	38.077	24.77	12.22	2.53	2.47	2.47	G0BB	l	1
86.36	42.35	32.6	4.6	1.73	1.73	1.73	I028	k	1
86.98	38.51	28.86	5.12	1.92	1.92	1.92	I035	k	1
87.072	38.709	27.25	5.81	1.79	1.75	1.75	AL35	l	1
87.17	43.27	31.26	2.91	1.73	1.73	1.73	I026	k	1
87.19	40.83	30.52	4.13	1.82	1.72	1.72	I032	k	1
87.28	42.25	32.35	3.39	2.42	2.42	2.42	I029	k	1
87.601	43.808	30.05	4.96	0.32	0.31	0.31	URUM	m	1
87.89	50.24	26.3	-4.82	1.43	1.34	1.34	KURA	g	1
88.14	47.85	28.65	-1.74	1.04	1.04	1.04	JB44	g	1
88.15	39.03	30.62	3.62	1.82	1.82	1.82	Y033	k	1
88.153	39.03	26.92	4.22	2.35	2.38	2.38	ROQG	l	1
88.153	39.03	28.76	4.82	1.55	1.34	1.34	RUOQ	a	1
88.18	39.02	28.32	2.41	1.92	1.92	1.92	I034	k	1
88.25	40.27	30.55	2.18	1.82	1.92	1.92	I033	k	1
88.265	39.446	25.42	5.01	2.79	1.89	1.89	LOBU	a	1
88.32	43.35	32.19	0.82	1.73	1.73	1.73	I025	k	1
88.42	50.07	27.28	-2.36	1.53	1.44	1.44	CHAG	g	1
88.593	37.563	40.21	-0.54	2.34	2.29	2.29	AL10	l	1
88.63	42.82	31.57	0.02	1.73	1.73	1.73	I027	k	1
88.849	39.027	26.3	3.63	2.44	2.47	2.47	POWR	l	1
88.899	39.241	25.59	3.11	2.32	1.81	1.81	MILA	a	1
89.141	38.849	24.81	1.57	2.48	1.82	1.82	KUMU	a	1
89.2	38.72	29.16	2.98	1.72	1.72	1.72	G172	k	1
89.282	38.614	23.69	-4.76	1.62	1.67	1.67	PAXI	l	1
89.905	38.409	29.6	3.89	2.78	1.88	1.88	KLSA	a	1
89.926	38.409	31.97	3.16	1.7	1.75	1.75	SCAN	l	1
89.932	38.404	32.47	3.66	2.44	2.01	2.01	SCAS	l	1
89.94	48.98	28.69	-1.57	1.14	1.04	1.04	ULGI	g	1
89.968	38.391	27.99	4.04	3	1.98	1.98	HAPI	a	1
90.085	38.391	31.17	5.96	1.94	1.6	1.6	TERR	a	1
90.25	42.9	32.26	0.97	1.73	1.73	1.73	I006	k	1
90.418	38.376	31.5	5.14	2.54	1.83	1.83	MULI	a	1
90.442	37.274	32.86	8.09	2.06	1.93	1.93	Y196	l	1
90.8	38.29	35.35	4.06	1.81	1.71	1.71	G171	k	1

Continued on next page...

Table B.1 – Continued from previous page

Long	Lat	Velocity (mm/yr)				Corr	Site	Source†	EXC‡
°E	°N	East	North	σ E	σ N				
90.907	38.285	30.08	3.36	2.31	1.76	1.76	HATU	a	1
90.98	38.59	33.51	2.53	1.13	1.04	1.04	JB32	g	1
91.083	38.764	30.74	1.07	2.25	2.29	2.29	AL03	l	1
91.47	43.48	32.27	-0.75	1.63	1.63	1.63	I003	k	1
91.59	53.67	26.19	-6.21	1.44	1.34	1.34	ABAK	g	1
91.62	47.96	30.45	-4.02	1.04	1.04	1.04	HOVA	g	1
91.63	47.76	29.17	-1.92	1.14	1.04	1.04	HOVD	g	1
91.821	37.887	32.78	4.9	3.4	1.92	1.92	MANG	a	1
92.08	49.97	27.58	-3.98	1.14	1.04	1.04	ULAA	g	1
92.439	28.432	44.41	10.73	2.14	1.86	1.86	LOZ1	m	1
92.794	55.993	24.9	-6.1	0.42	0.39	0.39	KSTU	m	1
92.794	55.993	21.72	-0.45	0.91	1.21	1.21	KSTU	a	1
93	39.29	32.02	-0.36	1.91	1.72	1.72	G165	k	1
93.339	29.9	48.04	3.26	0.99	0.83	0.83	GBD1	m	1
93.41	38.81	34.21	-1.66	1.13	1.04	1.04	JB31	g	1
93.49	39.64	29.99	-0.62	1.91	1.72	1.72	G163	k	1
93.5	37.9	35.15	1.9	1.81	1.71	1.71	G170	k	1
93.57	52.44	24.89	-5.93	1.43	1.34	1.34	ARAD	g	1
93.63	42.81	31.32	-2.39	1.03	1.04	1.04	JB43	g	1
94.32	39.95	31.48	-1.84	2.01	2.01	2.01	GA05	k	1
94.327	39.953	32.16	-2.46	0.84	0.78	0.78	DHS1	m	1
94.36	38.81	33.7	-0.78	2.11	1.91	1.91	G167	k	1
94.55	39.72	31.4	-1.06	1.91	1.82	1.82	G162	k	1
94.67	43.24	31.08	-2.58	1.63	1.63	1.63	I001	k	1
94.758	40.157	32.75	-0.94	3.02	1.67	1.67	DUNH	a	1
94.797	36.221	39.83	3.11	0.65	0.57	0.57	GLM1	m	1
94.81	40.17	30.88	-2.15	1.82	1.72	1.72	G161	k	1
94.857	39.514	29.9	-1.98	1.54	1.12	1.12	SUBE	a	1
94.86	39.51	31.37	-2.05	1.91	1.82	1.82	G164	k	1
94.87	36.43	34.23	1.97	1.13	1.04	1.04	JB30	g	1
94.874	36.433	35.24	1.69	0.79	0.73	0.73	GOLM	a	1
94.892	29.541	45.64	-2.77	0.98	0.83	0.83	PQX1	m	1
95	40.55	30.36	-2.12	1.72	1.72	1.72	G160	k	1
95	38.06	32.84	-1.07	1.91	1.81	1.81	G169	k	1
95.02	50.25	24.45	-7.29	1.43	1.33	1.33	ERZN	g	1
95.085	30.103	48.13	-0.66	1.88	1.66	1.66	TOM1	a	1
95.3	41.57	33.64	-0.54	1.92	1.92	1.92	AS20	k	1
95.32	39.33	33.73	-2.99	2.21	2.11	2.11	GA12	k	1
95.377	37.834	35.69	0.64	1.51	1.12	1.12	DACA	a	1
95.38	37.83	37.81	-0.78	1.51	1.51	1.51	Y345	k	1
95.396	37.618	36.45	0	0.93	0.83	0.83	DQD1	m	1

Continued on next page...

Table B.1 – Continued from previous page

Long	Lat	Velocity (mm/yr)				Corr	Site	Source†	EXC‡
°E	°N	East	North	σ E	σ N				
95.46	41.07	31.22	-3.48	1.72	1.72	1.72	G123	k	1
95.61	39.71	30.21	-1.89	1.82	1.82	1.82	G145	k	1
95.71	40.08	30.4	-2.93	1.82	1.82	1.82	G131	k	1
95.738	29.87	47.63	-5.92	1.25	0.92	0.92	ZMZ1	a	1
95.738	29.87	47.63	-5.92	1.25	0.92	0.92	ZMZ1	m	1
95.8	40.514	29.86	-3.87	1.36	1.15	1.15	ANXI	a	1
95.8	37.51	33.66	-1.11	1.81	1.81	1.81	G151	k	1
95.8	40.51	28.85	-4.15	1.03	1.04	1.04	JB28	g	1
95.87	49.62	26.85	-5.51	1.14	1.04	1.04	TES1	g	1
96.06	38.97	37.26	-4.51	2.31	2.21	2.21	GA13	k	1
96.094	29.745	42.18	-8.88	1.95	1.61	1.61	SOZ1	a	1
96.25	46.55	30.66	-6.07	1.13	1.04	1.04	ALTA	g	1
96.321	21.89	28.36	-4.12	2.2	0.91	0.91	ZIBI	f	1
96.7	37.36	33.89	0.52	1.81	1.81	1.81	G156	k	1
96.71	40.64	29.2	-4.95	1.82	1.72	1.72	G125	k	1
96.748	39.903	29.75	-4.52	2.26	1.42	1.42	CHMA	a	1
96.75	40.04	31	-3.75	1.82	1.82	1.82	G130	k	1
96.75	39.9	30.2	-3.55	1.82	1.82	1.82	G139	k	1
96.763	29.505	43.25	-10.75	0.88	0.81	0.81	RWZ1	m	1
96.78	47.61	30.19	-7.42	1.13	1.04	1.04	ULIA	g	1
96.82	37.6	33.58	-1.02	2.41	2.31	2.31	GA20	k	1
96.83	-12.19	46.94	46.17	1.53	1.46	1.46	COCO	g	1
96.834	-12.188	40.63	51.09	0.52	0.35	0.35	COCO	a	1
96.89	41.13	31.18	-4.22	2.02	2.02	2.02	GA01	k	1
97.012	40.285	30.98	-3.19	2.03	1.35	1.35	YUME	a	1
97.05	41.85	30.16	-4.69	1.62	1.63	1.63	G122	k	1
97.08	40.29	30.17	-4.96	1.82	1.82	1.82	G128	k	1
97.27	33.9	45.75	-4.69	2.31	2.21	2.21	DS39	k	1
97.38	37.38	34.61	-1.94	1.03	1.04	1.04	DLHA	g	1
97.39	33.18	50.62	-6.02	1.71	1.71	1.71	Y224	k	1
97.44	40.03	29.83	-5.16	1.82	1.82	1.82	G129	k	1
97.68	40.27	29.91	-6.04	1.82	1.82	1.82	G127	k	1
97.7	39.57	31.01	-4.23	1.82	1.82	1.82	G138	k	1
97.729	37.377	35.08	-1.05	1.54	1.12	1.12	DELI	a	1
97.777	29.727	42.29	-12.91	1.26	1.14	1.14	ZUG1	m	1
97.81	37.35	34.98	-1.21	2.31	2.21	2.21	GA24	k	1
97.92	39.85	30.58	-5.1	1.82	1.82	1.82	G137	k	1
97.98	49.08	29.39	-7.16	1.13	1.04	1.04	BOL2	g	1
98	39.19	31.18	-5.21	1.81	1.82	1.82	G144	k	1
98.05	49.21	28.67	-8.69	1.04	1.04	1.04	BOL1	g	1
98.1	36.27	35.24	0.73	1.91	1.81	1.81	J002	k	1

Continued on next page...

Table B.1 – Continued from previous page

Long	Lat	Velocity (mm/yr)				Corr	Site	Source†	EXC‡
°E	°N	East	North	σ E	σ N				
98.153	33.02	50.32	-4.26	0.48	0.41	0.41	SEX1	m	1
98.167	36.431	38.24	0.38	0.7	0.59	0.59	XRH1	m	1
98.172	39.852	31.78	-5.67	0.74	0.62	0.62	HCY1	m	1
98.188	39.841	30.55	-6.3	1.28	1.18	1.18	G136	b	1
98.2	33.06	45.85	-4.65	2.21	2.21	2.21	DS40	k	1
98.21	34.89	43.71	-2.58	1.71	1.71	1.71	J005	k	1
98.268	34.868	44.65	-1.42	0.48	0.42	0.42	MDX1	m	1
98.27	38.97	32.85	-5.18	1.81	1.81	1.81	G147	k	1
98.34	37.31	35.33	-2.37	1.91	1.91	1.91	G154	k	1
98.46	36.94	36.02	-2.69	1.71	1.71	1.71	G159	k	1
98.46	36.44	36.31	-1.38	2.11	2.11	2.11	GA28	k	1
98.496	39.758	30.25	-4.52	1.05	0.93	0.93	JIUQ	a	1
98.5	39.71	29.82	-6.27	1.82	1.82	1.82	G135	k	1
98.595	29.691	43.15	-14.57	1.02	0.86	0.86	MKZ1	m	1
98.66	37.58	36.51	-3.67	1.91	1.81	1.81	G150	k	1
98.67	40.71	30.8	-6.75	2.02	2.02	2.02	GA03	k	1
98.78	38.81	33.2	-3.83	2.11	2.01	2.01	GA15	k	1
98.8	39.41	31.39	-6.05	2.41	2.41	2.41	G142	k	1
98.8	48.71	29.04	-8.78	1.13	1.04	1.04	IKUL	g	1
98.85	37.98	33.99	-4.93	1.91	1.81	1.81	G149	k	1
98.89	39.91	30.38	-6.99	1.82	1.72	1.72	G132	k	1
98.909	31.947	43.54	-5.56	2.16	1.98	1.98	QUER	a	1
98.93	36.77	36.67	-4.23	2.11	2.01	2.01	CJ06	k	1
98.98	50.18	27.53	-9.34	1.04	1.04	1.04	BZUR	g	1
99.01	37.3	36.37	-4.16	1.81	1.81	1.81	G153	k	1
99.07	36.8	36.06	-3.37	1.91	1.81	1.81	G158	k	1
99.075	40.275	31.73	-8.65	0.76	0.67	0.67	CSD4	m	1
99.075	40.275	29.85	-6.23	1.11	1.1	1.1	G041	b	1
99.193	31.938	46.66	-11.75	1.79	1.79	1.79	J009	c	1
99.32	37.34	34.64	-3.05	2.11	2.01	2.01	GA25	k	1
99.33	38.65	30.74	-4.29	1.81	1.81	1.81	GA18	k	1
99.49	37.13	36.02	-4.6	1.81	1.81	1.81	G152	k	1
99.56	38.44	32.32	-6.95	1.81	1.81	1.81	G148	k	1
99.565	38.445	34.39	-5.12	2.32	1.6	1.6	YIEN	a	1
99.6	39.7	30.61	-6.1	1.82	1.72	1.72	G133	k	1
99.61	39.15	31.01	-6.29	1.82	1.72	1.72	G143	k	1
99.62	38.83	31.61	-6.28	1.81	1.72	1.72	G146	k	1
99.642	33.767	44.73	-4.86	2.79	1.91	1.91	DAR1	m	1
99.661	33.96	42.87	-5.59	1.55	1.56	1.56	Y222	c	1
99.688	33.804	43.47	-6.6	1.82	1.83	1.83	J006	c	1
99.7	40.46	30.09	-5.45	1.82	1.72	1.72	GA02	k	1

Continued on next page...

Table B.1 – Continued from previous page

Long	Lat	Velocity (mm/yr)				Corr	Site	Source†	EXC‡
°E	°N	East	North	σ E	σ N				
99.796	22.728	27.62	-12.3	1.14	0.86	0.86	ZTN1	m	1
99.8	52.54	25.18	-6.79	1.04	1.05	1.05	ORLK	g	1
99.81	39.41	28.92	-7.52	1.03	1.04	1.04	JB29	g	1
99.814	39.41	32.55	-6.57	1.35	1.12	1.12	GAOT	a	1
99.9	36.69	35.98	-4.01	1.71	1.71	1.71	G157	k	1
99.94	31.626	48.13	-12.08	2.69	1.94	1.94	GAZ2	m	1
99.96	39.58	29.77	-6.5	1.72	1.72	1.72	GA08	k	1
99.97	35.62	37.06	-3.5	1.71	1.61	1.61	J003	k	1
100.006	31.618	45.09	-13.97	1.77	1.78	1.78	H182	c	1
100.021	31.614	47.75	-11.73	2.25	1.97	1.97	GPmZ	a	1
100.021	31.614	45.29	-13.07	1.49	1.59	1.59	Y267	c	1
100.06	35.92	36.75	-3.53	1.41	1.41	1.41	G0DT	k	1
100.09	49.66	27.37	-8.52	1.13	1.04	1.04	MURN	g	1
100.1	39	31.06	-7.43	1.82	1.72	1.72	GA16	k	1
100.11	37.43	35.26	-4.89	1.81	1.71	1.71	GA23	k	1
100.15	39.72	30.14	-7.46	1.72	1.72	1.72	G044	k	1
100.16	37.31	36.65	-5	1.81	1.71	1.71	G075	k	1
100.2	40.98	29.2	-7.44	1.03	1.04	1.04	DXIN	g	1
100.236	38.19	35.88	-7.36	1.96	1.34	1.34	QILI	a	1
100.24	38.18	32.14	-5.64	1.71	1.72	1.72	G062	k	1
100.241	31.32	45.56	-16.33	1.77	1.77	1.77	H057	c	1
100.27	36.62	36.64	-5.91	1.71	1.71	1.71	G090	k	1
100.28	37.8	33.44	-5.34	1.81	1.71	1.71	GA19	k	1
100.297	31.646	43.67	-13.05	1.77	1.77	1.77	H056	c	1
100.307	30.925	43.34	-18.24	1.76	1.76	1.76	H063	c	1
100.309	30.942	42.93	-15.32	3.03	2.57	2.57	XINL	a	1
100.309	30.942	44.54	-18.74	1.47	1.48	1.48	Y270	c	1
100.32	39.24	29.33	-8.7	1.72	1.72	1.72	G048	k	1
100.334	32.275	42.38	-8.36	1.78	1.69	1.69	H042	c	1
100.35	38.61	31.13	-6.49	1.72	1.72	1.72	G054	k	1
100.36	36.61	36.33	-5.64	2.51	2.51	2.51	CS21	k	1
100.43	37.61	36.22	-5.78	1.71	1.71	1.71	G071	k	1
100.448	38.927	32.09	-8.62	2.26	1.59	1.59	ZHAN	a	1
100.45	38.93	28.22	-8.43	2.41	2.41	2.41	GC18	k	1
100.48	37.22	36.12	-6.39	1.71	1.71	1.71	G076	k	1
100.482	37.217	37.52	-5.46	2.87	1.74	1.74	HAER	a	1
100.508	33.367	42.19	-5.92	1.52	1.52	1.52	Y225	c	1
100.55	36.22	36.91	-4.38	1.71	1.71	1.71	G097	k	1
100.56	37.72	34.81	-6.62	1.81	1.81	1.81	GA21	k	1
100.595	33.093	39.68	-6.64	1.79	1.7	1.7	H029	c	1
100.728	31.862	38.44	-10.97	1.67	1.68	1.68	H039	c	1

Continued on next page...

Table B.1 – Continued from previous page

Long	Lat	Velocity (mm/yr)				Corr	Site	Source†	EXC‡
°E	°N	East	North	σ E	σ N				
100.73	38.88	29.59	-7.7	1.72	1.72	1.72	G051	k	1
100.75	31.297	40.62	-15.47	1.66	1.67	1.67	H054	c	1
100.75	31.297	42.15	-13.57	1.04	0.91	0.91	XIAL	a	1
100.75	31.297	40.32	-16.77	1.47	1.48	1.48	Y268	c	1
100.79	39.61	29.67	-7.74	1.72	1.62	1.62	G045	k	1
100.79	44.47	30.28	-9.14	1.13	1.04	1.04	KHAR	g	1
100.83	38.35	30.48	-6.12	1.72	1.72	1.72	G059	k	1
100.83	38.41	29.18	-4.52	1.81	1.72	1.72	GC14	k	1
100.83	38.415	34.43	-6.4	2.31	1.45	1.45	MINL	a	1
100.92	51.62	25.99	-9.66	1.04	1.04	1.04	MOND	g	1
100.929	31.143	42	-16.52	1.76	1.76	1.76	H062	c	1
100.93	37.961	37.49	-7.23	2.89	1.71	1.71	ERBO	a	1
100.94	37.97	32.27	-7.74	1.71	1.62	1.62	G065	k	1
100.96	36.4	36.66	-4.7	1.71	1.71	1.71	G094	k	1
101.01	36.88	36.46	-6.23	1.61	1.61	1.61	G082	k	1
101.06	41.96	31.3	-8.2	1.63	1.63	1.63	G040	k	1
101.06	39.5	30.04	-7.32	1.72	1.72	1.72	GA09	k	1
101.07	32.319	40.22	-8.96	1.77	1.68	1.68	H041	c	1
101.11	36.45	36.05	-4.55	1.71	1.71	1.71	G100	k	1
101.139	30.991	38.98	-15.17	1.46	1.47	1.47	Y269	c	1
101.14	38.93	29.64	-7.42	1.72	1.72	1.72	G141	k	1
101.152	38.936	33.4	-8.4	1.78	1.33	1.33	HONG	a	1
101.163	30.955	38.47	-15.38	1.75	1.76	1.76	H053	c	1
101.2	38.72	30.13	-8.94	1.72	1.62	1.62	G052	k	1
101.24	36.7	35.94	-5.29	1.61	1.61	1.61	G084	k	1
101.31	43.09	29.74	-8.76	1.13	1.03	1.03	UNDU	g	1
101.35	38.16	32.62	-7.26	1.72	1.62	1.62	G055	k	1
101.4	37.46	35.92	-6.96	1.62	1.62	1.62	G070	k	1
101.425	37.479	37.42	-7.27	1.89	1.37	1.37	QING	a	1
101.44	36.08	37.11	-7.33	2.41	2.41	2.41	G103	k	1
101.44	45.67	28.09	-10.92	1.13	1.04	1.04	TEEG	g	1
101.47	35.04	38.1	-1.81	2.21	2.21	2.21	DS04	k	1
101.482	33.429	39.61	-7.29	1.69	1.7	1.7	H027	c	1
101.486	30.075	42.1	-22.47	1.44	1.28	1.28	H067	b	1
101.5	30.5	40.39	-19.26	1.14	1.05	1.05	JB35	g	1
101.5	30.51	41.79	-12.28	2.8	2.49	2.49	QIAN	a	1
101.5	30.51	39.73	-16.04	2.07	1.88	1.88	Y271	c	1
101.51	30.04	41.01	-21	2	1.63	1.63	XDQ1	m	1
101.524	30.326	39.92	-21.87	1.74	1.75	1.75	H079	c	1
101.525	30.545	39.54	-12.14	2.2	1.67	1.67	XIC1	m	1
101.54	36.49	36.4	-6.17	1.61	1.61	1.61	G089	k	1

Continued on next page...

Table B.1 – Continued from previous page

Long	Lat	Velocity (mm/yr)				Corr	Site	Source†	EXC‡
°E	°N	East	North	σ E	σ N				
101.61	50.1	26.93	-7.22	1.04	1.04	1.04	ERBL	g	1
101.613	34.716	37.62	-6.33	1.73	1.73	1.73	J001	c	1
101.615	31.77	37.16	-11.61	1.76	1.67	1.67	H040	c	1
101.63	36.98	37.19	-7.01	1.61	1.61	1.61	G080	k	1
101.654	36.66	36.31	-5.98	1.16	0.97	0.97	XINI	a	1
101.66	39.22	29.38	-8.78	1.72	1.62	1.62	G047	k	1
101.66	36.66	37.99	-4.91	1.71	1.71	1.71	GC05	k	1
101.706	32.902	39.68	-9.84	1.68	1.68	1.68	H028	c	1
101.74	38.3	31.88	-7.78	1.72	1.62	1.62	G058	k	1
101.77	36.6	37.01	-6.6	1.13	1.04	1.04	XNIN	g	1
101.788	30.074	37.89	-20.04	1.64	1.74	1.74	H066	c	1
101.8	47.52	30.04	-10.64	1.13	1.04	1.04	TSET	g	1
101.87	30.95	42.28	-12.54	1.71	1.71	1.71	H052	k	1
101.879	30.887	41.94	-7.88	2.59	1.73	1.73	DBA1	m	1
101.919	31.794	38.3	-9.87	2.24	1.78	1.78	KEY1	m	1
101.93	36.557	38.21	-5.27	0.5	0.45	0.45	XXK1	m	1
101.99	36.21	36.55	-6.19	1.61	1.61	1.61	G096	k	1
102.01	37.32	36.15	-6.52	1.62	1.62	1.62	G074	k	1
102.03	35.92	36.55	-5.59	1.61	1.61	1.61	G102	k	1
102.05	35.54	36.95	-6.09	1.61	1.61	1.61	G109	k	1
102.063	31.477	36.79	-12.71	1.5	1.51	1.51	Y279	c	1
102.076	31.449	38.79	-10.67	2.62	1.89	1.89	YJW1	m	1
102.08	29.688	37.15	-16.61	1.74	1.64	1.64	H078	c	1
102.096	31.466	36.46	-13.03	1.17	1.1	1.1	H047	b	1
102.1	38.39	31.83	-7.58	2.11	2.11	2.11	GC11	k	1
102.102	38.393	31.67	-7.23	2.39	1.56	1.56	HEXI	a	1
102.11	38.28	31.53	-7.98	1.72	1.62	1.62	G060	k	1
102.126	34	38.76	-7.97	1.7	1.71	1.71	H018	c	1
102.15	38.43	31.83	-7.5	1.72	1.72	1.72	G057	k	1
102.16	30.076	33.17	-12.93	1.98	0.93	0.93	SWS3	m	1
102.21	51.76	25.81	-9.99	1.04	1.04	1.04	BADA	g	1
102.26	38.14	31.42	-8.12	1.62	1.62	1.62	G061	k	1
102.26	36.12	36.02	-6.16	1.61	1.61	1.61	G098	k	1
102.29	29.848	34.34	-13.77	1.64	1.64	1.64	H073	c	1
102.31	31.71	35.26	-11.39	1.14	1.05	1.05	JB34	g	1
102.32	37.96	32.11	-7.13	1.62	1.62	1.62	G064	k	1
102.32	38.7	30.6	-7.95	1.62	1.62	1.62	G134	k	1
102.35	51.6	25.61	-9.42	1.04	1.04	1.04	HARA	g	1
102.37	34.17	35.8	-12.84	1.61	1.41	1.41	Y231	k	1
102.38	36.5	39.21	-7.9	1.61	1.61	1.61	G087	k	1
102.44	35.12	36.8	-6.78	1.61	1.61	1.61	G115	k	1

Continued on next page...

Table B.1 – Continued from previous page

Long	Lat	Velocity (mm/yr)				Corr	Site	Source†	EXC‡
°E	°N	East	North	σ E	σ N				
102.501	32.786	38.41	-9.36	1.67	1.68	1.68	H031	c	1
102.502	34.589	36.94	-6.47	1.71	1.72	1.72	H015	c	1
102.54	35.84	36.09	-6.53	1.61	1.61	1.61	G106	k	1
102.56	36.89	36.59	-7.16	1.61	1.62	1.62	G081	k	1
102.57	39.13	30.57	-8.64	1.72	1.62	1.62	G049	k	1
102.62	37.51	34.68	-7	1.62	1.62	1.62	G066	k	1
102.644	37.781	34.35	-8.06	0.66	0.6	0.6	MZZ1	m	1
102.645	37.781	33.77	-8.93	1.18	1.19	1.19	G063	b	1
102.652	37.886	32.91	-8.24	1.63	1.23	1.23	WUWE	a	1
102.66	51.77	24.25	-9.3	1.43	1.33	1.33	AKHL	g	1
102.67	31.85	34.38	-13.59	1.66	1.66	1.66	H046	c	1
102.744	30.703	37.24	-12.38	3.48	1.05	1.05	RJJ2	m	1
102.775	30.992	33.54	-12.01	1.65	1.65	1.65	H051	c	1
102.78	39.41	30.24	-9.01	1.62	1.62	1.62	G046	k	1
102.79	46.26	29.47	-10.07	1.52	1.33	1.33	ARVA	g	1
102.79	35.88	36.07	-7.5	1.61	1.61	1.61	G105	k	1
102.81	35.26	35.96	-7.29	1.61	1.61	1.61	G113	k	1
102.81	49.45	26.17	-8.61	1.04	1.04	1.04	NSEL	g	1
102.817	29.789	33.79	-13.31	1.64	1.64	1.64	H072	c	1
102.841	30.253	34.41	-13.62	1.64	1.64	1.64	H061	c	1
102.845	37.438	35.76	-8.8	1.89	1.39	1.39	GULA	a	1
102.85	37.44	33.35	-8.16	1.62	1.62	1.62	G069	k	1
102.89	38.42	31.84	-9	1.62	1.62	1.62	G056	k	1
102.89	36.33	36.75	-7.54	1.61	1.61	1.61	G093	k	1
102.89	34.95	37.45	-7.8	1.61	1.61	1.61	G118	k	1
102.96	49.29	27.07	-9.15	1.13	1.04	1.04	SSEL	g	1
102.98	37.15	35.84	-7.59	1.72	1.62	1.62	G073	k	1
102.991	33.571	39.18	-9.8	1.68	1.69	1.69	H026	c	1
103	51.92	24.48	-10.49	1.14	1.14	1.14	TORY	g	1
103.002	29.975	34.99	-12.46	1.64	1.64	1.64	H065	c	1
103.002	29.975	33.49	-12.26	1.44	1.45	1.45	Y283	c	1
103.003	29.975	38.83	-6.8	2.76	2.2	2.2	YAAN	a	1
103.02	46.12	31.36	-8.83	1.42	1.13	1.13	ARVX	g	1
103.08	51.81	26.29	-11.61	1.14	1.14	1.14	TOR1	g	1
103.11	38.65	28.61	-9.47	1.72	1.62	1.62	GC10	k	1
103.113	38.645	29.02	-9.89	2.59	1.51	1.51	MINQ	a	1
103.145	31.008	34.71	-13.21	1.64	1.65	1.65	H050	c	1
103.147	34.109	36.37	-9.84	1.69	1.7	1.7	H017	c	1
103.16	36.89	35.82	-8.13	1.62	1.62	1.62	G079	k	1
103.166	32.075	36.34	-12.13	1.66	1.66	1.66	H037	c	1
103.17	31.461	33.8	-12.06	1.55	1.37	1.37	ZGL2	m	1

Continued on next page...

Table B.1 – Continued from previous page

Long	Lat	Velocity (mm/yr)				Corr	Site	Source†	EXC‡
°E	°N	East	North	σ E	σ N				
103.19	38.54	30.8	-9.49	1.72	1.62	1.62	G053	k	1
103.21	35.57	35.52	-8.5	1.61	1.61	1.61	G108	k	1
103.22	52.26	24.1	-10.25	1.04	1.04	1.04	HADR	g	1
103.247	34.749	37.27	-8.38	1.71	1.72	1.72	H013	c	1
103.25	36.71	36.01	-8.25	1.62	1.62	1.62	G083	k	1
103.261	29.228	34.83	-13.42	1.63	1.64	1.64	H081	c	1
103.33	35.93	36.01	-8.05	1.61	1.61	1.61	G101	k	1
103.34	35.41	36	-8.74	1.61	1.61	1.61	G112	k	1
103.36	38.85	30.97	-8.35	1.62	1.62	1.62	G050	k	1
103.38	37.56	32.19	-8.81	1.62	1.62	1.62	G068	k	1
103.41	30.415	32.17	-12.07	1.64	1.64	1.64	H060	c	1
103.42	36.15	36.49	-8.78	1.61	1.61	1.61	G095	k	1
103.435	32.931	36.43	-10.31	1.67	1.67	1.67	H025	c	1
103.44	37.15	35.09	-7.91	1.62	1.62	1.62	G091	k	1
103.468	29.602	33.33	-12.88	1.63	1.64	1.64	H076	c	1
103.472	36.173	39.25	-8.04	0.86	0.79	0.79	HSC3	m	1
103.48	32.883	33.24	-12.17	2.01	1.76	1.76	SBP2	m	1
103.486	31.14	32.53	-12.03	1.4	1.13	1.13	SWP3	m	1
103.52	48.8	27.07	-9.28	1.04	1.04	1.04	BULG	g	1
103.612	31.474	34.98	-12.84	1.65	1.65	1.65	H045	c	1
103.613	32.591	34.91	-11.85	1.66	1.67	1.67	H030	c	1
103.64	51.68	25.23	-10.54	1.33	1.43	1.43	TALY	g	1
103.66	37.23	32.56	-7.58	1.72	1.72	1.72	GA26	k	1
103.692	31.06	34.16	-13.86	1.64	1.65	1.65	H049	c	1
103.7	51.65	25.83	-9.86	1.04	1.04	1.04	SLYU	g	1
103.71	35.29	35.66	-8.63	1.61	1.61	1.61	G117	k	1
103.725	32.396	34.59	-13.27	3.05	1.35	1.35	MJZ1	m	1
103.727	33.937	36.12	-9.7	1.69	1.69	1.69	H020	c	1
103.732	32.361	34.21	-13.65	1.17	1.1	1.1	H034	b	1
103.74	51.77	25.61	-9.67	1.04	1.04	1.04	KULT	g	1
103.84	35.38	34.75	-9.57	1.61	1.61	1.61	G111	k	1
103.845	30.041	30.92	-11.58	1.64	1.64	1.64	H064	c	1
103.865	30.692	33.44	-12.6	1.64	1.64	1.64	H059	c	1
103.89	33.28	37.94	-7.72	1.14	1.04	1.04	JB33	g	1
103.99	36.49	36.43	-9.04	1.62	1.62	1.62	G092	k	1
103.99	36	34.93	-11.33	2.41	2.41	2.41	G099	k	1
104.073	34.403	35.59	-11.39	1.7	1.7	1.7	H014	c	1
104.073	29.652	34.38	-12.74	1.63	1.64	1.64	H070	c	1
104.074	30.687	33.81	-11.53	0.48	0.35	0.35	CHDU	m	1
104.077	30.732	32.89	-10.83	1.45	1.19	1.19	H058	b	1
104.09	37.24	32.61	-9.6	1.62	1.62	1.62	G072	k	1

Continued on next page...

Table B.1 – Continued from previous page

Long	Lat	Velocity (mm/yr)				Corr	Site	Source†	EXC‡
°E	°N	East	North	σ E	σ N				
104.1	35.04	35.32	-9.43	1.61	1.61	1.61	G114	k	1
104.13	36.85	36.61	-10.39	1.62	1.62	1.62	G078	k	1
104.16	35.88	35.61	-9.17	1.61	1.61	1.61	G104	k	1
104.187	31.353	34.03	-13.09	1.65	1.65	1.65	H044	c	1
104.23	33.23	39.19	-13.71	1.61	1.61	1.61	H024	k	1
104.316	52.219	24.82	-9.39	0.15	0.14	0.14	IRKJ	m	1
104.316	52.219	24.82	-9.39	0.15	0.14	0.14	IRKT	m	1
104.33	37.45	31.68	-9.67	1.62	1.62	1.62	G067	k	1
104.355	36.603	34.28	-10.44	2.44	1.62	1.62	BAIY	a	1
104.36	36.66	36.68	-10.65	1.62	1.62	1.62	G086	k	1
104.36	36.6	33.98	-8.45	2.51	2.51	2.51	GC02	k	1
104.384	34.046	35.06	-10.87	1.69	1.69	1.69	H016	c	1
104.401	33.787	34.95	-11.97	1.68	1.69	1.69	H019	c	1
104.43	43.59	32.14	-9.36	1.13	1.03	1.03	DALA	g	1
104.441	31.157	35.2	-13.65	1.64	1.65	1.65	H048	c	1
104.444	31.802	33.92	-12.96	1.65	1.65	1.65	H035	c	1
104.48	34.85	39.9	-6.76	1.18	1.1	1.1	G119	b	1
104.497	32.465	31.24	-14.63	2.03	1.58	1.58	ZHM2	m	1
104.51	40.74	29.98	-9.94	1.63	1.63	1.63	G042	k	1
104.536	30.374	32.67	-12.57	1.64	1.64	1.64	H071	c	1
104.54	35.05	35.37	-10.55	1.61	1.61	1.61	G116	k	1
104.55	35.54	34.17	-11.36	1.61	1.61	1.61	G107	k	1
104.559	31.365	31.71	-10.9	1.48	1.31	1.31	JSP2	m	1
104.571	32.405	34.32	-12.3	1.66	1.66	1.66	H032	c	1
104.625	33.001	34.22	-13.02	1.67	1.67	1.67	H022	c	1
104.63	36.91	34.05	-10.83	1.62	1.62	1.62	G077	k	1
104.65	33.621	34.53	-12.24	1.49	1.49	1.49	Y232	c	1
104.66	28.857	33.34	-11.77	2.84	0.89	0.89	SLW2	m	1
104.74	36.43	36.54	-10.94	1.62	1.62	1.62	G085	k	1
104.782	31.486	33.38	-12.45	1.65	1.65	1.65	H043	c	1
104.81	40.16	30.15	-10	1.63	1.63	1.63	G043	k	1
104.824	33.423	35.01	-12.08	1.67	1.68	1.68	H021	c	1
104.832	32.182	33.59	-13.47	1.65	1.66	1.66	H033	c	1
104.89	51.85	24.24	-9.55	1.04	1.04	1.04	LIST	g	1
104.92	34.47	34.42	-11.73	1.61	1.61	1.61	G121	k	1
104.94	34.71	34.92	-11.94	1.61	1.61	1.61	G120	k	1
104.97	36.09	35.11	-11.49	1.62	1.62	1.62	G019	k	1
105.01	35.73	34.01	-10.49	1.62	1.62	1.62	G021	k	1
105.02	35.41	34.21	-13.08	1.62	1.62	1.62	G026	k	1
105.13	38.05	30.26	-10.7	1.62	1.62	1.62	G001	k	1
105.18	37.58	29.97	-9.6	1.62	1.62	1.62	G004	k	1

Continued on next page...

Table B.1 – Continued from previous page

Long	Lat	Velocity (mm/yr)				Corr	Site	Source†	EXC‡
°E	°N	East	North	σ E	σ N				
105.22	37.24	30.77	-10.5	1.62	1.62	1.62	G006	k	1
105.226	32.571	32.86	-12.48	1.66	1.66	1.66	H010	c	1
105.25	36.66	33.77	-11.49	1.62	1.62	1.62	G011	k	1
105.27	36.93	31.57	-10.8	1.62	1.62	1.62	G008	k	1
105.285	33.781	33.37	-11.81	1.68	1.68	1.68	H006	c	1
105.29	36.5	35.77	-11.39	1.62	1.62	1.62	G014	k	1
105.306	32.607	35.78	-12.92	2.41	1.96	1.96	CGP2	m	1
105.306	34.108	33.47	-12.32	1.68	1.69	1.69	H003	c	1
105.31	36.66	35.66	-11.8	1.62	1.62	1.62	GC31	k	1
105.313	36.657	33.03	-9.78	2.71	1.82	1.82	GPmY	a	1
105.37	34.79	33.17	-12.86	1.61	1.61	1.61	G035	k	1
105.38	39.07	29.71	-10.81	1.63	1.63	1.63	GC29	k	1
105.38	35.14	33.38	-11.82	1.04	1.04	1.04	JB27	g	1
105.383	39.07	29.27	-6.5	2.57	1.58	1.58	XILI	a	1
105.41	28.87	33.4	-13.17	1.15	1.05	1.05	LUZH	g	1
105.457	32.018	34.15	-12.86	1.35	1.19	1.19	H012	b	1
105.463	32.016	28.07	-13.95	1.67	1.38	1.38	TJP2	m	1
105.5	53.06	22.55	-8.91	1.04	1.05	1.05	BAYA	g	1
105.5	35.61	33.35	-12.62	1.62	1.62	1.62	G023	k	1
105.55	37.52	30.42	-10.4	1.62	1.62	1.62	G003	k	1
105.595	33.697	33.33	-13.49	1.68	1.68	1.68	H005	c	1
105.62	36.51	33.83	-11.48	1.62	1.62	1.62	G012	k	1
105.62	36.28	34.23	-12.97	1.62	1.62	1.62	G015	k	1
105.63	33.4	33.74	-17.68	1.61	1.61	1.61	H008	k	1
105.66	34.87	33.04	-13.83	1.62	1.62	1.62	G033	k	1
105.67	37.36	30.21	-11.12	1.62	1.62	1.62	G005	k	1
105.67	38.81	30.33	-10.72	1.03	1.04	1.04	JB09	g	1
105.7	38.44	30.68	-10.77	1.63	1.63	1.63	D095	k	1
105.7	34.59	33.43	-12.54	1.61	1.61	1.61	G037	k	1
105.76	39.75	30.54	-10.74	1.63	1.63	1.63	D085	k	1
105.79	35.08	32.82	-12.87	1.62	1.62	1.62	G030	k	1
105.8	35.96	33.71	-14.81	1.62	1.62	1.62	G018	k	1
105.81	34.25	32.52	-14.95	1.61	1.61	1.61	G039	k	1
105.814	33.891	33.81	-13.35	1.68	1.69	1.69	H002	c	1
105.83	32.448	33.1	-13.43	1.66	1.66	1.66	H011	c	1
105.88	36.97	31.59	-10.36	1.62	1.62	1.62	G007	k	1
105.89	37.54	29.87	-10.39	1.62	1.62	1.62	G002	k	1
105.92	37.89	29.16	-9.81	2.42	2.42	2.42	D097	k	1
105.99	36.28	33.48	-11.37	1.62	1.62	1.62	G013	k	1
105.997	38.385	30.68	-7.1	2.06	1.51	1.51	YING	a	1
106	38.39	29.84	-10.75	1.63	1.63	1.63	GC30	k	1

Continued on next page...

Table B.1 – Continued from previous page

Long	Lat	Velocity (mm/yr)				Corr	Site	Source†	EXC‡
°E	°N	East	North	σ E	σ N				
106.01	35.17	33.59	-12.93	1.62	1.62	1.62	G028	k	1
106.02	51.17	26.69	-11.52	1.04	0.95	0.95	UDUN	g	1
106.023	32.962	34.18	-13.29	1.66	1.67	1.67	H009	c	1
106.03	30.8	32.81	-12.75	1.14	1.05	1.05	JB24	g	1
106.09	30.798	37.67	-13.69	2.46	2.11	2.11	NACH	a	1
106.1	36.63	31.56	-11.51	1.62	1.62	1.62	G010	k	1
106.12	39.03	30.11	-10.41	1.63	1.63	1.63	D088	k	1
106.12	35.6	31.07	-14.98	1.62	1.62	1.62	G022	k	1
106.155	33.34	33.68	-13.53	1.67	1.67	1.67	H007	c	1
106.16	34.75	34.18	-13.56	1.62	1.62	1.62	G034	k	1
106.2	38.74	30.9	-10.52	1.63	1.63	1.63	D091	k	1
106.2	35.67	32.26	-13.4	1.62	1.62	1.62	G020	k	1
106.21	38.48	30.81	-13.81	1.63	1.63	1.63	D094	k	1
106.21	35.01	33.97	-15.08	1.62	1.62	1.62	G031	k	1
106.22	36.02	32.46	-13.72	1.62	1.62	1.62	G017	k	1
106.22	45.8	28.9	-10.72	1.13	1.04	1.04	MAND	g	1
106.25	50.23	26.21	-12.07	1.04	1.04	1.04	SUKG	g	1
106.35	39.2	29.87	-10.98	1.63	1.63	1.63	D087	k	1
106.35	37.81	30.41	-11.82	1.63	1.63	1.63	D096	k	1
106.36	36.84	31.53	-12.68	1.62	1.62	1.62	G009	k	1
106.4	35.46	32.24	-13.35	1.62	1.62	1.62	G025	k	1
106.4	34.52	32.05	-13.31	1.62	1.62	1.62	G036	k	1
106.48	39.07	29.96	-12.31	1.63	1.63	1.63	D089	k	1
106.49	50.74	26.8	-11.23	1.04	0.95	0.95	KIAT	g	1
106.509	33.915	32.34	-12.33	1.68	1.68	1.68	H001	c	1
106.53	35.24	31.43	-13.37	1.62	1.62	1.62	G027	k	1
106.56	38.55	30.56	-12.4	1.63	1.63	1.63	D093	k	1
106.58	52.79	23.55	-9.27	1.14	1.04	1.04	ANGA	g	1
106.58	35.46	32.92	-13.89	1.62	1.62	1.62	G024	k	1
106.65	36.1	31.1	-13.73	1.62	1.62	1.62	G016	k	1
106.68	37.45	30.27	-12.99	1.62	1.63	1.63	D098	k	1
106.68	34.95	31.81	-13.8	1.62	1.62	1.62	G110	k	1
106.68	33.12	32.67	-12.33	1.14	1.04	1.04	JB23	g	1
106.69	38.79	30.24	-12.85	1.63	1.63	1.63	D090	k	1
106.72	39.49	30.51	-12.09	1.63	1.63	1.63	D086	k	1
106.75	39.92	29.49	-12.71	1.63	1.64	1.64	D083	k	1
106.81	39.68	29.79	-11.82	1.63	1.63	1.63	D084	k	1
106.82	34.89	32.69	-13.03	1.62	1.62	1.62	G032	k	1
106.867	33.678	34.29	-12.32	0.99	0.82	0.82	TYP1	m	1
106.867	33.678	34.29	-12.32	0.99	0.82	0.82	TYP2	m	1
106.9	47.92	29.35	-11.8	1.23	1.13	1.13	UB01	g	1

Continued on next page...

Table B.1 – Continued from previous page

Long	Lat	Velocity (mm/yr)				Corr	Site	Source†	EXC‡
°E	°N	East	North	σ E	σ N				
106.924	33.617	32.3	-14.23	1.67	1.68	1.68	H004	c	1
106.98	41.43	28.79	-12.15	1.64	1.64	1.64	D042	k	1
107	40.32	29.14	-12.6	1.64	1.64	1.64	D053	k	1
107.05	47.87	28.38	-11.86	1.02	1.02	1.02	ULA1	g	1
107.05	40.26	29.63	-13.51	1.93	1.93	1.93	X001	k	1
107.052	47.865	28.05	-11.27	1.34	0.95	0.95	ULAB	m	1
107.053	40.264	29.57	-9.02	1.35	1.12	1.12	DENG	a	1
107.14	34.43	32.36	-13.5	1.62	1.62	1.62	G038	k	1
107.15	40.9	29.59	-12.67	1.64	1.64	1.64	D047	k	1
107.19	36.77	31.22	-12.4	1.92	1.92	1.92	D062	k	1
107.23	38.48	30.97	-12.68	1.63	1.63	1.63	D059	k	1
107.29	34.09	33.04	-13.62	1.62	1.62	1.62	D082	k	1
107.38	34.47	32.73	-13.96	1.62	1.62	1.62	D074	k	1
107.39	35.29	31.82	-12.69	1.62	1.62	1.62	D065	k	1
107.41	40.76	28.76	-14.53	2.03	2.03	2.03	D051	k	1
107.44	37.78	30.36	-12.8	1.53	1.53	1.53	YANC	k	1
107.58	34.43	31.5	-13.61	1.62	1.62	1.62	D073	k	1
107.62	51.81	26.66	-13.2	1.04	1.04	1.04	ULAN	g	1
107.62	51.81	24.76	-11.3	1.14	1.04	1.04	ULAZ	g	1
107.64	34.07	32.5	-14.31	1.62	1.62	1.62	D081	k	1
107.74	53.33	23.48	-8.75	1.14	1.14	1.14	UZUR	g	1
107.89	41.09	28.87	-12.37	1.65	1.65	1.65	D046	k	1
107.95	40.79	28.48	-13.27	1.64	1.64	1.64	D050	k	1
107.982	33.529	33.49	-13.7	1.67	1.68	1.68	F053	c	1
108	39.09	29.24	-12.8	1.64	1.64	1.64	D057	k	1
108.015	39.258	30.08	-9.67	1.25	1.08	1.08	ERTU	a	1
108.02	39.26	29.43	-14.02	1.93	1.83	1.83	X002	k	1
108.09	35.06	32.4	-13.89	1.13	1.04	1.04	JB08	g	1
108.16	34.11	31.73	-12.84	1.62	1.62	1.62	D080	k	1
108.19	34.3	31.53	-13.95	1.62	1.62	1.62	D077	k	1
108.23	34.5	32.62	-13.77	1.62	1.62	1.62	D072	k	1
108.24	52.97	25.27	-11.26	1.04	1.04	1.04	TURK	g	1
108.26	41.1	28.11	-12.47	1.65	1.65	1.65	D045	k	1
108.4	41.03	29.15	-9.13	1.67	1.54	1.54	HB03	a	1
108.51	41.57	29.35	-10.96	1.75	1.65	1.65	D041	k	1
108.518	41.511	28.61	-11.99	1.78	1.59	1.59	GI02	a	1
108.64	40.86	28.17	-12.85	1.65	1.65	1.65	D049	k	1
108.72	39.85	28.9	-13.12	1.74	1.64	1.64	D055	k	1
108.91	34.55	31.03	-13.74	1.62	1.62	1.62	D071	k	1
108.91	34.05	32.34	-11.72	1.62	1.62	1.62	D079	k	1
108.99	34.18	27.92	-9.75	1.33	1.33	1.33	XIAA	k	1

Continued on next page...

Table B.1 – Continued from previous page

Long	Lat	Velocity (mm/yr)				Corr	Site	Source†	EXC‡
°E	°N	East	North	σ E	σ N				
109	34.97	31.41	-14.38	1.63	1.63	1.63	D066	k	1
109.049	32.694	32.17	-13.06	1.66	1.67	1.67	F055	c	1
109.106	33.658	32.77	-13.79	1.68	1.68	1.68	F054	c	1
109.14	41.02	25.68	-10.89	1.75	1.65	1.65	D044	k	1
109.15	52.12	27.69	-11.86	1.24	1.14	1.14	HORN	g	1
109.221	34.369	32.63	-14.63	0.51	0.47	0.47	XIAN	m	1
109.221	34.369	30.53	-13.75	1.51	0.53	0.53	XIAN	a	1
109.43	36.65	31.01	-13.65	1.63	1.63	1.63	D061	k	1
109.48	40.64	28.64	-12.96	1.65	1.65	1.65	D048	k	1
109.527	38.302	31.97	-12.87	1.7	1.55	1.55	GI71	a	1
109.63	34.99	31.02	-12.53	1.63	1.63	1.63	D068	k	1
109.71	34.46	32.02	-14.23	1.63	1.63	1.63	D070	k	1
109.8	41.22	28.16	-12.27	1.66	1.66	1.66	D043	k	1
109.8	39.35	29.05	-12.87	1.65	1.65	1.65	D056	k	1
109.82	38.29	29.7	-13.53	1.64	1.64	1.64	D058	k	1
109.82	35.59	31.28	-14.1	1.63	1.63	1.63	D064	k	1
109.923	33.88	31.77	-13.1	1.68	1.69	1.69	D078	c	1
109.94	40.3	28.89	-13.06	1.65	1.65	1.65	D052	k	1
109.95	34.81	30.88	-14.5	1.63	1.63	1.63	D069	k	1
109.966	41.755	27.08	-8.81	1.72	1.55	1.55	HB04	a	1
109.97	41.77	27.8	-13.04	1.66	1.66	1.66	D040	k	1
109.97	34.35	31.49	-14.09	1.63	1.63	1.63	D075	k	1
109.98	40.6	27.47	-13.28	1.65	1.65	1.65	D007	k	1
110.01	39.82	28.5	-13.25	1.65	1.65	1.65	D054	k	1
110.034	40.656	30.14	-8.6	1.67	1.53	1.53	HB06	a	1
110.21	-7.63	29.33	-9.01	1.56	1.32	1.32	BUTU	g	1
110.377	-7.722	32.74	-11.48	1.21	2.21	2.21	JOGY	a	1
110.52	-66.283	0.98	-10.2	0.6	0.61	0.61	CAS1	m	1
110.59	47.26	26.42	-11.96	1.23	1.04	1.04	UNDE	g	1
110.85	48.52	25.31	-15.03	1.23	1.13	1.13	BATS	g	1
111.03	38.49	30.22	-13.51	1.13	1.04	1.04	JB07	g	1
111.446	40.754	30.19	-10.21	1.67	1.53	1.53	HB07	a	1
111.709	41.515	29.11	-8.75	1.6	1.51	1.51	HB08	a	1
111.71	41.52	28.51	-11.78	1.03	1.04	1.04	JB18	g	1
112.662	37.715	30.71	-14.52	1.67	1.5	1.5	GI72	a	1
112.664	-7.118	31.9	-14.83	2	2.11	2.11	SURA	a	1
113.032	39.509	30.47	-10.67	1.73	1.56	1.56	HB10	a	1
113.178	41.101	27.1	-13.53	1.67	1.54	1.54	HB11	a	1
113.252	38.706	28.15	-11.49	1.65	1.51	1.51	HB12	a	1
113.315	40.224	29.39	-12.2	1.58	1.48	1.48	HB13	a	1
113.32	38.74	29.92	-14.63	1.03	1.04	1.04	JB01	g	1

Continued on next page...

Table B.1 – Continued from previous page

Long	Lat	Velocity (mm/yr)				Corr	Site	Source†	EXC‡
°E	°N	East	North	σ E	σ N				
113.373	37.082	33.24	-14.86	1.68	1.5	1.5	GI74	a	1
113.416	40.645	28.36	-9.51	1.66	1.53	1.53	HB14	a	1
113.657	39.055	29.01	-14.16	1.65	1.51	1.51	HB15	a	1
113.772	39.772	30.18	-14.51	1.69	1.54	1.54	HB16	a	1
113.989	41.104	28.73	-10.67	1.73	1.57	1.57	HB17	a	1
114.18	38.842	30.51	-12.42	1.61	1.49	1.49	HB18	a	1
114.227	39.425	30.16	-11.69	1.69	1.54	1.54	HB19	a	1
114.295	40.424	30.49	-11.05	1.74	1.57	1.57	HB20	a	1
114.352	38.037	32	-10.25	1.75	1.55	1.55	GI78	a	1
114.58	48.09	25.02	-14.44	1.13	1.04	1.04	CHOI	g	1
114.634	40.215	29.99	-11.38	1.64	1.51	1.51	HB21	a	1
114.68	-8.147	26.44	-9.91	0.39	0.28	0.28	BALI	i	1
114.728	39.907	28.46	-11.43	1.69	1.54	1.54	HB22	a	1
114.741	39.334	31.07	-12.97	1.72	1.55	1.55	HB23	a	1
114.751	40.873	27.78	-9.97	1.63	1.52	1.52	HB24	a	1
114.928	40.669	28.62	-10.63	1.75	1.58	1.58	HB25	a	1
115.055	38.902	31.58	-11.74	1.64	1.5	1.5	HB26	a	1
115.151	-8.76	32.83	-10.22	2.9	1.91	1.91	DENP	a	1
115.4	39.729	30.56	-16.02	1.67	1.53	1.53	HB27	a	1
115.467	40.352	28.04	-15.19	2.79	2.28	2.28	HB28	a	1
115.531	40.208	26.66	-11.94	1.78	1.59	1.59	HB29	a	1
115.617	39.473	29.31	-15.27	1.33	1.18	1.18	HB30	a	1
115.682	40.365	26.67	-13.22	1.74	1.57	1.57	HB31	a	1
115.817	39.651	28.57	-12.93	1.72	1.55	1.55	HB32	a	1
115.846	40.87	27.04	-11.84	1.57	1.44	1.44	HB34	a	1
115.871	38.599	32.01	-16.1	1.66	1.51	1.51	HB35	a	1
115.892	39.609	29.7	-13.91	0.31	0.3	0.3	BJFS	m	1
115.938	39.047	31.23	-10.03	1.68	1.52	1.52	HB36	a	1
115.945	40.473	26.02	-11.45	1.74	1.57	1.57	HB37	a	1
115.965	39.452	32.22	-13.91	1.7	1.53	1.53	HB38	a	1
116.041	39.785	28.97	-11.93	1.35	1.19	1.19	HB40	a	1
116.1	43.9	28.56	-15.45	1.03	1.04	1.04	JB17	g	1
116.118	39.604	26.63	-12.53	1.98	1.6	1.6	HB41	a	1
116.161	39.862	28.1	-10.95	1.67	1.53	1.53	HB42	a	1
116.22	40.25	28.32	-13.07	1.03	1.04	1.04	BJSH	g	1
116.245	40.196	28.3	-12.52	1.37	1.18	1.18	HB43	a	1
116.482	39.138	33.14	-13.8	1.64	1.5	1.5	HB44	a	1
116.593	38.699	29.79	-8.71	1.65	1.5	1.5	HB45	a	1
116.623	40.73	28.64	-15.47	1.53	1.43	1.43	HB46	a	1
116.797	39.939	31.17	-9.38	1.67	1.52	1.52	HB49	a	1
116.944	40.438	27.68	-12.35	1.75	1.56	1.56	HB48	a	1

Continued on next page...

Table B.1 – Continued from previous page

Long	Lat	Velocity (mm/yr)				Corr	Site	Source†	EXC‡
°E	°N	East	North	σ E	σ N				
117.325	39.67	30.74	-14.22	1.36	1.18	1.18	HB52	a	1
117.53	40.08	27.46	-12.15	1.03	1.04	1.04	JIXN	g	1
117.562	40.472	26.91	-12.36	1.44	1.22	1.22	HB54	a	1
117.861	39.359	29.88	-15.97	1.79	1.58	1.58	HB57	a	1
117.914	40.961	25.88	-12.07	1.66	1.5	1.5	HB58	a	1
117.971	37.483	31.93	-12.62	1.76	1.54	1.54	HB59	a	1
118.247	40.19	26.98	-12.42	1.76	1.56	1.56	HB62	a	1
118.701	39.546	31.48	-15.91	1.6	1.48	1.48	HB66	a	1
118.915	40.417	27.5	-12.74	1.65	1.49	1.49	HB68	a	1
119.331	39.695	24.04	-11.31	1.91	1.61	1.61	HB69	a	1
119.382	-1.855	13.55	-5.85	2.02	1.62	1.62	LARA	i	1
119.46	-1.427	21.26	-9.69	0.83	0.59	0.59	BARA	i	1
119.47	39.83	26.81	-14.34	1.13	1.04	1.04	JB02	g	1
119.549	-5.026	31.27	-14.65	1.91	1.21	1.21	UJUN	a	1
119.58	-5.15	26.02	-7.5	1.41	1.23	1.23	UJPD	g	1
119.59	-0.87	19.9	-6.26	1.3	1.11	1.11	WATA	g	1
119.59	-0.87	19.9	-6.36	1.65	1.16	1.16	WATP	g	1
119.65	-3.98	25.03	-9.3	1.33	1.2	1.2	PARE	g	1
119.74	49.27	24.99	-13.99	1.04	1.04	1.04	HLAR	g	1
119.774	40.754	28.51	-15.02	1.72	1.53	1.53	HB71	a	1
119.83	40.083	26.56	-14.15	1.72	1.53	1.53	HB72	a	1
119.837	-0.906	17.83	3.32	1.12	1.36	1.36	P14P	i	1
119.84	-0.91	21.99	0.48	1.66	1.16	1.16	PL14	g	1
119.906	-0.916	17.64	8.5	0.94	1.17	1.17	PALP	i	1
119.91	-0.92	25.99	6.86	1.37	1.16	1.16	PALU	g	1
120.005	-0.248	14.44	25.54	1.44	0.96	0.96	DONG	i	1
120.011	-1.512	10.08	4.6	1.81	1.52	1.52	SUNG	i	1
120.09	-0.71	14.44	24.22	1.36	1.11	1.11	TOBO	g	1
120.09	-0.71	20.24	23.12	1.65	1.15	1.15	TOBP	g	1
120.32	-1.42	11.98	7.36	1.32	1.17	1.17	WUAS	g	1
120.37	-3.54	22.36	-6.67	1.43	1.23	1.23	REDO	g	1
120.428	-1.007	14.59	27.21	0.91	0.77	0.77	SULI	i	1
120.43	36.05	29.09	-15.24	1.13	1.05	1.05	JB03	g	1
120.434	0.482	13.49	34	2.34	1.53	1.53	PALA	i	1
120.6	18.52	-47.43	8.35	1.31	0.87	0.87	LAOA	g	1
120.707	37.787	28.97	-13.47	1.7	1.52	1.52	HB74	a	1
120.726	37.936	29.7	-15.39	1.73	1.54	1.54	HB75	a	1
120.79	1.12	21.56	30.68	1.39	1.11	1.11	TOLI	g	1
120.85	0.45	16.01	28.06	1.34	1.08	1.08	TOMI	g	1
120.863	1.318	20.59	23.99	3.16	1.79	1.79	LING	i	1
120.904	-1.908	1.93	7.86	2.2	1.48	1.48	KAMB	i	1

Continued on next page...

Table B.1 – Continued from previous page

Long	Lat	Velocity (mm/yr)				Corr	Site	Source†	EXC‡
°E	°N	East	North	σ E	σ N				
120.91	-2.6	16.7	-3.68	1.41	1.21	1.21	MALI	g	1
120.987	24.798	28.51	-13.11	0.49	0.44	0.44	TCMS	m	1
120.987	24.798	28.51	-13.11	0.49	0.44	0.44	TNML	m	1
121.08	14.64	-30.63	-0.18	1.34	1.16	1.16	PIMO	g	1
121.164	24.954	29.36	-16.33	1.4	1.36	1.36	TWTF	m	1
121.236	38.92	26.87	-18.08	1.64	1.48	1.48	GI84	a	1
121.436	-1.01	-5.89	12.9	2	1.24	1.24	AMPA	i	1
121.49	-4.58	24.72	-1.44	1.36	1.23	1.23	TOAR	g	1
121.536	25.021	32.54	-17.2	0.72	1.02	1.02	TAIW	a	1
121.537	25.021	35.73	-13.73	1.25	1.13	1.13	TAIW	m	1
121.599	42.053	24.09	-15.05	1.67	1.51	1.51	HB76	a	1
121.74	39.09	25.66	-15.19	1.13	1.04	1.04	JB16	g	1
121.77	-8.71	29.42	22.86	1.59	1.4	1.4	ENDE	g	1
121.77	42.76	25.75	-13.28	1.03	1.04	1.04	JB15	g	1
122.161	37.384	28.84	-15.28	2.01	1.66	1.66	HB78	a	1
122.17	46.06	25.12	-13.85	1.04	1.04	1.04	JB14	g	1
122.237	-8.58	23.9	63.79	2.7	2.21	2.21	MAUM	a	1
122.73	10.97	20.76	2.04	1.39	0.91	0.91	ILOI	g	1
122.772	-1.04	-3.47	14.85	2.74	1.54	1.54	LUWU	i	1
122.772	-1.033	2.65	6.04	2	2.31	2.31	LUWU	a	1
122.8	-5.47	27.44	6.16	1.56	1.31	1.31	BAUB	g	1
123.663	-10.11	32.36	46.2	2.4	1.41	1.41	KUPA	a	1
124.1	50.39	22.62	-12.9	1.04	1.05	1.05	JB13	g	1
124.28	-9.78	39.64	35.88	1.64	1.45	1.45	KAPA	g	1
124.34	13.57	-18.8	35.54	1.19	0.87	0.87	VIRA	g	1
125.064	1.331	22.17	-9.12	1.75	1.45	1.45	KEMA	i	1
125.064	1.331	19.92	-7.49	2.58	1.46	1.46	MANA	i	1
125.44	43.79	24.32	-14.05	1.04	1.04	1.04	CHAN	g	1
125.445	43.791	29.37	-12.51	1.4	0.73	0.73	CC06	f	1
125.51	7.08	-23.17	-7.07	1.3	0.94	0.94	DAVA	g	1
125.528	-8.491	39.84	40.85	2.2	0.92	0.92	DILI	a	1
125.74	-8.06	40.79	38.68	1.66	1.41	1.41	LIRA	g	1
125.99	-2.05	-11.86	15.12	1.64	1.23	1.23	SANA	g	1
126.429	-7.882	37.63	47.53	2.8	0.92	0.92	WETA	a	1
126.739	26.348	36.68	-46.75	1.61	1.64	1.64	6743	b	1
127.054	37.276	26.8	-15.31	0.56	0.52	0.52	SUWN	m	1
127.144	26.373	38.46	-44.63	1.6	1.62	1.62	6742	b	1
127.342	0.86	-54.97	13.77	1.42	0.87	0.87	TERN	i	1
127.366	36.374	19.71	-17.24	2.89	2.69	2.69	TAEJ	m	1
127.374	36.399	26.19	-14.98	0.23	0.22	0.22	DAEJ	m	1
127.769	26.145	38.84	-36.4	2.48	2.57	2.57	4100	b	1

Continued on next page...

Table B.1 – Continued from previous page

Long	Lat	Velocity (mm/yr)				Corr	Site	Source†	EXC‡
°E	°N	East	North	σ E	σ N				
128.089	-3.683	7.84	14.14	1.11	0.92	0.92	AMBG	a	1
128.117	-3.775	12.87	18.67	1.85	0.91	0.91	AMBO	i	1
128.144	26.708	38.71	-39.08	2.18	2.18	2.18	6738	b	1
128.248	26.859	36.37	-39.67	1.5	1.51	1.51	6737	b	1
128.432	27.032	34.35	-37.77	1.47	1.49	1.49	5495	b	1
128.619	32.634	27.36	-18.26	0.93	0.98	0.98	6698	b	1
128.651	27.401	33.5	-36.57	1.42	1.44	1.44	6735	b	1
128.843	32.669	26.97	-17.48	0.89	0.89	0.89	0462	m	1
128.843	32.669	25.78	-17.33	0.63	0.64	0.64	5462	b	1
128.894	27.817	33.34	-35.62	1.37	1.39	1.39	6734	b	1
129.026	32.886	25.72	-18.32	0.87	0.93	0.93	6692	b	1
129.311	34.268	23.97	-15.41	0.78	0.82	0.82	5457	b	1
129.482	34.655	23.82	-15.78	0.75	0.78	0.78	5456	b	1
129.489	28.399	28.67	-33.81	1.28	1.3	1.3	5494	b	1
129.49	43	22.67	-14.71	1.14	1.05	1.05	JB12	g	1
129.537	33.362	23.18	-16.46	0.81	0.86	0.86	5459	b	1
129.68	62.031	18.55	-14.26	0.25	0.24	0.24	YAKT	m	1
129.681	62.031	20.13	-13.07	0.57	0.56	0.56	YAKZ	d	1
129.681	62.031	21.86	-12.1	1.11	1.12	1.12	YAKZ	i	1
129.691	33.063	24.77	-18.01	0.82	0.87	0.87	5460	b	1
129.693	28.487	28.64	-27.9	1.26	1.28	1.28	6730	b	1
129.735	33.743	23.03	-16.31	0.77	0.81	0.81	5458	b	1
129.795	31.769	27.77	-24.38	0.91	0.97	0.97	5487	b	1
129.85	33.476	24.2	-16.44	0.78	0.82	0.82	4091	b	1
129.94	33.196	23.94	-15.36	0.79	0.84	0.84	6689	b	1
129.955	33.372	23.68	-16.73	0.78	0.82	0.82	6770	b	1
129.987	32.326	23.92	-22.25	0.86	0.9	0.9	5467	b	1
129.99	32.945	22.5	-18.21	0.8	0.86	0.86	6772	b	1
130.085	32.525	22.83	-22.47	0.84	0.87	0.87	6774	b	1
130.094	33.098	21.75	-18.67	0.79	0.83	0.83	5455	b	1
130.136	31.416	30.12	-27.47	0.93	0.97	0.97	6777	b	1
130.155	32.637	22.66	-22.46	0.82	0.86	0.86	5463	b	1
130.166	32.796	22.62	-19.39	0.8	0.85	0.85	6693	b	1
130.18	32.197	23.09	-17.26	0.86	0.9	0.9	6717	b	1
130.19	32.013	25.61	-23.38	0.97	1.05	1.05	4096	b	1
130.198	30.461	30.31	-26.33	1.03	1.07	1.07	6725	b	1
130.269	33.275	22.15	-16.89	0.89	0.89	0.89	0454	m	1
130.269	33.275	22.66	-16.22	0.52	0.54	0.54	5454	b	1
130.271	32.871	21.52	-22.53	0.79	0.84	0.84	5461	b	1
130.275	30.785	29.46	-27.28	0.98	1.02	1.02	6723	b	1
130.278	31.717	28.86	-25.18	0.88	0.93	0.93	5488	b	1

Continued on next page...

Table B.1 – Continued from previous page

Long	Lat	Velocity (mm/yr)				Corr	Site	Source†	EXC‡
°E	°N	East	North	σ E	σ N				
130.291	32.661	21.42	-23.14	0.81	0.86	0.86	6697	b	1
130.299	31.264	31.47	-25.23	0.93	0.98	0.98	4098	b	1
130.336	32.793	19.72	-20.42	0.79	0.84	0.84	6694	b	1
130.352	32.722	21.59	-20.75	0.79	0.85	0.85	6696	b	1
130.424	30.396	28.76	-26.75	1.02	1.05	1.05	6727	b	1
130.43	32.582	21.05	-23.24	0.8	0.85	0.85	6773	b	1
130.445	33.346	21.7	-14.18	0.74	0.79	0.79	6771	b	1
130.466	31.504	29.71	-39.12	0.9	0.94	0.94	4097	b	1
130.469	31.675	26.12	-24.85	0.88	0.92	0.92	6776	b	1
130.477	33.731	23.35	-15.38	0.72	0.76	0.76	4087	b	1
130.548	32.933	21.04	-18.82	0.77	0.81	0.81	5464	b	1
130.565	33.206	20.88	-17.96	0.74	0.79	0.79	5453	b	1
130.598	32.058	21.04	-25.85	0.98	0.99	0.99	0485	m	1
130.598	32.057	22.3	-26.09	0.58	0.59	0.59	5485	b	1
130.638	30.382	30.13	-27.75	1	1.04	1.04	5493	b	1
130.701	33.327	20.21	-16.36	0.73	0.78	0.78	6688	b	1
130.723	31.106	32.89	-26.05	0.93	0.97	0.97	5491	b	1
130.749	33.745	21.62	-14.68	0.7	0.75	0.75	6685	b	1
130.76	31.855	28.96	-21.36	0.85	0.9	0.9	5486	b	1
130.765	32.842	19.42	-19.88	0.76	0.8	0.8	5465	b	1
130.824	33.64	20.63	-13.33	0.7	0.75	0.75	6687	b	1
130.829	33.465	19.16	-14.95	0.71	0.76	0.76	5452	b	1
130.836	31.617	34.19	-27.7	0.88	0.91	0.91	5489	b	1
130.866	32.048	21.19	-25.61	0.83	0.86	0.86	6714	b	1
130.91	44.43	22.3	-15.22	1.14	1.05	1.05	SUIY	g	1
130.914	33.996	22.01	-13.61	0.67	0.72	0.72	4079	b	1
130.916	33.19	18.66	-16.73	0.73	0.77	0.77	6710	b	1
130.943	34.295	21.03	-14.4	0.92	0.93	0.93	0408	m	1
130.943	34.295	21.89	-14.03	0.47	0.48	0.48	5408	b	1
130.968	33.331	17.88	-14.16	0.71	0.76	0.76	4089	b	1
131.021	31.74	27.59	-27.03	0.85	0.89	0.89	5482	b	1
131.066	34.18	22.69	-11.83	0.66	0.7	0.7	6670	b	1
131.079	31.965	20.16	-23.47	0.82	0.86	0.86	5481	b	1
131.121	33.27	16.41	-14.98	0.71	0.76	0.76	6707	b	1
131.13	-12.84	34.36	53.31	1.91	1.81	1.81	DARW	g	1
131.152	34.764	22.22	-12.35	0.63	0.67	0.67	6668	b	1
131.169	33.496	16.23	-13.55	0.68	0.74	0.74	5471	b	1
131.17	46.65	20.85	-14.04	1.05	1.06	1.06	JB10	g	1
131.185	32.246	12.58	-24.55	0.79	0.83	0.83	5479	b	1
131.254	-0.869	-39.89	27.56	2.7	1.02	1.02	SORO	a	1
131.286	33.978	16.05	-14.74	0.65	0.7	0.7	5413	b	1

Continued on next page...

Table B.1 – Continued from previous page

Long	Lat	Velocity (mm/yr)				Corr	Site	Source[†]	EXC[‡]
°E	°N	East	North	σ E	σ N				
131.291	25.954	-35.14	23.33	1.48	1.48	1.48	6746	b	1
131.306	31.842	23.95	-24.49	0.83	0.86	0.86	6715	b	1
131.307	-7.936	43.15	45.97	3.1	0.82	0.82	SAUM	a	1
131.346	34.189	19.79	-10.98	0.65	0.68	0.68	5411	b	1
131.347	33.254	12.32	-15.67	0.74	0.8	0.8	5472	b	1
131.386	33.079	10.42	-15.63	0.71	0.75	0.75	6708	b	1
131.486	32.069	16.16	-18.82	0.79	0.83	0.83	6713	b	1
131.516	32.17	15.57	-18.26	0.78	0.82	0.82	5480	b	1
131.531	34.057	18.79	-14.21	1.46	1.46	1.46	5412	b	1
131.563	34.284	17.2	-6.9	0.63	0.67	0.67	5409	b	1
131.579	33.228	6.64	-14	0.68	0.74	0.74	6709	b	1
131.588	33.35	8.43	-12.88	0.67	0.72	0.72	6706	b	1
131.61	34.616	21.16	-12.18	0.61	0.64	0.64	4076	b	1
131.757	32.704	5.57	-9.24	0.72	0.76	0.76	5476	b	1
131.798	33.239	5.43	-11.5	1.46	1.46	1.46	5473	b	1
131.83	34.039	16.25	-9.7	0.65	0.68	0.68	6671	b	1
131.864	34.44	17.48	-11.63	0.6	0.64	0.64	6659	b	1
131.923	34.767	17.27	-13.62	0.58	0.62	0.62	5388	b	1
131.926	43.197	21.81	-15.03	0.83	0.84	0.84	VLAD	i	1
131.953	34.259	15.97	-10.38	0.61	0.64	0.64	5410	b	1
132.014	34.571	20.57	-12.71	0.59	0.62	0.62	6658	b	1
132.104	33.975	13.05	-10.08	0.62	0.65	0.65	5414	b	1
132.195	34.37	18.01	-8.64	0.59	0.62	0.62	6665	b	1
132.219	34.191	14.8	-11.21	0.6	0.63	0.63	6769	b	1
132.265	-2.9	-26.94	39.04	2.51	1.72	1.72	FAKF	a	1
132.269	34.575	17.08	-12.51	0.57	0.61	0.61	5404	b	1
132.277	34.727	18.51	-11.93	0.57	0.6	0.6	5399	b	1
132.281	33.469	4.18	-6.72	0.64	0.67	0.67	4086	b	1
132.345	34.369	16.49	-9.8	0.58	0.62	0.62	5406	b	1
132.456	34.261	14.8	-9.8	0.58	0.62	0.62	6666	b	1
132.457	34.893	18.65	-12.39	0.55	0.59	0.59	6657	b	1
132.463	34.539	16.81	-10.87	0.57	0.6	0.6	5403	b	1
132.487	33.611	5.14	-7.99	0.62	0.66	0.66	6680	b	1
132.544	33.178	-1.25	-4.42	0.65	0.68	0.68	6681	b	1
132.562	32.964	-7.17	-1.43	0.67	0.7	0.7	5437	b	1
132.575	34.34	17.79	-7.84	0.57	0.61	0.61	4078	b	1
132.684	33.722	4.5	-6.97	0.61	0.64	0.64	5434	b	1
132.704	32.841	-9.32	3.21	0.67	0.71	0.71	5449	b	1
132.743	35.393	23.67	-13.76	0.54	0.56	0.56	5384	b	1
132.782	33.959	11.35	-6.35	0.59	0.62	0.62	6679	b	1
132.793	33.172	-5.25	-2.09	0.65	0.67	0.67	5447	b	1

Continued on next page...

Table B.1 – Continued from previous page

Long	Lat	Velocity (mm/yr)				Corr	Site	Source†	EXC‡
°E	°N	East	North	σ E	σ N				
132.82	34.335	16.93	-10.6	0.56	0.59	0.59	6768	b	1
132.824	34.571	20.4	-12.12	0.58	0.61	0.61	5402	b	1
132.852	34.812	20.28	-11.57	0.54	0.58	0.58	6663	b	1
132.884	34.21	13.78	-6.15	0.57	0.6	0.6	6667	b	1
132.99	34.078	11	-7.72	0.57	0.6	0.6	5430	b	1
132.999	32.991	-11.56	1.85	0.65	0.68	0.68	5448	b	1
133.01	34.379	15.42	-5.76	0.55	0.59	0.59	5405	b	1
133.059	35.434	23.03	-12.78	0.51	0.54	0.54	4074	b	1
133.107	34.672	17.81	-10.98	0.54	0.57	0.57	5401	b	1
133.12	34.943	17.82	-17.97	0.9	0.89	0.89	0398	m	1
133.12	34.943	18.99	-14.02	0.38	0.4	0.4	5398	b	1
133.125	-5.251	16.85	56.21	1.41	0.72	0.72	TUAL	a	1
133.129	33.215	-8.92	0.5	0.63	0.66	0.66	6684	b	1
133.138	35.563	17.26	-7.52	2.01	2.01	2.01	6656	b	1
133.189	34.252	14.7	-6.95	0.55	0.59	0.59	6678	b	1
133.228	33.327	-8.29	1.83	0.62	0.65	0.65	6683	b	1
133.24	36.285	23.03	-14.72	0.51	0.53	0.53	5382	b	1
133.281	33.468	-5.89	1.4	0.61	0.63	0.63	5443	b	1
133.288	34.45	16.6	-9.34	0.54	0.58	0.58	6767	b	1
133.338	34.778	17.84	-11.02	0.53	0.56	0.56	6664	b	1
133.396	34.993	18.65	-15.45	0.53	0.54	0.54	6662	b	1
133.403	33.408	-9.35	1.01	0.61	0.63	0.63	5445	b	1
133.439	35.346	18.64	-13.27	1.55	1.5	1.5	0379	m	1
133.462	33.818	12.18	6.87	0.6	0.63	0.63	6682	b	1
133.528	34.549	16.79	-10.33	2.01	2.01	2.01	4077	b	1
133.598	34.81	18.62	-11.09	0.52	0.55	0.55	5394	b	1
133.656	33.767	0.81	-4.15	0.57	0.6	0.6	5438	b	1
133.681	33.937	4.42	-5.83	0.56	0.59	0.59	5419	b	1
133.694	-3.62	-19.45	54.08	2.01	1.41	1.41	KAIM	a	1
133.699	35.49	20.22	-12.11	0.5	0.52	0.52	4073	b	1
133.715	34.217	12.2	-7.88	0.54	0.58	0.58	5427	b	1
133.757	34.579	17.88	-10.68	0.52	0.56	0.56	6766	b	1
133.781	34.383	17.24	-9.35	0.53	0.57	0.57	6677	b	1
133.797	34.438	16.68	-8.59	0.53	0.56	0.56	5397	b	1
133.805	33.654	-3.58	-1.36	0.59	0.62	0.62	5439	b	1
133.875	34.04	7.3	-5.38	0.55	0.58	0.58	6674	b	1
133.904	33.506	-9.19	1.16	0.6	0.61	0.61	5442	b	1
133.929	34.791	15.67	-16.42	0.52	0.54	0.54	5395	b	1
133.961	34.982	18.14	-12.04	0.51	0.53	0.53	5393	b	1
133.999	34.445	13.15	-13.01	2.01	2.01	2.01	6676	b	1
134.007	33.428	-12.68	1.65	0.6	0.62	0.62	5444	b	1

Continued on next page...

Table B.1 – Continued from previous page

Long	Lat	Velocity (mm/yr)				Corr	Site	Source†	EXC‡
°E	°N	East	North	σ E	σ N				
134.047	35.457	20.48	-15.26	0.5	0.52	0.52	5378	b	1
134.049	34.051	6.72	-6.91	0.55	0.58	0.58	5417	b	1
134.05	-0.886	-41.93	36.14	1.71	1.21	1.21	MANO	a	1
134.058	33.877	3.1	-2.54	0.56	0.59	0.59	5421	b	1
134.107	33.604	-6.92	0.19	0.58	0.6	0.6	5440	b	1
134.166	34.658	17.9	-13.75	0.52	0.54	0.54	5396	b	1
134.176	34.81	19.78	-12.66	0.52	0.54	0.54	6765	b	1
134.23	34.038	7.99	-9.13	0.55	0.58	0.58	5418	b	1
134.235	35.021	18.72	-13.41	0.51	0.53	0.53	5391	b	1
134.237	35.266	18.71	-13.2	0.5	0.52	0.52	5380	b	1
134.242	34.255	12.71	-10.68	0.53	0.56	0.56	5426	b	1
134.281	33.528	-10.48	-2.38	0.58	0.6	0.6	5441	b	1
134.301	33.79	8.99	-2.57	0.59	0.62	0.62	6675	b	1
134.312	-5.987	34.33	57.91	2.31	0.82	0.82	ARUX	a	1
134.314	34.472	17.25	-11.68	0.52	0.55	0.55	5425	b	1
134.32	35.1	17.69	-2.58	0.5	0.52	0.52	5390	b	1
134.325	35.361	18.42	-10.83	0.5	0.52	0.52	6655	b	1
134.331	35.586	17.85	-21.53	0.5	0.52	0.52	4072	b	1
134.352	34.097	8.36	-9.13	0.54	0.57	0.57	5415	b	1
134.404	34.998	17.29	-14.59	0.51	0.53	0.53	5346	b	1
134.52	34.67	17.4	-13.02	0.52	0.54	0.54	5357	b	1
134.533	33.725	-3.09	-4.23	0.57	0.59	0.59	5423	b	1
134.545	34.897	17.21	-13.21	0.51	0.53	0.53	5350	b	1
134.56	34.06	5.69	-9.41	0.54	0.57	0.57	5416	b	1
134.582	35.437	20.34	-11.38	0.49	0.52	0.52	5341	b	1
134.586	35.094	17.17	-12.6	0.5	0.52	0.52	5344	b	1
134.66	34.864	16.03	-11.79	0.51	0.53	0.53	6762	b	1
134.677	35.621	17.48	-12.11	0.49	0.51	0.51	6645	b	1
134.729	35.461	16.7	-13.9	0.49	0.52	0.52	6646	b	1
134.735	34.334	11.64	-11.79	0.53	0.55	0.55	5362	b	1
134.736	34.224	9.88	-8.71	0.53	0.56	0.56	5363	b	1
134.767	34.985	15.95	-13.3	0.5	0.52	0.52	5347	b	1
134.771	35.163	17.73	-13.43	0.5	0.52	0.52	6648	b	1
134.818	35.315	16.27	-12.03	0.49	0.52	0.52	5342	b	1
134.829	34.787	15.47	-13.29	0.51	0.53	0.53	5354	b	1
134.932	35.556	17.59	-14.21	0.9	0.89	0.89	0328	m	1
134.932	35.556	16.36	-14.83	0.35	0.37	0.37	5328	b	1
134.945	34.936	14.59	-9.92	0.51	0.52	0.52	6649	b	1
134.966	34.67	15.15	-11.8	0.52	0.53	0.53	5358	b	1
134.973	35.091	14.92	-11.61	0.5	0.52	0.52	5345	b	1
134.997	34.805	15.22	-12.01	0.51	0.53	0.53	5352	b	1

Continued on next page...

Table B.1 – Continued from previous page

Long	Lat	Velocity (mm/yr)				Corr	Site	Source†	EXC‡
°E	°N	East	North	σ E	σ N				
135.022	35.238	14.12	-10.41	0.49	0.52	0.52	6647	b	1
135.024	34.577	12.68	-13.82	0.52	0.54	0.54	5359	b	1
135.034	35.685	16.89	-12.91	0.48	0.51	0.51	6640	b	1
135.046	48.521	20.94	-13.95	1.07	1.03	1.03	KHAJ	i	1
135.164	35.292	15.4	-13.06	0.49	0.52	0.52	5329	b	1
135.172	34.687	9.87	-12.16	0.52	0.53	0.53	5356	b	1
135.173	35.752	18.2	-14.54	0.48	0.5	0.5	5327	b	1
135.18	33.914	1.16	-6.01	0.55	0.57	0.57	5372	b	1
135.182	35.105	16.15	-15.48	0.5	0.52	0.52	5343	b	1
135.233	35.55	15.64	-13.67	0.48	0.51	0.51	4057	b	1
135.326	34.977	14.27	-11.17	0.5	0.52	0.52	5348	b	1
135.342	34.791	10.5	-10.89	0.51	0.53	0.53	5353	b	1
135.358	34.256	6.8	-9.38	0.55	0.55	0.55	5368	b	1
135.364	34.406	8.66	-10.67	0.53	0.55	0.55	5340	b	1
135.367	35.164	13.89	-11.49	0.5	0.52	0.52	5331	b	1
135.38	34.724	9.05	-12.35	0.52	0.53	0.53	5355	b	1
135.396	33.744	-3.41	-7.24	0.57	0.58	0.58	5375	b	1
135.431	34.084	5.46	-12.53	0.54	0.56	0.56	6651	b	1
135.481	34.527	6.89	-11.28	0.53	0.54	0.54	5337	b	1
135.508	33.785	-1.96	-7.48	0.57	0.58	0.58	5374	b	1
135.528	34.312	6.05	-10.27	0.53	0.55	0.55	6650	b	1
135.549	35.276	12.52	-10.61	0.49	0.52	0.52	6642	b	1
135.564	35.077	13.81	-11.97	0.5	0.52	0.52	5332	b	1
135.587	34.425	6.47	-11.11	0.53	0.54	0.54	5339	b	1
135.59	34.222	7.14	-11.35	0.54	0.55	0.55	5370	b	1
135.599	33.506	-11.46	-3.8	0.59	0.59	0.59	5377	b	1
135.609	35.463	14.94	-14.31	0.49	0.51	0.51	5262	b	1
135.627	34.479	6.07	-10.92	0.53	0.54	0.54	5338	b	1
135.665	34.988	10.99	-10.98	0.51	0.52	0.52	5333	b	1
135.685	34.778	7.63	-12.66	0.52	0.53	0.53	5335	b	1
135.704	34.388	5.85	-10.7	0.53	0.55	0.55	5366	b	1
135.706	34.698	5.76	-12.9	0.52	0.53	0.53	6763	b	1
135.731	34.539	4.89	-12.06	0.54	0.55	0.55	5365	b	1
135.764	33.483	-9.03	-5.09	0.59	0.59	0.59	4070	b	1
135.772	34.953	7.22	-12.94	0.51	0.52	0.52	6644	b	1
135.774	35.209	11.55	-13.8	0.5	0.52	0.52	5330	b	1
135.79	34.882	7.89	-15.32	0.51	0.52	0.52	6760	b	1
135.864	34.747	5.99	-12.67	0.52	0.53	0.53	5334	b	1
135.871	35.137	8.75	-14.36	0.5	0.52	0.52	5322	b	1
135.906	34.94	7.69	-14.13	0.51	0.52	0.52	5324	b	1
135.908	35.534	12.92	-11.85	2.01	2.01	2.01	5261	b	1

Continued on next page...

Table B.1 – Continued from previous page

Long	Lat	Velocity (mm/yr)				Corr	Site	Source[†]	EXC[‡]
°E	°N	East	North	σ E	σ N				
135.913	35.351	11.66	-14.25	0.49	0.52	0.52	5319	b	1
135.964	34.038	1.23	-8.64	0.55	0.57	0.57	5367	b	1
135.99	35.945	17.91	-16.02	0.48	0.49	0.49	5259	b	1
136.011	33.741	-6.34	-6.93	0.58	0.59	0.59	5316	b	1
136.041	35.086	6.56	-12.43	0.51	0.52	0.52	6639	b	1
136.05	34.567	3.46	-13.51	0.53	0.54	0.54	5364	b	1
136.054	35.466	10.89	-12.5	0.49	0.51	0.51	5318	b	1
136.055	34.869	7.02	-12.63	0.52	0.53	0.53	5326	b	1
136.056	35.837	13.1	-14.68	0.48	0.5	0.5	6580	b	1
136.063	35.319	9.73	-14.2	0.5	0.52	0.52	5320	b	1
136.086	33.875	-3.92	-8.21	0.57	0.58	0.58	5315	b	1
136.145	34.986	6.51	-13.31	0.51	0.53	0.53	5323	b	1
136.158	35.095	7.19	-12.55	0.53	0.54	0.54	4062	b	1
136.173	36.231	17.52	-12.98	0.47	0.49	0.49	4055	b	1
136.183	34.743	8.01	-13.82	0.52	0.53	0.53	5310	b	1
136.197	35.793	13.88	-13.83	0.49	0.51	0.51	5260	b	1
136.198	35.557	10.54	-12.82	0.49	0.51	0.51	5317	b	1
136.236	35.269	9.27	-12.89	0.5	0.52	0.52	5321	b	1
136.248	-1.167	-12.54	88.26	1.72	1.15	1.15	BIAK	i	1
136.265	35.42	9.76	-12.74	0.5	0.52	0.52	6638	b	1
136.279	36.146	16.63	-12.5	0.48	0.49	0.49	5257	b	1
136.296	34.932	4.57	-13.4	0.52	0.53	0.53	5325	b	1
136.33	34.649	3.37	-15.02	0.53	0.55	0.55	6635	b	1
136.334	34.433	1.95	-11.14	0.53	0.55	0.55	5312	b	1
136.343	34.208	-2.25	-8.47	0.55	0.56	0.56	6637	b	1
136.389	36.394	18	-14.04	0.89	0.89	0.89	0255	m	1
136.389	36.394	17.12	-14.43	0.35	0.36	0.36	5255	b	1
136.393	34.855	4.13	-12.25	0.52	0.53	0.53	6634	b	1
136.505	35.985	12.57	-13.39	0.48	0.49	0.49	5258	b	1
136.505	35.105	8.12	-11.73	0.52	0.53	0.53	5308	b	1
136.54	34.285	-2.81	-8.4	0.55	0.56	0.56	5313	b	1
136.55	35.372	7.54	-13.56	0.5	0.52	0.52	5291	b	1
136.551	34.547	0.89	-10.6	0.53	0.55	0.55	5311	b	1
136.593	35.228	5.39	-16.01	0.51	0.53	0.53	5294	b	1
136.605	36.37	16.58	-14.86	0.47	0.49	0.49	6578	b	1
136.611	35.633	7.35	-12.43	0.49	0.51	0.51	5286	b	1
136.628	34.431	-0.42	-8.72	0.54	0.55	0.55	6636	b	1
136.634	36.165	15.58	-14.62	0.48	0.49	0.49	5256	b	1
136.637	34.914	2.49	-12.74	0.52	0.54	0.54	5309	b	1
136.65	36.663	15.79	-14.18	0.47	0.49	0.49	4054	b	1
136.687	35.488	4.07	-13.7	0.51	0.52	0.52	5288	b	1

Continued on next page...

Table B.1 – Continued from previous page

Long	Lat	Velocity (mm/yr)				Corr	Site	Source†	EXC‡
°E	°N	East	North	σ E	σ N				
136.694	35.051	3.68	-11.88	0.52	0.53	0.53	6633	b	1
136.719	37.157	17.15	-14.38	0.46	0.48	0.48	6575	b	1
136.729	35.405	5.39	-13.08	0.5	0.52	0.52	5290	b	1
136.756	36.817	18.33	-13.89	0.47	0.48	0.48	6577	b	1
136.772	37.001	17.93	-13.53	0.89	0.89	0.89	0254	m	1
136.772	37.001	18.21	-14.44	0.34	0.35	0.35	5254	b	1
136.812	62.784	18.69	-14.99	1.63	1.62	1.62	TKL1	i	1
136.821	34.253	-4.52	-8.09	0.55	0.56	0.56	5314	b	1
136.829	35.19	3.72	-12.79	0.51	0.53	0.53	5299	b	1
136.832	34.904	2.93	-9.92	2.01	2.01	2.01	6632	b	1
136.863	35.867	7.48	-12.56	0.49	0.5	0.5	5282	b	1
136.895	-4.503	31.3	56.56	1.71	0.82	0.82	TIMI	a	1
136.9	35.526	5.24	-12.81	0.5	0.52	0.52	4060	b	1
136.904	36.261	11.94	-13.86	0.48	0.5	0.5	6617	b	1
136.919	37.85	18.95	-13.77	0.46	0.48	0.48	5252	b	1
136.921	36.402	13.24	-11.51	2.01	2.01	2.01	5251	b	1
136.93	35.335	4.46	-12.61	0.51	0.53	0.53	5298	b	1
136.953	36.033	7.12	-14.09	0.48	0.5	0.5	5280	b	1
136.975	35.758	3.53	-11.84	0.49	0.51	0.51	5283	b	1
136.996	36.741	16.56	-13.28	0.47	0.48	0.48	5248	b	1
137.032	36.65	16.15	-12.47	0.47	0.49	0.49	6573	b	1
137.139	37.307	17.58	-12.93	0.46	0.48	0.48	6574	b	1
137.147	36.335	11.8	-12.37	0.48	0.49	0.49	5279	b	1
137.174	35.612	3.71	-12.41	0.5	0.52	0.52	5287	b	1
137.195	36.634	16.33	-13.6	0.47	0.49	0.49	5249	b	1
137.201	35.912	3.39	-11.16	0.51	0.53	0.53	6619	b	1
137.278	34.649	-2.42	-11.18	0.54	0.56	0.56	5306	b	1
137.363	36.286	7.02	-15.12	0.48	0.49	0.49	6618	b	1
137.37	36.737	15.18	-13.6	0.47	0.48	0.48	6572	b	1
137.425	35.657	2.48	-12.16	0.51	0.52	0.52	5284	b	1
137.44	36.579	11.58	-12.93	2.01	2.01	2.01	5250	b	1
137.487	36.929	13.58	-13.02	0.47	0.48	0.48	4052	b	1
137.535	35.973	3.42	-13.02	0.49	0.51	0.51	5281	b	1
137.588	35.247	3.58	-12.21	0.53	0.54	0.54	5278	b	1
137.598	35.88	2.97	-11.96	0.5	0.51	0.51	6614	b	1
137.696	35.784	2.41	-12.22	0.9	0.89	0.89	0274	m	1
137.696	35.784	0.79	-11.5	0.36	0.38	0.38	5274	b	1
137.815	35.521	2.07	-11.73	0.52	0.54	0.54	5276	b	1
137.872	36.706	11.48	-12.81	0.48	0.49	0.49	5266	b	1
137.874	37.045	10.89	-11.38	0.47	0.48	0.48	5245	b	1
137.903	36.322	3.22	-9.49	0.48	0.5	0.5	5270	b	1

Continued on next page...

Table B.1 – Continued from previous page

Long	Lat	Velocity (mm/yr)				Corr	Site	Source†	EXC‡
°E	°N	East	North	σ E	σ N				
137.925	35.317	2.27	-13.48	0.53	0.55	0.55	5277	b	1
137.983	36.121	0.97	-10.06	0.49	0.51	0.51	5273	b	1
138.038	35.556	1.97	-11.79	0.52	0.54	0.54	5275	b	1
138.1	37.161	13.28	-11.23	0.47	0.48	0.48	5243	b	1
138.199	36.865	9.46	-8.85	0.48	0.49	0.49	5247	b	1
138.214	36.026	-0.2	-9.58	0.51	0.52	0.52	6612	b	1
138.216	36.208	-1.18	-8.91	0.49	0.51	0.51	5271	b	1
138.242	37.057	8.61	-10.68	0.47	0.49	0.49	6569	b	1
138.247	36.665	3.37	-11.27	0.93	0.92	0.92	0267	m	1
138.247	36.665	3.28	-10.43	0.36	0.36	0.36	5267	b	1
138.273	37.816	11.22	-14	0.46	0.48	0.48	5235	b	1
138.316	35.856	0.85	-9.45	0.52	0.53	0.53	5263	b	1
138.333	37.231	9.06	-11.42	0.34	0.36	0.36	5241	b	1
138.334	37.231	10.4	-11.1	0.89	0.89	0.89	0241	m	1
138.362	36.133	-0.9	-9.65	0.19	0.17	0.17	USUD	m	1
138.37	38.024	12.26	-12.29	0.46	0.48	0.48	6565	b	1
138.436	36.802	-1.31	-10.47	0.48	0.5	0.5	5265	b	1
138.461	36.131	-1.33	-9.74	0.51	0.52	0.52	5272	b	1
138.472	38.063	11.74	-13.35	0.46	0.48	0.48	5233	b	1
138.513	38.319	11.13	-12.64	0.45	0.48	0.48	5232	b	1
138.516	37.348	8.29	-11.82	0.47	0.48	0.48	6567	b	1
138.553	36.508	-1.52	-11.96	0.93	0.93	0.93	0221	m	1
138.553	36.508	-4.17	-13.59	0.43	0.43	0.43	5221	b	1
138.583	35.974	-1.65	-9.06	0.52	0.53	0.53	6613	b	1
138.591	36.616	-5.17	-11.8	0.49	0.51	0.51	6591	b	1
138.609	37.079	2.48	-11.18	0.47	0.49	0.49	5244	b	1
138.69	35.65	-1.41	-9.29	0.54	0.56	0.56	6606	b	1
138.695	35.747	-0.68	-10.49	0.53	0.55	0.55	5264	b	1
138.707	37.536	10.59	-11.05	0.47	0.48	0.48	6566	b	1
138.777	34.855	-9.25	-12.96	1.45	1.45	1.45	6620	b	1
138.781	37.667	7.01	-12	0.47	0.48	0.48	5237	b	1
138.79	37.311	3.52	-10.62	0.47	0.49	0.49	5240	b	1
138.831	36.993	0.38	-12.2	0.48	0.5	0.5	5246	b	1
138.906	36.697	-2.64	-11.2	0.49	0.51	0.51	4044	b	1
138.912	36.143	-2.75	-11.18	0.52	0.53	0.53	6593	b	1
138.934	37.166	0.26	-10.99	0.48	0.5	0.5	5242	b	1
138.95	-4.04	31.29	49.79	1.74	1.4	1.4	WAME	g	1
138.95	-4.066	26.48	43.34	3.4	1.91	1.91	WAME	a	1
138.989	37.896	6.81	-12.05	0.47	0.48	0.48	4050	b	1
138.998	37.468	3.11	-11.7	0.47	0.49	0.49	5239	b	1
139.02	37.32	1.44	-11.73	0.47	0.49	0.49	6568	b	1

Continued on next page...

Table B.1 – Continued from previous page

Long	Lat	Velocity (mm/yr)				Corr	Site	Source†	EXC‡
°E	°N	East	North	σ E	σ N				
139.026	35.512	-3.6	-7.74	0.55	0.56	0.56	6607	b	1
139.057	36.539	-2.76	-10.9	0.5	0.52	0.52	6752	b	1
139.059	37.662	2.62	-9.67	0.47	0.49	0.49	5238	b	1
139.067	36.235	-2.54	-9.21	0.52	0.53	0.53	6592	b	1
139.074	37.752	4.41	-11.45	0.47	0.49	0.49	6571	b	1
139.076	35.987	-3.17	-9.75	0.53	0.55	0.55	5223	b	1
139.225	36.77	-2.34	-12.25	0.5	0.52	0.52	5220	b	1
139.253	38.465	5.58	-11.87	0.46	0.48	0.48	5231	b	1
139.269	36.004	-2.73	-9.65	0.54	0.56	0.56	6753	b	1
139.33	36.422	-4.15	-11.31	0.52	0.53	0.53	5222	b	1
139.351	37.929	0.33	-10.63	0.47	0.49	0.49	5234	b	1
139.364	37.303	0.76	-11.9	0.48	0.5	0.5	5206	b	1
139.366	35.801	-2.55	-7.55	0.54	0.56	0.56	6755	b	1
139.37	35.616	-3.6	-3.38	0.55	0.57	0.57	6758	b	1
139.446	42.061	3.46	-15.24	0.45	0.46	0.46	6527	b	1
139.462	38.056	-1.11	-10.78	2.01	2.01	2.01	6564	b	1
139.478	37.686	1.47	-11.17	0.47	0.49	0.49	5236	b	1
139.49	36.624	-7.34	-8.12	0.53	0.55	0.55	6589	b	1
139.504	37.281	-0.42	-12.04	0.49	0.51	0.51	5207	b	1
139.51	38.231	-1.88	-11.38	0.47	0.49	0.49	4049	b	1
139.529	37.473	0.15	-11.16	0.48	0.5	0.5	5204	b	1
139.548	39.186	8.77	-10.68	0.45	0.47	0.47	5194	b	1
139.586	37.097	-0.92	-10.21	0.49	0.51	0.51	6563	b	1
139.619	36.666	-5	-11.79	0.51	0.53	0.53	5218	b	1
139.726	36.402	-4.31	-10.43	0.53	0.55	0.55	4043	b	1
139.742	38.146	-3.56	-9.44	0.47	0.49	0.49	5197	b	1
139.765	32.464	-24.9	12.2	0.79	0.8	0.8	6602	b	1
139.776	39.968	7.84	-9.3	0.44	0.46	0.46	4030	b	1
139.806	36.979	-4.11	-11.31	0.5	0.52	0.52	6586	b	1
139.809	38.895	3.1	-8.96	0.46	0.48	0.48	4032	b	1
139.811	36.204	-1.42	-10.3	0.54	0.56	0.56	3003	b	1
139.832	38.594	1.17	-9.62	0.89	0.89	0.89	0196	m	1
139.832	38.594	-0.32	-9.36	0.34	0.34	0.34	5196	b	1
139.854	36.776	-4.95	-13.11	0.51	0.53	0.53	6587	b	1
139.871	37.261	-3.49	-13.13	0.49	0.52	0.52	5209	b	1
139.908	39.206	5.35	-9.49	0.46	0.47	0.47	5191	b	1
139.923	36.599	-6.4	-10.88	0.53	0.54	0.54	5219	b	1
139.928	40.578	3.6	-10.89	0.89	0.89	0.89	0154	m	1
139.932	36.115	-0.42	-7.96	0.55	0.57	0.57	6583	b	1
139.957	38.76	-0.3	-10.27	0.46	0.48	0.48	5195	b	1
139.988	36.301	-5.45	-10.08	0.54	0.56	0.56	6582	b	1

Continued on next page...

Table B.1 – Continued from previous page

Long	Lat	Velocity (mm/yr)				Corr	Site	Source†	EXC‡
°E	°N	East	North	σ E	σ N				
140.004	42.131	2.51	-13.53	0.45	0.46	0.46	5145	b	1
140.039	36.854	-6.5	-12.32	0.52	0.54	0.54	5217	b	1
140.041	41.466	6.77	-11.81	0.44	0.46	0.46	4023	b	1
140.045	39.826	5.24	-9.21	0.45	0.46	0.46	6552	b	1
140.049	40.247	4.16	-10.49	1.44	1.44	1.44	5184	b	1
140.071	41.803	0.14	-10.39	0.44	0.46	0.46	6530	b	1
140.073	37.567	-5.73	-13.56	0.49	0.51	0.51	5202	b	1
140.077	38.197	-5.09	-7.26	0.47	0.49	0.49	5199	b	1
140.078	36.365	-5.45	-10.09	0.54	0.56	0.56	5215	b	1
140.087	36.106	-4.59	-10.07	0.2	0.16	0.16	TSKB	m	1
140.094	37.964	-5.78	-8.88	0.48	0.49	0.49	5198	b	1
140.107	42.008	1.18	-9.53	0.9	0.9	0.9	0021	m	1
140.107	42.008	1.52	-10.93	0.33	0.33	0.33	4021	b	1
140.132	39.936	3.98	-7.97	0.44	0.46	0.46	5186	b	1
140.136	37.424	-7.31	-12.39	0.5	0.52	0.52	6561	b	1
140.162	39.164	0.51	-7.25	0.46	0.48	0.48	5192	b	1
140.165	36.952	-7.6	-11.99	0.52	0.54	0.54	6585	b	1
140.179	36.542	-7.64	-11.17	2.01	2.01	2.01	6590	b	1
140.233	42.786	1.7	-13.49	0.47	0.47	0.47	5131	b	1
140.234	39.658	5.8	-7.54	0.45	0.47	0.47	5188	b	1
140.26	37.126	-7	-12.93	0.89	0.89	0.89	0210	m	1
140.26	37.126	-8.05	-12.21	0.37	0.38	0.38	5210	b	1
140.264	40.271	2.8	-9.11	0.44	0.46	0.46	5182	b	1
140.271	38.148	-6.36	-7.5	0.47	0.49	0.49	6557	b	1
140.273	40.779	5.25	-11.09	0.43	0.45	0.45	4026	b	1
140.293	36.651	-7.02	-9.73	0.54	0.55	0.55	5213	b	1
140.316	41.599	5.3	-12.42	0.89	0.89	0.89	0149	m	1
140.316	41.599	4.13	-12.09	0.33	0.33	0.33	5149	b	1
140.319	38.758	-2.68	-6.79	0.46	0.48	0.48	4033	b	1
140.325	37.362	-10.45	-9.58	0.52	0.54	0.54	4039	b	1
140.366	38.331	-7.6	-8.93	0.47	0.49	0.49	4035	b	1
140.373	37.621	-8.4	-9.74	0.49	0.51	0.51	6560	b	1
140.387	39.549	1.09	-7.66	0.46	0.48	0.48	5189	b	1
140.402	40.007	3.07	-8.16	0.45	0.46	0.46	5185	b	1
140.413	36.862	-8.62	-9.86	0.53	0.55	0.55	5212	b	1
140.414	-8.467	30.24	53.28	1.51	0.53	0.53	AUKE	a	1
140.443	37.99	-9.71	-10.22	0.48	0.5	0.5	5180	b	1
140.452	40.91	4.51	-11.51	0.43	0.45	0.45	6542	b	1
140.466	37.683	-12.29	-11.19	0.49	0.51	0.51	5200	b	1
140.476	36.344	-5.78	-10.26	0.89	0.89	0.89	0216	m	1
140.476	36.344	-6.4	-9.92	0.39	0.41	0.41	5216	b	1

Continued on next page...

Table B.1 – Continued from previous page

Long	Lat	Velocity (mm/yr)				Corr	Site	Source[†]	EXC[‡]
°E	°N	East	North	σ E	σ N				
140.479	40.624	4.13	-13.19	0.43	0.45	0.45	6540	b	1
140.491	41.185	2.91	-10.88	0.44	0.45	0.45	6534	b	1
140.498	36.743	-10	-10.44	0.54	0.56	0.56	6581	b	1
140.499	43.057	4.72	-13.86	0.89	0.89	0.89	0126	m	1
140.499	43.057	5.22	-14.99	0.35	0.36	0.36	5126	b	1
140.516	-2.556	8.28	37.11	1.51	0.63	0.63	SENT	a	1
140.544	36.181	-5.7	-9.53	0.57	0.58	0.58	3004	b	1
140.544	42.985	4.84	-15.56	0.47	0.47	0.47	5127	b	1
140.56	39.327	1.98	-8.44	0.46	0.48	0.48	5190	b	1
140.562	37.089	-12.6	-8.49	0.53	0.55	0.55	5211	b	1
140.577	40.325	3.01	-7.19	0.44	0.46	0.46	5181	b	1
140.597	39.749	2.74	-9.03	0.46	0.47	0.47	5187	b	1
140.63	39.052	-3.19	-5.59	0.46	0.48	0.48	5193	b	1
140.662	37.325	-11.55	-8.77	0.52	0.54	0.54	5205	b	1
140.715	41.977	4.7	-11.07	0.45	0.47	0.47	6529	b	1
140.733	39.703	2.87	-9.34	0.46	0.48	0.48	6553	b	1
140.748	41.826	1.34	-11.38	0.45	0.46	0.46	4022	b	1
140.754	36.8	-11.98	-11.03	0.54	0.56	0.56	5214	b	1
140.769	39.351	-3.89	-5.7	0.46	0.49	0.49	6544	b	1
140.802	38.749	-8.92	-6.16	0.47	0.49	0.49	5174	b	1
140.803	40.644	4.63	-10.47	0.44	0.46	0.46	6541	b	1
140.822	41.146	4.31	-9.68	0.44	0.46	0.46	6535	b	1
140.829	40.841	3.07	-11.39	0.44	0.46	0.46	4025	b	1
140.844	38.03	-14.37	-8.36	0.49	0.51	0.51	5179	b	1
140.848	38.546	-11	-6.52	0.47	0.5	0.5	6548	b	1
140.851	38.412	-12.57	-7.36	0.48	0.5	0.5	5177	b	1
140.861	43.209	6.22	-14.28	0.49	0.49	0.49	6517	b	1
140.872	40.913	2.09	-10.62	1.44	1.44	1.44	6536	b	1
140.88	41.455	3.32	-12.39	0.44	0.46	0.46	5150	b	1
140.902	37.091	-12.93	-6.74	0.54	0.56	0.56	4041	b	1
140.946	37.818	-15.78	-8.91	0.5	0.52	0.52	6558	b	1
140.954	38.317	-14.62	-7.41	0.49	0.51	0.51	4037	b	1
140.964	39.701	-5.21	-5.75	0.46	0.48	0.48	5165	b	1
140.99	38.815	-9.62	-5.26	0.48	0.49	0.49	5173	b	1
140.994	37.285	-13.52	-9.61	0.53	0.55	0.55	5208	b	1
141.007	37.534	-15.35	-7.93	0.52	0.54	0.54	5203	b	1
141.066	39.953	-0.93	-12.99	1.44	1.44	1.44	6543	b	1
141.076	40.291	2.23	-10.45	0.45	0.47	0.47	5157	b	1
141.132	40.862	-0.05	-9.68	0.45	0.47	0.47	6537	b	1
141.148	38.539	-14.79	-4.48	0.48	0.5	0.5	5176	b	1
141.165	39.851	-3.91	-8.39	0.46	0.48	0.48	5163	b	1

Continued on next page...

Table B.1 – Continued from previous page

Long	Lat	Velocity (mm/yr)				Corr	Site	Source†	EXC‡
°E	°N	East	North	σ E	σ N				
141.198	40.625	0.37	-12.65	0.45	0.47	0.47	5153	b	1
141.213	41.301	0.2	-11.54	0.45	0.47	0.47	4024	b	1
141.213	38.425	-17.39	-5.63	0.49	0.5	0.5	6549	b	1
141.225	39.98	-2.27	-8.96	0.46	0.48	0.48	5161	b	1
141.29	42.971	0.79	-14.84	0.48	0.48	0.48	5128	b	1
141.294	40.291	-0.3	-10.99	0.46	0.47	0.47	5159	b	1
141.33	44.427	11.43	-12.93	0.57	0.58	0.58	5106	b	1
141.431	43.405	3.24	-13.72	0.89	0.89	0.89	0117	m	1
141.431	43.405	4.23	-13.68	0.37	0.38	0.38	5117	b	1
141.441	38.449	-18.08	-6.59	2.01	2.01	2.01	4036	b	1
141.447	41.405	-0.55	-10.18	0.45	0.47	0.47	6533	b	1
141.449	38.683	-18.23	-5.54	0.89	0.89	0.89	0175	m	1
141.449	38.683	-16.82	-5.32	0.36	0.36	0.36	5175	b	1
141.462	40.049	-2.73	-11.12	0.46	0.48	0.48	5160	b	1
141.501	38.301	-20.8	-5.24	0.5	0.52	0.52	6550	b	1
141.51	43.854	5.23	-11.01	0.89	0.89	0.89	0008	m	1
141.54	43.077	1.74	-13.75	0.49	0.5	0.5	6520	b	1
141.577	42.884	0.45	-12.75	0.48	0.48	0.48	6522	b	1
141.602	42.655	-2.8	-13.14	0.47	0.48	0.48	5136	b	1
141.675	39.596	-4.74	-8.11	0.47	0.49	0.49	6547	b	1
141.713	40.405	-4.46	-12.34	0.46	0.47	0.47	5158	b	1
141.731	42.983	-1.28	-11.26	0.49	0.5	0.5	4014	b	1
141.741	44.892	12.58	-12.92	0.89	0.89	0.89	0104	m	1
141.741	44.892	14.06	-12.47	0.44	0.45	0.45	5104	b	1
141.75	45.403	12.09	-9.9	0.89	0.89	0.89	0001	m	1
141.75	45.403	14.25	-10.86	0.47	0.48	0.48	4001	b	1
141.756	44.398	11.03	-11.14	0.59	0.59	0.59	4003	b	1
141.789	40.133	-2.35	-10.83	0.46	0.48	0.48	4027	b	1
141.804	39.849	-6.43	-11.15	0.46	0.49	0.49	5164	b	1
141.891	43.248	-3.19	-11.5	1.44	1.44	1.44	6516	b	1
141.94	39.572	-6.13	-11.33	0.48	0.5	0.5	4028	b	1
141.951	39.869	-2.21	-12.76	0.89	0.89	0.89	0162	m	1
141.951	39.869	-3.52	-12.56	0.35	0.35	0.35	5162	b	1
141.955	39.458	-7.88	-13.29	2.01	2.01	2.01	5167	b	1
142.06	42.481	4.27	-12.88	0.47	0.48	0.48	5141	b	1
142.065	49.076	14.31	-15.03	1.12	1.11	1.11	UGLE	i	1
142.065	49.076	14.31	-15.03	1.12	1.11	1.11	UGLE	a	1
142.119	46.75	12.45	-13.99	1.61	1.72	1.72	YS10	m	1
142.13	47.057	12.8	-11.5	2.7	2.43	2.43	HOLS	m	1
142.152	44.007	5.82	-12.14	0.56	0.56	0.56	5110	b	1
142.157	49.637	13.67	-15.49	2.55	2.56	2.56	BOSH	a	1

Continued on next page...

Table B.1 – Continued from previous page

Long	Lat	Velocity (mm/yr)				Corr	Site	Source†	EXC‡
°E	°N	East	North	σ E	σ N				
142.17	45.336	11.6	-12.47	0.93	0.93	0.93	0101	m	1
142.17	45.336	11.35	-12.31	0.47	0.47	0.47	5101	b	1
142.265	44.728	10.1	-12.39	0.63	0.63	0.63	5105	b	1
142.296	42.727	-6.41	-9.76	0.89	0.89	0.89	0133	m	1
142.296	42.727	-6.12	-9.24	0.37	0.38	0.38	5133	b	1
142.392	47.03	13.6	-13.83	1.55	1.68	1.68	YS11	m	1
142.402	42.98	-8.2	-6.28	0.5	0.51	0.51	4012	b	1
142.482	43.59	-2.46	-8.9	0.53	0.54	0.54	4007	b	1
142.516	46.779	10.07	-12.92	1.6	1.86	1.86	PTRL	m	1
142.537	45.002	9.72	-12.99	0.67	0.67	0.67	5103	b	1
142.543	49.69	15.27	-15.16	2.65	2.67	2.67	AIVA	i	1
142.552	46.889	12	-13.71	1.51	1.75	1.75	YS04	m	1
142.568	46.827	12.18	-14.65	1.66	1.99	1.99	YS09	m	1
142.6	46.984	12.21	-16.66	1.6	1.67	1.67	YS08	m	1
142.626	44.295	6.08	-11.11	0.89	0.89	0.89	0107	m	1
142.626	44.294	6.18	-11.62	0.44	0.44	0.44	5107	b	1
142.63	47.075	13.11	-14.72	1.62	1.87	1.87	YS06	m	1
142.657	46.741	11.68	-13.47	1.47	1.75	1.75	YS05	m	1
142.657	46.972	11.71	-15.24	1.67	1.9	1.9	YS07	m	1
142.676	46.898	11.67	-15.45	1.9	1.9	1.9	YS03	m	1
142.717	47.03	13.32	-17.92	0.58	0.58	0.58	YSSK	m	1
142.717	47.03	14.57	-16.23	0.88	0.85	0.85	YUZN	m	1
142.759	48.573	12.38	-14.94	2.64	2.65	2.65	PORE	a	1
142.81	43.166	-7.82	-7.48	0.52	0.53	0.53	6518	b	1
142.817	49.838	13.73	-14.89	2.24	2.22	2.22	PBDN	i	1
142.824	46.633	9.71	-10.56	1.18	1.26	1.26	KORS	m	1
142.846	46.969	11.57	-14.05	1.58	1.76	1.76	YS12	m	1
142.935	42.131	-11.62	-7.24	0.5	0.5	0.5	5144	b	1
142.946	53.602	15.02	-16.45	0.81	0.8	0.8	OKHA	i	1
142.964	44.582	6.67	-12.94	0.64	0.64	0.64	6502	b	1
143.103	42.699	-10.74	-3	0.52	0.53	0.53	5134	b	1
143.156	42.006	-13.64	-6.04	0.51	0.51	0.51	4019	b	1
143.222	46.825	10.62	-15.5	2.98	2.26	2.26	OHOT	m	1
143.242	64.566	15.96	-16.11	1.36	1.35	1.35	UNR1	i	1
143.27	49.922	13.11	-18.34	2.57	2.58	2.58	PERV	i	1
143.316	42.125	-19.26	-4.37	0.51	0.52	0.52	6532	b	1
143.329	46.498	10.05	-11.8	1.5	1.66	1.66	BUSS	m	1
143.334	44.006	1.34	-10.37	0.61	0.61	0.61	5111	b	1
143.461	42.552	-14.44	-1.56	0.54	0.53	0.53	5138	b	1
143.562	43.289	-8.22	-5.61	0.58	0.58	0.58	5121	b	1
143.646	50.049	13.23	-16.13	2.55	2.56	2.56	PILG	i	1

Continued on next page...

Table B.1 – Continued from previous page

Long	Lat	Velocity (mm/yr)				Corr	Site	Source†	EXC‡
°E	°N	East	North	σ E	σ N				
143.787	43.849	0.64	-10.23	0.62	0.63	0.63	5114	b	1
143.804	50.292	14.22	-16.8	2.73	2.75	2.75	OKRG	i	1
143.927	42.895	-12.14	-0.72	0.58	0.58	0.58	5112	b	1
144.126	43.121	-12.37	-1.23	0.43	0.43	0.43	5124	b	1
144.127	43.121	-11.91	-0.99	0.89	0.89	0.89	0124	m	1
144.293	43.989	-2.69	-9.67	0.66	0.66	0.66	6505	b	1
144.325	43.233	-13.15	-1.37	0.62	0.62	0.62	5122	b	1
144.598	43.307	-13.84	0.12	0.68	0.68	0.68	6515	b	1
144.719	42.982	-17.94	-0.54	0.63	0.63	0.63	6531	b	1
144.774	43.409	-13.83	-2.58	0.66	0.66	0.66	5116	b	1
144.843	43.057	-17.36	-0.91	0.65	0.64	0.64	5125	b	1
144.87	13.59	-13.03	-0.28	1.14	1.03	1.03	GUAM	g	1
145.115	43.382	-16.52	-2.23	0.69	0.69	0.69	5118	b	1
145.131	43.662	-11.2	-4.82	0.71	0.71	0.71	5115	b	1
145.186	44.019	-0.67	-5.85	0.73	0.73	0.73	5109	b	1
146.993	-6.674	26.37	50.56	1.08	1.04	1.04	LAE1	m	1
147.19	-9.43	33.91	48.71	2.26	1.75	1.75	MORE	g	1
147.431	61.883	13.77	-21.64	1.33	1.33	1.33	KUL1	i	1
147.876	61.645	8.3	-14.93	1.52	1.54	1.54	OMK1	m	1
148.168	62.779	12.34	-19.03	1.25	1.25	1.25	SUS1	i	1
150.77	59.576	11.93	-16.72	1.76	1.74	1.74	MAG0	m	1
151.887	7.447	-71.67	21.1	1.05	0.99	0.99	TRUK	i	1
152.392	61.13	11.84	-21.3	2.3	2.23	2.23	TAL1	i	1
152.422	62.925	10.17	-19.5	1.2	1.18	1.18	SEY2	i	1
153.979	24.29	-71.09	20.64	1.15	1.07	1.07	MARC	i	1
155.77	62.518	9.3	-18.61	2.27	2.21	2.21	OMS1	i	1
155.962	54.304	3.89	-16.84	2.25	2.22	2.22	SOBL	i	1
156.244	52.661	-2.76	-13.18	2.3	2.25	2.25	UBR1	i	1
156.575	52.928	-2.52	-12.72	2.53	2.58	2.58	UBR2	i	1
156.738	57.091	8.15	-17.79	2.26	2.23	2.23	UHAZ	i	1
156.81	51.466	-6.26	-14.6	2.21	2.2	2.2	PAUZ	i	1
157.536	53.325	-1.26	-11.11	2.3	2.37	2.37	MAL1	i	1
158.213	53.28	-3.42	-9.76	2.21	2.18	2.18	KORC	i	1
158.607	53.067	-6.38	-9.08	0.48	0.46	0.46	PETP	m	1
158.607	53.067	-2.35	-11.55	1.17	1.18	1.18	PETR	i	1
158.623	54.693	2.3	-14.95	2.25	2.18	2.18	MILK	i	1
158.65	53.023	-9.14	-9.18	2.36	2.35	2.35	PETS	i	1
158.686	57.759	6.42	-21.76	1.67	1.65	1.65	_TIG	i	1
158.697	55.93	6.18	-17.15	1.03	1.04	1.04	_ES1	i	1
158.936	-54.5	-12.22	31.19	0.36	0.36	0.36	MAC1	i	1
159.197	53.142	-9.6	-7.74	2.18	2.16	2.16	NALY	i	1

Continued on next page...

Table B.1 – Continued from previous page

Long	Lat	Velocity (mm/yr)				Corr	Site	Source†	EXC‡
°E	°N	East	North	σ E	σ N				
159.865	56.042	4.44	-18.18	2.05	2.05	2.05	KOZY	i	1
160.062	56.254	5.73	-16.89	2.08	2.1	2.1	MAYS	i	1
160.856	56.318	9.13	-16.94	1.02	1.02	1.02	_KLU	i	1
161.194	54.585	-9.85	-6.89	2.2	2.18	2.18	KRON	i	1
162.593	56.265	-5.35	-11.7	2.07	2.06	2.06	UKAM	i	1
162.711	56.258	-1.86	-10.29	0.95	0.95	0.95	_KBG	i	1
163.067	59.243	7.01	-19.67	2.23	2.2	2.2	OSSO	i	1
165.984	55.192	-28.88	13.96	0.96	0.96	0.96	_BKI	i	1
166.147	60.445	1.51	-27.45	1.1	1.09	1.09	_TIL	i	1
166.211	62.456	6.71	-19.37	0.87	0.87	0.87	_KMS	i	1
166.438	68.076	7.56	-22.96	0.81	0.81	0.81	BILI	m	1
167.73	8.722	-71.45	26.65	0.57	0.41	0.41	KWJ1	i	1
167.73	8.722	-70.3	26.45	0.74	0.55	0.55	KWJ1	a	1
174.834	-36.603	1.01	36.58	0.48	0.4	0.4	AUCK	a	1
183.434	-43.956	-42.34	29.39	1.04	0.58	0.58	CHAT	a	1
200.335	22.126	-61.79	31.63	2.23	2.2	2.2	KOKB	m	1
200.335	22.126	-64.34	31.2	0.43	0.3	0.3	KOKB	a	1
204.544	19.801	-65.78	30.7	0.51	0.42	0.42	MKEA	a	1
207.499	57.735	-12.93	-12.07	0.66	0.63	0.63	KODK	m	1
210.394	-17.577	-72.84	32.62	1.84	0.52	0.52	THTI	a	1
212.501	64.978	-9.09	-21.86	0.34	0.33	0.33	FAIR	m	1
224.778	60.751	-13.2	-13.97	0.86	0.85	0.85	WHIT	m	1
240.375	49.323	-13.56	-11.17	0.14	0.14	0.14	DRAO	m	1
243.111	35.425	-19.01	-4.62	0.8	0.79	0.79	GOL2	m	1
243.111	35.425	-18.64	-4.93	0.35	0.33	0.33	GOLD	i	1
245.519	62.481	-17.69	-11.51	0.25	0.24	0.24	YELL	m	1
251.881	34.302	-13.69	-8.67	0.14	0.13	0.13	PIE1	m	1
254.767	40.131	-15.23	-7.45	0.22	0.21	0.21	TMGO	m	1
255.274	40.182	-14.99	-7.24	0.18	0.17	0.17	PLTC	m	1
255.985	30.681	-12.62	-6.75	0.14	0.12	0.12	MDO1	m	1
258.022	54.726	-17.88	-7.68	0.24	0.24	0.24	FLIN	m	1
264.134	50.259	-18.24	-5.01	0.24	0.24	0.24	DUBO	m	1
265.911	58.759	-18.94	-3.64	0.46	0.45	0.45	CHUR	m	1
268.425	41.772	-15.77	-2.09	0.16	0.15	0.15	NLIB	m	1
279.616	25.614	-9.92	1.39	1.62	1.55	1.55	RCM6	i	1
281.929	45.956	-16.51	1.97	0.18	0.18	0.18	ALGO	m	1
283.173	39.022	-14.78	3.52	0.14	0.14	0.14	GODE	m	1
288.507	-16.466	8.75	11.75	0.53	0.44	0.44	AREQ	m	1
288.507	42.613	-14.72	4.72	0.37	0.35	0.35	WES2	m	1
289.331	-33.15	20.98	13.47	0.55	0.54	0.54	SANT	m	1
291.175	76.537	-22.4	5.18	0.79	0.79	0.79	THU3	i	1

Continued on next page...

Table B.1 – Continued from previous page

Long	Lat	Velocity (mm/yr)				Corr	Site	Source†	EXC‡
°E	°N	East	North	σ E	σ N				
291.212	76.537	-21.92	5.16	0.37	0.36	0.36	THU1	m	1
293.167	54.832	-18.47	6.59	0.44	0.44	0.44	SCH2	m	1
295.304	32.37	-12.15	7.89	0.21	0.19	0.19	BRMU	m	1
302.1	-63.321	15.81	9.78	0.86	0.86	0.86	OHIG	i	1
307.194	5.252	-2.47	12.21	0.66	0.51	0.51	KOUR	m	1
307.322	47.595	-14.15	12.59	0.18	0.17	0.17	STJO	m	1
309.055	66.987	-17.17	12.25	0.35	0.33	0.33	KELY	m	1
312.122	-15.947	-2.54	10.88	0.23	0.23	0.23	BRAZ	m	1
321.574	-3.877	-2.51	11.1	0.7	0.66	0.66	FORT	m	1
342.535	14.685	18.06	19.63	1.39	1.27	1.27	DAKA	d	1
344.367	27.764	17.42	16.55	0.13	0.13	0.13	MAS1	m	1
345.588	-7.951	-4.45	9.2	0.81	0.61	0.61	ASC1	a	1
350.119	-40.349	24	16.62	0.94	0.97	0.97	GOUG	a	1
350.898	30.053	16.5	19.02	1.47	1.03	1.03	BAHA	d	1
351.381	33.162	19.9	19.1	1.57	1.05	1.05	SALA	d	1
351.601	43.364	24.85	20.43	1.37	1.15	1.15	ACOR	d	1
351.982	31.665	16.79	17.49	2.36	1.53	1.53	MARO	d	1
353.109	32.834	16.94	19.85	1.37	1.02	1.02	KBGA	d	1
353.133	33.976	17.19	16.35	0.67	0.66	0.66	IAVH	d	1
353.145	33.998	17.18	16.35	0.67	0.66	0.66	RABT	d	1
353.384	31.934	18.49	19.38	1.28	1.02	1.02	AZIL	d	1
353.794	36.464	16.81	16.56	0.5	0.49	0.49	SFER	d	1
354.102	30.415	16.71	18.16	1.47	1.01	1.01	ZARA	d	1
354.76	6.871	23.44	17.39	0.71	0.7	0.7	YKRO	d	1
354.892	33.54	17.62	16.08	0.84	0.83	0.83	IFRN	d	1
355.366	32.769	18.81	19.1	1.37	1.02	1.02	MBLD	d	1
355.465	32.255	17.86	17.47	1.52	1.04	1.04	RIC0	d	1
355.75	40.429	20.45	14.47	0.93	0.88	0.88	MADR	m	1
355.813	31.549	16.89	19.56	1.57	1.06	1.06	ERFD	d	1
356.048	40.444	21.38	15.59	0.51	0.5	0.5	VILL	m	1
356.048	40.444	20.38	15.59	0.32	0.23	0.23	VILL	a	1
359.519	38.339	21.25	16.5	0.92	0.87	0.87	ALAC	d	1
0	0	11.23	38.54	7.5	8.23	8.23	Sta.	k	2
27.708	-25.887	7.01	18.48	7.71	3.61	3.61	HARK	a	2
55.479	-4.674	31.57	18.64	4.07	3.53	3.53	SEY1	e	2
72.21	42.445	28.03	-0.69	3.52	3.44	3.44	TALA	a	2
73.997	44.208	26.72	-3.99	2.87	2.82	2.82	SUMK	a	2
74.336	39.842	32.14	14.6	4.33	3.72	3.72	ULUG	a	2
74.426	39.024	25.9	15.45	5.01	4.22	4.22	MUJI	a	2
74.751	42.999	31.14	-3.81	2.87	2.81	2.81	CHUM	a	2
74.951	38.662	27.17	19.6	5.07	4.35	4.35	BULU	a	2

Continued on next page...

Table B.1 – Continued from previous page

Long	Lat	Velocity (mm/yr)				Corr	Site	Source†	EXC‡
°E	°N	East	North	σ E	σ N				
75.25	39.718	34.04	14.06	4.3	3.72	3.72	WUQI	a	2
75.315	42.621	31.05	-0.33	3.17	3.1	3.1	SHAS	a	2
75.388	40.517	24.11	8.94	4.35	3.73	3.73	TURG	a	2
75.404	40.094	27.92	7.23	4.47	3.82	3.82	QIAK	a	2
75.447	36.851	22.15	17.93	5.32	4.41	4.41	KUNJ	a	2
75.479	38.853	33.46	15.5	5.29	4.43	4.43	GAZE	a	2
75.51	39.311	33.56	17.25	5.21	4.41	4.41	WUPA	a	2
75.899	39.195	30.85	12.22	4.36	3.77	3.77	AKTO	a	2
76.027	38.341	29.72	16.8	4.57	3.88	3.88	QIAE	a	2
76.174	38.935	37.75	11.37	4.32	3.72	3.72	YENG	a	2
76.294	31.897	29.61	26.12	7.17	3.5	3.5	JWAL	m	2
76.463	38.656	31.23	20.68	4.39	3.84	3.84	KIZI	a	2
76.512	39.806	27.35	12.28	4.95	4.25	4.25	SUGU	a	2
76.69	37.862	20.5	18.42	4.43	3.76	3.76	KOSR	a	2
76.734	39.497	26.65	17.23	4.99	4.22	4.22	JIAS	a	2
76.889	40.204	29.97	0.93	7.54	6.67	6.67	HAEJ	a	2
76.978	40.844	29.18	7.46	4.21	3.66	3.66	QIQI	a	2
76.981	36.846	17.74	21.23	5.28	4.03	4.03	AKME	a	2
77.005	36.577	24.8	21.75	4.62	3.78	3.78	MAZA	a	2
77.175	37.396	28.4	19.82	4.47	3.82	3.82	KOKY	a	2
77.277	38.174	32.76	19.48	4.76	3.85	3.85	ZEPU	a	2
77.624	38.904	34.8	17.48	4.57	3.82	3.82	MARK	a	2
77.906	37.258	27.03	14.1	4.48	3.84	3.84	KELI	a	2
78.037	39.714	31.78	7.74	4.17	3.69	3.69	KALA	a	2
78.246	37.559	27.82	19.14	4.42	3.77	3.77	PISH	a	2
78.451	40.942	29.34	10.76	4.16	3.64	3.64	AKQI	a	2
78.54	39.776	36.01	11.5	4.19	3.69	3.69	BACH	a	2
78.966	39.877	36.98	10.75	4.3	3.75	3.75	AKTA	a	2
79.035	40.503	34.56	10.24	4.22	3.71	3.71	KALP	a	2
79.21	30.49	23.56	26.62	3.33	2.24	2.24	TUNG	k	2
79.45	30.465	2.08	52.01	3.46	3.09	3.09	GARU	m	2
79.56	30.53	30.37	28.11	4.22	2.43	2.43	AULI	k	2
79.581	35.459	31.33	19.1	3.27	3.14	3.14	THAI	a	2
79.62	29.64	37.17	31.16	4.12	3.03	3.03	KTML	k	2
79.8	32.427	28.47	14.53	3.33	3.15	3.15	SQHE	a	2
80.239	41.143	35.09	7.81	4.15	3.67	3.67	AKSU	a	2
80.392	40.643	34.2	10.21	4.2	3.69	3.69	AWAT	a	2
83.257	43.398	32.27	-0.04	3.29	3.18	3.18	XYUA	a	2
85.14	31.02	35.92	17.36	3.51	3.41	3.41	TCOQ	k	2
85.538	38.081	31.42	-1.32	3.22	3.12	3.12	QIMO	a	2
85.74	29.59	38.88	18.84	3.71	3.41	3.41	SHOT	k	2

Continued on next page...

Table B.1 – Continued from previous page

Long	Lat	Velocity (mm/yr)				Corr	Site	Source†	EXC‡
°E	°N	East	North	σ E	σ N				
86.02	28.29	38.22	21.74	3.61	1.93	1.93	WT11	e	2
86.93	27.97	40	26.12	3.71	3.61	3.61	SCOL	k	2
87.177	43.471	35.03	7.79	3.53	3.39	3.39	GUAO	m	2
87.766	31.891	41.7	14.22	3.32	3.15	3.15	NYMA	a	2
88.5	27.09	37.09	29.51	8.5	4.21	4.21	DELO	k	2
88.85	50.59	26.52	-3.61	4.87	4.34	4.34	YAZU	g	2
88.898	39.243	22.8	3.43	4.77	3.61	3.61	HOTL	l	2
89.63	38.468	24.28	2.06	3.66	2.03	2.03	NICE	a	2
90.131	38.031	32.17	5.47	3.88	4.2	4.2	COOL	l	2
90.96	29.28	48.04	14.39	3.61	3.51	3.51	GGAR	k	2
90.982	38.588	33.98	-0.71	3.29	3.15	3.15	XORK	a	2
91.85	25.53	41.77	28.46	7.6	3.81	3.81	SHIL	k	2
91.91	38.09	37.07	-2.2	3.31	2.91	2.91	AL23	k	2
91.985	32.986	45.57	4.09	3.36	3.16	3.16	TGLA	a	2
93.052	35.088	42.54	2.11	3.4	3.17	3.17	WUDA	a	2
93.24	29.88	56.08	-0.61	3.21	2.53	2.53	GNGB	e	2
93.412	38.809	35.74	-7.63	3.29	3.15	3.15	LEHU	a	2
93.626	42.81	34.31	-10.13	3.29	3.16	3.16	HAMI	a	2
93.91	35.52	42.16	-0.1	3.7	2.71	2.71	BUDO	k	2
94.831	36.346	35.65	0.17	4.33	2.95	2.95	GLMD	a	2
96.46	36.38	37.59	0.61	3.01	2.71	2.71	G0CQ	k	2
96.868	29.391	39.29	-12.63	3.33	3.14	3.14	RAWU	a	2
96.988	32.997	46.14	-3.99	3.32	3.15	3.15	YUSH	a	2
97.819	0.559	28.98	24.86	4.2	2.8	2.8	D952	a	2
99.918	22.554	25.19	-12.49	3.4	3.19	3.19	LANC	a	2
100.449	-0.942	24.04	18.56	3.9	3.6	3.6	SPG2	a	2
100.76	1.653	52.53	-12	4.9	5.5	5.5	BLMS	a	2
101.033	12.764	31.28	-8.25	4.56	2.96	2.96	RYNG	i	2
101.097	6.733	28.25	-7.4	6.91	4.36	4.36	PATN	i	2
101.139	30.991	33.68	-14.1	4.05	3.06	3.06	DAOF	a	2
101.219	1.222	43.11	-5.89	4.6	5.7	5.7	DURI	a	2
101.27	25.21	26.64	-22.74	4.2	2.31	2.31	H137	k	2
101.497	30.495	43.15	-18.24	3.29	3.13	3.13	QLIN	a	2
101.512	28.996	30.68	-17.48	4.34	3.01	3.01	JIUL	a	2
102.164	-5.256	22.51	18.04	7.9	3.4	3.4	ENGG	a	2
102.219	27.902	39.75	-18.03	4.42	3.26	3.26	XICH	a	2
102.306	31.706	35.72	-8.92	3.33	3.15	3.15	BARK	a	2
102.48	24.95	38.25	-23.94	3.9	3.4	3.4	AN07	k	2
102.74	24.27	33.69	-16.61	3.6	3.31	3.31	JC02	k	2
102.81	24.81	30.32	-20.13	3.7	3.3	3.3	CG06	k	2
102.89	25.06	32.63	-16.85	3.9	3.3	3.3	DQ03	k	2

Continued on next page...

Table B.1 – Continued from previous page

Long	Lat	Velocity (mm/yr)				Corr	Site	Source†	EXC‡
°E	°N	East	North	σ E	σ N				
102.99	24.95	36.42	-16.97	4	3.4	3.4	YZ05	k	2
103.04	25.35	32.94	-19.89	4.1	3.3	3.3	SM04	k	2
103.28	50.38	27.81	-8.37	2.72	3.26	3.26	ZAKM	g	2
103.526	28.843	35.75	-16.34	3.34	3.14	3.14	MABI	a	2
103.889	33.276	38.74	-6.33	3.34	3.16	3.16	JZAI	a	2
105.379	35.141	33.53	-10.46	3.28	3.14	3.14	TWEI	a	2
105.638	-6.489	22.92	-10.19	6.4	2.42	2.42	BPIL	a	2
105.669	38.809	32.68	-10.86	3.33	3.17	3.17	AZUO	a	2
105.69	-10.45	35.33	54.84	4	1.61	1.61	XMAS	a	2
106.034	30.804	34.81	-12.71	3.35	3.15	3.15	NCHO	a	2
106.665	26.415	32.21	-12.14	3.33	3.15	3.15	GYAN	a	2
106.681	33.116	35.81	-13.97	3.32	3.15	3.15	MIXN	a	2
106.831	22.107	32.27	-12.51	3.36	3.15	3.15	PXIN	a	2
108.086	35.058	35.1	-13.14	3.29	3.15	3.15	BXIN	a	2
109.412	0.807	26.23	-17.88	5.1	3.3	3.3	KAYA	a	2
110.219	1.586	17.2	-9.93	4.1	1.12	1.12	T030	f	2
110.254	30.812	32.67	-14.12	3.29	2.96	2.96	TG24	a	2
110.306	25.186	34.81	-18.78	3.34	3.14	3.14	GUIL	a	2
110.328	30.635	33.27	-16.84	3.31	2.96	2.96	TG27	a	2
110.468	31.407	36.93	-16.08	3.39	2.98	2.98	TG11	a	2
111.029	38.488	30.39	-13.97	3.32	3.17	3.17	XIXN	a	2
111.119	30.666	33.11	-14.64	3.23	2.9	2.9	TG29	a	2
111.67	-2.686	24.06	-11.11	3.9	1.81	1.81	PANG	a	2
112.335	16.834	29.14	-14.12	3.38	3.22	3.22	YDAO	a	2
113.105	34.521	30.26	-12.24	3.3	3.15	3.15	ZHZH	a	2
113.181	36.226	30.64	-14.61	3.33	3.16	3.16	CZHI	a	2
114.755	-3.424	17.49	-13.66	8.8	2.31	2.31	BANJ	a	2
115.047	27.059	32.14	-16.76	3.33	3.15	3.15	JEAN	a	2
116.104	43.903	24.94	-13.45	3.32	3.18	3.18	XHOT	a	2
118.693	-8.487	15.28	-7.13	2.51	4.9	4.9	BIMA	a	2
119.034	31.654	32.55	-15.2	3.34	3.16	3.16	LISH	a	2
119.474	39.825	29.24	-14.57	3.35	3.17	3.17	BEID	a	2
120.301	-9.606	29.62	12.83	6.3	2.11	2.11	WAIN	a	2
120.427	36.053	30.02	-12.67	3.34	3.17	3.17	QDAO	a	2
120.478	-8.54	2.26	4.45	5.5	4	4	RUTE	a	2
120.78	27.971	33.28	-21.26	3.36	3.16	3.16	WENZ	a	2
121.74	39.092	27.76	-12.05	3.34	3.17	3.17	DLIA	a	2
122.172	46.062	27.01	-15.34	3.35	3.2	3.2	UHOT	a	2
122.736	-4.227	23.24	7.23	5.14	2.81	2.81	KEND	i	2
124.103	50.39	22.47	-12.06	3.33	3.22	3.22	JAGD	a	2
124.692	24.642	35.33	-55.41	3.43	3.6	3.6	6748	b	2

Continued on next page...

Table B.1 – Continued from previous page

Long	Lat	Velocity (mm/yr)				Corr	Site	Source†	EXC‡
°E	°N	East	North	σ E	σ N				
124.925	1.536	23.33	-14.62	4.2	2.01	2.01	MANA	a	2
125.575	9.647	-17.53	19.17	4.45	2.8	2.8	SURI	i	2
126.969	46.65	15.3	-10.29	3.35	3.21	3.21	SUIH	a	2
127.38	0.825	-61.72	-6.13	5.9	3.21	3.21	TERN	a	2
127.644	-1.341	-35.09	3.18	3.2	2.51	2.51	OBIX	a	2
129.489	43.003	25.46	-13.71	3.35	3.2	3.2	YANJ	a	2
129.775	-4.489	33.26	32.39	4	1.72	1.72	BAPI	a	2
131.17	46.65	22.67	-19.28	3.73	3.39	3.39	SHUA	a	2
136.09	-1.16	-32.06	91.23	6.9	6.7	6.7	BIAK	a	2
136.24	-1.862	-5.07	40.23	5.9	5.4	5.4	YAPE	a	2
141.133	39.135	0.55	-17.27	3.95	3.96	3.96	MIZU	m	2
157.474	53.333	-1.41	-13.37	3.22	3.23	3.23	MALK	i	2
159.481	54.025	1.18	-15.12	4.15	4.1	4.1	KRM9	i	2
204.544	19.801	-67.4	32.38	2.94	2.92	2.92	MKEA	m	2
234.75	71.99	-12.5	-0.37	4.81	4.51	4.51	SACH	m	2
242.239	70.736	-19.15	-9.31	3.37	3.17	3.17	HOLM	i	2
243.111	35.425	-14.67	-16.72	6.26	4.95	4.95	GOL2	m	2
265.106	74.691	-29.45	5.45	2.89	2.85	2.85	RESO	i	2
288.507	-16.466	-5.1	5.17	3.47	3.3	3.3	AREQ	i	2

†- *GPS data sources*
- *a* - Bock et al., 2003
- *b* - Zhang et al., 2004
- *c* - Shen et al., 2005
- *d* - Reilinger et al., 2006
- *e* - Bettinelli et al., 2006
- *f* - Socquet et al., 2006
- *g* - Calais et al., 2006
- *h* - Jade et al., 2007
- *i* - Simons et al., 2007
- *j* - Sol et al., 2007
- *k* - Gan et al., 2007
- *l* - Kogan and Steblov, 2008
- *m* - Banerjee et al., 2008

‡- *GPS site exclusion reasons (see text for full explaination)*
- *U* - Used in inversion
- *1* - Outside study area
- *2* - High error

3 - Duplicate site

Table B.2: Detailed segment geometry of the elastic dislocations that bound the blocks in the India model.

Segment	Start Point		End Point		Locking Depth	Dip	Slip Rate (mm/yr)		
Number	Long °E	Lat °N	Long °E	Lat °N	(km)	°	Strike-Slip	Dip-Slip	Tensile
1	26.598	-26.764	26.632	-28.335	15	90	7.0	0.0	-2.5
2	26.598	-26.764	27.978	-26.207	15	90	5.0	0.0	5.5
3	26.632	-28.335	37.563	-37.145	15	90	3.8	0.0	-6.2
4	27.509	-24.423	27.978	-26.207	15	90	6.4	0.0	-3.9
5	27.509	-24.423	33.111	-21.293	15	90	5.5	0.0	5.0
6	28.971	-2.697	33.677	-8.94	15	90	4.1	0.0	-6.3
7	28.971	-2.697	32.208	5.673	15	90	7.6	0.0	0.0
8	32.208	5.673	36.192	5.092	15	90	1.8	0.0	7.3
9	32.232	-47.095	37.563	-37.145	15	90	6.9	0.0	1.7
10	32.232	-47.095	67.986	-26.574	15	90	-2.6	0.0	-5.7
11	33.111	-21.293	33.677	-8.94	15	90	7.1	0.0	-2.0
12	34.37	27.29	35.01	29.61	15	90	12.5	0.0	3.9
13	34.37	27.29	35.57	25.55	15	90	10.7	0.0	-7.9
14	35.01	29.61	35.58	31.32	15	90	12.3	0.0	6.1
15	35.47	31.38	35.58	31.32	15	90	10.1	0.0	-9.8
16	35.47	31.38	35.72	33.68	18	90	13.3	0.0	5.5
17	35.57	25.55	43.607	11.99	15	90	10.5	0.0	-15.4
18	35.72	33.68	36.31	34.44	15	90	8.9	0.0	12.2
19	36.192	5.092	37.609	5.96	15	90	6.0	0.0	4.4
20	36.31	34.44	36.43	36.63	15	90	14.0	0.0	7.3
21	36.43	36.63	36.629	37.025	15	90	10.5	0.0	12.6
22	36.629	37.025	36.83	37.42	15	90	10.5	0.0	13.0
23	36.83	37.42	38.65	38.2	15	90	0.1	0.0	17.5
24	37.609	5.96	41.435	11.28	15	90	7.3	0.0	1.6
25	38.65	38.2	40.27	38.83	15	90	-0.3	0.0	18.8
26	40.27	38.83	42.498	36.803	15	90	-18.7	0.0	6.3

Continued on next page...

Table B.2 – Continued from previous page

Segment	Start Point		End Point		Locking Depth	Dip	Slip Rate (mm/yr)		
Number	Long °E	Lat °N	Long °E	Lat °N	(km)	°	Strike-Slip	Dip-Slip	Tensile
27	41.435	11.28	43.607	11.99	15	90	5.1	0.0	5.4
28	42.498	36.803	44.005	36.521	15	30	-10.6	20.3	0.0
29	43.607	11.99	47.193	12.364	0	90	-12.1	0.0	-13.1
30	44.005	36.521	45.587	34.893	15	30	-19.4	10.1	0.0
31	45.587	34.893	45.82	33.44	15	30	-21.6	-1.2	0.0
32	45.82	33.44	48.96	31.39	15	30	-15.1	19.3	0.0
33	47.193	12.364	51.265	13.186	0	90	-13.7	0.0	-14.7
34	48.96	31.39	51.43	29.42	15	30	-16.3	21.0	0.0
35	51.265	13.186	52.236	14.643	0	90	-21.2	0.0	-2.3
36	51.43	29.42	51.64	28.23	15	90	-24.7	0.0	5.5
37	51.64	28.23	54.25	26.85	15	30	-10.7	27.9	0.0
38	52.236	14.643	56.234	14.643	0	90	9.4	0.0	20.8
39	54.25	26.85	57.12	27.62	15	90	11.9	0.0	25.6
40	56.234	14.643	59.363	14.913	15	90	-1.6	0.0	-5.2
41	56.234	14.643	58.222	12.731	15	90	5.8	0.0	-19.0
42	56.993	9.909	58.222	12.731	15	90	20.7	0.0	-2.9
43	56.993	9.909	62.319	4.673	15	90	3.7	0.0	-23.3
44	57.12	27.62	57.3	26.67	15	90	-27.9	0.0	8.9
45	57.3	26.67	57.49	25.72	15	90	-27.7	0.0	9.9
46	57.49	25.72	57.8	25.05	15	90	-24.8	0.0	16.4
47	57.8	25.05	61.44	24.44	15	30	1.2	35.9	0.0
48	59.363	14.913	59.91	15.413	15	90	-4.5	0.0	-3.1
49	59.91	15.413	60.729	19.42	15	90	-5.5	0.0	0.0
50	60.729	19.42	62.186	22.151	15	90	-5.3	0.0	-1.6
51	61.44	24.44	65.89	24.9	15	30	11.5	36.5	0.0
52	62.186	22.151	65.89	24.9	15	90	-4.2	0.0	-3.7
53	62.319	4.673	64.396	3.018	15	90	0.9	0.0	-26.8
54	64.396	3.018	65.444	3.173	15	90	-19.6	0.0	-19.8

Continued on next page...

Table B.2 – Continued from previous page

Segment	Start Point		End Point		Locking Depth	Dip	Slip Rate (mm/yr)		
Number	Long °E	Lat °N	Long °E	Lat °N	(km)	°	Strike-Slip	Dip-Slip	Tensile
55	65.213	-18.118	67.458	-16.7	15	90	35.7	0.0	1.2
56	65.213	-18.118	66.335	-19.95	15	90	1.5	0.0	-36.9
57	65.444	3.173	66.264	2.627	15	90	-1.1	0.0	-28.4
58	65.89	24.9	66.184	26.773	15	90	29.1	0.0	-2.3
59	65.981	-14.16	66.225	-11.334	15	90	22.1	0.0	-22.1
60	65.981	-14.16	67.458	-16.7	15	90	5.1	0.0	-33.8
61	66.184	26.773	71.55	34.595	15	90	28.0	0.0	11.1
62	66.225	-11.334	67.222	-9.788	15	90	29.1	0.0	-6.7
63	66.264	2.627	66.739	1.018	15	90	17.5	0.0	-23.2
64	66.335	-19.95	68.699	-21.191	15	90	-17.6	0.0	-35.2
65	66.739	1.018	67.857	-1.652	15	90	14.8	0.0	-26.3
66	67.222	-9.788	68.221	-6.842	15	90	26.9	0.0	-10.5
67	67.857	-1.652	68.452	-4.004	15	90	18.7	0.0	-25.3
68	67.986	-26.574	69.939	-25.562	15	90	-2.8	0.0	-4.3
69	68.221	-6.842	69.047	-6.825	15	90	-5.3	0.0	-1.3
70	68.221	-6.842	68.452	-4.004	15	90	26.1	0.0	-19.2
71	68.699	-21.191	69.939	-25.562	15	90	14.5	0.0	-40.3
72	69.047	-6.825	70.538	-6.985	15	90	-5.1	0.0	-1.2
73	69.939	-25.562	78.26	-40.807	15	90	14.9	0.0	-53.3
74	70.538	-6.985	73.348	-7.651	15	90	-5.0	0.0	-0.4
75	71.55	34.595	74.632	32.753	18	8	-5.0	18.2	0.0
76	71.55	34.595	75.774	36.626	15	90	4.1	0.0	14.7
77	73.348	-7.651	73.884	-4.318	15	90	0.9	0.0	6.1
78	73.884	-4.318	74.828	-4.512	15	90	-7.2	0.0	0.9
79	74.51	39.887	75.774	36.626	15	90	27.0	0.0	-4.4
80	74.51	39.887	77.739	39.887	15	90	0.3	0.0	25.5
81	74.632	32.753	75.885	31.42	18	8	-9.4	15.5	0.0
82	74.828	-4.512	76.21	-5.039	15	90	-7.4	0.0	0.6

Continued on next page...

Table B.2 – Continued from previous page

Segment	Start Point		End Point		Locking Depth	Dip	Slip Rate (mm/yr)		
Number	Long °E	Lat °N	Long °E	Lat °N	(km)	°	Strike-Slip	Dip-Slip	Tensile
83	75.774	36.626	80.872	35.846	15	90	9.5	0.0	-2.2
84	75.774	36.626	78.489	33.634	15	90	3.7	0.0	-3.3
85	75.885	31.42	76.925	30.433	18	8	-8.3	15.7	0.0
86	76.21	-5.039	78.067	-4.928	15	90	-6.3	0.0	4.6
87	76.925	30.433	78.205	29.607	18	8	-5.0	16.7	0.0
88	77.739	39.887	82.761	41.727	15	90	11.2	0.0	15.6
89	78.067	-4.928	99.226	-3.16	15	90	-6.4	0.0	12.1
90	78.205	29.607	79.352	28.967	18	8	-3.6	16.6	0.0
91	78.26	-40.807	163.25	-46.913	15	90	22.3	0.0	-68.6
92	78.489	33.634	80.905	31.102	15	90	-4.1	0.0	2.8
93	78.489	33.634	79.801	33.353	15	90	8.3	0.0	0.0
94	79.352	28.967	79.939	28.7	18	8	-2.1	16.6	0.0
95	79.801	33.353	83.104	36.287	15	90	41.5	0.0	-1.8
96	79.801	33.353	86.675	31.681	15	90	-14.6	0.0	-20.5
97	79.939	28.7	80.925	28.327	18	6	-0.8	16.4	0.0
98	80.872	35.846	83.104	36.287	15	90	5.7	0.0	-11.5
99	80.905	31.102	84.424	29.557	15	90	-2.4	0.0	4.3
100	80.925	28.327	81.752	28.007	18	6	-0.8	16.1	0.0
101	81.752	28.007	83.005	27.58	18	6	0.1	15.8	0.0
102	82.761	41.727	86.493	41.464	15	90	4.3	0.0	12.1
103	83.005	27.58	84.312	27.18	18	6	0.8	15.4	0.0
104	83.104	36.287	86.247	37.641	15	90	41.2	0.0	-3.1
105	84.312	27.18	86.045	26.647	18	8	1.0	14.9	0.0
106	84.424	29.557	86.292	29.501	15	90	-0.3	0.0	5.0
107	86.045	26.647	87.138	26.46	18	8	-0.2	15.1	0.0
108	86.045	26.647	86.616	28.433	15	90	0.3	0.0	-5.0
109	86.247	37.641	92.427	39.006	15	90	13.7	0.0	5.8
110	86.247	37.641	91.368	36.025	15	90	22.7	0.0	12.0

Continued on next page...

Table B.2 – Continued from previous page

Segment	Start Point		End Point		Locking Depth	Dip	Slip Rate (mm/yr)		
Number	Long °E	Lat °N	Long °E	Lat °N	(km)	°	Strike-Slip	Dip-Slip	Tensile
111	86.292	29.501	86.616	28.433	15	90	-3.2	0.0	-6.8
112	86.292	29.501	86.675	31.681	15	90	5.1	0.0	-9.5
113	86.493	41.464	88.911	41.043	15	90	3.2	0.0	7.6
114	86.675	31.681	90.063	31.601	15	90	-4.1	0.0	1.5
115	87.138	26.46	88.511	26.48	18	8	3.1	16.3	0.0
116	88.511	26.48	89.885	26.487	18	8	5.6	14.0	0.0
117	88.511	26.48	89.119	27.758	15	90	4.6	0.0	2.3
118	88.911	41.043	91.014	41.201	15	90	4.9	0.0	2.5
119	89.119	27.758	89.924	28.498	15	90	4.3	0.0	-0.1
120	89.885	26.487	93.511	26.86	18	8	6.5	17.1	0.0
121	89.885	26.487	90.004	25.201	15	90	-4.0	0.0	2.3
122	89.924	28.498	90.311	30.06	15	90	2.6	0.0	-6.5
123	90.004	25.201	92.009	25.021	15	90	2.7	0.0	6.1
124	90.063	31.601	91.711	31.155	15	90	-5.0	0.0	4.7
125	90.311	30.06	91.711	31.155	15	90	7.4	0.0	-8.7
126	91.014	41.201	92.427	39.006	15	90	1.1	0.0	2.2
127	91.059	24.022	92.681	20.05	40	15	-18.3	15.5	0.0
128	91.059	24.022	92.009	25.021	15	90	-26.6	0.0	-4.8
129	91.368	36.025	94.336	35.706	15	90	23.9	0.0	-0.7
130	91.711	31.155	96.113	29.735	15	90	8.5	0.0	4.2
131	91.899	11.203	91.901	9.703	40	18	-19.8	25.2	0.0
132	91.899	11.203	92.114	12.92	40	18	-22.6	22.6	0.0
133	91.901	9.703	92.092	8.095	40	18	-16.8	27.3	0.0
134	92.009	25.021	95.454	26.213	15	90	-16.3	0.0	-2.0
135	92.092	8.095	93.016	4.994	38	15	-12.1	29.2	0.0
136	92.114	12.92	92.818	14.308	40	18	-28.4	13.7	0.0
137	92.427	39.006	96.621	40.011	15	90	8.3	0.0	2.2
138	92.427	39.006	95.184	37.347	15	90	0.7	0.0	5.6

Continued on next page...

Table B.2 – Continued from previous page

Segment	Start Point		End Point		Locking Depth	Dip	Slip Rate (mm/yr)		
Number	Long °E	Lat °N	Long °E	Lat °N	(km)	°	Strike-Slip	Dip-Slip	Tensile
139	92.681	20.05	94.105	18.085	40	15	-15.4	10.9	0.0
140	92.818	14.308	94.285	16.204	40	15	-30.2	8.2	0.0
141	92.822	4.493	93.016	4.994	0	90	-26.7	0.0	14.6
142	92.822	4.493	93.807	2.988	40	15	-3.6	31.2	0.0
143	93.511	26.86	95.671	27.74	18	8	13.3	21.9	0.0
144	93.737	10.202	93.778	8.373	15	90	-18.0	0.0	-9.4
145	93.737	10.202	95.202	11.14	15	90	-1.1	0.0	-21.0
146	93.778	8.373	94.078	7.08	15	90	-19.4	0.0	-4.6
147	93.807	2.988	96.015	1.705	40	15	10.3	29.2	0.0
148	94.078	7.08	95.065	5.8	15	90	-19.4	0.0	4.7
149	94.105	18.085	94.285	16.204	40	15	-17.1	-3.7	0.0
150	94.127	23.944	94.162	21.309	15	90	-2.4	0.0	15.6
151	94.127	23.944	95.454	26.213	15	90	-7.9	0.0	6.3
152	94.162	21.309	94.512	19.179	15	90	0.4	0.0	22.0
153	94.285	16.204	94.723	17.523	15	90	-12.5	0.0	28.0
154	94.336	35.706	97.177	34.061	15	90	17.0	0.0	-4.7
155	94.336	35.706	96.762	35.647	15	90	11.2	0.0	5.5
156	94.512	19.179	94.723	17.523	15	90	-0.4	0.0	26.9
157	95.065	5.8	97.816	3.524	30	90	-17.7	0.0	10.5
158	95.184	37.347	97.448	37.026	15	90	2.8	0.0	3.1
159	95.202	11.14	95.24	12.645	15	90	-18.3	0.0	-11.6
160	95.24	12.645	95.718	12.831	15	90	3.9	0.0	-21.7
161	95.454	26.213	97.095	26.792	0	90	-24.0	0.0	4.1
162	95.671	27.74	96.838	27.344	0	90	-8.1	0.0	28.7
163	95.692	13.389	95.718	12.831	15	90	-19.4	0.0	-10.9
164	95.692	13.389	96.533	14.122	15	90	-3.7	0.0	-22.3
165	95.817	23.853	95.989	22.919	15	90	-22.1	0.0	0.1
166	95.817	23.853	96.917	25.923	0	90	-17.3	0.0	-17.8

Continued on next page...

Table B.2 – Continued from previous page

Segment	Start Point		End Point		Locking Depth	Dip	Slip Rate (mm/yr)		
Number	Long °E	Lat °N	Long °E	Lat °N	(km)	°	Strike-Slip	Dip-Slip	Tensile
167	95.989	22.919	97.98	23.243	15	90	8.5	0.0	-0.2
168	95.989	22.919	96.032	21.221	15	90	-23.1	0.0	-9.3
169	96.015	1.705	96.959	0.327	50	15	-2.7	30.5	0.0
170	96.032	21.221	96.217	19.29	15	90	-23.6	0.0	-5.8
171	96.113	29.735	97.501	28.144	15	90	6.4	0.0	4.4
172	96.217	19.29	96.533	14.122	15	90	-20.1	0.0	-12.5
173	96.217	19.29	99.097	19.855	15	90	8.9	0.0	2.8
174	96.621	40.011	99.599	38.973	15	90	5.4	0.0	5.8
175	96.762	35.647	97.299	35.573	15	90	10.5	0.0	5.3
176	96.838	27.344	97.501	28.144	15	90	-1.2	0.0	6.3
177	96.838	27.344	97.095	26.792	0	90	-23.3	0.0	19.5
178	96.917	25.923	97.095	26.792	0	90	-22.4	0.0	-17.7
179	96.959	0.327	97.883	-1.23	25	15	-4.6	30.0	0.0
180	97.177	34.061	99.22	32.56	15	90	17.4	0.0	-4.4
181	97.299	35.573	102.174	34.024	15	90	9.6	0.0	3.6
182	97.448	37.026	100.268	37.055	15	90	3.2	0.0	0.9
183	97.816	3.524	100.054	0.535	30	90	-19.9	0.0	8.1
184	97.883	-1.23	98.595	-2.352	40	15	-3.7	29.7	0.0
185	97.98	23.243	99.325	23.741	0	90	8.8	0.0	1.6
186	98.595	-2.352	99.226	-3.16	35	15	-1.0	29.7	0.0
187	99.097	19.855	101.641	20.918	15	90	9.5	0.0	2.2
188	99.22	32.56	101.819	30.376	15	90	17.6	0.0	-5.1
189	99.226	-3.16	100.705	-5.171	50	15	-21.1	34.4	0.0
190	99.325	23.741	100.134	24.475	0	90	9.3	0.0	0.6
191	99.599	38.973	102.155	37.367	15	90	4.1	0.0	5.8
192	100.054	0.535	100.532	-0.668	30	90	-21.6	0.0	3.9
193	100.134	24.475	100.413	25.464	0	90	8.9	0.0	-2.1
194	100.268	37.055	102.155	37.367	15	90	3.1	0.0	-1.1

Continued on next page...

Table B.2 – Continued from previous page

Segment	Start Point		End Point		Locking Depth	Dip	Slip Rate (mm/yr)		
Number	Long °E	Lat °N	Long °E	Lat °N	(km)	°	Strike-Slip	Dip-Slip	Tensile
195	100.413	25.464	100.673	26.894	15	90	1.5	0.0	-1.3
196	100.413	25.464	101.826	23.685	70	90	-5.8	0.0	4.8
197	100.532	-0.668	101.759	-2.654	30	90	-20.5	0.0	8.6
198	100.673	26.894	101.766	27.959	15	90	1.2	0.0	2.4
199	100.705	-5.171	102.135	-6.944	15	15	-19.7	36.0	0.0
200	101.641	20.918	103.004	21.5	15	90	9.5	0.0	3.2
201	101.759	-2.654	104.638	-5.66	30	90	-18.2	0.0	14.4
202	101.766	27.959	102.318	29.013	15	90	2.4	0.0	4.5
203	101.819	30.376	102.318	29.013	15	90	18.2	0.0	2.7
204	101.826	23.685	103.116	23.074	70	90	-2.8	0.0	7.3
205	102.135	-6.944	105.146	-8.524	15	15	-4.4	42.0	0.0
206	102.155	37.367	104.775	37.324	15	90	9.8	0.0	-0.8
207	102.174	34.024	105.639	33.715	15	90	9.2	0.0	-4.1
208	102.197	27.964	102.878	26.906	15	90	7.7	0.0	-6.2
209	102.197	27.964	102.318	29.013	15	90	9.5	0.0	0.6
210	102.318	29.013	105.639	33.715	15	90	-0.4	0.0	3.0
211	102.878	26.906	103.17	25.86	15	90	9.2	0.0	-5.2
212	103.004	21.5	103.116	23.074	15	90	7.6	0.0	-6.3
213	103.116	23.074	103.587	22.837	70	90	-1.5	0.0	4.7
214	103.116	23.074	103.152	24.761	15	90	10.4	0.0	-5.2
215	103.152	24.761	103.17	25.86	15	90	10.4	0.0	-3.8
216	103.587	22.837	106.263	20.106	70	90	-2.9	0.0	3.5
217	104.092	51.633	106.616	41.741	70	90	-3.2	0.0	-0.8
218	104.092	51.633	108.107	53.034	70	90	-0.8	0.0	-3.0
219	104.638	-5.66	105.3	-7.077	30	90	-22.2	0.0	9.2
220	104.775	37.324	105.622	37.12	15	90	10.0	0.0	0.2
221	105.146	-8.524	107.901	-9.924	0	30	-15.4	73.5	0.0
222	105.146	-8.524	105.3	-7.077	0	90	-24.0	0.0	-2.9

Continued on next page...

Table B.2 – Continued from previous page

Segment	Start Point		End Point		Locking Depth	Dip	Slip Rate (mm/yr)		
Number	Long °E	Lat °N	Long °E	Lat °N	(km)	°	Strike-Slip	Dip-Slip	Tensile
223	105.622	37.12	106.52	36.638	15	90	9.6	0.0	2.1
224	105.639	33.715	106.655	35.42	15	90	-2.0	0.0	0.8
225	105.786	38.305	107.079	39.418	15	90	-1.5	0.0	-5.4
226	105.786	38.305	106.454	37.383	15	90	-5.9	0.0	-0.6
227	106.263	20.106	119.866	12.531	0	90	-1.6	0.0	1.9
228	106.454	37.383	106.52	36.638	15	90	-4.9	0.0	-3.4
229	106.52	36.638	106.655	35.42	15	90	-0.2	0.0	4.0
230	106.616	41.741	109.387	40.968	70	90	0.6	0.0	-1.2
231	106.616	41.741	106.622	41.256	15	90	-4.6	0.0	-1.8
232	106.622	41.256	107.079	39.418	15	90	-4.9	0.0	-1.4
233	106.655	35.42	108.28	34.659	70	90	0.6	0.0	-0.4
234	107.901	-9.924	121.911	-11.189	30	30	6.9	81.7	0.0
235	108.107	53.034	109.768	55.595	70	90	-2.5	0.0	-1.5
236	108.28	34.659	110.406	34.73	70	90	0.1	0.0	-1.1
237	109.387	40.968	111.092	40.67	70	90	0.5	0.0	-0.7
238	109.768	55.595	142.406	54.636	70	90	-0.6	0.0	-1.9
239	110.406	34.73	113.499	40.037	70	90	-1.3	0.0	-1.6
240	111.092	40.67	112.498	40.476	70	90	0.4	0.0	-0.3
241	112.498	40.476	113.499	40.037	70	90	0.5	0.0	0.2
242	112.884	4.714	115.187	8.428	0	90	-3.2	0.0	3.8
243	112.884	4.714	119.24	-0.291	0	90	3.8	0.0	4.1
244	113.499	40.037	120.407	35.949	70	90	3.1	0.0	-0.5
245	115.187	8.428	118.146	7.142	0	90	-4.0	0.0	-2.9
246	118.146	7.142	121.415	9.875	0	90	-4.5	0.0	2.0
247	119.24	-0.291	119.629	0.007	0	90	5.4	0.0	-2.4
248	119.422	0.968	119.629	0.007	0	90	0.1	0.0	-5.9
249	119.422	0.968	119.605	1.807	0	90	2.5	0.0	-5.2
250	119.605	1.807	121.309	1.985	0	90	5.7	0.0	0.9

Continued on next page...

Table B.2 – Continued from previous page

Segment	Start Point		End Point		Locking Depth	Dip	Slip Rate (mm/yr)		
Number	Long °E	Lat °N	Long °E	Lat °N	(km)	°	Strike-Slip	Dip-Slip	Tensile
251	119.866	12.531	121.027	22.4	0	90	3.7	0.0	6.6
252	119.866	12.531	121.415	9.875	0	90	5.7	0.0	2.4
253	120.407	35.949	132.119	28.812	70	90	3.0	0.0	-0.5
254	121.027	22.4	121.715	23.522	0	90	1.0	0.0	7.0
255	121.309	1.985	122.824	1.91	0	90	5.5	0.0	1.9
256	121.415	9.875	125.518	3.507	0	90	4.6	0.0	-4.1
257	121.715	23.522	124.74	23.642	0	90	-5.2	0.0	4.5
258	121.911	-11.189	125.538	-9.808	30	30	38.1	75.0	0.0
259	122.824	1.91	124.514	2.511	0	90	5.8	0.0	-0.1
260	122.836	-7.024	125.538	-9.808	15	90	45.5	0.0	-60.0
261	122.836	-7.024	123.01	-5.997	15	90	74.7	0.0	1.3
262	123.01	-5.997	123.495	-4.576	0	90	73.5	0.0	13.9
263	123.495	-4.576	123.811	-3.65	0	90	73.5	0.0	14.5
264	123.684	-2.188	123.811	-3.65	0	0	73.1	-16.0	0.0
265	123.684	-2.188	124.801	-0.482	15	90	2.2	0.0	4.6
266	123.684	-2.188	152.121	-2.852	0	90	8.6	0.0	71.6
267	124.514	2.511	125.518	3.507	0	90	5.3	0.0	-2.4
268	124.74	23.642	127.811	24.043	0	90	-4.7	0.0	4.8
269	124.801	-0.482	125.57	0.288	15	90	1.2	0.0	5.2
270	125.518	3.507	125.976	2.781	0	90	5.8	0.0	0.4
271	125.57	0.288	126.497	2.028	15	90	2.7	0.0	4.9
272	125.976	2.781	126.497	2.028	0	90	5.8	0.0	0.0
273	127.811	24.043	132.119	28.812	0	90	-0.1	0.0	6.2
274	132.119	28.812	133.353	31.774	0	90	0.8	0.0	2.5
275	133.353	31.774	134.945	32.435	25	10	-1.1	2.2	0.0
276	134.945	32.435	136.817	33.007	30	20	-1.2	2.1	0.0
277	136.817	33.007	138.765	34.904	30	25	-0.1	2.3	0.0
278	137.776	38.591	137.838	36.577	20	20	1.3	1.4	0.0

Continued on next page...

Table B.2 – Continued from previous page

Segment	Start Point		End Point		Locking Depth	Dip	Slip Rate (mm/yr)		
Number	Long °E	Lat °N	Long °E	Lat °N	(km)	°	Strike-Slip	Dip-Slip	Tensile
279	137.776	38.591	138.436	39.77	30	20	0.7	1.7	0.0
280	137.838	36.577	138.107	35.608	25	25	1.6	1.3	0.0
281	138.107	35.608	138.437	35.256	25	25	1.9	0.5	0.0
282	138.436	39.77	138.662	42.758	30	20	1.2	1.1	0.0
283	138.437	35.256	138.765	34.904	25	25	1.9	0.6	0.0
284	138.662	42.758	138.91	45.745	50	20	1.2	0.8	0.0
285	138.91	45.745	142.642	45.791	70	90	-0.5	0.0	1.1
286	142.284	51.077	142.642	45.791	70	90	1.0	0.0	0.2
287	142.284	51.077	142.745	53.474	70	90	1.0	0.0	-0.1
288	142.406	54.636	142.745	53.474	70	90	0.9	0.0	-0.5
289	152.121	-2.852	164.629	-9.718	0	90	-25.1	0.0	61.1
290	163.25	-46.913	176.226	-20.032	0	90	-46.2	0.0	-37.6
291	164.629	-9.718	167.905	-16.076	0	90	-53.4	0.0	29.7
292	167.905	-16.076	176.226	-20.032	0	90	-28.7	0.0	49.4

Appendix C

GPS velocities and segment geometry used in the Aegean Plate model

Table C.1: GPS Velocities Used in Aegean Plate Inversion - ITRF 2008 Reference Frame

Long	Lat	Velocity (mm/yr)				Corr	Site	Source†	EXC‡
°E	°N	East	North	σ E	σ N				
-5.240	6.871	21.94	18.37	0.70	0.69	0.001	YKRO	REI	U
0.336	50.867	16.89	16.43	0.07	0.07	-0.137	HERS	GPS	U
1.481	43.561	19.17	16.64	0.33	0.37	-0.064	TOUL	GPS	U
1.481	43.561	19.65	16.11	0.09	0.08	-0.003	TLSE	GPS	U
4.359	50.798	17.71	15.91	0.07	0.07	-0.059	BRUS	GPS	U
4.677	45.879	19.61	15.95	0.07	0.07	-0.023	SJDV	GPS	U
5.354	43.279	20.08	15.81	0.11	0.09	-0.002	MARS	GPS	U
5.810	52.178	18.02	16.16	0.07	0.07	-0.123	KOSG	GPS	U
6.605	52.915	17.65	16.35	0.08	0.07	-0.075	WSRT	GPS	U
6.921	43.755	20.37	16.08	0.07	0.08	-0.017	GRAS	GPS	U
7.351	48.415	19.44	15.59	0.15	0.12	-0.101	WELS	GPS	U
7.465	46.877	19.80	16.25	0.07	0.07	-0.042	ZIMM	GPS	U
7.661	45.063	20.34	15.88	0.07	0.09	-0.057	TORI	GPS	U
8.921	44.419	20.93	15.68	0.08	0.06	-0.112	GENO	GPS	U
8.973	39.136	21.69	15.89	0.07	0.08	-0.118	CAGL	GPS	U
9.672	0.354	22.44	19.27	0.16	0.17	0.004	NKLG	GPS	U
9.785	47.515	19.88	15.89	0.21	0.22	-0.023	PFAN	GPS	U
10.233	45.565	20.51	16.10	0.17	0.14	-0.023	BRIX	GPS	U
11.280	48.086	20.26	15.69	0.17	0.18	-0.029	OBE2	GPS	U
11.329	44.488	21.84	17.74	0.21	0.18	0.013	BOLO	GPS	U
11.337	46.499	19.75	16.23	0.09	0.09	-0.035	BZRG	GPS	U
11.865	78.930	10.74	14.26	0.17	0.16	0.009	NYA1	GPS	U
11.926	57.395	17.22	14.66	0.06	0.07	-0.018	ONSA	GPS	U
12.435	46.008	20.48	16.96	0.23	0.21	-0.053	CANV	GPS	U
12.584	38.008	21.91	18.12	0.14	0.14	-0.024	MILO	GPS	U
12.879	49.144	20.28	15.41	0.07	0.07	-0.110	WTZR	GPS	U
12.974	46.557	21.04	16.29	0.16	0.13	-0.007	ZOUF	GPS	U
13.066	52.379	19.07	15.27	0.07	0.07	-0.101	POTS	GPS	U
13.552	-1.632	18.53	21.36	0.41	0.52	0.030	MSKU	GPS	U
14.786	49.914	20.00	15.10	0.07	0.07	-0.048	GOPE	GPS	U
15.155	37.286	21.12	19.76	0.19	0.20	0.011	HAGA	GPS	U
15.494	47.067	21.85	15.55	0.06	0.06	-0.083	GRAZ	GPS	U
15.554	38.205	22.97	18.16	0.34	0.33	-0.037	MESS	GPS	U
17.074	52.277	20.01	14.61	0.06	0.07	-0.033	BOR1	GPS	U
17.879	-29.669	18.26	19.66	0.34	0.33	-0.019	SBOK	GPS	U
18.158	-32.973	17.46	19.81	0.36	0.35	0.000	LGBN	GPS	U
18.440	-34.188	16.45	19.51	0.32	0.27	-0.069	SIMO	GPS	U
18.469	-33.951	16.50	19.68	1.41	1.09	-0.021	MBRY	GPS	U
19.282	47.790	22.17	14.56	0.08	0.07	-0.041	PENC	GPS	U

Continued on next page...

Table C.1 – Continued from previous page

Long	Lat	Velocity (mm/yr)				Corr	Site	Source†	EXC‡
°E	°N	East	North	σ E	σ N				
19.762	-31.482	17.95	20.16	0.36	0.35	-0.016	CALV	GPS	U
20.026	39.866	20.03	13.34	0.56	0.65	-0.025	SARA	GPS	U
20.342	38.180	18.15	11.07	0.11	0.11	0.003	GERO	HOL	U
20.473	39.291	20.88	15.19	1.30	1.60	0.000	PARG	HOL	U
20.509	38.132	14.29	6.06	1.40	1.80	0.000	LKTR	HOL	U
20.543	38.563	19.22	9.53	0.10	0.11	0.002	DUKA	HOL	U
20.548	38.371	16.25	7.94	1.30	1.60	0.000	ASSO	HOL	U
20.577	38.460	19.64	7.03	1.20	1.10	0.000	FISK	HOL	U
20.585	38.619	20.13	7.89	0.32	0.38	-0.074	PONT	GPS	U
20.589	38.177	17.32	3.72	0.25	0.20	-0.006	VLSM	GPS	U
20.665	39.734	21.22	11.87	0.38	0.38	0.035	KRTS	FLO	U
20.670	53.892	20.19	14.25	0.07	0.07	-0.039	LAMA	GPS	U
20.674	38.781	21.68	4.76	0.32	0.32	-0.007	SPAN	GPS	U
20.678	38.167	17.00	5.84	1.70	2.20	0.000	TSAR	HOL	U
20.702	37.931	13.44	3.45	0.11	0.20	0.002	SKIN	HOL	U
20.732	38.364	15.97	4.02	2.30	2.80	0.000	SARA	HOL	U
20.799	37.675	7.10	-2.55	0.80	0.80	0.000	LOGO	HOL	U
20.808	37.655	8.90	-0.64	0.11	0.11	0.003	KERI	HOL	U
20.811	-32.380	17.19	19.50	0.19	0.17	-0.061	SUTH	GPS	U
20.811	-32.381	17.03	19.44	0.24	0.24	-0.067	SUTM	GPS	U
20.846	38.910	18.89	3.37	1.20	1.50	0.000	VONW	HOL	U
20.880	39.463	18.49	11.44	1.40	1.80	0.000	TERO	HOL	U
20.971	39.157	17.47	10.24	1.20	1.00	0.000	ARTC	HOL	U
20.987	39.162	17.37	10.04	0.70	0.60	0.000	ARTB	HOL	U
20.989	37.723	9.11	-2.27	1.60	1.80	0.000	KSSI	HOL	U
21.014	37.250	4.99	-3.35	0.80	0.90	0.000	STRF	HOL	U
21.032	52.097	20.80	14.37	0.07	0.07	-0.053	JOZE	GPS	U
21.120	38.494	15.00	-0.84	1.70	2.30	0.000	ATKO	HOL	U
21.122	38.370	11.62	-0.93	1.70	2.20	0.000	MESS	HOL	U
21.142	37.890	6.27	-10.54	0.53	0.54	-0.035	CG59	FLO	U
21.165	38.864	17.24	11.54	0.20	0.40	0.000	AMFI	HOL	U
21.291	38.697	12.48	8.83	1.60	2.00	0.000	L2PE	HOL	U
21.394	39.634	22.22	9.66	0.44	0.53	0.020	TRIG	FLO	U
21.465	38.056	9.31	-8.96	0.25	0.25	-0.023	RLS_	GPS	U
21.486	38.655	16.70	7.31	0.62	0.62	-0.073	PRSL	FLO	U
21.580	38.014	7.48	-12.57	0.72	0.82	0.012	CG61	FLO	U
21.644	37.490	1.12	-12.14	1.60	1.90	0.000	ZAHA	HOL	U
21.705	36.826	4.19	-11.07	0.21	0.21	0.092	METH	FLO	U
21.787	38.284	3.85	-6.44	0.73	0.83	-0.017	0137	GPS	U
21.798	38.905	15.97	4.44	0.24	0.34	-0.054	KRPN	FLO	U
21.808	38.105	8.23	-9.64	0.81	0.82	0.069	L000	FLO	U

Continued on next page...

Table C.1 – Continued from previous page

Long	Lat	Velocity (mm/yr)				Corr	Site	Source†	EXC‡
°E	°N	East	North	σ E	σ N				
21.835	37.244	0.38	-11.75	1.30	1.70	0.000	AETO	HOL	U
21.849	38.339	11.35	-1.52	0.52	0.43	-0.032	DREP	FLO	U
21.878	36.791	3.93	-10.64	0.27	0.35	-0.060	XRIS	FLO	U
21.899	37.430	6.00	-10.84	0.25	0.26	0.032	VASS	FLO	U
21.903	38.445	11.77	5.97	1.21	1.31	-0.029	I000	FLO	U
21.925	37.702	1.93	-10.61	1.11	1.21	-0.018	DOXA	FLO	U
21.928	38.427	11.27	1.90	0.15	0.14	-0.057	EYPA	GPS	U
21.939	38.328	10.37	-9.55	1.31	1.41	0.000	N000	FLO	U
21.950	38.066	7.86	-10.98	1.31	1.31	0.001	G000	FLO	U
21.954	38.194	9.37	-15.27	0.52	0.52	-0.033	R000	FLO	U
21.958	39.237	18.21	5.70	0.24	0.33	-0.057	CG06	FLO	U
21.973	38.228	9.14	-12.72	1.20	1.50	0.000	LAKA	HOL	U
21.980	38.529	10.78	5.86	1.31	1.31	0.089	H000	FLO	U
22.016	38.410	9.29	1.63	0.42	0.52	-0.043	M000	FLO	U
22.046	38.210	9.89	-11.02	0.18	0.17	-0.054	KOUN	GPS	U
22.065	38.154	5.79	-8.50	1.81	2.01	0.060	F000	FLO	U
22.073	38.365	8.53	-1.36	0.18	0.19	-0.046	TRIZ	GPS	U
22.085	38.215	10.30	-13.51	0.71	0.81	0.001	E106	FLO	U
22.102	38.191	9.50	-8.71	0.91	1.01	0.030	E000	FLO	U
22.134	38.237	11.61	-10.12	1.41	1.41	0.010	D000	FLO	U
22.184	38.322	7.95	-2.20	0.19	0.21	-0.056	PSAR	GPS	U
22.192	38.130	9.51	-9.74	1.51	1.51	0.010	CG43	FLO	U
22.197	38.607	8.64	-0.90	0.61	0.62	0.001	LEVK	FLO	U
22.201	38.529	12.84	0.62	0.21	0.17	-0.045	LIDO	GPS	U
22.239	38.181	10.03	-8.45	1.51	1.51	-0.010	T000	FLO	U
22.242	39.089	18.25	3.12	0.33	0.33	-0.083	CG08	FLO	U
22.252	37.171	2.36	-13.59	0.52	0.62	-0.002	MLVN	FLO	U
22.263	38.472	7.55	1.57	1.41	1.41	0.030	B000	FLO	U
22.273	38.385	8.34	-2.15	0.42	0.52	-0.053	IT18	FLO	U
22.355	37.525	4.12	-15.37	0.71	0.71	-0.035	TR00	FLO	U
22.380	38.143	6.76	-11.70	0.71	0.71	-0.018	X000	FLO	U
22.384	36.493	6.44	-11.36	0.26	0.26	0.055	KERY	FLO	U
22.388	37.034	3.47	-12.10	1.40	1.70	0.000	SRTA	HOL	U
22.392	38.376	5.77	-2.07	1.41	1.41	-0.010	CT00	FLO	U
22.397	38.640	10.17	0.15	1.80	1.61	-0.109	CG22	FLO	U
22.409	37.098	4.41	-11.76	0.43	0.52	-0.053	STRV	FLO	U
22.413	36.475	0.26	-10.57	1.60	2.00	0.000	GERM	HOL	U
22.430	37.850	5.96	-13.65	1.80	1.91	-0.059	CG62	FLO	U
22.557	38.493	10.41	-3.21	0.51	0.61	-0.047	CS00	FLO	U
22.559	38.095	7.99	-12.96	0.81	0.81	-0.028	Y000	FLO	U
22.577	38.399	9.51	-1.33	0.61	0.71	-0.019	CG32	FLO	U

Continued on next page...

Table C.1 – Continued from previous page

Long	Lat	Velocity (mm/yr)				Corr	Site	Source†	EXC‡
°E	°N	East	North	σ E	σ N				
22.618	37.972	0.01	-12.29	0.52	0.52	-0.044	OBSR	FLO	U
22.623	38.651	15.64	1.36	2.60	2.70	0.000	CG20	HOL	U
22.643	38.010	7.72	-14.99	0.52	0.52	-0.026	CG44	FLO	U
22.656	37.347	2.99	-5.39	0.71	0.81	0.051	OREI	FLO	U
22.687	37.525	4.40	-14.67	2.50	2.40	-0.080	KIVE	FLO	U
22.737	37.860	6.63	-14.63	0.81	0.81	0.001	CJ00	FLO	U
22.737	37.087	5.60	-6.86	1.81	1.91	-0.049	KOSM	FLO	U
22.790	38.525	10.46	-3.67	1.01	0.81	0.069	CG29	FLO	U
22.806	38.752	15.06	-3.86	0.71	0.71	0.010	CG21	FLO	U
22.809	38.343	8.96	-4.10	0.51	0.61	-0.047	CP00	FLO	U
22.823	37.184	5.33	-13.77	0.24	0.33	-0.179	LEON	FLO	U
22.858	37.887	4.47	-12.26	0.81	0.81	0.050	CK00	FLO	U
22.861	38.624	13.48	-6.88	0.61	0.61	0.019	CG24	FLO	U
22.864	38.261	11.48	-5.32	1.31	1.31	-0.020	CG45	FLO	U
22.869	38.428	9.77	-8.00	0.51	0.52	-0.019	CG33	FLO	U
22.875	37.723	6.96	-14.80	0.52	0.61	0.012	CG63	FLO	U
22.911	37.065	5.44	-7.62	0.61	0.62	-0.034	PIGA	FLO	U
22.939	38.294	5.19	-11.14	1.11	1.11	-0.010	CN00	FLO	U
22.940	37.795	6.78	-13.51	0.52	0.61	-0.027	CG64	FLO	U
22.945	38.021	7.59	-13.18	0.42	0.42	-0.053	CG47	FLO	U
22.945	38.888	14.59	-1.38	0.23	0.32	-0.186	NEVA	FLO	U
22.956	38.216	4.70	-6.75	1.11	1.11	-0.010	CM00	FLO	U
22.984	36.307	6.70	-12.80	0.34	0.43	-0.053	KYRA	FLO	U
22.999	38.653	12.65	-4.84	0.50	0.52	-0.017	ATAL	GPS	U
23.015	36.275	7.31	-11.12	0.25	0.25	0.018	KITH	FLO	U
23.029	38.253	7.31	-8.27	0.81	0.71	0.029	CG46	FLO	U
23.034	38.755	14.31	-5.54	0.24	0.24	-0.070	ARKI	GPS	U
23.042	36.735	4.09	-12.56	1.60	2.00	0.000	MONE	HOL	U
23.068	37.709	6.01	-17.55	2.00	2.00	0.060	DMNA	FLO	U
23.093	37.804	6.22	-16.15	0.71	0.81	-0.028	CG65	FLO	U
23.114	37.414	4.32	-10.31	0.61	0.61	-0.027	KOIL	FLO	U
23.132	38.020	12.63	-12.22	0.42	0.52	-0.036	MKPG	FLO	U
23.202	38.566	12.45	-9.37	0.51	0.61	-0.039	CG28	FLO	U
23.213	38.097	7.35	-12.84	0.42	0.42	-0.018	CG49	FLO	U
23.222	38.427	9.26	-9.80	0.51	0.61	0.009	CG34	FLO	U
23.297	35.873	6.04	-11.94	1.70	1.80	0.000	AKIT	HOL	U
23.299	37.442	2.16	-13.06	2.30	1.80	0.060	ILOK	FLO	U
23.341	38.785	10.08	-8.59	0.71	0.81	-0.010	CG26	FLO	U
23.355	38.209	6.69	-13.46	0.42	0.52	-0.066	CG50	FLO	U
23.386	37.561	7.29	-12.96	0.16	0.16	-0.015	MENA	FLO	U
23.445	38.066	9.01	-15.50	1.21	1.21	0.010	CG57	FLO	U

Continued on next page...

Table C.1 – Continued from previous page

Long	Lat	Velocity (mm/yr)				Corr	Site	Source†	EXC‡
°E	°N	East	North	σ E	σ N				
23.459	37.328	4.81	-15.52	0.71	0.71	-0.028	HYDR	FLO	U
23.463	38.843	15.20	-8.20	0.61	0.61	0.028	CG27	FLO	U
23.469	37.464	-0.19	-14.91	2.50	2.50	0.010	VRMS	FLO	U
23.533	35.311	7.60	-11.76	0.29	0.21	0.009	XRSO	FLO	U
23.540	38.445	10.23	-10.57	0.61	0.61	-0.049	CG35	FLO	U
23.566	35.422	7.03	-9.84	1.70	1.90	0.000	SFIN	HOL	U
23.587	38.643	11.93	-10.25	0.51	0.61	-0.030	CG36	FLO	U
23.615	38.018	6.65	-13.15	0.51	0.61	-0.077	CG58	FLO	U
23.701	38.145	7.48	-11.95	0.61	0.71	0.076	PRNI	FLO	U
23.718	38.632	8.67	-11.09	0.61	0.61	-0.011	CG37	FLO	U
23.743	38.430	8.88	-11.52	0.61	0.61	-0.002	CG41	FLO	U
23.854	38.230	7.61	-12.57	0.52	0.61	-0.040	CG53	FLO	U
23.864	38.047	7.40	-11.65	0.43	0.30	-0.048	NOA1	GPS	U
23.931	35.325	7.15	-11.28	0.45	0.44	-0.100	OMAL	FLO	U
23.933	38.079	8.55	-11.00	0.33	0.30	-0.067	DION	GPS	U
23.944	37.822	6.75	-13.86	0.52	0.61	-0.096	CG66	FLO	U
23.963	38.388	7.84	-13.38	0.52	0.61	-0.078	CG52	FLO	U
23.993	-30.665	16.99	19.27	0.42	0.40	-0.062	DEAR	GPS	U
24.071	35.533	7.89	-12.02	0.16	0.18	-0.076	TUC2	GPS	U
24.081	34.831	8.46	-12.40	0.32	0.30	-0.018	GVDS	FLO	U
24.096	35.218	8.30	-11.46	0.23	0.22	-0.018	ANOP	FLO	U
24.109	34.839	8.16	-12.63	0.17	0.17	-0.072	GVD0	GPS	U
24.109	38.661	9.26	-11.47	0.61	0.62	-0.041	CG38	FLO	U
24.188	38.345	8.79	-13.54	0.52	0.52	-0.078	CG55	FLO	U
24.368	37.623	6.07	-14.60	1.90	1.81	0.040	TZIA	FLO	U
24.383	36.676	5.58	-15.72	0.71	0.71	-0.040	MILS	FLO	U
24.392	38.086	7.76	-13.33	0.33	0.33	-0.209	SEVA	FLO	U
24.395	60.218	19.96	12.74	0.09	0.09	0.008	METS	GPS	U
24.410	37.363	5.89	-12.67	0.42	0.42	-0.113	KYNS	FLO	U
24.419	35.172	5.94	-10.63	1.60	1.90	0.000	DAMN	HOL	U
24.438	38.058	7.87	-13.24	0.62	0.62	-0.003	OCHI	FLO	U
24.519	36.747	7.52	-12.44	0.17	0.17	-0.022	MLOS	FLO	U
24.543	38.887	11.34	-10.63	0.43	0.43	-0.104	NSKR	FLO	U
24.643	38.808	10.17	-12.07	0.81	0.72	0.045	SKYR	FLO	U
24.694	35.404	7.05	-14.39	0.36	0.44	-0.216	ROML	FLO	U
24.890	35.289	5.96	-12.61	1.20	1.10	0.000	ANYA	HOL	U
24.906	37.756	1.22	-14.70	2.50	2.11	0.049	AGFA	FLO	U
24.913	34.981	9.01	-14.80	0.27	0.26	-0.031	AKYR	FLO	U
25.126	39.851	8.36	0.57	0.45	0.37	-0.070	LIMN	FLO	U
25.181	39.897	8.16	0.58	0.31	0.26	-0.057	LEMN	GPS	U
25.333	37.487	6.36	-13.75	0.62	0.62	-0.091	MYKN	FLO	U

Continued on next page...

Table C.1 – Continued from previous page

Long	Lat	Velocity (mm/yr)				Corr	Site	Source†	EXC‡
°E	°N	East	North	σ E	σ N				
25.357	36.358	8.21	-13.95	0.21	0.20	-0.061	SNTR	FLO	U
25.379	37.449	7.28	-13.27	0.53	0.53	-0.172	MKN2	FLO	U
25.406	36.463	4.93	-16.74	0.82	0.72	-0.070	THRA	FLO	U
25.429	36.422	7.40	-16.82	0.28	0.32	-0.041	NOMI	GPS	U
25.439	36.346	6.55	-17.78	0.35	0.35	-0.405	THIR	FLO	U
25.610	35.261	8.21	-14.68	0.28	0.27	-0.022	NEAP	FLO	U
25.611	-33.985	15.79	19.43	0.38	0.34	-0.071	PELB	GPS	U
25.737	35.004	7.16	-15.02	1.73	0.75	0.145	IERA	FLO	U
26.082	39.501	2.90	4.24	0.96	0.97	-0.017	AMAN	REI	U
26.085	38.443	4.59	-10.39	0.46	0.46	-0.194	XIOS	FLO	U
26.157	39.731	2.84	4.13	0.93	0.95	-0.018	KEST	REI	U
26.174	39.973	7.30	3.68	0.67	0.62	-0.012	SUBA	REI	U
26.189	39.614	3.78	3.43	0.93	0.95	-0.025	BDER	REI	U
26.206	35.129	8.26	-15.79	0.44	0.50	-0.321	ZAKR	FLO	U
26.216	39.726	2.60	3.67	0.95	0.96	0.001	KRKE	REI	U
26.268	43.599	22.83	12.75	1.33	1.25	-0.005	TSAR	REI	U
26.270	43.600	23.54	12.18	0.61	0.51	0.000	TSAR	BUR	U
26.317	39.785	3.67	4.07	0.95	0.99	0.001	EZIN	REI	U
26.385	38.311	6.26	-9.11	0.69	0.67	-0.002	CEIL	REI	U
26.406	36.586	9.58	-17.81	0.47	0.47	-0.207	ASTP	FLO	U
26.451	39.234	4.16	-0.20	0.48	0.42	-0.147	LESV	FLO	U
26.535	39.580	3.33	6.73	0.94	0.96	0.004	HOBS	REI	U
26.700	39.311	5.03	1.49	0.76	0.70	0.003	AYKA	REI	U
26.707	39.326	2.77	3.41	0.73	0.71	-0.009	AYVA	REI	U
26.717	38.427	5.18	-0.58	0.29	0.34	-0.093	MNTS	FLO	U
26.732	39.653	1.15	5.94	0.94	0.93	0.023	KCAM	REI	U
26.871	40.601	10.27	9.02	0.91	0.94	0.055	KVAK	REI	U
26.880	40.396	4.52	6.59	0.90	0.92	0.035	SEVK	REI	U
26.885	39.010	2.84	-0.34	1.78	1.75	-0.019	ESEN	REI	U
26.910	40.029	4.06	4.52	0.93	0.93	0.040	BAH1	REI	U
26.929	36.752	7.87	-14.46	0.50	0.49	-0.212	KOSI	FLO	U
26.989	37.780	4.56	-11.88	0.49	0.49	-0.234	SAMO	FLO	U
27.085	38.019	4.02	-6.52	0.69	0.62	-0.069	OZDE	REI	U
27.112	39.244	4.26	1.03	1.67	1.72	-0.004	D5DU	REI	U
27.174	35.550	11.11	-18.45	0.50	0.40	0.000	KPTH	HOL	U
27.214	40.171	3.82	4.06	0.92	0.93	0.050	ARAK	REI	U
27.217	39.897	4.21	4.72	0.62	0.61	0.017	KIRE	REI	U
27.224	35.493	11.89	-18.47	0.50	0.54	-0.296	KRPT	FLO	U
27.269	39.577	3.10	6.71	0.95	0.94	0.043	EGMI	REI	U
27.301	40.381	5.53	7.54	0.89	0.89	0.049	KABI	REI	U
27.308	38.711	6.55	-1.62	0.77	0.72	0.004	BAYO	REI	U

Continued on next page...

Table C.1 – Continued from previous page

Long	Lat	Velocity (mm/yr)				Corr	Site	Source†	EXC‡
°E	°N	East	North	σ E	σ N				
27.316	39.024	3.31	-0.21	0.76	0.71	0.013	YAYA	REI	U
27.394	36.380	12.66	-17.17	0.43	0.35	-0.092	TILO	GPS	U
27.394	36.681	12.37	-16.77	0.65	0.61	-0.030	KNID	REI	U
27.423	37.032	8.23	-12.95	0.67	0.59	-0.047	BODR	REI	U
27.424	39.785	0.91	4.58	0.73	0.72	0.022	ALAN	REI	U
27.486	37.818	4.45	-5.88	0.91	0.87	-0.018	SOKE	REI	U
27.586	40.588	8.75	7.24	1.14	1.06	0.008	MISL	REI	U
27.590	39.295	7.20	0.81	1.64	1.66	-0.011	D7DU	REI	U
27.629	40.245	3.83	7.56	0.92	0.93	0.054	UKIR	REI	U
27.687	-25.890	18.33	18.55	0.15	0.14	-0.069	HRAO	GPS	U
27.707	-25.887	17.76	18.93	0.21	0.19	-0.126	HARB	GPS	U
27.708	-25.887	21.92	19.29	0.83	0.76	-0.096	HARK	GPS	U
27.763	40.059	0.99	10.08	0.94	0.94	0.045	KOCB	REI	U
27.781	35.952	16.48	-16.03	0.58	0.53	-0.077	KATC	GPS	U
27.816	40.400	2.89	9.78	0.69	0.68	0.014	ERDE	REI	U
27.836	37.196	6.64	-11.93	0.64	0.59	-0.054	CAMK	REI	U
27.873	39.006	3.00	2.71	0.68	0.66	0.014	AKGA	REI	U
27.906	39.722	2.74	8.47	0.71	0.63	0.003	BALI	REI	U
27.963	36.772	10.05	-12.95	0.60	0.54	-0.035	MARM	REI	U
28.000	38.248	3.50	0.38	0.93	0.87	-0.009	ODME	REI	U
28.081	37.609	3.43	-7.94	0.64	0.55	-0.050	CINE	REI	U
28.121	36.214	14.71	-12.85	0.30	0.30	0.001	ARHA	HOL	U
28.311	-15.426	20.07	18.59	0.35	0.36	-0.046	ZAMB	GPS	U
28.373	40.398	4.73	11.68	1.23	1.06	-0.013	YENI	REI	U
28.427	37.175	6.17	-7.83	0.74	0.69	-0.046	MULA	REI	U
28.483	38.315	1.57	-0.25	0.96	0.89	0.004	ALSE	REI	U
28.671	39.046	2.98	6.48	0.71	0.67	-0.004	DMIR	REI	U
28.779	40.167	3.60	10.28	0.93	0.93	0.056	HAGA	REI	U
28.826	36.762	8.64	-7.12	0.98	0.79	-0.013	DLMN	REI	U
28.882	40.481	5.77	17.74	1.99	1.68	-0.014	FIST	REI	U
28.923	39.930	0.61	12.28	0.96	0.95	0.057	GIRE	REI	U
29.048	37.566	3.06	-2.54	1.02	0.97	-0.052	TAVA	REI	U
29.102	40.136	0.62	9.74	0.71	0.70	-0.001	ULUD	REI	U
29.106	40.270	3.21	13.22	0.92	0.92	0.043	DTAS	REI	U
29.111	40.165	2.79	12.03	0.93	0.93	0.056	ZEYA	REI	U
29.136	37.941	2.51	4.99	0.67	0.64	-0.008	PAMU	REI	U
29.141	40.122	4.61	10.44	0.79	0.76	-0.006	ULDA	REI	U
29.143	40.639	8.37	13.86	0.71	0.69	0.003	CINA	REI	U
29.146	40.460	3.93	14.60	0.92	0.92	0.043	GEML	REI	U
29.261	40.200	2.95	11.41	0.93	0.93	0.051	CATA	REI	U
29.288	40.485	8.63	14.21	1.81	1.55	0.006	KUTE	REI	U

Continued on next page...

Table C.1 – Continued from previous page

Long	Lat	Velocity (mm/yr)				Corr	Site	Source†	EXC‡
°E	°N	East	North	σ E	σ N				
29.392	37.448	3.35	1.57	0.99	0.89	-0.060	GKPN	REI	U
29.439	36.720	9.35	1.21	0.68	0.63	-0.046	SIRA	REI	U
29.451	40.787	20.76	11.62	0.14	0.17	-0.065	TUBI	GPS	U
29.514	40.164	2.69	12.52	0.97	0.95	0.053	HMZA	REI	U
29.535	37.185	5.18	-0.56	0.83	0.81	-0.022	YSFC	REI	U
29.585	40.667	10.95	14.64	0.94	0.93	0.045	OLUK	REI	U
29.648	36.194	14.52	3.99	0.71	0.55	-0.056	KASO	REI	U
29.781	60.533	20.83	11.85	0.23	0.23	0.010	SVTL	GPS	U
29.810	36.971	4.31	4.15	0.82	0.81	-0.021	KYBS	REI	U
29.889	40.066	3.45	6.11	1.95	1.80	-0.016	KPKL	REI	U
29.908	40.438	6.42	10.88	0.60	0.60	0.003	IGAZ	REI	U
29.929	40.425	6.43	10.90	0.60	0.60	0.003	IUCK	REI	U
30.026	40.465	7.36	10.94	0.66	0.62	-0.008	MEKE	REI	U
30.134	40.690	11.17	12.60	0.79	0.81	0.010	SMAS	REI	U
30.297	37.689	5.27	3.98	0.57	0.52	-0.029	BURD	REI	U
30.497	50.364	22.26	12.81	0.11	0.11	-0.065	GLSV	GPS	U
30.609	36.829	12.40	4.41	0.64	0.59	-0.037	ANTG	REI	U
30.637	39.658	0.29	10.77	0.97	0.90	0.015	ESKI	REI	U
30.638	40.614	10.61	11.29	0.58	0.59	0.012	KTOP	REI	U
30.644	38.769	3.17	9.97	0.84	0.74	0.018	AFYO	REI	U
30.655	40.628	10.66	11.23	0.58	0.59	0.012	KKAP	REI	U
30.679	40.552	7.20	11.87	0.67	0.70	0.026	BOZS	REI	U
30.680	40.538	7.20	11.87	0.67	0.70	0.026	AGUZ	REI	U
30.738	-0.602	24.29	17.78	0.19	0.21	-0.063	MBAR	GPS	U
30.761	40.589	11.15	11.34	0.78	0.79	0.000	AGOK	REI	U
30.804	40.386	4.69	10.63	0.63	0.63	0.039	TEBA	REI	U
30.862	40.555	7.03	12.31	0.96	0.97	0.041	PINA	REI	U
30.975	-25.475	17.36	18.10	0.35	0.34	-0.115	NSPT	GPS	U
31.121	37.762	8.02	7.50	0.92	0.74	-0.102	AKSU	REI	U
31.814	39.564	4.03	9.99	0.79	0.68	0.018	SIVR	REI	U
32.078	-28.796	16.24	18.04	0.22	0.19	-0.159	RBAY	GPS	U
32.160	36.431	13.68	11.91	0.64	0.60	-0.060	SEKI	REI	U
32.759	39.887	1.26	11.74	0.12	0.14	-0.088	ANKR	GPS	U
33.191	37.378	11.21	14.61	0.61	0.60	0.005	MELE	REI	U
33.396	35.141	19.07	15.07	0.09	0.09	-0.103	NICO	GPS	U
34.256	36.566	13.77	16.27	0.14	0.13	-0.092	MERS	GPS	U
34.552	36.900	12.83	16.19	1.08	0.96	0.029	MER0	REI	U
34.803	39.106	5.51	15.62	1.50	1.49	-0.025	ABDI	REI	U
34.813	39.801	5.96	17.10	0.67	0.65	0.005	YOZG	REI	U
34.875	40.453	7.13	16.47	0.94	0.91	-0.016	KKIR	REI	U
35.870	36.397	19.81	21.07	1.70	1.62	-0.001	ULCN	REI	U

Continued on next page...

Table C.1 – Continued from previous page

Long	Lat	Velocity (mm/yr)				Corr	Site	Source†	EXC‡
°E	°N	East	North	σ E	σ N				
35.880	32.029	22.86	17.35	0.50	0.54	-0.094	AMMN	GPS	U
35.940	36.456	15.62	21.25	1.04	1.00	0.003	ULUC	REI	U
36.100	29.139	27.14	24.18	0.88	0.86	0.001	HALY	REI	U
36.131	36.050	20.15	21.72	0.66	0.64	-0.015	SENK	REI	U
36.137	36.899	14.11	21.09	0.51	0.51	-0.012	DORT	REI	U
36.180	36.540	15.36	23.67	1.73	1.75	-0.033	ISKE	REI	U
36.245	38.231	11.29	19.84	1.59	1.44	-0.016	PNLR	REI	U
36.285	33.510	22.21	23.02	0.39	0.69	-0.046	UDMC	GPS	U
36.330	37.572	11.06	20.36	1.66	1.60	-0.031	ANDR	REI	U
36.378	26.458	28.86	25.72	1.77	1.77	-0.002	ALWJ	REI	U
36.465	36.531	17.87	23.30	0.90	0.82	0.007	ABAK	REI	U
36.524	36.788	17.46	21.56	0.68	0.68	-0.004	HASA	REI	U
36.570	55.115	22.95	11.70	0.15	0.15	-0.028	MOBN	GPS	U
36.643	37.088	17.79	22.37	0.76	0.72	-0.016	FEVZ	REI	U
36.759	55.699	23.55	12.03	0.23	0.23	-0.029	ZWEN	GPS	U
36.972	37.190	17.10	22.95	0.50	0.51	-0.009	SAKZ	REI	U
36.996	37.522	15.88	21.92	0.56	0.58	-0.020	KMAR	REI	U
37.106	36.685	17.37	21.83	1.77	1.74	-0.060	KILI	REI	U
37.113	37.747	13.28	19.60	0.70	0.69	-0.011	ABEY	REI	U
37.220	38.179	11.98	20.62	0.67	0.68	-0.017	ELBI	REI	U
37.224	56.028	23.04	11.17	0.20	0.24	-0.027	MDVO	GPS	U
37.436	37.518	17.90	22.71	0.69	0.71	-0.014	ALAR	REI	U
37.574	36.901	18.63	24.91	0.57	0.54	-0.012	GAZI	REI	U
37.869	38.050	11.97	20.86	0.69	0.68	-0.014	ALTP	REI	U
37.886	37.541	18.25	23.70	0.74	0.73	-0.011	CKRH	REI	U
37.902	37.237	18.55	24.74	0.69	0.69	-0.021	ARGA	REI	U
37.958	39.454	8.16	21.09	0.45	0.44	0.001	SINC	REI	U
38.215	38.456	13.83	21.97	0.74	0.72	-0.012	MLT1	REI	U
38.215	38.456	13.83	21.97	0.74	0.72	-0.012	MLTY	REI	U
38.231	37.747	17.80	25.11	0.83	0.80	-0.002	ADYI	REI	U
38.584	9.081	25.45	18.16	1.00	0.79	-0.010	KOLO	REI	U
38.766	9.035	25.43	17.97	0.54	0.47	-0.003	ADD0	REI	U
39.164	39.613	6.60	20.56	0.93	0.87	-0.026	KMAH	REI	U
39.254	38.640	11.76	21.71	1.24	1.20	-0.046	GMKV	REI	U
39.282	8.472	27.61	17.68	0.65	0.57	0.011	BOKU	REI	U
39.438	8.292	28.40	17.35	0.72	0.58	0.028	SELA	REI	U
39.520	8.258	28.68	16.84	0.60	0.54	-0.005	BOLO	REI	U
39.524	39.071	8.43	22.71	1.45	1.30	-0.004	TUNC	REI	U
39.531	8.266	28.68	16.84	0.60	0.54	-0.005	REDG	REI	U
39.631	21.369	33.26	26.58	1.79	1.78	-0.001	JEDD	REI	U
39.805	37.847	16.61	25.82	0.75	0.74	-0.006	KRCD	REI	U

Continued on next page...

Table C.1 – Continued from previous page

Long	Lat	Velocity (mm/yr)				Corr	Site	Source†	EXC‡
°E	°N	East	North	σ E	σ N				
40.052	38.963	11.94	20.52	1.58	1.36	-0.012	KAKO	REI	U
40.194	-2.996	26.77	16.66	0.16	0.18	-0.075	MALI	GPS	U
40.650	37.246	19.20	27.18	0.80	0.76	-0.023	KIZ2	REI	U
40.651	37.247	19.20	27.18	0.80	0.76	-0.023	KIZI	REI	U
42.045	19.211	35.16	27.94	0.91	0.88	0.005	NAMA	REI	U
42.954	14.769	36.00	27.88	1.04	0.92	0.012	HODE	REI	U
44.190	15.348	35.25	25.20	1.05	0.90	0.004	SANA	REI	U
45.040	12.812	36.61	28.34	1.09	0.93	0.010	ADEN	REI	U
46.401	24.911	32.41	29.46	0.41	0.54	-0.157	SOLA	GPS	U
48.409	30.246	25.99	27.10	1.23	1.09	0.003	KHOS	REI	U
48.773	15.947	37.17	28.89	1.19	1.12	-0.005	SYON	REI	U
49.038	14.486	36.65	32.67	1.28	1.20	-0.011	MKLA	REI	U
50.608	26.209	31.13	30.06	0.13	0.16	-0.149	BAHR	GPS	U
51.082	28.919	27.86	29.87	0.82	0.76	0.001	ALIS	REI	U
54.004	26.883	29.59	30.09	1.63	1.18	0.012	LAMB	REI	U
55.479	-4.674	25.17	11.68	0.16	0.17	-0.121	SEY1	GPS	U
55.572	-21.208	18.65	11.07	0.29	0.31	-0.156	REUN	GPS	U
56.112	22.187	35.19	32.20	0.28	0.40	-0.151	YIBL	GPS	U
56.233	26.208	30.62	31.83	1.54	1.16	0.014	KHAS	REI	U
58.561	56.430	25.14	6.13	0.14	0.15	-0.004	ARTU	GPS	U
58.569	23.564	33.23	33.08	1.25	1.08	0.001	MUSC	REI	U
83.235	54.841	27.13	-1.16	0.19	0.20	-0.056	NVSK	GPS	U
88.360	69.362	22.15	-2.04	0.15	0.16	-0.035	NRIL	GPS	U
92.794	55.993	24.38	-4.11	0.27	0.28	-0.108	KSTU	GPS	U
104.316	52.219	25.21	-6.69	0.13	0.13	-0.105	IRKT	GPS	U
128.866	71.635	16.90	-11.71	0.14	0.14	-0.102	TIXI	GPS	U
129.680	62.031	18.57	-12.49	0.18	0.17	-0.113	YAKT	GPS	U
342.106	28.764	16.23	16.94	0.16	0.17	0.088	LPAL	GPS	U
342.535	14.685	20.60	16.68	0.30	0.33	0.114	DAKA	GPS	U
344.367	27.764	16.78	17.42	0.09	0.10	0.110	MAS1	GPS	U
354.349	42.588	19.24	16.84	0.30	0.33	0.025	LEON	GPS	U
355.750	40.429	18.79	16.16	0.08	0.08	0.018	MADR	GPS	U
356.048	40.444	19.17	16.51	0.07	0.08	-0.048	VILL	GPS	U
358.551	38.041	19.41	16.60	0.33	0.35	0.063	MULA	GPS	U
-9.102	30.053	15.16	19.91	1.46	1.02	-0.021	BAHA	REI	1
-8.619	33.162	18.55	19.97	1.56	1.04	-0.028	SALA	REI	1
-8.399	43.364	23.56	21.14	1.37	1.14	-0.005	ACOR	REI	1
-8.018	31.665	15.44	18.37	2.36	1.52	0.002	MARO	REI	1
-6.891	32.834	15.60	20.73	1.36	1.01	-0.003	KBGA	REI	1
-6.867	33.976	15.84	17.21	0.65	0.64	0.003	IAVH	REI	1
-6.616	31.934	17.13	20.26	1.27	1.01	-0.018	AZIL	REI	1

Continued on next page...

Table C.1 – Continued from previous page

Long	Lat	Velocity (mm/yr)				Corr	Site	Source†	EXC‡
°E	°N	East	North	σ E	σ N				
-5.898	30.415	15.35	19.08	1.46	1.00	-0.019	ZARA	REI	1
-4.634	32.769	17.46	19.98	1.36	1.01	-0.014	MBLD	REI	1
-4.535	32.255	16.52	18.36	1.51	1.03	0.002	RIC0	REI	1
-4.187	31.549	15.53	20.46	1.56	1.05	-0.009	ERFD	REI	1
0.104	38.835	20.70	16.26	0.22	0.22	0.045	DENI	GPS	1
0.155	48.019	18.65	16.39	0.58	0.51	0.018	MAN2	GPS	1
0.155	48.019	17.64	15.71	0.63	0.49	-0.007	MANS	GPS	1
0.334	50.868	16.17	15.96	0.13	0.16	-0.029	HERT	GPS	1
0.492	40.821	20.03	15.79	0.13	0.13	0.034	EBRE	GPS	1
0.751	41.882	19.23	15.56	0.27	0.25	0.064	AVEL	GPS	1
0.976	42.694	19.45	16.42	0.12	0.13	0.032	ESCO	GPS	1
1.133	42.375	19.89	15.92	0.22	0.19	0.041	SORI	GPS	1
1.169	41.170	20.06	15.90	0.17	0.16	0.048	REUS	GPS	1
1.401	41.600	19.82	16.35	0.12	0.12	0.007	BELL	GPS	1
1.517	41.992	20.19	15.88	0.40	0.33	0.054	SONA	GPS	1
1.720	47.294	18.59	16.02	0.14	0.16	0.029	VFCH	GPS	1
1.914	41.293	20.23	16.26	0.19	0.22	0.035	GARR	GPS	1
1.973	42.478	20.06	16.18	0.12	0.09	0.026	LLIV	GPS	1
1.987	41.419	20.18	15.81	0.21	0.20	0.033	PLAN	GPS	1
2.052	45.403	19.30	15.85	0.21	0.18	0.017	EGLT	GPS	1
2.174	41.980	20.33	15.78	0.19	0.18	0.047	SBAR	GPS	1
2.335	48.836	18.24	15.98	0.14	0.14	-0.003	OPMT	GPS	1
2.429	41.540	19.95	16.11	0.16	0.16	0.047	MATA	GPS	1
2.587	48.841	18.48	15.81	0.17	0.19	-0.003	MLVL	GPS	1
2.625	39.553	18.54	16.57	0.13	0.14	0.010	MALL	GPS	1
2.728	43.681	19.98	16.08	0.42	0.31	-0.004	LACA	GPS	1
2.824	43.431	20.53	15.60	0.39	0.44	0.018	PARD	GPS	1
2.904	41.883	19.72	16.41	0.18	0.22	0.038	CASS	GPS	1
3.111	45.761	19.79	16.22	0.27	0.22	0.032	CLFD	GPS	1
3.253	36.810	20.14	16.13	0.66	0.44	0.005	EMAP	GPS	1
3.268	43.920	20.08	16.15	0.26	0.34	0.053	SLVT	GPS	1
3.316	42.319	20.35	15.91	0.13	0.13	0.028	CREU	GPS	1
3.400	50.934	17.18	15.90	0.10	0.11	0.014	DENT	GPS	1
3.466	43.296	19.74	15.35	0.47	0.39	0.072	AGDE	GPS	1
3.581	44.121	20.02	15.94	0.30	0.24	0.033	AIGL	GPS	1
3.865	43.637	20.07	16.01	0.14	0.14	0.036	MTPL	GPS	1
3.879	45.044	19.55	15.88	0.16	0.13	-0.001	PUYV	GPS	1
3.967	43.877	20.34	15.65	0.36	0.32	0.055	BAUB	GPS	1
4.156	44.369	19.91	16.06	0.11	0.11	0.010	BANN	GPS	1
4.288	45.125	19.88	15.96	0.14	0.11	-0.025	TENC	GPS	1
4.289	46.954	19.34	15.99	0.19	0.19	-0.002	AUTN	GPS	1

Continued on next page...

Table C.1 – Continued from previous page

Long	Lat	Velocity (mm/yr)				Corr	Site	Source†	EXC‡
°E	°N	East	North	σ E	σ N				
4.388	51.986	17.42	15.61	0.19	0.14	0.008	DELF	GPS	1
4.467	44.256	19.85	16.02	0.12	0.10	-0.028	SAUV	GPS	1
4.595	50.095	18.40	15.80	0.09	0.08	-0.004	DOUR	GPS	1
4.862	43.881	20.06	16.03	0.08	0.08	0.002	CHRN	GPS	1
5.145	50.002	18.41	15.70	0.12	0.14	0.004	REDU	GPS	1
5.219	53.363	18.12	14.61	0.15	0.12	0.004	TERS	GPS	1
5.245	50.690	18.44	15.58	0.12	0.10	-0.002	WARE	GPS	1
5.354	48.486	18.80	16.55	0.28	0.32	0.017	BUAN	GPS	1
5.399	45.117	20.20	15.83	0.17	0.18	0.031	LFAZ	GPS	1
5.484	43.941	20.13	15.96	0.14	0.11	0.001	RSTL	GPS	1
5.530	22.793	21.08	19.39	0.62	0.66	0.019	TAMP	GPS	1
5.599	59.018	15.16	15.59	0.11	0.11	-0.042	STAS	GPS	1
5.625	45.916	20.19	15.73	0.24	0.27	0.017	LEBE	GPS	1
5.684	50.758	17.97	15.61	0.12	0.09	0.004	EIJS	GPS	1
5.717	43.924	20.08	16.05	0.09	0.10	-0.047	MICH	GPS	1
5.762	45.235	19.39	15.79	0.11	0.14	0.002	STEY	GPS	1
5.787	43.676	20.32	16.02	0.09	0.09	-0.059	GINA	GPS	1
5.796	46.529	19.73	16.19	0.10	0.09	-0.038	JOUX	GPS	1
5.881	45.111	20.20	15.89	0.17	0.17	0.009	CHAM	GPS	1
5.911	44.633	19.54	16.56	0.35	0.23	-0.017	BURE	GPS	1
5.986	45.643	19.92	16.11	0.10	0.11	-0.043	FCLZ	GPS	1
5.989	47.247	19.65	15.94	0.19	0.20	0.000	BSCN	GPS	1
6.084	45.087	20.10	15.89	0.16	0.24	0.055	ALPE	GPS	1
6.359	45.304	19.62	15.82	0.08	0.09	0.080	CHTL	GPS	1
6.479	44.858	20.77	15.59	0.18	0.21	0.031	PUYA	GPS	1
6.601	43.220	20.50	15.87	0.17	0.17	0.019	TROP	GPS	1
6.628	45.692	19.81	15.06	0.23	0.27	-0.041	ROSD	GPS	1
6.662	44.662	21.31	15.49	0.34	0.51	-0.017	GUIL	GPS	1
6.666	53.579	17.83	15.51	0.20	0.14	0.006	BORJ	GPS	1
6.700	49.372	19.06	15.33	0.12	0.13	0.015	DILL	GPS	1
6.710	44.910	20.70	15.18	0.32	0.35	0.033	JANU	GPS	1
6.710	45.214	19.92	15.74	0.10	0.08	-0.081	MODA	GPS	1
6.747	53.564	17.72	15.35	0.24	0.17	-0.021	BORK	GPS	1
6.764	50.674	18.50	16.18	0.10	0.11	-0.020	EUSK	GPS	1
6.882	50.525	18.85	15.74	0.12	0.12	-0.015	EFBG	GPS	1
6.977	44.268	20.67	15.73	0.19	0.24	-0.056	RABU	GPS	1
7.017	45.128	20.40	15.35	0.25	0.25	-0.017	GRAV	GPS	1
7.032	47.923	19.92	15.34	0.38	0.37	0.034	MAKS	GPS	1
7.054	43.611	20.53	15.86	0.16	0.11	-0.024	SOPH	GPS	1
7.061	45.770	19.59	15.36	0.16	0.17	0.021	MRGE	GPS	1
7.140	45.468	20.53	15.46	0.22	0.26	-0.001	AGNE	GPS	1

Continued on next page...

Table C.1 – Continued from previous page

Long	Lat	Velocity (mm/yr)				Corr	Site	Source†	EXC‡
°E	°N	East	North	σ E	σ N				
7.197	48.217	20.39	15.57	0.48	0.35	0.021	AUBU	GPS	1
7.265	45.148	20.56	15.64	0.22	0.16	-0.038	RSPX	GPS	1
7.268	47.438	19.90	15.98	0.31	0.30	0.023	LUCE	GPS	1
7.300	43.726	20.78	15.91	0.10	0.08	0.015	NICE	GPS	1
7.321	45.737	20.37	15.57	0.48	0.44	-0.013	AO01	GPS	1
7.351	48.415	18.62	15.22	0.29	0.30	-0.117	WLBH	GPS	1
7.465	46.877	20.17	16.14	0.35	0.36	0.016	ZIM2	GPS	1
7.465	46.877	19.81	15.84	0.15	0.17	0.009	ZIMJ	GPS	1
7.554	44.395	20.92	16.87	0.63	0.52	-0.003	CUNE	GPS	1
7.639	45.015	20.77	15.50	0.18	0.14	-0.005	IENG	GPS	1
7.640	48.549	19.42	15.56	0.11	0.13	-0.011	ENTZ	GPS	1
7.661	44.648	20.84	15.52	0.21	0.20	-0.004	SAVI	GPS	1
7.684	48.622	19.49	15.75	0.07	0.07	-0.014	STJ9	GPS	1
7.763	48.580	19.90	15.59	0.31	0.27	0.033	EOST	GPS	1
7.765	45.042	20.42	14.64	0.17	0.16	0.023	OATO	GPS	1
7.827	44.389	20.76	15.30	0.18	0.16	0.022	MOND	GPS	1
7.877	54.186	17.97	15.48	0.22	0.20	-0.009	HEL2	GPS	1
7.893	54.175	17.77	15.97	0.08	0.08	-0.021	HELG	GPS	1
7.927	45.074	20.58	15.63	0.15	0.15	0.008	MONC	GPS	1
8.048	45.561	20.44	15.45	0.19	0.18	0.014	BIEL	GPS	1
8.081	44.446	21.00	15.68	0.34	0.22	0.037	PARO	GPS	1
8.106	45.192	20.46	15.06	0.29	0.23	0.008	CRE1	GPS	1
8.203	44.906	20.13	15.97	0.17	0.19	-0.003	ASTI	GPS	1
8.261	46.314	20.06	16.08	0.29	0.25	-0.038	DEVE	GPS	1
8.293	54.759	18.11	15.12	0.18	0.21	0.002	HOE2	GPS	1
8.325	48.331	20.18	15.79	0.24	0.27	0.046	BFO1	GPS	1
8.342	52.588	18.52	15.86	0.16	0.14	0.010	DIEP	GPS	1
8.411	49.011	19.24	15.58	0.31	0.33	-0.012	KARJ	GPS	1
8.411	49.011	19.69	15.69	0.12	0.13	0.000	KARL	GPS	1
8.533	39.311	22.18	16.54	0.36	0.37	0.019	IGLE	GPS	1
8.567	40.721	21.75	15.73	0.24	0.25	0.027	SAS_	GPS	1
8.610	50.228	19.11	15.56	0.15	0.18	0.016	BADH	GPS	1
8.614	45.447	20.33	15.93	0.10	0.09	-0.011	NOVA	GPS	1
8.616	44.923	19.72	16.61	0.29	0.27	-0.018	ALES	GPS	1
8.680	46.042	20.18	15.84	0.19	0.16	0.003	CARZ	GPS	1
8.703	45.849	20.18	14.97	0.27	0.23	0.021	GAVI	GPS	1
8.730	50.220	18.54	15.59	0.11	0.10	0.005	KLOP	GPS	1
8.746	45.999	21.32	16.11	0.08	0.54	0.009	LUIN	GPS	1
8.763	41.928	21.06	16.01	0.10	0.11	-0.043	AJAC	GPS	1
8.770	40.269	21.57	16.76	0.26	0.22	0.026	MACO	GPS	1
8.862	45.315	20.81	15.85	0.17	0.15	0.017	VIGE	GPS	1

Continued on next page...

Table C.1 – Continued from previous page

Long	Lat	Velocity (mm/yr)				Corr	Site	Source†	EXC‡
°E	°N	East	North	σ E	σ N				
8.881	44.415	21.39	15.52	0.46	0.30	0.048	GENV	GPS	1
8.973	39.136	21.66	15.95	0.10	0.11	-0.022	CAGZ	GPS	1
9.096	45.802	20.33	15.67	0.13	0.12	0.006	COMO	GPS	1
9.100	40.908	22.20	15.54	0.37	0.37	0.016	TEMP	GPS	1
9.106	39.743	22.09	14.72	0.55	0.45	0.032	ISIL	GPS	1
9.134	39.538	21.49	15.60	0.32	0.06	0.030	CA04	GPS	1
9.136	45.203	20.47	16.40	0.11	0.15	-0.010	PAVI	GPS	1
9.137	45.203	20.73	16.13	0.24	0.21	0.007	PVIA	GPS	1
9.197	44.823	20.81	16.29	0.19	0.20	-0.007	VARZ	GPS	1
9.229	45.480	20.41	16.12	0.19	0.18	0.014	MLNO	GPS	1
9.313	40.315	21.67	15.25	0.07	0.32	-0.017	NU01	GPS	1
9.383	44.771	21.74	16.83	0.38	0.32	0.013	BOBB	GPS	1
9.401	46.320	20.14	15.97	0.30	0.32	-0.022	CHIA	GPS	1
9.407	45.857	19.84	15.48	0.19	0.19	0.020	LECC	GPS	1
9.407	45.857	19.90	15.91	0.17	0.16	-0.023	LEC1	GPS	1
9.473	45.287	21.23	16.21	0.17	0.19	0.013	LODI	GPS	1
9.521	39.143	22.11	15.79	0.40	0.34	0.015	VILS	GPS	1
9.548	39.883	21.48	14.74	0.36	0.41	0.027	LANU	GPS	1
9.559	55.641	17.43	15.08	0.11	0.13	-0.004	SMID	GPS	1
9.567	46.134	20.23	15.75	0.32	0.27	-0.030	MORB	GPS	1
9.597	45.646	20.64	15.74	0.17	0.17	0.005	DALM	GPS	1
9.685	45.354	20.58	16.18	0.16	0.15	0.016	CREA	GPS	1
9.690	45.043	21.15	16.89	0.35	0.27	0.020	PIA1	GPS	1
9.690	45.043	20.83	16.97	0.32	0.20	0.020	PIAC	GPS	1
9.725	44.236	20.45	16.11	0.33	0.24	-0.015	BRUG	GPS	1
9.742	56.842	16.84	14.65	0.14	0.13	0.002	SULD	GPS	1
9.766	44.488	21.39	16.56	0.32	0.24	0.018	TARO	GPS	1
9.785	47.515	20.21	16.04	0.41	0.38	0.007	PFA2	GPS	1
9.829	45.794	20.90	15.67	0.26	0.27	-0.051	GAZZ	GPS	1
9.840	44.073	21.10	15.92	0.15	0.12	-0.008	LASP	GPS	1
9.850	46.170	21.21	14.74	0.27	0.25	-0.025	SOND	GPS	1
9.878	45.870	20.97	16.09	0.60	0.38	-0.022	PREM	GPS	1
9.892	43.426	20.82	15.72	0.15	0.17	-0.029	GROG	GPS	1
9.897	45.602	20.29	16.16	0.18	0.19	0.004	PALA	GPS	1
9.951	51.500	19.13	15.19	0.17	0.23	0.014	GOET	GPS	1
10.002	45.147	20.90	16.51	0.17	0.14	0.014	CREM	GPS	1
10.109	45.886	21.41	15.07	0.32	0.29	0.000	PORA	GPS	1
10.157	54.373	18.08	15.04	0.16	0.19	0.005	HOL2	GPS	1
10.177	45.880	21.32	15.85	0.33	0.21	-0.033	DARF	GPS	1
10.211	42.753	20.73	16.11	0.10	0.09	-0.030	ELBA	GPS	1
10.216	44.753	21.11	17.36	0.31	0.31	0.014	COLL	GPS	1

Continued on next page...

Table C.1 – Continued from previous page

Long	Lat	Velocity (mm/yr)				Corr	Site	Source†	EXC‡
°E	°N	East	North	σ E	σ N				
10.227	43.960	20.71	16.17	0.39	0.43	0.024	LU02	GPS	1
10.233	45.565	20.51	16.02	0.24	0.17	0.007	BREA	GPS	1
10.295	42.793	20.00	16.46	0.46	0.60	0.004	PFER	GPS	1
10.301	45.471	20.60	16.61	0.38	0.36	-0.024	CASN	GPS	1
10.310	43.547	21.26	16.22	0.38	0.39	0.000	LI02	GPS	1
10.312	44.765	21.62	17.25	0.17	0.17	-0.018	PARM	GPS	1
10.319	63.371	14.07	15.67	0.17	0.14	-0.034	TRDS	GPS	1
10.323	42.815	20.75	15.90	0.27	0.20	0.008	LI01	GPS	1
10.357	44.888	21.11	16.52	0.22	0.27	0.006	PR01	GPS	1
10.364	46.468	19.49	15.93	0.22	0.21	0.020	BORM	GPS	1
10.366	43.748	21.81	16.14	0.22	0.22	0.006	PISA	GPS	1
10.368	59.737	15.68	15.20	0.16	0.14	-0.011	OSLS	GPS	1
10.405	44.432	21.68	17.57	0.39	0.24	0.000	CAST	GPS	1
10.427	45.368	20.77	15.89	0.16	0.13	-0.012	CARP	GPS	1
10.460	52.296	19.04	15.59	0.08	0.08	-0.016	PTBB	GPS	1
10.476	53.051	18.75	15.31	0.09	0.10	-0.006	HOBU	GPS	1
10.500	43.850	21.71	16.63	0.22	0.21	-0.009	LUCC	GPS	1
10.524	45.618	21.23	15.57	0.23	0.21	-0.039	SALO	GPS	1
10.544	43.979	20.97	16.39	0.43	0.49	-0.014	LU03	GPS	1
10.544	43.979	21.33	16.70	0.28	0.28	-0.011	MOZZ	GPS	1
10.551	46.686	20.48	16.22	0.18	0.17	0.019	MABZ	GPS	1
10.617	45.462	22.75	16.86	0.47	0.48	0.022	SIR2	GPS	1
10.625	44.360	22.09	18.73	0.30	0.32	0.006	MO03	GPS	1
10.627	47.146	20.11	16.00	0.12	0.12	-0.011	KRBG	GPS	1
10.629	45.775	20.50	15.76	0.19	0.20	-0.010	MAGA	GPS	1
10.637	44.706	23.16	17.14	0.27	0.31	0.011	REGG	GPS	1
10.640	44.887	21.81	15.55	0.29	0.35	-0.009	RE01	GPS	1
10.662	44.918	21.16	16.37	0.28	0.26	0.007	GUAS	GPS	1
10.670	45.984	20.11	16.63	0.26	0.23	-0.061	RONC	GPS	1
10.676	46.363	20.62	14.36	0.34	0.34	0.006	PEJO	GPS	1
10.696	44.306	22.38	16.01	0.44	0.35	-0.012	BOR_	GPS	1
10.789	45.160	20.98	16.32	0.18	0.15	0.010	MANT	GPS	1
10.835	44.340	22.97	18.96	0.26	0.24	0.026	MO02	GPS	1
10.865	42.791	20.70	16.12	0.28	0.23	-0.005	CASP	GPS	1
10.889	42.937	20.90	16.97	0.45	0.45	0.049	GAVO	GPS	1
10.900	44.641	23.82	17.40	0.29	0.30	0.010	MO01	GPS	1
10.920	45.051	20.52	16.65	0.17	0.13	-0.020	SBPO	GPS	1
10.935	43.715	21.18	16.04	0.20	0.16	0.011	EMPO	GPS	1
10.949	44.629	21.21	18.96	0.19	0.17	0.000	MODE	GPS	1
10.949	44.629	21.52	18.36	0.21	0.24	0.011	MOPS	GPS	1
10.980	43.796	22.62	16.87	0.28	0.29	0.005	CRMI	GPS	1

Continued on next page...

Table C.1 – Continued from previous page

Long	Lat	Velocity (mm/yr)				Corr	Site	Source†	EXC‡
°E	°N	East	North	σ E	σ N				
10.994	45.438	21.09	15.98	0.36	0.34	-0.015	VR02	GPS	1
11.002	45.445	20.77	15.72	0.24	0.21	0.013	VERO	GPS	1
11.005	49.587	19.92	15.50	0.10	0.11	-0.013	ERLA	GPS	1
11.034	45.600	20.93	16.65	0.21	0.22	0.015	BOSC	GPS	1
11.042	45.894	20.32	16.51	0.15	0.14	-0.022	ROVE	GPS	1
11.066	44.897	21.26	16.81	0.88	0.68	-0.014	MO04	GPS	1
11.072	45.647	21.47	16.91	0.38	0.46	-0.011	ROVR	GPS	1
11.099	43.886	21.66	17.26	0.08	0.10	-0.022	PRAT	GPS	1
11.109	42.782	19.87	17.26	0.48	0.44	-0.006	GROA	GPS	1
11.111	44.287	23.29	16.55	0.30	0.29	-0.011	VERG	GPS	1
11.113	44.122	21.51	16.83	0.12	0.09	-0.102	BRAS	GPS	1
11.118	43.871	21.19	16.73	0.23	0.25	0.021	PO01	GPS	1
11.118	46.091	21.39	16.17	0.26	0.26	0.044	TREN	GPS	1
11.120	42.428	20.74	16.30	0.37	0.31	-0.006	GR01	GPS	1
11.120	42.428	21.24	16.00	0.36	0.20	-0.013	PSTE	GPS	1
11.123	45.777	21.01	16.20	0.24	0.25	0.073	PARR	GPS	1
11.131	42.428	20.67	15.86	0.16	0.11	-0.039	MAON	GPS	1
11.141	43.475	21.13	17.07	0.24	0.25	-0.002	SI02	GPS	1
11.142	46.419	21.21	16.23	0.20	0.18	0.007	SARN	GPS	1
11.143	46.098	20.74	16.36	0.23	0.21	-0.024	MOCA	GPS	1
11.148	44.265	21.31	17.49	0.35	0.46	0.003	GRZM	GPS	1
11.157	46.669	20.86	15.12	0.68	0.56	-0.012	MERA	GPS	1
11.164	43.868	22.00	16.84	0.21	0.18	-0.003	CALA	GPS	1
11.183	44.636	22.59	16.90	0.21	0.20	0.000	SGIP	GPS	1
11.190	44.645	22.33	17.62	0.31	0.32	0.006	PERS	GPS	1
11.214	43.796	21.41	17.74	0.26	0.20	-0.005	IGMI	GPS	1
11.269	45.184	21.80	16.96	0.35	0.34	-0.019	LEGN	GPS	1
11.278	48.084	20.28	16.29	0.55	0.06	-0.047	OBET	GPS	1
11.278	45.258	20.73	16.97	0.39	0.54	-0.056	BTAC	GPS	1
11.278	45.258	20.76	17.03	0.35	0.27	0.009	VR01	GPS	1
11.280	48.086	20.10	15.93	0.37	0.25	-0.059	OBER	GPS	1
11.286	44.838	20.99	16.77	0.44	0.29	0.017	MO05	GPS	1
11.300	45.007	22.25	17.43	0.27	0.25	0.006	SERM	GPS	1
11.320	44.493	21.38	18.77	0.48	0.42	0.004	BO01	GPS	1
11.338	43.315	20.77	16.45	0.16	0.15	0.013	SIEN	GPS	1
11.350	53.050	19.26	14.25	0.56	0.38	0.018	GOR2	GPS	1
11.350	53.050	18.30	15.05	0.21	0.17	-0.026	GORL	GPS	1
11.357	44.500	21.06	19.42	0.19	0.20	0.005	BOLG	GPS	1
11.363	45.718	20.75	17.05	0.42	0.30	0.010	SCHI	GPS	1
11.378	44.118	20.89	17.58	0.35	0.35	0.005	FIRE	GPS	1
11.386	47.313	20.98	15.86	0.42	0.40	0.002	HFL2	GPS	1

Continued on next page...

Table C.1 – Continued from previous page

Long	Lat	Velocity (mm/yr)				Corr	Site	Source†	EXC‡
°E	°N	East	North	σ E	σ N				
11.386	47.313	20.55	16.18	0.12	0.12	-0.044	HFLK	GPS	1
11.425	44.313	22.42	18.58	0.47	0.39	-0.001	MTRZ	GPS	1
11.426	46.898	20.82	16.19	0.14	0.15	-0.041	STBZ	GPS	1
11.460	47.208	20.16	16.56	0.47	0.49	-0.005	PAT2	GPS	1
11.460	47.208	19.78	16.77	0.18	0.20	-0.036	PATK	GPS	1
11.474	43.619	21.51	17.39	0.18	0.23	0.016	FIGL	GPS	1
11.509	46.069	21.08	15.98	0.27	0.22	0.005	SPER	GPS	1
11.525	45.866	20.32	16.26	0.15	0.13	0.018	ASIA	GPS	1
11.525	45.866	20.25	16.15	0.45	0.40	0.018	VI01	GPS	1
11.556	45.564	20.78	16.64	0.22	0.20	-0.014	VICE	GPS	1
11.568	48.149	20.46	15.97	0.12	0.12	0.003	MUEJ	GPS	1
11.599	44.833	21.21	17.59	0.10	0.10	-0.015	UNFE	GPS	1
11.601	44.828	21.63	16.75	0.31	0.25	0.014	FERR	GPS	1
11.615	50.645	19.29	15.13	0.41	0.27	-0.021	MOXA	GPS	1
11.616	50.642	19.37	14.94	0.33	0.23	-0.004	MOX2	GPS	1
11.627	44.814	21.25	17.64	0.26	0.25	0.005	FERA	GPS	1
11.647	44.520	22.13	17.96	0.13	0.10	-0.008	MSEL	GPS	1
11.647	44.520	22.65	17.48	0.11	0.15	-0.028	MEDI	GPS	1
11.669	44.625	21.94	17.76	0.27	0.26	0.022	BO03	GPS	1
11.677	45.343	20.50	17.38	0.12	0.12	-0.024	TEOL	GPS	1
11.682	46.423	20.73	15.96	0.25	0.25	-0.055	POZZ	GPS	1
11.718	44.348	23.28	17.89	0.32	0.32	0.001	ITIM	GPS	1
11.724	46.304	20.66	15.87	0.25	0.17	-0.020	FDOS	GPS	1
11.731	45.762	20.87	16.84	0.30	0.26	-0.007	BASS	GPS	1
11.783	45.087	20.85	17.54	0.13	0.13	0.004	ROVI	GPS	1
11.789	42.096	20.08	16.80	0.42	0.36	0.011	CVTV	GPS	1
11.795	45.640	20.26	16.70	0.27	0.31	0.017	CITD	GPS	1
11.827	46.032	20.38	16.92	0.27	0.23	0.002	MAVE	GPS	1
11.836	43.647	20.74	17.28	0.27	0.31	0.013	AR01	GPS	1
11.861	44.303	22.11	18.89	0.38	0.37	0.008	FAEZ	GPS	1
11.865	78.930	10.16	13.98	0.09	0.08	-0.005	NYAL	GPS	1
11.875	43.464	21.66	17.10	0.13	0.17	-0.003	AREZ	GPS	1
11.876	50.313	20.05	14.95	0.23	0.25	0.004	HOFJ	GPS	1
11.878	45.407	20.53	17.73	0.19	0.19	-0.073	UPAD	GPS	1
11.879	45.422	20.77	16.65	0.41	0.37	-0.009	PD01	GPS	1
11.896	45.411	21.18	16.83	0.14	0.11	-0.032	PADO	GPS	1
11.901	42.964	20.97	17.36	0.34	0.22	-0.008	SI01	GPS	1
11.902	46.193	20.38	16.39	0.28	0.32	-0.043	PASS	GPS	1
11.910	42.849	20.00	16.70	0.28	0.32	0.020	SACS	GPS	1
11.911	45.385	20.96	17.28	0.12	0.12	-0.036	VOLT	GPS	1
11.941	46.797	20.74	16.00	0.16	0.13	-0.012	BRBZ	GPS	1

Continued on next page...

Table C.1 – Continued from previous page

Long	Lat	Velocity (mm/yr)				Corr	Site	Source†	EXC‡
°E	°N	East	North	σ E	σ N				
11.966	43.329	20.82	17.90	0.34	0.29	-0.003	CAFI	GPS	1
11.969	45.533	21.27	17.05	0.39	0.40	-0.008	BORG	GPS	1
11.971	36.811	21.94	17.01	0.23	0.24	-0.003	PZIN	GPS	1
11.976	44.973	22.15	16.93	0.29	0.30	-0.006	FE01	GPS	1
11.978	43.259	20.94	17.40	0.46	0.43	0.009	CAMU	GPS	1
12.000	42.064	20.12	16.79	0.15	0.18	-0.020	TOLF	GPS	1
12.002	42.952	21.11	17.20	0.16	0.12	0.000	REPI	GPS	1
12.049	45.783	21.82	15.28	0.31	0.37	-0.068	MBEL	GPS	1
12.053	43.592	20.98	17.81	0.64	0.43	-0.022	IEMO	GPS	1
12.084	46.100	20.53	17.78	0.50	0.44	0.006	BRSE	GPS	1
12.101	54.170	18.55	15.15	0.12	0.10	-0.009	WARN	GPS	1
12.111	42.913	20.54	17.32	0.30	0.27	-0.003	MGAB	GPS	1
12.112	44.837	22.21	17.32	0.30	0.30	0.010	CODI	GPS	1
12.113	42.716	21.22	16.73	0.16	0.16	0.002	UNOV	GPS	1
12.120	42.418	20.97	16.72	0.24	0.23	-0.028	VITE	GPS	1
12.134	44.415	22.68	18.10	0.28	0.44	0.010	RA01	GPS	1
12.175	46.527	19.92	15.88	0.18	0.21	0.013	AFAL	GPS	1
12.177	42.257	20.28	17.75	0.43	0.40	-0.008	CAPR	GPS	1
12.192	44.405	22.59	17.53	0.33	0.43	-0.014	RAVE	GPS	1
12.203	46.137	21.06	16.16	0.35	0.30	-0.019	BL01	GPS	1
12.218	46.437	21.02	16.96	0.57	0.62	0.157	BORC	GPS	1
12.222	45.680	20.98	15.95	0.44	0.38	-0.016	TVSO	GPS	1
12.226	43.453	23.36	18.42	0.19	0.21	0.002	REMO	GPS	1
12.228	45.003	21.39	16.92	0.32	0.26	0.010	TGPO	GPS	1
12.239	45.490	20.16	18.17	0.31	0.27	0.020	MSTR	GPS	1
12.245	43.209	21.42	17.03	0.20	0.13	-0.001	CSSB	GPS	1
12.248	43.467	21.64	17.49	0.17	0.22	-0.017	CAIE	GPS	1
12.248	43.467	21.80	17.00	0.14	0.16	-0.011	CITT	GPS	1
12.257	45.664	20.60	17.19	0.13	0.13	-0.020	TREV	GPS	1
12.265	43.817	22.02	18.86	0.39	0.39	-0.006	PENB	GPS	1
12.285	43.279	21.48	17.03	0.30	0.31	-0.032	VALC	GPS	1
12.298	50.138	19.27	14.67	0.17	0.17	0.014	POUS	GPS	1
12.329	43.311	21.36	16.60	0.20	0.20	0.011	UMBE	GPS	1
12.355	42.055	20.81	17.09	0.29	0.28	0.002	OLGI	GPS	1
12.356	43.119	21.53	16.82	0.09	0.08	-0.012	UNPG	GPS	1
12.356	43.119	21.68	17.35	0.14	0.16	-0.008	UPG2	GPS	1
12.358	45.438	20.94	17.21	0.21	0.21	0.021	VEAR	GPS	1
12.360	47.418	20.15	15.68	0.35	0.36	0.001	KTZ2	GPS	1
12.374	51.354	19.37	14.97	0.20	0.23	-0.008	LEIP	GPS	1
12.394	43.111	21.37	17.16	0.20	0.14	-0.027	PERU	GPS	1
12.402	43.451	21.91	17.21	0.22	0.19	-0.027	PIET	GPS	1

Continued on next page...

Table C.1 – Continued from previous page

Long	Lat	Velocity (mm/yr)				Corr	Site	Source†	EXC‡
°E	°N	East	North	σ E	σ N				
12.407	43.382	21.78	17.32	0.17	0.19	-0.007	MVAL	GPS	1
12.407	42.782	21.23	17.11	0.16	0.18	0.014	RETO	GPS	1
12.408	42.781	21.94	16.25	0.42	0.40	0.013	TODI	GPS	1
12.422	41.905	19.86	16.51	0.16	0.17	-0.006	ROMA	GPS	1
12.451	43.934	22.72	18.53	0.18	0.18	-0.012	RSMN	GPS	1
12.493	41.893	21.06	16.55	0.15	0.17	-0.040	M0SE	GPS	1
12.500	55.739	18.07	14.81	0.11	0.12	-0.008	BUDP	GPS	1
12.515	41.828	21.17	17.21	0.07	0.08	-0.038	INGR	GPS	1
12.516	46.025	19.60	16.12	0.72	0.55	-0.012	PN01	GPS	1
12.525	43.263	23.14	16.24	0.22	0.20	-0.011	MURB	GPS	1
12.564	46.193	21.48	17.47	0.36	0.33	-0.022	BARC	GPS	1
12.564	45.630	20.80	17.60	0.32	0.21	0.010	SDNA	GPS	1
12.578	43.351	20.25	16.27	0.31	0.26	0.059	GUB2	GPS	1
12.578	43.343	21.37	16.75	0.43	0.38	-0.006	PG01	GPS	1
12.582	44.048	22.68	18.57	0.15	0.19	-0.021	ITRN	GPS	1
12.583	45.479	21.12	17.61	0.11	0.11	-0.040	CAVA	GPS	1
12.606	35.500	19.93	18.63	0.09	0.09	-0.149	LAMP	GPS	1
12.619	42.053	19.79	16.96	0.31	0.33	-0.019	MORO	GPS	1
12.640	43.701	22.41	18.56	0.38	0.48	-0.030	UNUB	GPS	1
12.650	42.567	19.28	16.79	0.21	0.23	-0.004	TERI	GPS	1
12.661	45.957	20.61	16.58	0.12	0.09	0.004	PORD	GPS	1
12.665	41.597	20.60	15.44	0.35	0.36	0.022	APRI	GPS	1
12.674	42.559	21.29	16.63	0.29	0.18	-0.041	UNTR	GPS	1
12.690	46.567	21.05	16.07	0.53	0.47	-0.051	SAPP	GPS	1
12.699	42.955	20.92	17.16	0.23	0.33	0.005	FOL1	GPS	1
12.703	41.811	22.02	17.32	0.18	0.16	-0.016	RMPO	GPS	1
12.704	42.956	21.42	16.97	0.16	0.18	0.012	REFO	GPS	1
12.782	43.234	22.97	18.09	0.17	0.28	0.016	ITGT	GPS	1
12.799	46.415	20.95	16.23	0.13	0.10	0.001	AMPE	GPS	1
12.807	43.689	23.38	18.79	0.28	0.29	-0.029	FOSS	GPS	1
12.833	45.767	21.28	17.68	0.26	0.20	0.007	PORT	GPS	1
12.833	45.767	21.36	17.85	0.43	0.33	0.006	VE02	GPS	1
12.857	42.408	21.03	15.57	0.18	0.18	-0.024	RIET	GPS	1
12.879	49.144	20.46	15.38	0.08	0.08	-0.018	WTZZ	GPS	1
12.891	57.715	17.43	14.54	0.11	0.10	-0.014	SPT0	GPS	1
12.893	43.893	21.41	19.00	0.50	0.41	-0.025	PES1	GPS	1
12.894	50.357	19.74	15.41	0.18	0.20	-0.011	MARJ	GPS	1
12.901	41.471	21.54	16.96	0.20	0.23	-0.021	LAT1	GPS	1
12.905	43.005	21.98	18.70	0.31	0.22	0.034	CESI	GPS	1
12.926	43.344	22.44	18.53	0.17	0.17	-0.018	ITFA	GPS	1
12.979	45.959	21.10	17.20	0.27	0.21	0.010	CODR	GPS	1

Continued on next page...

Table C.1 – Continued from previous page

Long	Lat	Velocity (mm/yr)				Corr	Site	Source†	EXC‡
°E	°N	East	North	σ E	σ N				
12.982	41.949	21.33	16.91	0.17	0.20	-0.029	CERT	GPS	1
12.988	46.241	20.49	16.52	0.17	0.13	-0.022	MPRA	GPS	1
12.993	42.456	23.02	16.45	0.23	0.27	-0.026	MTTO	GPS	1
13.001	46.414	21.09	16.23	0.30	0.26	-0.018	FUSE	GPS	1
13.009	46.674	21.54	16.60	0.56	0.40	0.084	KOE2	GPS	1
13.009	46.674	20.60	16.10	0.30	0.24	0.030	KOET	GPS	1
13.039	42.050	22.48	18.41	0.27	0.29	-0.042	OCRA	GPS	1
13.040	42.603	22.11	17.22	0.16	0.20	-0.020	LNSS	GPS	1
13.053	45.806	20.90	17.28	0.29	0.19	-0.039	PAZO	GPS	1
13.069	45.672	20.61	17.29	0.31	0.19	-0.004	BEVA	GPS	1
13.073	53.330	18.70	14.86	0.17	0.18	-0.013	NTZ1	GPS	1
13.080	37.512	20.66	18.15	0.55	0.36	0.007	SCIA	GPS	1
13.093	42.793	22.07	17.86	0.19	0.17	0.010	RENO	GPS	1
13.100	41.250	21.34	15.81	0.50	0.41	0.005	SFCI	GPS	1
13.110	47.803	20.49	16.62	0.38	0.34	0.008	SBG2	GPS	1
13.110	47.803	20.74	16.09	0.16	0.14	-0.023	SBGZ	GPS	1
13.124	43.503	22.59	17.97	0.18	0.16	-0.008	MOIE	GPS	1
13.124	43.112	22.78	18.33	0.15	0.11	-0.037	CAME	GPS	1
13.179	38.708	22.21	16.95	0.26	0.27	-0.037	USIX	GPS	1
13.198	46.407	20.75	16.50	0.12	0.08	0.006	MOGG	GPS	1
13.217	46.083	20.34	17.42	0.21	0.20	0.021	UNUD	GPS	1
13.228	46.055	20.82	16.33	0.41	0.43	0.015	UDI2	GPS	1
13.240	42.528	20.98	16.16	0.27	0.23	-0.045	MTRA	GPS	1
13.253	46.038	20.76	17.28	0.20	0.17	0.008	UDI1	GPS	1
13.253	46.037	20.53	17.72	0.34	0.32	-0.009	UDIN	GPS	1
13.304	37.894	21.35	18.95	0.21	0.17	-0.002	CORL	GPS	1
13.308	45.905	20.64	17.30	0.09	0.08	-0.010	PLMN	GPS	1
13.312	41.794	21.34	16.18	0.23	0.23	-0.009	GUAR	GPS	1
13.316	42.383	22.51	18.31	0.16	0.17	-0.017	INGP	GPS	1
13.335	43.063	23.94	19.43	0.43	0.06	-0.012	GUMA	GPS	1
13.337	42.332	21.05	16.89	0.66	0.76	0.000	ROPI	GPS	1
13.349	41.648	22.03	17.91	0.54	0.30	-0.059	FROS	GPS	1
13.350	42.368	21.92	17.65	0.10	0.11	-0.045	AQUI	GPS	1
13.374	42.366	20.62	16.70	0.25	0.27	-0.022	AQRA	GPS	1
13.379	42.338	20.30	16.25	0.36	0.33	-0.022	AQUN	GPS	1
13.384	41.673	21.79	14.94	0.49	0.43	0.005	ALAT	GPS	1
13.416	46.184	20.74	16.92	0.23	0.23	0.005	JOAN	GPS	1
13.422	40.795	21.29	16.77	0.17	0.14	0.002	VENT	GPS	1
13.436	45.925	20.88	17.67	0.10	0.11	-0.019	MDEA	GPS	1
13.451	43.294	24.00	18.73	0.25	0.21	0.005	MACE	GPS	1
13.486	48.203	21.32	15.74	0.28	0.28	-0.021	RIED	GPS	1

Continued on next page...

Table C.1 – Continued from previous page

Long	Lat	Velocity (mm/yr)				Corr	Site	Source†	EXC‡
°E	°N	East	North	σ E	σ N				
13.498	42.735	23.70	18.35	0.23	0.24	-0.039	VCRA	GPS	1
13.502	43.603	22.26	18.86	0.31	0.27	0.006	AN01	GPS	1
13.502	43.603	22.37	19.03	0.33	0.31	0.005	ANCG	GPS	1
13.515	46.548	21.32	16.19	0.14	0.18	-0.010	ACOM	GPS	1
13.515	42.138	21.16	19.75	0.48	0.39	-0.033	OVRA	GPS	1
13.542	46.333	20.89	16.85	0.34	0.27	-0.044	BOVE	GPS	1
13.544	43.465	23.75	18.73	0.29	0.28	0.018	CASF	GPS	1
13.560	41.810	21.54	18.31	0.24	0.37	-0.006	BLRA	GPS	1
13.592	42.855	22.81	18.14	0.46	0.07	-0.017	CSGP	GPS	1
13.593	46.502	21.25	16.22	0.36	0.32	-0.014	TARV	GPS	1
13.593	42.857	22.69	17.77	0.46	0.40	-0.005	ASCC	GPS	1
13.623	41.870	22.09	17.61	0.13	0.12	-0.022	VVLO	GPS	1
13.624	45.943	20.72	17.47	0.28	0.31	0.013	GORI	GPS	1
13.625	45.896	20.65	18.07	0.30	0.22	0.000	NOVG	GPS	1
13.637	42.823	22.87	17.67	0.24	0.24	-0.014	ASCO	GPS	1
13.643	54.514	18.86	14.91	0.13	0.12	-0.009	SASS	GPS	1
13.646	41.955	22.47	17.72	0.09	0.49	0.008	OTRA	GPS	1
13.680	42.650	23.42	18.85	0.34	0.38	-0.038	ITTE	GPS	1
13.698	42.657	22.02	17.34	0.27	0.26	-0.018	TERA	GPS	1
13.699	41.281	22.74	14.82	0.36	0.40	-0.015	FORM	GPS	1
13.712	41.717	21.67	17.62	0.22	0.22	-0.030	POFI	GPS	1
13.720	42.368	21.01	19.18	0.24	0.27	-0.040	CDRA	GPS	1
13.724	49.134	20.44	14.93	0.16	0.19	-0.020	VACO	GPS	1
13.730	51.030	19.97	15.80	0.11	0.13	-0.004	DRES	GPS	1
13.764	45.710	20.65	17.51	0.11	0.14	-0.022	TRIE	GPS	1
13.766	41.407	21.99	14.31	0.65	0.51	0.015	SGLI	GPS	1
13.771	47.377	21.17	16.31	0.14	0.10	-0.024	HKBL	GPS	1
13.788	45.661	20.39	17.36	0.31	0.34	0.011	TRI1	GPS	1
13.801	47.921	21.06	15.45	0.29	0.30	-0.019	GMND	GPS	1
13.849	44.877	21.30	18.89	0.29	0.31	-0.004	PUGS	GPS	1
13.851	46.607	21.40	16.00	0.10	0.11	-0.027	VLCH	GPS	1
13.871	42.976	24.87	18.39	0.37	0.32	0.020	GRAM	GPS	1
13.881	41.146	20.83	16.67	0.20	0.20	0.020	MODR	GPS	1
13.893	46.631	21.79	16.44	0.31	0.30	0.005	LANK	GPS	1
13.916	42.885	23.36	17.99	0.23	0.03	-0.038	MRRA	GPS	1
13.924	42.048	22.48	18.28	0.28	0.24	-0.026	SMRA	GPS	1
13.925	40.712	19.04	17.12	0.29	0.38	0.026	ISCY	GPS	1
13.974	41.195	20.62	16.91	0.31	0.46	0.036	CARI	GPS	1
13.995	48.570	20.78	15.32	0.27	0.25	-0.023	ROHR	GPS	1
14.002	42.658	22.87	17.93	0.11	0.11	-0.052	RSTO	GPS	1
14.002	42.659	23.07	17.97	0.13	0.13	-0.041	ITRA	GPS	1

Continued on next page...

Table C.1 – Continued from previous page

Long	Lat	Velocity (mm/yr)				Corr	Site	Source†	EXC‡
°E	°N	East	North	σ E	σ N				
14.002	42.268	22.25	17.98	0.30	0.28	-0.037	SCRA	GPS	1
14.007	42.552	22.82	17.81	0.19	0.23	-0.046	ATRA	GPS	1
14.021	48.158	21.11	15.25	0.27	0.24	-0.019	WEL2	GPS	1
14.024	40.765	19.38	15.27	0.15	0.13	-0.003	IPRO	GPS	1
14.026	37.990	21.57	20.05	0.27	0.30	-0.026	GBLM	GPS	1
14.034	41.734	21.86	20.39	0.30	0.38	-0.046	ALRA	GPS	1
14.050	40.876	19.12	17.53	0.12	0.12	-0.021	LICO	GPS	1
14.118	52.210	18.90	14.95	0.50	0.36	-0.024	LDBG	GPS	1
14.121	52.209	19.39	15.11	0.17	0.16	0.015	LDB2	GPS	1
14.145	42.385	21.87	17.38	0.43	0.54	-0.010	CHIE	GPS	1
14.152	41.704	22.67	17.82	0.14	0.18	-0.063	RNI2	GPS	1
14.172	46.344	21.65	16.32	0.23	0.31	0.006	RADO	GPS	1
14.225	40.878	23.34	18.17	0.23	0.23	-0.004	FRUL	GPS	1
14.229	42.124	22.23	18.95	0.27	0.26	-0.040	PBRA	GPS	1
14.234	41.415	21.71	16.64	0.32	0.28	0.000	VAGA	GPS	1
14.236	41.600	22.66	18.96	0.44	0.29	-0.003	ISER	GPS	1
14.248	45.567	21.00	16.90	0.29	0.40	0.024	ILIR	GPS	1
14.274	37.570	21.48	18.65	0.35	0.42	-0.010	ENNA	GPS	1
14.276	40.870	23.28	17.14	0.36	0.35	-0.007	NAPO	GPS	1
14.283	48.310	20.43	14.98	0.12	0.10	-0.008	LINZ	GPS	1
14.292	42.418	22.76	17.95	0.24	0.25	-0.022	FRRA	GPS	1
14.319	46.607	22.02	16.41	0.49	0.47	-0.009	KLAG	GPS	1
14.322	53.450	19.61	14.82	0.30	0.26	0.014	GELL	GPS	1
14.327	41.047	22.10	18.13	0.44	0.54	-0.009	NICY	GPS	1
14.335	41.327	22.07	16.71	0.39	0.36	0.000	ALIF	GPS	1
14.335	40.582	21.83	16.33	0.12	0.16	0.035	ENAV	GPS	1
14.343	47.525	22.52	16.09	0.44	0.47	0.071	RTM2	GPS	1
14.343	47.525	20.95	15.39	0.14	0.16	-0.038	RTMN	GPS	1
14.356	38.534	21.77	19.67	0.38	0.34	-0.071	IACL	GPS	1
14.362	37.223	21.26	20.02	0.18	0.15	-0.004	RAFF	GPS	1
14.374	40.626	21.63	16.62	0.47	0.33	-0.006	SORR	GPS	1
14.526	35.838	21.69	19.61	0.23	0.23	-0.023	MALT	GPS	1
14.529	41.364	22.67	17.25	0.26	0.24	0.011	PTRJ	GPS	1
14.544	46.048	21.27	17.29	0.09	0.14	-0.002	GSR1	GPS	1
14.550	41.767	23.89	18.51	0.15	0.17	-0.011	TRIV	GPS	1
14.556	40.871	21.13	16.82	0.10	0.12	-0.024	PACA	GPS	1
14.567	37.711	20.80	18.60	0.27	0.28	-0.003	GALF	GPS	1
14.575	38.564	22.70	18.89	0.31	0.42	-0.062	IFIL	GPS	1
14.594	41.546	22.94	18.17	0.16	0.17	0.011	BSSO	GPS	1
14.626	46.661	21.85	15.84	0.11	0.12	-0.020	VLKM	GPS	1
14.669	41.974	23.11	18.01	0.19	0.17	-0.014	FRES	GPS	1

Continued on next page...

Table C.1 – Continued from previous page

Long	Lat	Velocity (mm/yr)				Corr	Site	Source†	EXC‡
°E	°N	East	North	σ E	σ N				
14.678	41.560	25.10	17.73	0.34	0.33	-0.008	CABA	GPS	1
14.706	41.398	21.49	17.35	0.25	0.25	-0.013	SACR	GPS	1
14.708	42.110	22.56	17.87	0.24	0.25	-0.034	VTRA	GPS	1
14.713	37.596	20.81	19.07	0.34	0.26	-0.033	ECNV	GPS	1
14.716	37.178	19.96	18.49	0.25	0.28	-0.010	HVZN	GPS	1
14.740	38.157	22.82	20.91	0.29	0.26	-0.016	CAPO	GPS	1
14.783	36.959	21.21	19.37	0.20	0.24	-0.023	HMDC	GPS	1
14.783	40.912	22.26	18.36	0.31	0.35	-0.006	AVEY	GPS	1
14.794	46.590	21.18	16.90	0.34	0.30	-0.016	BLEI	GPS	1
14.811	41.223	22.34	17.56	0.20	0.19	0.011	PSB1	GPS	1
14.860	42.011	22.82	18.60	0.34	0.29	0.013	PETC	GPS	1
14.922	41.810	22.90	18.76	0.19	0.18	-0.022	LAR_	GPS	1
14.948	38.446	21.61	21.79	0.19	0.22	0.024	LOSV	GPS	1
14.952	38.409	24.02	21.12	0.23	0.20	-0.020	VCSP	GPS	1
14.987	40.547	20.10	17.14	0.47	0.46	-0.001	EBOL	GPS	1
14.990	36.876	21.56	19.74	0.11	0.11	-0.155	NOT1	GPS	1
14.990	36.876	20.86	19.76	0.29	0.29	-0.063	NOTO	GPS	1
15.008	45.907	21.99	16.75	0.24	0.32	0.008	TREB	GPS	1
15.017	41.409	23.64	19.46	0.32	0.49	-0.016	BART	GPS	1
15.032	37.283	22.72	18.51	0.40	0.44	-0.024	HCRL	GPS	1
15.060	41.073	22.08	17.54	0.13	0.14	-0.014	GROT	GPS	1
15.076	37.158	21.67	19.38	0.18	0.16	-0.006	SSYX	GPS	1
15.077	38.643	24.16	17.17	0.31	0.29	-0.060	CPAN	GPS	1
15.080	46.512	22.00	15.98	0.23	0.21	-0.015	SLOG	GPS	1
15.082	37.514	22.83	17.90	0.26	0.23	-0.002	EIIV	GPS	1
15.101	41.067	22.50	17.59	0.34	0.39	0.004	GRO1	GPS	1
15.114	38.639	20.92	17.84	0.22	0.24	-0.031	LI3D	GPS	1
15.122	36.960	21.63	19.86	0.18	0.19	-0.008	HAVL	GPS	1
15.127	41.706	23.40	19.17	0.38	0.36	-0.013	MELA	GPS	1
15.159	41.371	22.82	18.56	0.28	0.18	0.005	MOCO	GPS	1
15.168	40.783	22.87	17.76	0.22	0.27	-0.024	MCRV	GPS	1
15.184	40.931	21.82	17.83	0.35	0.34	-0.015	ANGE	GPS	1
15.193	45.579	22.29	17.34	0.25	0.24	-0.001	CRNO	GPS	1
15.205	52.738	19.34	14.40	0.35	0.32	0.006	GWWL	GPS	1
15.209	40.926	22.48	17.73	0.16	0.14	-0.008	SNAL	GPS	1
15.231	38.271	23.06	20.39	0.22	0.19	-0.020	MILA	GPS	1
15.234	38.803	23.34	18.06	0.23	0.30	0.001	SVIN	GPS	1
15.237	41.028	22.18	18.46	0.17	0.23	-0.013	CAFE	GPS	1
15.242	46.242	22.02	16.36	0.25	0.23	0.000	CELJ	GPS	1
15.254	37.935	24.78	22.29	0.20	0.19	-0.033	MMME	GPS	1
15.260	41.740	23.95	18.37	0.27	0.23	-0.006	SPCI	GPS	1

Continued on next page...

Table C.1 – Continued from previous page

Long	Lat	Velocity (mm/yr)				Corr	Site	Source†	EXC‡
°E	°N	East	North	σ E	σ N				
15.266	40.231	22.34	17.00	0.13	0.15	-0.018	VLUC	GPS	1
15.289	37.853	22.57	19.38	0.31	0.32	-0.011	TAOR	GPS	1
15.303	40.318	22.44	16.72	0.20	0.21	-0.020	CMPR	GPS	1
15.305	40.490	21.46	16.87	0.17	0.19	-0.014	CDRU	GPS	1
15.331	41.159	23.89	18.85	0.27	0.31	-0.008	ACCA	GPS	1
15.365	41.136	23.17	18.92	0.21	0.18	-0.014	SGTA	GPS	1
15.378	40.078	22.71	17.58	0.20	0.19	-0.011	BULG	GPS	1
15.489	40.756	23.74	19.13	0.26	0.24	-0.014	MRLC	GPS	1
15.508	38.264	23.13	19.37	0.17	0.20	-0.005	MSRU	GPS	1
15.532	41.452	23.42	19.03	0.25	0.23	-0.004	FOGG	GPS	1
15.554	38.184	23.33	17.73	0.38	0.37	-0.012	MESA	GPS	1
15.593	45.904	22.72	17.60	0.25	0.23	0.004	BREZ	GPS	1
15.616	40.955	23.52	19.06	0.25	0.17	0.000	VULT	GPS	1
15.630	40.074	21.60	16.95	0.40	0.29	-0.010	SAPR	GPS	1
15.633	48.203	21.36	15.25	0.08	0.08	-0.029	STPO	GPS	1
15.633	40.391	21.39	16.17	0.17	0.20	-0.037	SLCN	GPS	1
15.642	38.224	23.40	18.21	0.26	0.17	-0.005	VLSG	GPS	1
15.649	46.562	22.69	15.81	0.33	0.39	-0.005	MARI	GPS	1
15.651	38.108	23.88	18.37	0.14	0.17	-0.029	TGRC	GPS	1
15.700	38.003	24.07	17.76	0.23	0.20	0.004	MTTG	GPS	1
15.724	40.601	22.65	19.54	0.11	0.15	-0.025	TITO	GPS	1
15.744	41.755	24.16	20.03	0.25	0.17	-0.012	SGRT	GPS	1
15.751	40.266	23.17	18.64	0.20	0.24	-0.013	MTSN	GPS	1
15.802	40.326	23.27	19.25	0.20	0.22	-0.011	MCEL	GPS	1
15.816	39.994	22.38	18.42	0.19	0.23	0.057	CUCC	GPS	1
15.859	47.928	21.41	15.70	0.40	0.37	0.017	TRF2	GPS	1
15.859	47.928	20.87	15.29	0.36	0.28	-0.024	TRFB	GPS	1
15.866	40.184	24.04	19.17	0.20	0.21	-0.012	SIRI	GPS	1
15.881	46.417	22.34	15.43	0.25	0.26	0.002	PTUJ	GPS	1
15.883	46.953	21.70	15.52	0.32	0.29	-0.020	FLDB	GPS	1
15.886	38.607	24.07	18.27	0.25	0.22	-0.001	JOPP	GPS	1
15.894	38.260	24.04	18.03	0.28	0.31	0.008	CELL	GPS	1
15.895	38.422	22.88	18.09	0.15	0.20	0.002	GIOI	GPS	1
15.897	41.904	24.24	19.17	0.28	0.25	-0.010	ISCH	GPS	1
15.910	41.712	23.36	18.65	0.22	0.18	0.002	MSAG	GPS	1
15.942	40.787	23.23	19.27	0.28	0.24	-0.008	ACER	GPS	1
15.955	39.529	23.28	17.85	0.25	0.23	-0.014	CETR	GPS	1
15.960	40.944	23.22	19.22	0.17	0.18	-0.007	PALZ	GPS	1
16.007	37.953	24.29	17.84	0.23	0.23	-0.009	MPAZ	GPS	1
16.061	40.532	22.94	18.98	0.23	0.25	-0.030	PTRP	GPS	1
16.085	40.190	23.61	18.65	0.14	0.21	-0.018	SCHR	GPS	1

Continued on next page...

Table C.1 – Continued from previous page

Long	Lat	Velocity (mm/yr)				Corr	Site	Source†	EXC‡
°E	°N	East	North	σ E	σ N				
16.090	46.741	22.43	15.48	0.28	0.25	0.007	BODO	GPS	1
16.149	41.373	24.22	19.23	0.22	0.21	-0.009	MARG	GPS	1
16.196	41.061	23.36	19.19	0.19	0.21	-0.007	MRVN	GPS	1
16.211	39.254	23.53	18.48	0.18	0.24	-0.014	CARO	GPS	1
16.226	39.367	24.54	17.85	0.31	0.32	-0.013	ARCA	GPS	1
16.226	39.431	23.90	18.34	0.23	0.16	0.007	TVRN	GPS	1
16.254	40.917	24.04	18.86	0.24	0.22	-0.013	POGG	GPS	1
16.274	41.078	23.49	19.26	0.10	0.11	-0.027	CADM	GPS	1
16.288	39.446	23.59	18.76	0.25	0.23	0.013	LUZZ	GPS	1
16.310	39.201	22.94	18.71	0.47	0.51	-0.029	COSE	GPS	1
16.319	47.074	22.26	15.37	0.19	0.17	-0.069	GUES	GPS	1
16.346	46.572	22.00	15.23	0.27	0.27	0.000	VELI	GPS	1
16.373	48.219	20.50	15.00	0.11	0.12	-0.019	WIEN	GPS	1
16.404	47.738	21.49	15.50	0.15	0.16	-0.015	MTBG	GPS	1
16.435	40.381	23.66	19.15	0.17	0.18	-0.016	CRAC	GPS	1
16.438	38.449	24.16	17.90	0.18	0.19	-0.060	PLAC	GPS	1
16.439	43.507	23.16	18.56	0.36	0.37	-0.017	SPLT	GPS	1
16.441	40.604	23.29	19.08	0.19	0.15	-0.024	SVTO	GPS	1
16.449	39.340	24.44	18.07	0.28	0.27	-0.012	CAMO	GPS	1
16.547	39.278	23.58	18.49	0.38	0.34	-0.022	CRLM	GPS	1
16.560	64.698	15.43	14.75	0.17	0.16	0.001	VIL0	GPS	1
16.583	47.684	22.41	15.48	0.32	0.29	-0.004	SPRN	GPS	1
16.593	49.206	20.80	14.88	0.10	0.09	-0.004	TUBO	GPS	1
16.604	40.907	23.39	19.20	0.18	0.14	-0.018	AMUR	GPS	1
16.689	39.036	24.45	18.06	0.18	0.18	-0.056	SERS	GPS	1
16.705	40.649	23.18	19.05	0.07	0.06	-0.145	MATE	GPS	1
16.758	40.578	24.47	18.85	0.21	0.21	-0.016	GINO	GPS	1
16.776	39.226	25.16	18.26	0.21	0.27	-0.014	CCRI	GPS	1
16.816	39.485	23.88	18.32	0.24	0.19	0.001	PIPA	GPS	1
16.905	41.016	24.72	19.45	0.28	0.24	-0.021	VAL1	GPS	1
16.915	39.148	25.68	17.93	0.20	0.21	0.000	STSV	GPS	1
17.062	51.113	20.34	14.47	0.07	0.07	-0.047	WROC	GPS	1
17.064	40.789	24.51	18.83	0.16	0.15	-0.019	NOCI	GPS	1
17.089	-22.575	20.06	20.00	0.47	0.48	-0.078	WIND	GPS	1
17.118	54.472	19.18	13.95	0.39	0.34	0.001	REDZ	GPS	1
17.259	60.595	17.76	13.99	0.12	0.11	-0.008	MAR6	GPS	1
17.274	48.373	22.40	14.47	0.44	0.33	0.000	MOP2	GPS	1
17.274	48.373	21.57	14.94	0.18	0.14	-0.017	MOPI	GPS	1
17.292	46.964	21.73	14.93	0.24	0.18	0.000	SUME	GPS	1
17.359	40.835	24.85	18.95	0.27	0.26	-0.018	FASA	GPS	1
17.429	50.257	20.75	14.35	0.21	0.18	-0.021	BISK	GPS	1

Continued on next page...

Table C.1 – Continued from previous page

Long	Lat	Velocity (mm/yr)				Corr	Site	Source†	EXC‡
°E	°N	East	North	σ E	σ N				
17.965	40.385	24.46	18.47	0.22	0.22	-0.014	SASA	GPS	1
17.994	53.135	19.73	15.02	0.35	0.28	-0.002	BYDG	GPS	1
18.110	42.650	23.02	17.52	0.15	0.15	-0.037	DUBR	GPS	1
18.162	39.928	24.53	18.55	0.23	0.23	-0.020	UGEN	GPS	1
18.367	57.654	18.85	13.74	0.08	0.08	-0.007	VIS0	GPS	1
18.414	43.868	23.18	15.60	0.12	0.11	-0.021	SRJV	GPS	1
18.430	40.124	24.45	18.20	0.21	0.22	-0.026	GIUR	GPS	1
18.467	40.072	23.66	18.35	0.18	0.17	-0.024	SCTE	GPS	1
18.469	-33.951	17.29	19.15	0.78	0.56	-0.018	CTWN	GPS	1
18.681	45.561	22.64	15.07	0.10	0.09	-0.048	OSJE	GPS	1
18.731	-33.464	12.76	21.27	0.51	0.55	-0.016	MALM	GPS	1
18.837	-33.845	17.08	19.66	0.50	0.46	-0.023	STBS	GPS	1
18.938	69.663	14.57	14.99	0.13	0.11	0.008	TROM	GPS	1
18.940	69.663	15.20	14.91	0.15	0.13	0.048	TRO1	GPS	1
19.057	47.481	22.12	14.32	0.17	0.18	-0.007	BUTE	GPS	1
19.151	48.752	21.25	14.47	0.16	0.14	-0.002	BBYS	GPS	1
19.206	49.687	21.10	14.84	0.13	0.11	-0.032	ZYWI	GPS	1
19.223	-34.425	17.16	19.35	0.60	0.56	-0.018	HERM	GPS	1
19.223	-34.425	17.12	19.15	1.00	0.83	0.011	HNUS	GPS	1
19.379	39.856	20.14	17.30	0.70	0.70	0.000	OTHO	HOL	1
19.429	39.865	20.55	15.89	0.50	0.60	0.000	OTHF	HOL	1
19.460	51.779	21.23	14.53	0.37	0.39	0.002	LODZ	GPS	1
19.496	42.051	21.84	15.60	0.31	0.32	-0.032	SHKO	GPS	1
19.510	40.410	22.62	16.18	1.20	0.81	0.000	VLOR	BUR	1
19.797	39.712	21.62	17.26	0.40	0.40	0.000	ANOK	HOL	1
19.854	39.525	18.56	16.16	2.00	2.50	0.000	AMAT	HOL	1
19.861	39.749	19.32	14.05	1.30	1.60	0.000	PNTN	HOL	1
19.863	41.347	20.79	15.44	0.46	0.52	-0.030	TIRA	GPS	1
19.921	50.066	21.10	14.58	0.15	0.13	-0.018	KRAW	GPS	1
19.936	39.746	19.76	14.26	0.27	0.28	-0.044	KASI	GPS	1
19.946	40.708	21.61	14.60	0.51	0.65	-0.046	BERA	GPS	1
20.005	48.374	22.02	15.77	0.33	0.30	-0.001	RISO	GPS	1
20.128	39.236	23.55	17.64	0.20	0.30	0.000	PAXI	HOL	1
20.194	39.194	23.76	16.13	2.60	3.00	0.000	GAIO	HOL	1
20.213	49.195	21.31	14.22	0.35	0.33	0.155	LOMS	GPS	1
20.249	39.141	23.57	17.24	0.10	0.10	0.002	APAX	HOL	1
20.440	41.685	22.35	12.19	0.24	0.31	-0.020	PESH	GPS	1
20.470	41.590	22.76	12.14	1.00	0.71	0.000	MAQE	BUR	1
20.520	41.240	21.74	12.34	0.61	0.61	0.001	M124	BUR	1
20.540	41.770	23.55	11.73	0.71	0.61	0.001	0801	BUR	1
20.600	41.070	24.68	11.13	1.90	1.10	0.000	QTH2	BUR	1

Continued on next page...

Table C.1 – Continued from previous page

Long	Lat	Velocity (mm/yr)				Corr	Site	Source†	EXC‡
°E	°N	East	North	σ E	σ N				
20.671	46.555	22.40	14.42	0.11	0.11	-0.015	OROS	GPS	1
20.680	41.430	22.73	11.22	0.71	0.61	0.001	M123	BUR	1
20.794	41.127	24.01	11.65	0.11	0.13	-0.050	ORID	GPS	1
20.800	41.990	23.35	12.79	0.61	0.61	0.001	M108	BUR	1
20.820	40.930	23.44	12.40	0.71	0.61	0.001	0807	BUR	1
20.968	67.857	15.76	14.82	0.11	0.10	0.013	KIRU	GPS	1
21.016	37.250	6.19	-4.55	1.60	2.30	0.000	STRO	HOL	1
21.030	41.230	25.12	11.47	0.61	0.61	0.001	M125	BUR	1
21.032	52.098	21.06	13.88	0.13	0.13	-0.038	JOZ2	GPS	1
21.035	52.475	20.62	14.43	0.10	0.10	-0.013	BOGI	GPS	1
21.035	52.476	20.36	14.33	0.07	0.07	-0.035	BOGO	GPS	1
21.048	64.879	17.07	14.09	0.21	0.19	0.024	SKE0	GPS	1
21.050	41.660	23.65	11.56	0.71	0.61	0.001	M110	BUR	1
21.060	67.878	15.90	14.48	0.18	0.17	0.013	KIR0	GPS	1
21.119	55.715	20.03	13.82	0.45	0.43	-0.019	KLPD	GPS	1
21.180	41.000	24.09	11.04	0.71	0.61	0.001	M127	BUR	1
21.210	41.440	23.21	11.04	0.71	0.61	0.001	M122	BUR	1
21.256	-28.414	18.43	18.80	0.85	0.75	-0.067	UPTN	GPS	1
21.258	-28.407	17.68	20.06	0.58	0.56	-0.058	UPTA	GPS	1
21.269	40.519	23.56	11.33	0.10	0.10	0.001	KAST	HOL	1
21.400	41.700	22.80	11.01	0.80	0.80	0.000	M111	BUR	1
21.450	42.190	25.02	13.61	0.61	0.61	0.000	0802	BUR	1
21.650	41.330	23.00	10.68	0.71	0.61	0.000	M121	BUR	1
21.742	36.896	-2.88	-20.43	0.50	0.68	-0.056	PYLO	GPS	1
21.771	62.961	18.29	13.29	0.13	0.12	0.005	VAAS	GPS	1
21.787	38.284	6.72	-8.55	0.56	0.63	-0.030	PAT0	GPS	1
21.790	40.930	24.00	10.17	1.10	1.00	0.000	0806	BUR	1
21.800	41.990	23.11	11.05	0.71	0.71	0.000	M112	BUR	1
21.846	39.676	19.49	2.94	0.62	0.62	-0.036	LIPO	FLO	1
21.930	42.310	24.77	11.94	0.61	0.61	0.000	M104	BUR	1
21.936	39.764	19.00	4.32	1.31	1.01	0.020	OXIA	FLO	1
22.010	41.770	23.69	11.22	0.61	0.61	0.000	0804	BUR	1
22.014	39.565	21.58	5.54	0.30	0.41	-0.118	KLOK	GPS	1
22.120	42.030	23.35	10.31	0.71	0.61	0.000	M113	BUR	1
22.136	47.835	22.39	13.27	0.29	0.24	-0.029	NYIR	GPS	1
22.210	41.160	24.52	10.00	0.61	0.61	0.000	M129	BUR	1
22.241	39.608	20.85	-0.76	0.71	0.71	-0.038	CG02	FLO	1
22.298	48.632	21.85	13.65	0.09	0.08	-0.040	UZHL	GPS	1
22.310	41.510	23.28	10.39	0.71	0.61	0.000	M120	BUR	1
22.332	39.433	21.47	5.61	0.33	0.33	-0.099	CG03	FLO	1
22.382	-34.001	15.95	19.83	0.37	0.34	-0.042	GEOR	GPS	1

Continued on next page...

Table C.1 – Continued from previous page

Long	Lat	Velocity (mm/yr)				Corr	Site	Source†	EXC‡
°E	°N	East	North	σ E	σ N				
22.389	39.912	22.66	5.41	0.43	0.52	0.010	GDMN	FLO	1
22.510	41.780	22.66	11.35	0.71	0.61	0.000	M117	BUR	1
22.510	58.256	19.94	13.04	0.34	0.36	0.011	KURE	GPS	1
22.520	42.160	23.60	12.65	0.71	0.61	0.000	M114	BUR	1
22.544	39.937	25.29	7.98	0.25	0.25	-0.086	KRNA	FLO	1
22.574	-32.347	17.69	19.03	0.37	0.36	-0.039	BWES	GPS	1
22.586	49.433	21.37	13.93	0.37	0.34	-0.012	USDL	GPS	1
22.620	39.490	21.10	3.31	1.90	2.10	0.000	CG01	HOL	1
22.680	42.260	24.31	11.12	1.60	1.30	0.000	BOGS	BUR	1
22.700	42.500	24.56	11.82	0.71	0.70	0.000	ZEME	BUR	1
22.713	42.284	24.09	12.03	0.58	0.49	-0.046	KUST	GPS	1
22.720	42.680	23.53	10.32	0.80	0.80	0.000	DSEC	BUR	1
22.749	-29.668	17.51	19.31	0.35	0.34	-0.056	PSKA	GPS	1
22.770	43.610	23.17	12.30	0.51	0.51	0.000	VARB	BUR	1
22.780	41.330	24.09	10.62	0.61	0.61	0.000	0805	BUR	1
22.812	39.148	17.86	0.08	0.32	0.33	-0.121	CG09	FLO	1
22.820	42.360	24.41	11.90	0.80	0.80	0.000	CARV	BUR	1
22.860	42.000	24.48	12.11	0.61	0.61	0.000	0803	BUR	1
22.880	41.540	24.27	10.90	0.61	0.61	0.000	M119	BUR	1
22.900	42.750	23.65	9.39	0.80	0.80	0.000	BREZ	BUR	1
22.928	54.099	20.13	13.04	0.32	0.41	-0.001	SWKI	GPS	1
22.940	42.130	23.87	11.40	0.71	0.71	0.000	FROL	BUR	1
22.960	41.790	23.43	10.39	0.80	0.61	0.000	M116	BUR	1
23.004	40.567	24.72	5.86	0.20	0.18	-0.044	AUT1	GPS	1
23.060	42.860	22.96	11.57	0.51	0.51	0.000	SLIV	BUR	1
23.070	42.720	23.48	11.57	0.80	0.80	0.000	BANK	BUR	1
23.080	42.570	23.31	10.16	0.71	0.80	0.000	KRAL	BUR	1
23.090	42.390	24.34	10.86	0.71	0.71	0.000	DELA	BUR	1
23.125	41.459	23.96	12.22	1.32	1.27	-0.008	PETB	REI	1
23.127	52.035	20.83	13.94	0.49	0.56	0.003	BPDL	GPS	1
23.130	41.460	23.72	10.17	0.61	0.51	0.000	PECH	BUR	1
23.138	43.110	20.92	12.61	1.32	1.23	0.001	BERK	REI	1
23.140	43.110	23.63	12.26	0.51	0.51	0.000	BERK	BUR	1
23.170	42.510	24.04	10.45	0.80	0.80	0.000	BOSN	BUR	1
23.180	42.140	23.11	10.56	0.90	0.90	0.000	PADA	BUR	1
23.186	39.361	19.22	-2.90	0.81	0.71	-0.107	CG05	FLO	1
23.222	39.306	18.40	0.44	0.40	0.40	0.000	NEOH	HOL	1
23.250	42.280	24.20	12.25	0.71	0.71	0.000	SAPA	BUR	1
23.254	39.146	15.94	-5.33	0.71	0.71	-0.059	CG10	FLO	1
23.268	41.551	23.37	10.18	0.44	0.41	-0.035	SAND	GPS	1
23.269	42.668	23.88	13.06	0.69	0.75	-0.057	SOFA	GPS	1

Continued on next page...

Table C.1 – Continued from previous page

Long	Lat	Velocity (mm/yr)				Corr	Site	Source†	EXC‡
°E	°N	East	North	σ E	σ N				
23.272	39.182	17.75	-0.64	0.61	0.71	0.028	MKRH	FLO	1
23.280	42.560	21.65	11.93	0.90	0.90	0.000	CHER	BUR	1
23.360	42.870	24.91	11.62	0.61	0.61	0.000	VLTR	BUR	1
23.372	38.986	14.47	-4.87	0.61	0.61	-0.030	CG17	FLO	1
23.395	42.556	23.95	11.96	0.09	0.10	-0.066	SOFI	GPS	1
23.425	42.477	20.01	12.52	1.23	1.13	0.010	PLA1	REI	1
23.428	40.789	23.64	8.58	0.45	0.38	0.043	SOXO	FLO	1
23.430	42.480	23.58	12.12	0.51	0.51	0.000	PLA1	BUR	1
23.433	-27.461	18.27	18.97	0.35	0.34	-0.056	KMAN	GPS	1
23.490	42.600	23.47	11.11	0.90	0.90	0.000	LOZE	BUR	1
23.510	42.270	22.93	11.31	0.80	0.80	0.000	MALA	BUR	1
23.550	42.990	23.42	12.39	1.10	1.10	0.000	KOZN	BUR	1
23.558	47.652	22.56	13.52	0.24	0.23	-0.006	BAIA	GPS	1
23.569	41.823	22.48	10.93	1.34	1.30	-0.012	DOBR	REI	1
23.570	42.770	22.76	10.29	1.00	1.10	0.000	BUHO	BUR	1
23.570	41.820	23.42	11.40	0.51	0.51	0.000	DOBR	BUR	1
23.668	39.147	14.88	-5.61	1.50	1.70	0.000	CG11	HOL	1
23.730	42.480	26.23	10.08	0.80	0.80	0.000	VERI	BUR	1
23.760	42.140	23.40	11.47	0.80	0.80	0.000	BELM	BUR	1
23.765	44.338	23.05	12.69	0.33	0.29	-0.006	CRAI	GPS	1
23.800	42.780	24.29	11.66	0.90	0.90	0.000	VITA	BUR	1
23.854	42.064	25.05	11.74	0.08	0.40	-0.030	YUND	GPS	1
23.890	42.510	23.85	11.55	1.20	1.20	0.000	BELI	BUR	1
23.915	39.207	14.39	-7.34	1.30	1.50	0.000	CG12	HOL	1
23.916	41.597	23.06	9.96	1.25	1.21	-0.003	SAT1	REI	1
23.919	39.994	23.91	3.59	0.43	0.35	-0.020	STHN	FLO	1
23.920	41.600	24.02	10.86	0.51	0.51	0.000	SAT1	BUR	1
23.930	42.430	23.47	12.04	0.71	0.80	0.000	MUHO	BUR	1
24.015	49.836	21.59	13.86	0.11	0.10	-0.023	SULP	GPS	1
24.059	56.949	20.34	13.35	0.09	0.10	0.004	RIGA	GPS	1
24.060	42.290	23.22	11.32	0.80	0.80	0.000	VETR	BUR	1
24.244	41.375	24.57	11.24	0.50	0.52	0.009	SKAL	FLO	1
24.340	42.231	23.41	12.12	0.55	0.48	-0.032	PAZA	GPS	1
24.380	59.464	19.38	11.97	0.32	0.30	0.023	SUUR	GPS	1
24.395	60.218	19.81	12.65	0.14	0.14	0.003	METZ	GPS	1
24.535	-32.248	18.16	19.77	0.37	0.32	-0.062	GRNT	GPS	1
24.627	40.593	22.45	10.59	0.55	0.47	-0.043	THAS	FLO	1
24.630	43.360	23.82	11.93	1.30	1.30	0.000	KAIL	BUR	1
24.634	43.362	23.71	14.04	1.42	1.27	-0.004	KAIL	REI	1
24.741	41.696	23.83	11.68	0.38	0.31	-0.041	ROZH	GPS	1
24.750	42.150	24.25	11.23	0.51	0.51	0.000	PLDV	BUR	1

Continued on next page...

Table C.1 – Continued from previous page

Long	Lat	Velocity (mm/yr)				Corr	Site	Source†	EXC‡
°E	°N	East	North	σ E	σ N				
24.753	42.146	22.33	11.19	1.29	1.26	-0.013	PLO2	REI	1
24.807	-28.743	17.55	18.99	0.35	0.34	-0.068	KLEY	GPS	1
24.917	41.140	24.86	10.67	0.54	0.50	-0.038	DUTH	GPS	1
25.180	43.580	23.67	14.35	0.90	0.80	0.000	TATA	BUR	1
25.277	42.963	24.27	14.01	1.29	1.19	0.000	GABR	REI	1
25.280	42.960	23.70	12.23	0.41	0.41	0.000	GABR	BUR	1
25.299	54.653	20.95	13.39	0.17	0.17	-0.006	VLNS	GPS	1
25.400	41.550	24.36	11.33	0.51	0.51	0.000	MOMC	BUR	1
25.402	41.545	24.61	11.29	1.27	1.22	-0.009	MOMC	REI	1
25.513	40.466	21.78	10.34	1.00	1.30	0.000	SMTK	HOL	1
25.540	-25.805	18.25	17.80	0.42	0.40	-0.081	MFKG	GPS	1
25.566	40.928	25.15	10.57	0.44	0.46	-0.065	ASKT	FLO	1
26.126	44.464	23.41	12.11	0.08	0.09	-0.062	BUCU	GPS	1
26.265	39.246	4.91	-0.10	0.34	0.31	-0.048	PRKV	GPS	1
26.298	-29.104	14.85	14.92	0.38	0.37	-0.078	BFTN	GPS	1
26.309	42.075	23.43	13.25	1.24	1.19	-0.005	TOPO	REI	1
26.310	42.080	24.81	11.28	0.81	0.80	0.000	TOPO	BUR	1
26.389	67.421	17.74	13.02	0.18	0.19	0.036	SODA	GPS	1
26.466	58.266	20.61	12.24	0.39	0.46	0.022	TORA	GPS	1
26.507	-33.320	15.32	18.63	0.44	0.39	-0.076	GRHM	GPS	1
26.706	40.739	18.80	9.85	0.71	0.71	0.021	DOKU	REI	1
26.716	-30.680	16.65	19.15	0.36	0.34	-0.070	ANTH	GPS	1
26.725	43.488	22.57	12.78	1.34	1.27	-0.001	SHUM	REI	1
26.730	43.490	23.33	12.10	0.61	0.51	0.000	SHUM	BUR	1
26.912	46.562	22.08	13.39	0.22	0.21	-0.022	BACA	GPS	1
26.922	-31.908	15.75	19.23	0.38	0.35	-0.067	QTWN	GPS	1
27.231	31.346	22.12	17.69	0.88	0.77	0.003	MATR	REI	1
27.240	-27.664	17.40	18.99	0.34	0.33	-0.068	KSTD	GPS	1
27.393	40.811	20.21	8.31	0.71	0.68	-0.010	YENB	REI	1
27.440	42.670	24.59	12.09	0.41	0.41	0.000	BURG	BUR	1
27.442	42.666	24.41	12.58	1.26	1.22	-0.010	BURG	REI	1
27.480	42.480	24.72	11.99	0.81	0.71	0.000	BUTG	BUR	1
27.483	42.484	21.80	12.16	1.35	1.30	-0.003	BUTG	REI	1
27.537	59.422	20.60	12.26	0.46	0.39	0.034	TOIL	GPS	1
27.696	-23.687	18.32	18.28	0.34	0.31	-0.083	ERAS	GPS	1
27.766	-26.083	16.78	18.47	0.54	0.57	-0.094	KRUG	GPS	1
27.777	-25.636	17.74	18.43	0.82	0.78	-0.073	BRIT	GPS	1
27.779	41.827	24.56	12.90	0.73	0.69	-0.018	DEMI	REI	1
27.829	-33.038	16.02	19.16	0.36	0.33	-0.077	ELDN	GPS	1
27.904	-26.661	16.18	19.03	0.48	0.47	-0.101	VER1	GPS	1
27.923	43.203	25.83	11.11	0.46	0.47	-0.054	VARN	GPS	1

Continued on next page...

Table C.1 – Continued from previous page

Long	Lat	Velocity (mm/yr)				Corr	Site	Source†	EXC‡
°E	°N	East	North	σ E	σ N				
27.950	42.100	22.15	12.22	1.40	1.20	0.000	AHTG	BUR	1
27.960	40.971	26.51	12.38	0.65	0.62	-0.001	MAER	REI	1
28.283	-25.732	18.25	17.13	0.34	0.34	-0.096	PRET	GPS	1
28.293	41.475	25.04	12.24	1.16	1.05	-0.007	YALI	REI	1
28.334	-28.250	17.00	19.98	0.34	0.34	-0.082	BETH	GPS	1
28.341	-26.195	16.49	18.24	0.50	0.48	-0.093	BENI	GPS	1
28.365	41.052	22.23	13.69	1.15	1.06	-0.005	SELP	REI	1
28.373	-26.509	17.19	18.47	0.66	0.70	-0.098	HEID	GPS	1
28.406	-24.703	17.90	18.56	0.38	0.38	-0.099	NYLS	GPS	1
28.658	44.162	23.46	12.15	0.21	0.22	-0.042	COST	GPS	1
28.673	-31.549	16.22	18.58	0.35	0.34	-0.097	UMTA	GPS	1
28.733	-25.803	17.03	18.88	0.68	0.65	-0.090	BRNK	GPS	1
28.844	47.030	22.80	12.93	0.32	0.33	-0.022	IGEO	GPS	1
29.019	41.104	25.54	9.97	0.12	0.13	-0.080	ISTA	GPS	1
29.064	41.064	21.51	13.72	0.62	0.59	0.000	IKAN	REI	1
29.412	-25.162	17.90	18.69	0.39	0.39	-0.065	GDAL	GPS	1
29.423	40.821	15.16	13.55	0.68	0.68	0.031	GATE	REI	1
29.454	-25.774	17.86	18.69	0.34	0.33	-0.105	MBRG	GPS	1
29.466	-23.923	17.97	19.75	0.35	0.34	-0.088	PTBG	GPS	1
29.623	41.179	23.14	12.10	1.25	1.11	-0.022	SILE	REI	1
29.635	40.803	17.97	13.91	0.94	0.92	0.041	YUHE	REI	1
29.681	40.362	4.22	13.30	0.65	0.58	0.009	DERB	REI	1
29.782	-28.558	16.82	18.59	0.35	0.33	-0.108	LSMH	GPS	1
29.984	-26.498	17.77	19.20	0.35	0.34	-0.102	EMLO	GPS	1
29.987	-29.209	16.70	16.08	0.96	0.86	-0.081	MRIV	GPS	1
30.069	-30.146	15.84	16.01	0.79	0.76	-0.045	IXOP	GPS	1
30.090	-1.945	25.41	18.45	0.79	0.73	-0.047	NURK	GPS	1
30.096	62.391	20.45	11.72	0.17	0.15	0.044	JOEN	GPS	1
30.130	40.745	15.64	11.93	0.89	0.92	0.003	SISL	REI	1
30.185	-24.672	20.46	23.08	0.49	0.47	-0.105	SPRT	GPS	1
30.328	59.772	20.99	11.93	0.48	0.43	0.015	PULK	GPS	1
30.383	-29.601	15.83	18.52	0.43	0.41	-0.116	PMBG	GPS	1
30.384	-23.080	18.86	16.67	0.35	0.32	-0.080	TDOU	GPS	1
30.578	-29.071	16.95	16.84	0.91	0.85	-0.084	GREY	GPS	1
30.745	40.652	13.03	13.59	0.99	1.01	0.079	KMAL	REI	1
30.755	-30.286	16.13	16.78	0.94	0.91	-0.077	SCOT	GPS	1
30.827	40.735	16.25	11.95	0.73	0.74	0.014	KDER	REI	1
30.888	29.514	22.49	18.10	0.83	0.79	-0.001	MEST	REI	1
30.947	-29.965	16.46	18.38	0.41	0.43	-0.109	DRBN	GPS	1
31.031	70.336	17.33	12.15	0.16	0.14	0.053	VARS	GPS	1
31.134	-23.952	18.18	17.93	0.35	0.34	-0.108	PBWA	GPS	1

Continued on next page...

Table C.1 – Continued from previous page

Long	Lat	Velocity (mm/yr)				Corr	Site	Source†	EXC‡
°E	°N	East	North	σ E	σ N				
31.290	-29.344	16.73	19.30	0.83	0.78	-0.045	STAN	GPS	1
31.314	51.519	21.99	12.59	0.35	0.38	0.012	CNIV	GPS	1
31.343	29.862	23.06	18.70	0.58	0.69	-0.087	PHLW	GPS	1
31.344	29.862	22.90	18.08	0.55	0.52	-0.009	HELW	REI	1
31.421	-28.293	16.45	18.70	0.35	0.34	-0.115	ULDI	GPS	1
31.438	40.937	20.87	12.48	0.56	0.54	0.004	YIG2	REI	1
31.439	40.937	20.87	12.48	0.56	0.54	0.004	YIGI	REI	1
31.973	46.973	23.30	12.26	0.13	0.12	-0.035	MIKL	GPS	1
32.226	41.520	24.78	11.23	0.87	0.86	-0.012	HALI	REI	1
32.566	29.379	23.76	19.27	0.60	0.59	0.006	FANA	REI	1
32.570	40.881	17.94	12.41	0.75	0.69	-0.006	ISME	REI	1
33.102	29.141	24.22	18.97	0.70	0.66	0.006	ABOZ	REI	1
33.164	45.220	23.99	12.60	0.17	0.17	-0.059	EVPA	GPS	1
33.228	28.163	23.35	19.36	0.67	0.66	0.005	GARB	REI	1
33.391	27.919	23.45	19.41	0.66	0.65	0.002	ZEIT	REI	1
33.404	28.631	22.43	17.16	0.66	0.65	0.004	DERB	REI	1
33.494	27.686	23.69	17.25	0.66	0.65	0.000	GEMS	REI	1
33.596	28.269	22.20	18.44	0.59	0.58	0.004	TOUR	REI	1
33.832	27.244	22.05	17.94	0.83	0.78	-0.003	HURG	REI	1
33.883	27.961	20.81	20.83	1.01	1.01	-0.008	KENS	REI	1
33.991	44.413	24.06	12.27	0.13	0.13	-0.038	CRAO	GPS	1
33.995	28.639	24.53	18.44	1.03	1.04	-0.011	CATH	REI	1
34.184	27.846	22.04	19.29	0.59	0.58	0.001	SHAM	REI	1
34.284	31.228	26.86	17.17	0.22	0.26	-0.029	SLOM	GPS	1
34.314	28.178	23.26	20.07	0.88	0.81	-0.003	NABQ	REI	1
34.470	28.529	22.40	19.39	0.64	0.64	0.001	DAHA	REI	1
34.543	49.603	22.33	12.21	0.13	0.12	-0.028	POLV	GPS	1
34.607	31.708	23.09	18.96	0.22	0.23	-0.052	ALON	GPS	1
34.763	30.598	23.17	19.27	0.11	0.14	-0.105	RAMO	GPS	1
34.781	32.068	22.92	20.32	0.10	0.12	-0.064	TELA	GPS	1
34.866	31.378	22.79	19.01	0.15	0.16	-0.055	LHAV	GPS	1
34.890	32.488	22.01	19.51	0.16	0.18	-0.051	CSAR	GPS	1
34.921	29.509	24.88	20.78	0.10	0.12	-0.088	ELAT	GPS	1
34.928	30.992	23.23	19.25	0.21	0.21	-0.062	YRCM	GPS	1
35.023	32.779	22.27	19.71	0.12	0.11	-0.066	BSHM	GPS	1
35.036	30.038	24.17	20.59	0.20	0.24	-0.078	NRIF	GPS	1
35.089	31.723	23.81	19.07	1.18	1.12	-0.012	BARG	REI	1
35.145	33.023	21.91	20.04	0.10	0.11	-0.046	KABR	GPS	1
35.203	31.771	23.11	19.78	0.12	0.13	-0.010	JSLM	GPS	1
35.205	42.020	24.05	13.32	0.87	0.77	0.007	SINO	REI	1
35.209	32.102	22.70	20.16	0.34	0.34	-0.073	AREL	GPS	1

Continued on next page...

Table C.1 – Continued from previous page

Long	Lat	Velocity (mm/yr)				Corr	Site	Source†	EXC‡
°E	°N	East	North	σ E	σ N				
35.369	31.037	24.42	20.81	0.20	0.22	-0.058	DSEA	GPS	1
35.392	31.593	22.99	20.18	0.10	0.11	-0.100	DRAG	GPS	1
35.417	32.479	22.12	20.48	0.10	0.10	-0.056	GILB	GPS	1
35.674	34.115	21.63	21.41	0.33	0.37	-0.048	LAUG	GPS	1
35.688	32.995	22.41	23.32	0.11	0.12	-0.062	KATZ	GPS	1
35.771	33.182	22.32	22.49	0.11	0.12	-0.085	ELRO	GPS	1
36.336	41.299	25.11	14.16	0.98	0.99	0.049	SAMS	REI	1
36.894	-1.221	27.46	15.66	0.63	0.68	-0.085	RCMN	GPS	1
37.215	56.022	22.62	11.69	0.17	0.18	-0.009	MDVJ	GPS	1
38.049	44.552	24.48	9.96	1.50	1.32	-0.024	GELE	REI	1
38.906	48.457	25.46	10.29	0.60	0.67	-0.008	ALCI	GPS	1
39.242	44.704	24.55	10.78	1.27	1.13	0.018	GKL_	REI	1
39.584	-69.007	-4.00	2.84	0.14	0.13	-0.106	SYOG	GPS	1
39.702	40.974	25.93	13.24	0.48	0.46	0.009	AKTO	REI	1
39.776	40.995	25.35	13.36	0.16	0.19	-0.062	TRAB	GPS	1
40.194	-2.996	26.36	16.22	0.69	0.61	-0.101	MAL2	GPS	1
40.254	39.731	22.61	16.39	0.75	0.69	-0.015	MERC	REI	1
40.272	43.681	26.85	9.43	1.68	1.41	0.006	KRPO	REI	1
40.809	40.437	26.13	13.76	0.57	0.52	-0.015	ISPI	REI	1
41.057	38.959	18.82	21.90	1.43	1.20	-0.024	SOLH	REI	1
41.300	39.973	24.84	16.23	0.67	0.65	0.008	ERZU	REI	1
41.339	41.371	24.85	13.15	0.90	0.89	-0.017	HOPA	REI	1
41.454	39.186	19.71	21.08	2.01	1.29	-0.046	VART	REI	1
41.512	39.643	23.48	14.71	1.78	1.22	-0.072	TKMN	REI	1
41.565	43.788	25.22	11.27	0.10	0.11	-0.057	ZECK	GPS	1
41.794	38.754	20.97	25.02	0.84	0.70	0.105	KRKT	REI	1
41.990	40.548	27.48	15.26	0.93	0.90	0.020	OLTU	REI	1
42.062	42.721	24.90	13.50	0.50	0.50	-0.005	INGU	REI	1
42.133	41.648	24.90	15.33	0.67	0.67	-0.009	SHUA	REI	1
42.149	39.714	24.19	18.99	1.40	1.24	-0.022	KRYZ	REI	1
42.195	43.349	24.96	10.01	0.85	0.83	-0.006	ULKA	REI	1
42.457	37.528	19.35	25.26	2.72	1.24	0.042	SRNK	REI	1
42.471	42.022	27.63	14.25	0.75	0.70	-0.031	VANI	REI	1
42.547	38.488	20.14	24.12	1.52	1.20	-0.045	RESD	REI	1
42.667	43.743	25.78	12.15	0.81	0.82	-0.010	SHAT	REI	1
42.755	41.126	26.94	14.65	1.35	1.06	-0.012	ARDA	REI	1
42.787	44.011	25.27	11.28	0.85	0.85	-0.007	BEUG	REI	1
42.873	45.267	27.24	8.87	0.97	0.93	0.010	SVT1	REI	1
42.910	39.232	23.69	19.46	0.62	0.53	-0.031	PTNS	REI	1
43.026	39.719	26.54	18.64	0.69	0.66	-0.035	ARGI	REI	1
43.135	42.468	26.49	13.89	0.86	0.72	-0.008	KHOT	REI	1

Continued on next page...

Table C.1 – Continued from previous page

Long	Lat	Velocity (mm/yr)				Corr	Site	Source†	EXC‡
°E	°N	East	North	σ E	σ N				
43.170	40.685	27.18	15.85	0.60	0.51	-0.015	KARS	REI	1
43.341	38.549	20.77	23.06	0.86	0.84	0.014	KAL2	REI	1
43.382	42.578	25.79	9.37	0.74	0.67	0.013	KHUR	REI	1
43.400	42.349	28.05	15.85	0.70	0.61	0.025	SACC	REI	1
43.540	42.485	26.33	9.73	0.76	0.72	0.022	LESO	REI	1
43.753	42.978	26.71	10.33	0.87	0.87	-0.032	MATS	REI	1
43.759	38.997	20.83	21.31	2.09	1.42	-0.089	MRAD	REI	1
43.768	40.972	27.07	16.41	0.92	0.84	0.014	AMAS	REI	1
43.891	41.537	27.13	14.40	0.64	0.60	0.003	NINO	REI	1
43.954	40.609	27.72	17.94	0.83	0.82	-0.017	ARTI	REI	1
44.114	40.178	28.20	17.59	0.83	0.82	-0.017	MMOR	REI	1
44.145	39.556	25.12	16.84	2.12	1.29	-0.107	DBYZ	REI	1
44.364	41.031	29.34	15.76	0.84	0.79	0.003	STEP	REI	1
44.486	42.447	26.36	13.59	0.60	0.59	0.027	KRES	REI	1
44.503	40.227	28.44	17.13	0.11	0.13	-0.088	NSSP	GPS	1
44.526	41.831	27.17	16.19	0.59	0.56	0.020	NICH	REI	1
44.742	40.149	28.70	19.35	0.63	0.55	0.006	GARN	REI	1
44.826	41.377	34.49	14.84	2.69	1.70	0.057	SHUL	REI	1
44.859	40.526	27.20	14.96	1.12	0.84	-0.007	GAGA	REI	1
45.139	40.907	29.65	17.11	0.64	0.61	0.006	IJEV	REI	1
45.341	40.124	28.86	19.00	2.10	1.45	0.054	ASTG	REI	1
45.661	39.837	30.97	19.85	0.86	0.82	-0.015	JERM	REI	1
45.795	41.951	25.53	14.78	0.73	0.69	-0.015	KUDI	REI	1
46.093	39.536	30.21	19.38	0.99	0.88	0.026	NORA	REI	1
46.162	39.126	27.29	23.86	2.11	1.39	0.024	KAJR	REI	1
46.162	36.908	24.94	23.44	0.80	0.77	0.001	MIAN	REI	1
46.367	39.511	30.76	20.71	0.84	0.82	-0.011	GORI	REI	1
46.459	39.315	30.30	21.84	2.09	1.35	0.069	KARM	REI	1
46.511	41.652	26.97	14.42	0.64	0.64	0.002	KATE	REI	1
46.758	40.184	30.20	20.41	0.97	0.85	0.006	KASP	REI	1
46.760	39.753	29.74	20.48	0.93	0.81	0.002	SHOU	REI	1
46.842	43.026	27.62	12.87	0.56	0.56	-0.004	DUBK	REI	1
46.847	43.125	24.97	13.05	0.56	0.56	0.000	ZURA	REI	1
47.250	41.132	27.17	14.72	0.65	0.65	0.002	SHEK	REI	1
47.863	40.975	26.76	13.03	0.67	0.65	-0.004	KEBE	REI	1
47.930	36.232	24.55	21.91	1.25	1.12	0.011	BIJA	REI	1
48.148	40.333	30.53	18.88	0.99	0.86	0.009	KURD	REI	1
48.388	38.952	31.54	21.78	0.93	0.86	0.002	YARD	REI	1
48.419	38.706	31.33	20.98	0.91	0.81	0.003	GOSM	REI	1
48.529	41.595	26.85	10.07	0.96	0.86	0.004	SAMU	REI	1
48.551	40.614	28.90	10.54	0.89	0.80	-0.003	MEDR	REI	1

Continued on next page...

Table C.1 – Continued from previous page

Long	Lat	Velocity (mm/yr)				Corr	Site	Source†	EXC‡
°E	°N	East	North	σ E	σ N				
48.717	39.497	32.66	21.35	0.67	0.65	0.000	BILE	REI	1
49.120	41.066	27.20	10.67	0.89	0.80	0.003	SIYE	REI	1
49.426	40.025	30.34	10.51	0.69	0.66	0.005	SHIK	REI	1
50.748	32.367	26.37	21.68	1.21	1.09	-0.001	SHAH	REI	1
51.334	35.697	25.99	19.41	0.22	0.27	-0.065	TEHN	GPS	1
51.812	35.730	26.28	17.84	0.72	0.69	-0.001	BOOM	REI	1
51.885	35.223	28.18	17.55	1.27	1.25	0.016	PISH	REI	1
51.986	35.793	26.51	17.54	1.33	1.30	0.018	ABAL	REI	1
52.043	35.492	27.16	17.04	1.25	1.22	0.015	TANG	REI	1
52.059	35.701	25.79	16.46	1.25	1.24	0.014	DAMA	REI	1
52.157	35.868	26.90	15.33	1.32	1.30	0.021	MEHR	REI	1
52.285	36.588	24.72	14.04	1.13	1.10	0.007	MAHM	REI	1
52.305	36.206	24.10	17.12	1.40	1.29	0.021	HELI	REI	1
52.586	35.701	25.24	16.76	1.23	1.20	0.013	AMIN	REI	1
53.564	35.662	26.75	16.69	1.32	1.13	0.014	SEMN	REI	1
53.822	32.313	25.62	21.15	0.79	0.75	0.001	ARD1	REI	1
54.199	36.860	25.80	12.73	1.36	1.13	0.016	KORD	REI	1
54.608	30.079	28.63	23.43	1.30	1.11	0.007	HARA	REI	1
55.918	28.302	26.73	24.98	1.38	1.05	-0.025	HAJI	REI	1
56.070	33.369	28.81	18.15	1.27	1.10	0.006	ROBA	REI	1
57.119	30.277	28.20	23.01	2.28	1.37	0.034	KERM	REI	1
57.308	37.814	29.21	9.11	1.38	1.12	0.020	SHIR	REI	1
57.767	25.636	29.51	20.75	1.21	1.07	0.000	JASK	REI	1
58.464	35.293	27.79	12.55	0.82	0.76	-0.001	KASH	REI	1
59.480	36.335	27.02	4.50	1.76	1.53	0.008	MASH	REI	1
60.694	25.300	26.68	13.76	1.43	1.13	0.003	CHAC	REI	1
61.034	36.601	30.68	5.56	1.30	1.12	0.010	YAZT	REI	1
61.517	31.049	28.35	5.68	1.21	1.07	0.004	ZABO	REI	1
62.871	-67.605	-3.74	-2.16	0.14	0.13	-0.121	MAW1	GPS	1
66.885	39.135	27.96	5.57	0.12	0.13	-0.081	KIT3	GPS	1
70.256	-49.352	4.87	-2.79	0.15	0.13	-0.153	KERG	GPS	1
72.370	-7.270	47.41	33.14	0.14	0.14	-0.181	DGAR	GPS	1
73.526	4.189	45.91	35.42	0.35	0.46	-0.122	MALD	GPS	1
74.694	42.680	27.31	4.95	0.11	0.12	-0.141	POL2	GPS	1
74.751	42.999	26.82	2.71	0.13	0.15	-0.074	CHUM	GPS	1
77.017	43.179	28.14	3.89	0.13	0.14	-0.117	SELE	GPS	1
77.512	13.034	42.68	35.03	0.22	0.28	-0.104	BAN2	GPS	1
77.570	13.021	42.32	34.92	0.18	0.22	-0.177	IISC	GPS	1
77.973	-68.577	-3.02	-5.16	0.13	0.14	-0.107	DAV1	GPS	1
78.551	17.417	40.44	34.51	0.21	0.24	-0.181	HYDE	GPS	1
78.619	50.714	26.64	0.72	0.17	0.19	-0.080	KRTV	GPS	1

Continued on next page...

Table C.1 – Continued from previous page

Long	Lat	Velocity (mm/yr)				Corr	Site	Source†	EXC‡
°E	°N	East	North	σ E	σ N				
82.909	55.030	24.03	0.74	0.36	0.41	-0.088	NOVJ	GPS	1
82.910	55.031	26.77	-1.54	0.63	0.79	-0.062	NOVM	GPS	1
87.177	43.471	31.88	5.78	0.19	0.21	-0.128	GUAO	GPS	1
87.601	43.808	30.66	6.90	0.15	0.16	-0.137	URUM	GPS	1
91.104	29.657	47.13	14.84	0.19	0.22	-0.214	LHAS	GPS	1
91.104	29.657	46.52	15.58	0.14	0.17	-0.201	LHAZ	GPS	1
96.834	-12.188	46.19	51.14	0.16	0.18	-0.186	COCO	GPS	1
102.797	25.030	31.15	-18.51	0.15	0.18	-0.170	KUNM	GPS	1
104.316	52.219	25.46	-6.44	0.33	0.27	-0.147	IRKJ	GPS	1
107.052	47.865	28.22	-8.56	0.15	0.18	-0.196	ULAB	GPS	1
109.222	34.369	33.31	-10.76	0.37	0.48	-0.132	XIAN	GPS	1
110.520	-66.283	1.64	-9.74	0.13	0.13	-0.025	CAS1	GPS	1
114.357	30.532	31.73	-11.87	0.13	0.15	-0.177	WUHN	GPS	1
115.347	-29.047	40.09	58.55	0.29	0.37	-0.194	YAR1	GPS	1
115.347	-29.047	39.50	57.84	0.21	0.23	-0.141	YARR	GPS	1
115.885	-31.802	39.78	57.49	0.12	0.13	-0.139	PERT	GPS	1
115.893	39.609	30.71	-10.69	0.15	0.16	-0.201	BJFS	GPS	1
116.193	-31.049	38.54	58.07	0.22	0.22	-0.116	NNOR	GPS	1
117.097	-20.981	38.98	58.43	0.13	0.14	-0.159	KARR	GPS	1
120.987	24.798	30.10	-10.13	0.22	0.22	-0.245	TNML	GPS	1
120.987	24.798	29.44	-9.91	0.28	0.34	-0.208	TCMS	GPS	1
121.078	14.636	-28.49	7.06	0.17	0.18	-0.171	PIMO	GPS	1
121.165	24.954	32.45	-12.52	0.21	0.24	-0.215	TWTF	GPS	1
121.200	31.100	32.25	-12.49	0.12	0.14	-0.162	SHAO	GPS	1
125.444	43.791	25.95	-11.87	0.29	0.30	-0.195	CHAN	GPS	1
127.054	37.276	26.57	-12.87	0.13	0.15	-0.160	SUWN	GPS	1
127.366	36.374	26.55	-13.01	0.54	0.71	-0.099	TAEJ	GPS	1
127.375	36.399	26.75	-12.81	0.15	0.17	-0.168	DAEJ	GPS	1
131.133	-12.844	35.98	59.80	0.12	0.12	-0.127	DARW	GPS	1
132.894	-12.659	35.04	60.66	0.19	0.18	-0.101	JAB1	GPS	1
133.810	-31.867	29.12	58.82	0.13	0.14	-0.109	CEDU	GPS	1
133.886	-23.670	32.22	59.19	0.12	0.13	-0.111	ALIC	GPS	1
135.046	48.522	22.38	-13.68	0.19	0.20	-0.142	KHAJ	GPS	1
139.561	35.680	-1.74	-5.34	0.20	0.22	-0.142	MTKA	GPS	1
140.088	36.106	-3.69	-8.04	0.12	0.12	-0.109	TSKB	GPS	1
142.185	27.096	-36.52	12.34	0.13	0.16	-0.106	CCJM	GPS	1
144.803	13.433	-7.64	4.39	0.24	0.24	-0.094	GUUG	GPS	1
144.868	13.589	-8.62	4.76	0.12	0.14	-0.085	GUAM	GPS	1
144.975	-37.829	19.85	57.49	0.25	0.26	-0.047	MOBS	GPS	1
146.993	-6.674	27.40	52.82	0.33	0.31	-0.102	LAE1	GPS	1
147.056	-19.269	28.97	56.02	0.13	0.13	-0.074	TOW2	GPS	1

Continued on next page...

Table C.1 – Continued from previous page

Long	Lat	Velocity (mm/yr)				Corr	Site	Source†	EXC‡
°E	°N	East	North	σ E	σ N				
147.439	-42.805	14.10	56.14	0.12	0.13	-0.013	HOB2	GPS	1
148.980	-35.399	18.20	55.87	0.13	0.13	-0.032	TIDB	GPS	1
150.770	59.576	7.78	-20.65	0.28	0.27	-0.086	MAG0	GPS	1
153.979	24.290	-71.15	23.34	0.20	0.22	-0.070	MCIL	GPS	1
158.607	53.067	-5.19	-7.26	0.16	0.17	-0.078	PETP	GPS	1
158.936	-54.500	-11.70	31.27	0.14	0.13	0.038	MAC1	GPS	1
166.410	-22.270	20.17	45.89	0.21	0.22	0.024	NOUM	GPS	1
166.438	68.076	8.85	-20.59	0.19	0.19	-0.081	BILI	GPS	1
166.669	-77.838	9.88	-11.62	0.13	0.13	0.035	MCM4	GPS	1
167.730	8.722	-69.49	30.26	0.30	0.35	0.061	KWJ1	GPS	1
170.511	-45.870	-41.02	30.89	0.45	0.46	0.047	OUS2	GPS	1
172.655	-43.703	-34.25	31.50	0.17	0.17	0.040	MQZG	GPS	1
174.834	-36.603	4.19	39.90	0.13	0.13	0.040	AUCK	GPS	1
183.434	-43.956	-40.52	33.17	0.14	0.12	0.069	CHAT	GPS	1
189.278	-14.326	-63.11	34.43	0.27	0.25	0.088	ASPA	GPS	1
200.335	22.126	-62.35	34.17	0.09	0.11	0.122	KOKB	GPS	1
202.136	21.303	-62.73	34.49	0.12	0.15	0.124	HNLC	GPS	1
203.743	20.707	-61.93	34.64	0.12	0.16	0.161	MAUI	GPS	1
204.544	19.801	-62.62	34.96	0.11	0.13	0.136	MKEA	GPS	1
210.394	-17.577	-65.92	34.46	0.17	0.17	0.137	THTI	GPS	1
212.501	64.978	-7.03	-22.50	0.10	0.11	0.017	FAIR	GPS	1
224.778	60.751	-11.05	-13.27	0.13	0.13	0.137	WHIT	GPS	1
226.473	68.306	-12.59	-16.78	0.19	0.18	0.149	INVK	GPS	1
231.865	50.640	-12.42	-10.67	0.09	0.09	0.130	HOLB	GPS	1
234.750	71.990	-15.91	-14.65	0.65	0.69	0.120	SACH	GPS	1
235.914	49.295	-8.80	-8.32	0.10	0.11	0.185	NANO	GPS	1
236.513	48.390	-8.13	-7.88	0.08	0.09	0.123	ALBH	GPS	1
239.384	34.556	-43.08	23.58	0.10	0.11	0.117	VNDP	GPS	1
240.317	48.132	-12.82	-10.23	0.15	0.18	0.281	BREW	GPS	1
240.375	49.323	-13.11	-10.33	0.08	0.09	0.112	DRAO	GPS	1
241.827	34.205	-37.53	13.29	0.09	0.10	0.127	JPLM	GPS	1
242.239	70.736	-17.14	-12.31	0.19	0.19	0.164	HOLM	GPS	1
243.111	35.425	-17.49	-3.43	0.08	0.10	0.113	GOLD	GPS	1
243.334	31.871	-40.89	20.29	0.14	0.17	0.248	CIC1	GPS	1
243.578	32.892	-38.61	16.54	0.10	0.11	0.201	MONP	GPS	1
245.519	62.481	-17.20	-11.24	0.10	0.10	0.118	YELL	GPS	1
245.707	50.871	-14.66	-10.93	0.13	0.13	0.226	PRDS	GPS	1
250.617	-27.148	67.05	-6.31	0.24	0.30	0.138	EISL	GPS	1
250.656	-27.125	66.53	-5.57	0.33	0.29	0.111	ISPA	GPS	1
251.881	34.302	-12.81	-6.63	0.08	0.10	0.128	PIE1	GPS	1
255.985	30.681	-12.01	-5.51	0.09	0.10	0.136	MDO1	GPS	1

Continued on next page...

Table C.1 – Continued from previous page

Long	Lat	Velocity (mm/yr)				Corr	Site	Source†	EXC‡
°E	°N	East	North	σ E	σ N				
258.022	54.726	-17.82	-7.29	0.11	0.12	0.197	FLIN	GPS	1
263.998	64.318	-19.47	-3.98	0.21	0.25	0.150	BAKE	GPS	1
264.134	50.259	-17.73	-4.88	0.12	0.12	0.209	DUBO	GPS	1
265.106	74.691	-20.47	-5.07	0.21	0.22	0.127	RESO	GPS	1
265.911	58.759	-18.01	-3.85	0.12	0.13	0.174	CHUR	GPS	1
268.425	41.772	-15.50	-1.20	0.10	0.11	0.158	NLIB	GPS	1
269.480	14.590	5.19	3.38	0.17	0.20	0.186	GUAT	GPS	1
269.696	-0.743	50.57	10.12	0.24	0.25	0.185	GLPS	GPS	1
269.696	-0.743	50.92	11.13	0.33	0.44	0.158	GALA	GPS	1
270.883	13.697	6.73	8.60	0.20	0.22	0.151	SSIA	GPS	1
273.751	12.149	5.27	5.79	0.20	0.22	0.159	MANA	GPS	1
279.838	25.735	-9.62	2.62	0.27	0.32	0.205	AOML	GPS	1
282.934	38.921	-15.19	3.76	0.25	0.31	0.139	USN3	GPS	1
282.934	38.919	-14.76	3.82	0.12	0.13	0.152	USNO	GPS	1
283.173	39.022	-15.05	3.88	0.09	0.10	0.124	GODE	GPS	1
284.238	20.012	-6.06	4.52	0.18	0.18	0.157	SCUB	GPS	1
284.376	45.454	-16.32	3.80	0.12	0.12	0.182	NRC1	GPS	1
285.919	4.640	-0.62	15.96	0.16	0.17	0.096	BOGT	GPS	1
286.975	-36.844	33.41	21.05	0.30	0.29	0.111	CONZ	GPS	1
289.120	-53.137	5.10	12.07	0.20	0.22	0.095	PARC	GPS	1
289.331	-33.150	20.72	16.79	0.15	0.14	0.084	SANT	GPS	1
291.175	76.537	-22.39	5.00	0.18	0.20	0.048	THU2	GPS	1
291.175	76.537	-22.35	4.70	0.17	0.18	0.011	THU3	GPS	1
291.212	76.537	-21.75	5.20	0.22	0.26	0.031	THU1	GPS	1
291.778	44.395	-15.43	6.85	0.13	0.14	0.126	BARH	GPS	1
292.249	-53.786	3.82	12.55	0.28	0.28	0.097	RIOG	GPS	1
293.008	44.909	-15.44	6.93	0.13	0.15	0.147	EPRT	GPS	1
293.167	54.832	-17.31	7.78	0.15	0.16	0.118	SCH2	GPS	1
294.592	-24.728	4.47	12.19	0.20	0.23	0.057	UNSA	GPS	1
295.304	32.370	-11.62	9.22	0.10	0.12	0.106	BRMU	GPS	1
295.416	17.757	10.17	13.60	0.10	0.13	0.088	CRO1	GPS	1
295.530	-31.528	3.74	12.69	0.36	0.55	0.092	CORD	GPS	1
295.949	-64.775	13.65	9.78	0.96	0.73	0.086	PALM	GPS	1
295.966	67.559	-18.29	8.56	0.28	0.33	0.030	QIKI	GPS	1
296.389	44.684	-15.35	8.40	0.19	0.20	0.134	HLFX	GPS	1
297.660	82.494	-21.22	5.02	0.25	0.26	-0.028	ALRT	GPS	1
298.311	56.537	-16.37	10.33	0.19	0.19	0.050	NAIN	GPS	1
302.068	-34.907	-1.22	11.96	0.15	0.16	0.058	LPGS	GPS	1
302.099	-63.321	14.36	10.00	0.29	0.36	0.102	OHI3	GPS	1
302.099	-63.321	13.81	11.22	0.28	0.24	0.122	OHI2	GPS	1
302.100	-63.321	14.50	9.60	0.44	0.42	0.049	OHIG	GPS	1

Continued on next page...

Table C.1 – Continued from previous page

Long	Lat	Velocity (mm/yr)				Corr	Site	Source†	EXC‡
°E	°N	East	North	σ E	σ N				
307.322	47.595	-15.01	12.85	0.09	0.10	0.062	STJO	GPS	1
309.055	66.987	-17.92	11.61	0.10	0.11	-0.024	KELY	GPS	1
312.122	-15.948	-3.78	12.84	0.14	0.15	0.046	BRAZ	GPS	1
313.952	60.715	-16.55	13.27	0.17	0.17	-0.024	QAQ1	GPS	1
315.015	-22.687	-4.46	12.44	0.27	0.27	0.094	CHPI	GPS	1
321.574	-3.877	-4.80	12.95	0.17	0.21	0.071	FORT	GPS	1
321.575	-3.877	-4.91	13.01	0.36	0.37	0.082	BRFT	GPS	1
328.874	39.454	-8.69	19.92	0.58	0.76	0.028	FLRS	GPS	1
332.847	38.719	14.08	16.54	0.93	0.83	0.054	TERC	GPS	1
334.337	37.748	12.18	16.21	0.14	0.14	0.066	PDEL	GPS	1
337.017	16.755	19.07	16.29	0.29	0.28	0.112	TGCV	GPS	1
338.045	64.139	-10.72	20.56	0.11	0.10	-0.060	REYK	GPS	1
338.045	64.139	-10.26	19.39	0.17	0.17	-0.022	REYZ	GPS	1
343.092	32.648	15.39	17.92	0.40	0.45	0.074	FUNC	GPS	1
343.500	28.308	15.88	16.59	0.55	0.62	0.117	IZAN	GPS	1
344.802	64.267	13.91	14.86	0.11	0.10	-0.078	HOFN	GPS	1
345.588	-7.951	-5.36	11.29	0.18	0.21	0.038	ASC1	GPS	1
350.119	-40.349	21.09	19.19	0.28	0.22	-0.052	GOUG	GPS	1
350.582	38.693	17.87	16.81	0.09	0.09	0.023	CASC	GPS	1
351.187	42.184	17.89	16.63	0.24	0.21	0.060	VIGO	GPS	1
351.332	37.099	17.77	17.39	0.10	0.13	0.059	LAGO	GPS	1
351.411	41.106	17.85	17.06	0.13	0.13	0.054	GAIA	GPS	1
352.355	54.395	13.06	16.73	0.60	0.57	0.002	ENIS	GPS	1
352.663	54.984	14.85	16.92	0.59	0.57	0.011	FOYL	GPS	1
353.080	37.200	18.13	17.02	0.32	0.38	0.070	HUEL	GPS	1
353.146	33.998	16.45	17.78	0.11	0.11	0.031	RABT	GPS	1
353.236	62.023	11.55	17.01	0.33	0.07	0.009	TORS	GPS	1
353.658	39.479	18.60	16.99	0.11	0.12	0.031	CACE	GPS	1
353.794	36.464	17.23	17.06	0.54	0.52	0.070	ROAP	GPS	1
353.794	36.464	15.96	17.14	0.08	0.09	0.013	SFER	GPS	1
354.068	54.577	15.71	16.09	0.31	0.29	-0.003	BELF	GPS	1
354.457	50.103	15.92	16.28	0.17	0.15	0.011	NEWL	GPS	1
354.504	40.945	19.20	16.56	0.24	0.23	0.023	SALA	GPS	1
354.637	35.562	15.80	17.09	0.14	0.21	0.059	TETN	GPS	1
354.689	35.896	15.77	17.50	0.25	0.21	0.033	CEUT	GPS	1
354.694	35.892	15.85	17.50	0.37	0.43	0.070	CEU1	GPS	1
354.892	33.540	16.96	17.56	0.17	0.18	0.048	IFRN	GPS	1
355.279	37.916	19.10	16.32	0.17	0.16	0.054	COBA	GPS	1
355.292	41.703	18.22	16.50	0.31	0.37	0.028	VALA	GPS	1
355.503	48.381	16.66	16.82	0.11	0.12	-0.011	BRST	GPS	1
355.588	48.445	17.14	16.34	0.19	0.20	0.017	GUIP	GPS	1

Continued on next page...

Table C.1 – Continued from previous page

Long	Lat	Velocity (mm/yr)				Corr	Site	Source†	EXC‡
°E	°N	East	North	σ E	σ N				
355.607	36.726	19.03	15.51	0.19	0.22	0.062	MALA	GPS	1
355.750	40.429	18.80	16.13	0.12	0.12	0.006	MAD2	GPS	1
355.781	57.486	13.92	16.60	0.17	0.17	-0.025	INVE	GPS	1
355.781	57.486	15.74	16.57	0.68	0.65	0.010	INVR	GPS	1
356.036	39.675	19.33	15.68	0.28	0.29	0.046	SONS	GPS	1
356.202	43.472	18.85	16.38	0.16	0.10	0.038	CANT	GPS	1
356.573	47.746	17.30	16.23	0.26	0.27	0.012	PLOE	GPS	1
356.911	40.525	18.94	16.40	0.09	0.09	0.026	YEBE	GPS	1
357.158	-71.674	-0.67	10.54	0.18	0.18	-0.047	VESL	GPS	1
357.360	53.345	15.89	16.17	0.12	0.14	-0.018	DARE	GPS	1
357.541	36.853	19.09	16.10	0.11	0.11	0.041	ALME	GPS	1
358.001	38.248	19.86	16.51	0.41	0.43	0.047	MORA	GPS	1
358.131	38.115	19.34	14.91	0.39	0.36	0.031	CRVC	GPS	1
358.144	38.978	19.06	15.41	0.27	0.28	0.045	ALBA	GPS	1
358.315	55.213	15.56	16.44	0.14	0.11	-0.045	MORP	GPS	1
358.673	38.471	19.74	15.24	0.41	0.41	0.062	JUMX	GPS	1
358.674	38.502	20.67	16.52	0.31	0.33	0.054	JUMI	GPS	1
358.690	37.593	19.60	18.37	0.40	0.37	0.089	MAZA	GPS	1
358.781	46.159	18.34	16.25	0.10	0.12	0.021	LROC	GPS	1
358.791	39.569	19.38	16.33	0.20	0.18	0.038	UTIE	GPS	1
358.875	37.992	20.05	17.15	0.33	0.34	0.033	MURX	GPS	1
358.876	40.351	19.63	16.13	0.30	0.34	0.045	TERU	GPS	1
358.878	37.990	20.20	16.62	0.30	0.33	0.054	MURC	GPS	1
358.941	39.061	20.12	15.35	0.27	0.33	0.042	AYOR	GPS	1
359.005	37.606	19.77	17.18	0.53	0.67	0.023	CRTG	GPS	1
359.118	41.633	20.21	16.07	0.18	0.22	0.046	ZARA	GPS	1
359.139	37.731	20.88	17.48	0.28	0.30	0.054	ALCA	GPS	1
359.319	37.975	19.78	17.10	0.17	0.18	0.035	TORR	GPS	1
359.519	38.339	20.08	16.56	0.09	0.08	0.016	ALAC	GPS	1
359.527	38.698	19.86	16.74	0.17	0.17	0.058	ALCO	GPS	1
359.592	46.134	18.54	16.22	0.12	0.12	0.026	CHIZ	GPS	1
359.656	39.436	19.92	15.86	0.21	0.20	0.034	VCIA	GPS	1
359.660	51.421	16.67	15.76	0.15	0.16	-0.027	NPLD	GPS	1
359.662	39.481	20.42	16.08	0.10	0.10	0.029	VALE	GPS	1
359.898	40.618	20.10	15.39	0.24	0.24	0.042	MORE	GPS	1
359.917	39.905	20.43	15.79	0.17	0.16	0.041	BORR	GPS	1
20.372	38.221	19.95	9.87	3.50	4.80	0.000	K2AM	HOL	2
21.889	38.257	14.06	-10.84	4.20	3.80	-0.010	K000	FLO	2
22.142	38.397	9.32	-5.81	3.30	2.60	0.379	CG30	FLO	2
22.285	38.348	11.05	0.35	9.10	6.60	-0.270	CG31	FLO	2
22.644	37.750	6.10	-10.32	3.00	2.90	0.130	MLDR	FLO	2

Continued on next page...

Table C.1 – Continued from previous page

Long	**Lat**	**Velocity (mm/yr)**				**Corr**	**Site**	**Source**†	**EXC**‡
°E	**°N**	**East**	**North**	σ **E**	σ **N**				
23.172	37.296	2.42	-14.95	3.00	2.80	0.060	PHEL	FLO	2
23.206	37.475	-0.56	-13.33	3.00	2.90	0.100	DDYM	FLO	2
23.541	37.756	5.44	-17.18	3.20	3.00	-0.040	AFIA	FLO	2
23.996	37.955	13.96	-14.46	3.30	3.20	0.160	LTSA	FLO	2
24.065	38.166	7.47	-12.24	4.60	3.80	-0.040	AGMA	FLO	2
24.585	38.805	17.06	-9.56	3.20	2.41	-0.010	CG40	FLO	2

†- *GPS data sources*
GPS - THIS STUDY
BUR - Burchfield et al., 2006
FLO - Floyd et al., 2010
HOL - Hollenstein et al., 2008
REI - Reilinger et al., 2006

‡- *GPS site exclusion reasons (see text for full explaination)*
U - Used in inversion
1 - Outside study area
2 - High error
3 - Duplicate site

Table C.2: Detailed segment geometry of the elastic dislocations that bound blocks in the Aegean model.

Segment	Start Point		End Point		Locking Depth	Dip
Number	Long °E	Lat °N	Long °E	Lat °N	(km)	°
Hellenic Subduction Segments						
1	21.033	36.847	23.105	35.197	30	20
2	23.105	35.197	24.4	34.25	30	20
3	24.4	34.25	25.2	34.253	30	20
4	25.2	34.253	26	34.25	30	20
5	26	34.25	27.306	35.319	30	20
6	27.306	35.319	28.64	36.361	30	20
7	-38.115	29.505	-14.226	-35.129	15	90
8	-38.115	29.505	350.629	38.202	15	90
9	-14.226	-35.129	32.232	-47.095	15	90
10	-5.684	35.95	350.629	38.202	15	90
11	-5.684	35.95	7.183	37.511	15	90
12	7.183	37.511	19.89	37.764	15	90
13	19.733	40.042	20.789	39.066	15	90
14	19.733	40.042	20.933	39.851	15	90
15	19.89	37.764	21.033	36.847	15	90
16	19.89	37.764	20.789	39.066	15	90
17	20.789	39.066	21.323	38.334	15	90
18	20.933	39.851	23.501	38.883	15	90
19	21.033	36.847	21.084	37.885	15	90
20	21.084	37.885	21.323	38.334	15	90
21	21.323	38.334	21.681	38.324	15	90
22	21.681	38.324	22.063	38.313	15	90
23	22.063	38.313	22.403	38.252	15	90
24	22.403	38.252	22.606	38.199	15	90
25	22.606	38.199	22.994	38.014	15	90
26	22.994	38.014	23.29	38.149	15	90
27	22.994	38.014	24.259	36.363	15	90
28	23.29	38.149	23.501	38.883	15	90
29	23.501	38.883	24.089	39.099	15	90
30	23.685	39.422	23.897	39.783	15	90
31	23.685	39.422	24.336	39.178	15	90
32	23.897	39.783	24.68	40.132	15	90
33	24.089	39.099	24.336	39.178	15	90
34	24.259	36.363	26.455	36.249	15	90
35	24.336	39.178	24.983	38.931	15	90
36	24.68	40.132	27.291	40.705	15	90
37	24.983	38.931	25.241	38.798	15	90

Continued on next page...

Table C.2 – Continued from previous page

Segment	Start		End		Locking Depth	Dip
Number	Long °E	Lat °N	Long °E	Lat °N	KM	°
38	24.983	38.931	25.423	39.331	15	90
39	25.241	38.798	25.607	38.667	15	90
40	25.423	39.331	27.187	39.639	15	90
41	25.607	38.667	28.362	38.49	15	90
42	26.455	36.249	27.206	36.739	15	90
43	26.598	-26.764	27.978	-26.207	15	90
44	26.598	-26.764	26.632	-28.335	15	90
45	26.632	-28.335	37.563	-37.145	15	90
46	27.187	39.639	27.871	40.061	15	90
47	27.206	36.739	28.996	37.856	15	90
48	27.291	40.705	28.642	40.902	15	90
49	27.509	-24.423	27.978	-26.207	15	90
50	27.509	-24.423	33.111	-21.293	15	90
51	27.871	40.061	29.004	40.137	15	90
52	28.362	38.49	28.906	38.019	15	90
53	28.64	36.361	29.546	37.394	15	90
54	28.64	36.361	31.26	35.009	15	90
55	28.642	40.902	31.087	40.587	15	90
56	28.906	38.019	29.031	37.878	15	90
57	28.971	-2.697	32.208	5.673	15	90
58	28.971	-2.697	33.677	-8.94	15	90
59	28.996	37.856	29.031	37.878	15	90
60	29.004	40.137	29.541	40.369	15	90
61	29.031	37.878	29.265	37.644	15	90
62	29.265	37.644	29.546	37.394	15	90
63	29.541	40.369	31.087	40.587	15	90
64	31.087	40.587	34.827	41.131	15	90
65	31.26	35.009	33.225	34	15	90
66	32.208	5.673	36.192	5.092	15	90
67	32.232	-47.095	67.986	-26.574	15	90
68	32.232	-47.095	37.563	-37.145	15	90
69	33.111	-21.293	33.677	-8.94	15	90
70	33.225	34	33.809	34.433	15	90
71	33.809	34.433	34.609	35	15	90
72	34.37	27.29	35.01	29.61	15	90
73	34.37	27.29	35.57	25.55	15	90
74	34.609	35	35.634	35.7	15	90
75	34.827	41.131	39.988	39.687	15	90
76	35.01	29.61	35.58	31.32	15	90
77	35.47	31.38	35.58	31.32	15	90
78	35.47	31.38	35.72	33.68	15	90

Continued on next page...

Table C.2 – Continued from previous page

Segment	Start		End		Locking Depth	Dip
Number	Long °E	Lat °N	Long °E	Lat °N	KM	°
79	35.57	25.55	43.607	11.99	15	90
80	35.634	35.7	36.43	36.63	15	90
81	35.72	33.68	36.31	34.44	15	90
82	36.192	5.092	37.609	5.96	15	90
83	36.31	34.44	36.43	36.63	15	90
84	36.43	36.63	36.629	37.025	15	90
85	36.629	37.025	36.83	37.42	15	90
86	36.83	37.42	38.65	38.2	15	90
87	37.609	5.96	41.435	11.28	15	90
88	38.65	38.2	40.27	38.83	15	90
89	39.988	39.687	41.054	39.048	15	90
90	40.27	38.83	42.498	36.803	15	90
91	40.27	38.83	41.054	39.048	15	90
92	41.435	11.28	43.607	11.99	15	90
93	42.498	36.803	44.005	36.521	15	90
94	43.607	11.99	47.193	12.364	15	90
95	44.005	36.521	45.587	34.893	15	90
96	45.587	34.893	45.82	33.44	15	90
97	45.82	33.44	48.96	31.39	15	90
98	47.193	12.364	51.265	13.186	15	90
99	48.96	31.39	51.43	29.42	15	90
100	51.265	13.186	52.236	14.643	15	90
101	51.43	29.42	51.64	28.23	15	90
102	51.64	28.23	54.25	26.85	15	90
103	52.236	14.643	56.234	14.643	15	90
104	54.25	26.85	57.12	27.62	15	90
105	56.234	14.643	59.363	14.913	15	90
106	56.234	14.643	58.222	12.731	15	90
107	56.993	9.909	62.319	4.673	15	90
108	56.993	9.909	58.222	12.731	15	90
109	57.12	27.62	57.3	26.67	15	90
110	57.3	26.67	57.49	25.72	15	90
111	57.49	25.72	57.8	25.05	15	90
112	57.8	25.05	61.44	24.44	15	90
113	59.363	14.913	59.91	15.413	15	90
114	59.91	15.413	60.729	19.42	15	90
115	60.729	19.42	62.186	22.151	15	90
116	61.44	24.44	65.89	24.9	15	90
117	62.186	22.151	65.89	24.9	15	90
118	62.319	4.673	64.396	3.018	15	90
119	64.396	3.018	65.444	3.173	15	90

Continued on next page...

Table C.2 – Continued from previous page

Segment	Start		End		Locking Depth	Dip
Number	Long °E	Lat °N	Long °E	Lat °N	KM	°
120	65.213	-18.118	67.458	-16.7	15	90
121	65.213	-18.118	66.335	-19.95	15	90
122	65.444	3.173	66.264	2.627	15	90
123	65.981	-14.16	67.458	-16.7	15	90
124	65.981	-14.16	66.225	-11.334	15	90
125	66.225	-11.334	67.222	-9.788	15	90
126	66.264	2.627	66.739	1.018	15	90
127	66.335	-19.95	68.699	-21.191	15	90
128	66.739	1.018	67.857	-1.652	15	90
129	67.222	-9.788	68.221	-6.842	15	90
130	67.857	-1.652	68.452	-4.004	15	90
131	67.986	-26.574	69.939	-25.562	15	90
132	68.221	-6.842	68.452	-4.004	15	90
133	68.699	-21.191	69.939	-25.562	15	90